Dissertation zur Erlangung des Doktorgrades
der Fakultät für Chemie und Pharmazie
der Ludwig-Maximilians-Universität München

A novel class of mRNA lipid nanoparticles (LNPs) optimized by the chemical evolution approach

Franziska Haase, geb. Freitag
aus Düsseldorf, Deutschland
2024

Erklärung

Diese Dissertation wurde im Sinne von § 7 der Promotionsordnung vom 28. November 2011 von Herrn Prof. Dr. Ernst Wagner betreut.

Eidesstattliche Versicherung

Diese Dissertation wurde eigenständig und ohne unerlaubte Hilfe erarbeitet.

München, 20.03.2024

.....

Franziska Haase

Dissertation eingereicht am 27.03.2024

1. Gutachter: **Prof. Dr. Ernst Wagner**

2. Gutachter: **Prof. Dr. Olivia Merkel**

Mündliche Prüfung am 16.05.2024

Meiner Familie

“Science doesn’t always go forwards. It’s a bit like doing a Rubik’s cube. You sometimes have to make more of a mess with a Rubik’s cube before you can get it to go right.” – Jocelyn Bell Burnell

Table of Contents

1 Introduction 7

1.1 Nucleic acid therapeutics: Challenges and Opportunities in nucleic acid delivery 7

1.2 Nonviral delivery of nucleic acids 8

1.2.1 Requirements on carriers and delivery systems 8

1.2.2 Approaches for synthetic carrier optimization 11

1.2.3 Lipid nanoparticles as lead nonviral delivery system 12

1.3 Aim of the thesis 14

2 Optimizing synthetic nucleic acid and protein nanocarriers: the chemical evolution approach 16

2.1 Introduction 18

2.2 Chemical evolution of delivery nanoagents 19

2.2.1 Molecular conjugates 20

2.2.2 Poly amino acid diblock polymers 22

2.2.3 Multi-block copolymer libraries 23

2.2.4 Combinatorial chemistry libraries 26

2.2.5 Sequence-defined macromolecules 28

2.2.6 Barcoded evolution of nanoagents *in vivo* 38

2.3 Optimizing for various macromolecular cargos 41

2.3.1 pDNA delivery 43

2.3.2 siRNA delivery 48

2.3.3 mRNA delivery 53

2.3.4 Intracellular protein delivery 56

2.3.5 Delivery of genome-editing nucleases 59

2.4 Conclusions 62

3 Lipoamino bundle LNPs for efficient mRNA transfection of dendritic cells and macrophages show high spleen selectivity 67

3.1 Introduction 69

3.2 Materials and methods 72

3.2.1 Materials 72

3.2.2 Synthesis of cationizable carriers 73

3.2.3 mRNA LNP formulation 78

3.2.4 Physicochemical characterization of LNPs 80

3.2.5 *In vitro* characterization 81

3.2.6 *In vivo* activity of mRNA LNPs in mice 85

3.2.7 Statistical analysis 88

3.3 Results and discussion 89

3.3.1 mRNA LNP formulation with novel ionizable LAF-Stp carriers 89

3.3.2 Physicochemical characterization of mRNA LNPs 92

3.3.3 Biological evaluation of LAF-Stp carriers in mRNA LNPs 95

3.3.4 Mechanistic studies on endosomal escape of mRNA LNPs 104

3.3.5 Screen of mRNA LNPs in presence of full serum 107

3.3.6 *In vivo* application of mRNA LNPs 109

3.4 Conclusion 114

4 Summary 116

6 Appendix 118

7 References 122

8 Publications 147

9 Acknowledgements 148

1 Introduction

This chapter is intended to provide a concise introduction into the topic of therapeutic nucleic acids and their application fields to contextualize the experimental data presented in the thesis within a broader framework. It does not aim to comprehensively address the entire scientific field.

1.1 Nucleic acid therapeutics: Challenges and Opportunities in nucleic acid delivery

Nucleic acid therapeutics have emerged as a groundbreaking advance in modern medicine, once the molecular structure of nucleic acids was unraveled [1, 2]. This discovery paved the way for the identification of genes associated with diseases [3], offering the potential to address a myriad of genetic and acquired diseases, such as infections, various forms of cancer and genetic disorders at their root cause [4, 5]. These therapeutic agents, including DNA, mRNA, siRNA or genome editing tools such as CRISPR-Cas9, have the ability to precisely modulate gene expression, correct genetic mutations, and influence a variety of cellular processes [6-8]. In recent times there has been an increasing number of clinical trials and market approvals for such therapeutic approaches [5, 9-11]. However, while the potential of nucleic acid therapeutics is immense, realizing their full capability depends on overcoming the substantial challenges associated with effective delivery [6].

Several critical factors play a role in the translation of various approaches into clinically viable nucleic acid therapeutics [12]. The core challenge resides in the efficient and precise delivery of nucleic acids to the target cells and tissues. It is essential to recognize that nucleic acid delivery is not a one-size-fits-all endeavor and different cargos impose distinct requirements on their carriers [13-15]. The requirements for delivering nucleic acids can vary significantly based on the specific therapeutic goals. In the end, the drug product should be biocompatible, exhibit adequate extracellular stability while maintaining intracellular release of the nucleic acid in its active form at the target location and overcoming various extra- and intracellular barriers depending on the route of application. Therefore, nucleic acids, characterized by their comparatively large size, negative charge, and limited biological stability, require suitable delivery systems for cargo protection and stability [6, 16, 17]. In the past,

clinical gene therapy trails have mostly been delivered using viral vectors [5], while non-viral formulations, have been less prevalent [10, 18].

Synthetic cationic polymer- or lipid-based nanocarriers, including polyplexes, lipoplexes, and lipopolyplexes [19], have been explored as non-viral delivery system, but also more complex formulations such as LNPs have gained recognition in recent years. LNP-based mRNA vaccines have shown promise in addressing the COVID-19 pandemic [20, 21], siRNA LNPs have reached the market as RNAi Therapeutic, for Hereditary Transthyretin Amyloidosis [22], and Cas9 mRNA LNPs have been successfully used for *in vivo* genetic correction by CRISPR Cas9/sgRNA in patients [23].

1.2 Nonviral delivery of nucleic acids

1.2.1 Requirements on carriers and delivery systems

Efficient nucleic acid delivery is a major bottleneck in the translation of therapeutic nucleic acid formulations into clinical practice [6]. Crucially, effective nonviral nucleic acid delivery demands carriers or delivery systems that possess several essential attributes, such as stability to protect nucleic acids from degradation, and the capacity to efficiently facilitate cellular uptake, endosomal escape and cargo release inside the cell [24-26]. Additionally, these carriers must be biocompatible, non-immunogenic, and ideally, capable of targeting specific cells or tissues with precision. Synthetic carriers have more and more emerged as essential tools for achieving these goals, offering several advantages over viral vectors, such as less induction of immune system, versatility in size and design of the carrier and better production upscaling [27-29].

To meet the diverse requirements of nucleic acid delivery, nonviral carriers and delivery systems should provide protection for the fragile nucleic acid cargo from enzymatic degradation and rapid clearance from the blood stream, as already mentioned. This is crucial to ensure the stability and integrity of the cargo, provide protection against nucleases and increase circulation time. The interaction between negatively charged nucleic acid and positively charged carrier plays an important role for nucleic acid complexation within nanoparticles [6]. This process is driven by entropy and results in the formation of nanoscale complexes (e.g. polyplexes) [30]. The size, shape and

surface chemistry of nanoparticles play a decisive role in systemic administration, significantly influencing pharmacokinetics and biodistribution [31]. Particles smaller than 10 nm get directly cleared by the kidneys [32, 33], whereas particles larger than 200 nm undergo rapid removal from the bloodstream via the reticuloendothelial system (RES) [34, 35], or accumulate in tumors with high vascularity due to the enhanced permeability and retention (EPR) effect [36].

A billion years of evolutionary defense mechanisms aimed at preventing invading RNAs from entering cells had to be overcome [37]. However, these carriers must be still capable of promoting cellular uptake by endocytosis, as their size, charge and hydrophilicity prevent passive diffusion across cell membrane's lipid bilayers **(Figure 1)**. Endosomes also consisting of a lipid bilayer, capture 99% of the cargo, often permitting only 1% to escape [38, 39]. Inside the endosomes, the pH gradually drops to pH 6.0 in early endosomes up to pH 5.5 in late endosomes, which results in endosomal rupture or endosomal escape followed by cargo release [40]. This implies both the efficient transport of nucleic acids across the cell membrane and their cargo release inside the cell, where they can develop their biological effects. LNPs, for example, exhibit neutral surfaces in plasma, but with an ideal pKa of 6.4, they become selectively cationic charged in the acidic environment within endosomes, thereby facilitating endosomal escape [9, 40, 41].

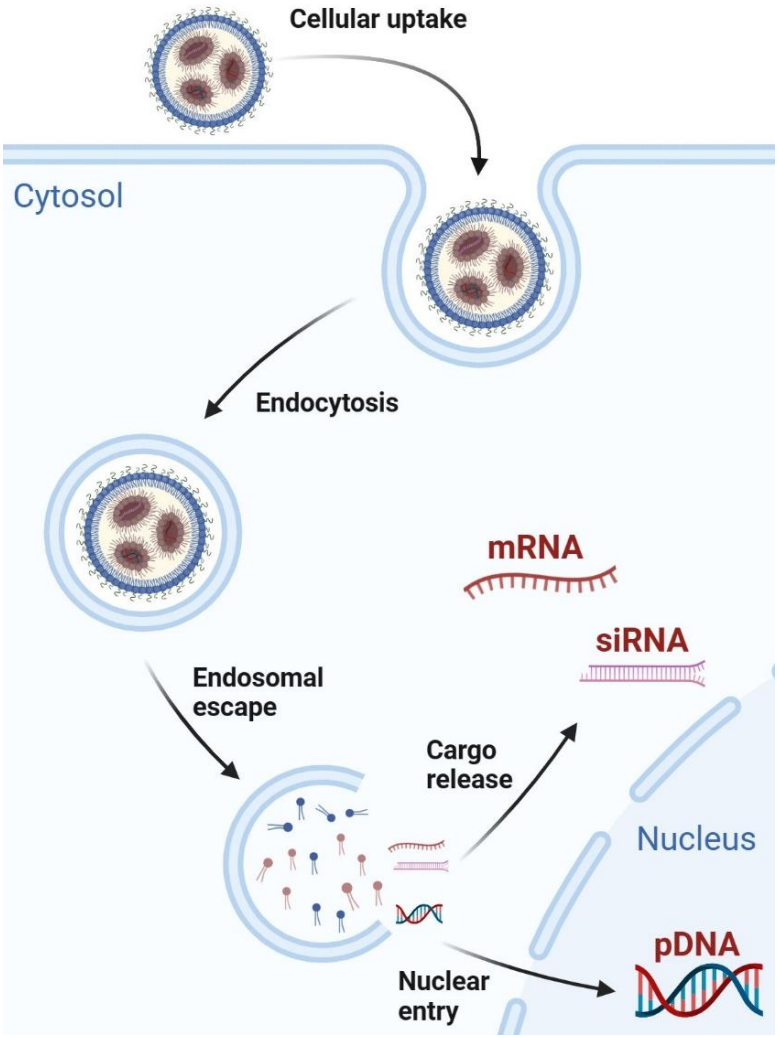

Figure 1. Nonviral transfection process. Cellular uptake of a nonviral carrier system (e.g. LNPs) via endocytosis, followed by endosomal escape and release of the different cargos (mRNA, siRNA, pDNA). Created with BioRender.com

As mentioned above, cell membrane lipid bilayers serve as the primary barriers for the efficient transport of large and negatively charged nucleic acids. To enhance cellular internalization, electrostatic interactions between the cell membrane and nanoparticles can be employed. However, endocytosis is generally less specific and effective than passive targeting via receptor-mediated uptake [42]. A convenient strategy to promote efficient and target specific cellular uptake is the incorporation of targeting ligands, such as peptides, glycopeptides or antibodies to the carrier system. These ligands can be chosen from receptors that are overexpressed in cancer or target cells [43, 44]. These targeted nanoparticles can accumulate in the appropriate tissue and then selectively reach target cells, thus reducing off-target effects and minimizing potential

side effects. Another advantageous feature for delivery systems is the bio-responsive adaption of their properties based on stimuli, such as changes in pH, redox potential, or temperature [45].

A notable recent hurdle is the weak *in vitro/in vivo* correlation, emphasizing the limitations of cell culture testing for therapeutic application [46-48]. Formulations that demonstrate strong *in vitro* activity can perform completely different *in vivo*, and relying on *in vitro* studies to select best-performing carriers may exclude highly efficient *in vivo* candidates [49]. Via intravenous application, nanoparticles are confronted with various additional hurdles not present *in vitro*. Once entering the blood, blood components lead to the formation of a protein corona, which modifies physicochemical characteristics, biological and pharmacokinetic activity and toxicity of the nanoparticle [50, 51]. This biological coating can even conceal the intended effects of the nanoparticle *in vivo* and lead to a loss of function [52]. Additionally, plasma proteins and blood cells in biological environment can effect nanoparticle aggregation [53]. Functionalizing nanoparticles surfaces with e. g. PEG as shielding agent can mitigate unspecific protein corona formation and decrease aggregation. This stealth effect improves particle durability and decreases immunogenicity by escaping immune system recognition and clearance [54-56].

1.2.2 Approaches for synthetic carrier optimization

Viruses have evolved diverse tactics to enter cells and transfer nucleic acids by biological evolution. Since they are synthesized inside cells using naturally occurring nucleotides and amino acids, their chemical composition is constrained. By using a range of synthetic molecules, delivery methods can be developed that exceed natural limits of viral evolution [57]. Nevertheless, viruses as highly effective delivery systems serve as templates for artificial nucleic acid carriers that mimic viral behavior [58].

Employing precise synthetic techniques, such as solid phase peptide synthesis (SPPS), libraries of carriers with defined sequences can be methodically generated and their structure-activity relationships can then be identified through high-throughput screenings [59-61]. These strategies pave the way for chemical evolution of sequence defined, virus-inspired delivery systems [14].

There are multiple different options, especially in the formulation of LNPs, beginning from molar ratio variations up to the use of different helper lipids and ionizable lipids/carriers, which make the formulation development very complex. Even slight variations in the formulation process can impact physicochemical, biological or pharmacological properties, which in turn affect the reproducibility [62]. The many variables impede to systematically examine all possibilities. Carrier optimization requires understanding critical factors that contribute to product variability to ensure their control or elimination, according to the Quality by Design (QbD) approach [63, 64]. Design of Experiments (DoE) tools as statistical analysis can be applied to systemically optimize nanoparticle formulations by establishing mathematical connections between the influencing factors of a process and its resulting output [65, 66]. Further approaches such as *in silico* methods can virtually predict and evaluate *in vivo* activity of infinite carriers via machine learning techniques [67]. These strategies lead to systematically enhanced, specific and precisely optimized carriers for nucleic acid delivery.

1.2.3 Lipid nanoparticles as lead nonviral delivery system

LNPs represent a promising and versatile class of nonviral nanocarriers that have recently attracted appreciable attention in the field of drug delivery and gene therapy [68]. Their origin lies in the development of liposomes containing lipids, organized in a bilayer structure, which separates the interior aqueous solution from the exterior [69, 70]. LNPs as enhanced version of liposomes with a liposome-like structure are composed of four lipids, which form more complex particles **(Figure 2)**. The incorporation of ionizable cationic lipids leads to strong electrostatic interactions with the negatively charged nucleic acids, resulting in highly efficient encapsulation inside the particle, and simultaneously facilitating endosomal escape and nucleic acid release into the cytosol. PEG lipids affect LNP's particle size, dispersity and stability due to the hydrophilic steric PEG chains reaching outside the particle's surface. Beside that they influence blood circulation, biodistribution and immune response. Cholesterol stabilizes lipid bilayers by filling in gaps between phospholipids, resulting in narrowing the lipid bilayer and decreasing particle permeability and leakage. The last component is a phospholipid, which stabilizes transitional structures during membrane fusion and bilayer disruption [71, 72]. Therefore, the unique property of LNPs lies in the efficiently

transport of various bioactive molecules, such as small molecule drugs, nucleic acids (pDNA, mRNA, siRNA, sgRNA) and proteins to specific target sites within the body [73].

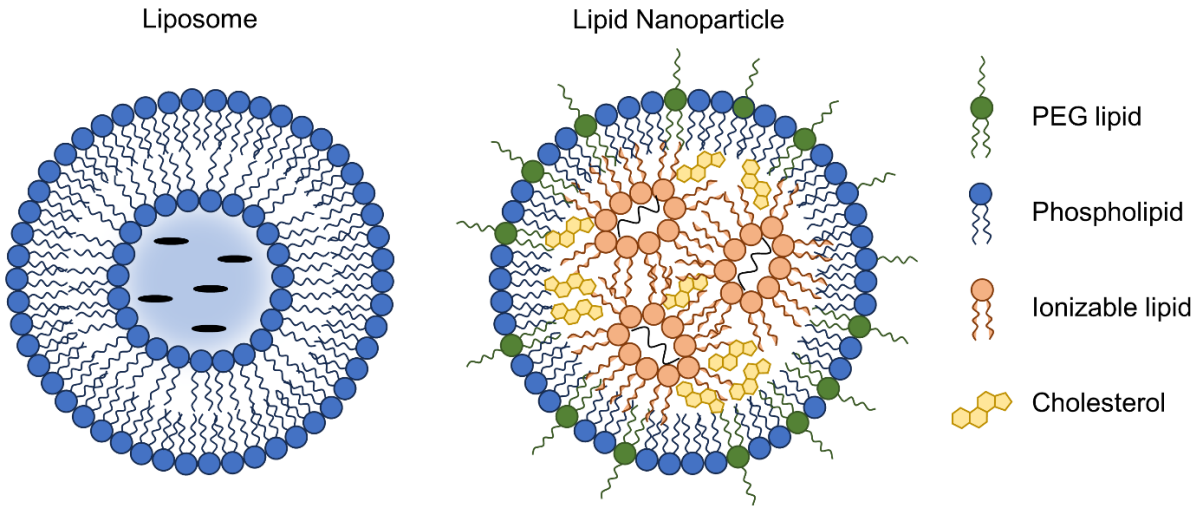

Figure 2. Liposome vs lipid nanoparticle. Liposomes consist of a ring of phospholipid bilayer surrounding an internal aqueous core. LNPs comprise a single phospholipid outer layer encapsulating multilayer cores, resulting from electrostatic complexation between ionizable lipids and nucleic acids.

The initial demonstration of the *in vivo* efficiency of LNPs focused on silencing genes in hepatocytes through i.v. administration of siRNA [74]. This pioneering study utilized the ionizable cationic lipid DLinDMA. The choice of the cationic lipid was found to be crucial [41], initiating an extensive research effort in lipid synthesis. This effort led to the discovery of DLin-MC3-DMA, which has become the widely recognized "gold standard" cationic lipid for gene silencing in liver cells and was used in the first FDA approved siRNA drug Onpattro (Patisiran) for the treatment of hereditary transthyretin amyloidosis [22, 75].

The development and widespread use of LNPs have been facilitated by their biocompatibility, stability, and ease of functionalization for tailored applications. This versatility has made LNPs a focus of pharmaceutical research, with emphasis on optimizing their structure and composition for improved drug delivery efficiency. LNPs have shown remarkable potential in overcoming some of the challenges associated

with traditional drug delivery systems, including poor solubility, rapid degradation, and nonspecific distribution in the body [71]. Furthermore, LNPs are capable of protecting encapsulated cargos from enzymatic degradation, enable targeted delivery by surface modifications, and improve cellular uptake. All of these are crucial factors in improving therapeutic outcomes while minimizing adverse effects [76].

In order to supply the high demand of LNP-based drug products, a highly reproducible, scalable and rapid production technology is required. Microfluidics as nonturbulent mixing technique meets all of these requirements and enables the control of physicochemical properties and the production of homogenous, size-controlled LNPs [77, 78].

1.3 Aim of the thesis

Nonviral gene therapy has attracted increasing attention as a new and safe delivery method compared to viral vectors. While polymeric gene delivery has a history spanning over half a century, more and more lipid-based therapeutics have captured the market in recent years, starting with Patisiran (Onpattro™) in 2018 [6, 22]. Although showing promising clinical effects, the development of safe and effective LNPs as delivery systems faces several challenges, particularly in their design and production. Continuous optimization of lipids, molar ratios, lipid compositions and manufacturing techniques resulted in progressively enhanced efficiency. Comprehension of delivery steps and understanding of the specific requirements of different nucleic acids and targets for their carriers forms the basis for this improvement. Searching for the optimal conditions and finding the best individual solution for the appropriate scientific problem by adjusting the right variables, is the key issue [79].

Aim of the thesis was to develop a lipid nanoparticle mediated delivery system for nucleic acid delivery, in particular for mRNA. For this purpose, a library of sequence defined carriers with different topologies should be generated via SPPS as described in Thalmayr et al. [80]. In general, all synthesized carriers should have a cationizable polar domain (Stp) for FLuc mRNA complexation and a pH-dependent cationizable lipidic domain (LAF) for lipidic integration into the particle and improved intracellular release. The structures of these carriers should differ in topology (U-shape, bundle), in hydrophilic/lipophilic balance within the carriers and in LAF type. The most obvious

approach should be to compare ourselves with two of the most popular and efficient ionizable lipids, DLin-MC3-DMA, which is used in Patisiran, and SM-102, the lipid in the Moderna vaccine as part of the global COVID-19 pandemic, as well as unsaturated oleic acid instead of the LAF motif. Deeper understanding of the role of helper lipids (cholesterol, phospholipids, PEG lipids) should be necessary to find the best selection and combination for the LNP composition, particularly as helper lipids also have an effect on particle behavior. Additionally, the formulation procedure (mixing technique, dialysis vs dilution, etc.) depending on the application was to be figured out.

The next important step should be to test and evaluate different molar lipidic and N/P ratios. Through comprehensive screenings of the synthesized library, including physicochemical characterization (size distribution, zeta potential, encapsulation efficiency, apparent surface pK_a, stability), biological evaluation in different cell lines (tumor cell lines, macrophages and dendritic cells) and mechanistic studies on endosomal escape, the best performing candidates should be identified. Moreover, *in vitro* studies in the presence of full serum should be performed for a better *in vivo* prediction. The most efficient carrier of each topology should then be compared with the gold standards DLin-MC3-DMA and SM-102 *in vivo* by intravenous application in tumor-bearing A/J mice and the organ specific mRNA expression was to be evaluated. Based on these results, the best candidate should be chosen for eGFP mRNA delivery in tumor-free A/J mice aiming to characterize the cell type specific transfection efficiency of immune cells in the liver, spleen and lungs.

2 Optimizing synthetic nucleic acid and protein nanocarriers: the chemical evolution approach

Franziska Freitag[a] and *Ernst Wagner*[a, b *]

[a] Pharmaceutical Biotechnology, Center for System-Based Drug Research, Ludwig-Maximilians-Universität (LMU), Munich, Germany

[b] Center for Nanoscience (CeNS), Ludwig-Maximilians-Universität (LMU), Munich, Germany

* Corresponding author. Pharmaceutical Biotechnology, LMU, Butenandtstrasse 5-13, D-81377 Munich, Germany. E-mail: ernst.wagner@cup.uni-muenchen.de

This chapter is adapted from a review article published in **Advanced Drug Delivery Reviews 2021, Volume 168, Pages 30-54 (ref.: [14]), Copyright Elsevier.**

Abstract

Optimizing synthetic nanocarriers is like searching for a needle in a haystack. How to find the most suitable carrier for intracellular delivery of a specified macromolecular nanoagent for a given disease target location? Here, we review different synthetic 'chemical evolution' strategies that have been pursued. Libraries of nanocarriers have been generated either by unbiased combinatorial chemistry or by variation and novel combination of known functional delivery elements. Like in natural evolution, definition of nanocarriers as sequences, as barcode or design principle, may fuel chemical evolution. Screening in appropriate test system may not only provide delivery candidates, but also a refined understanding of cellular delivery including novel, unpredictable mechanisms. Combined with rational design and computational algorithms, candidates can be further optimized in subsequent evolution cycles into nanocarriers with improved safety and efficacy. Optimization of nanocarriers differs for various cargos, as illustrated for plasmid DNA, siRNA, mRNA, proteins, or genome-editing nucleases.

Graphical abstract

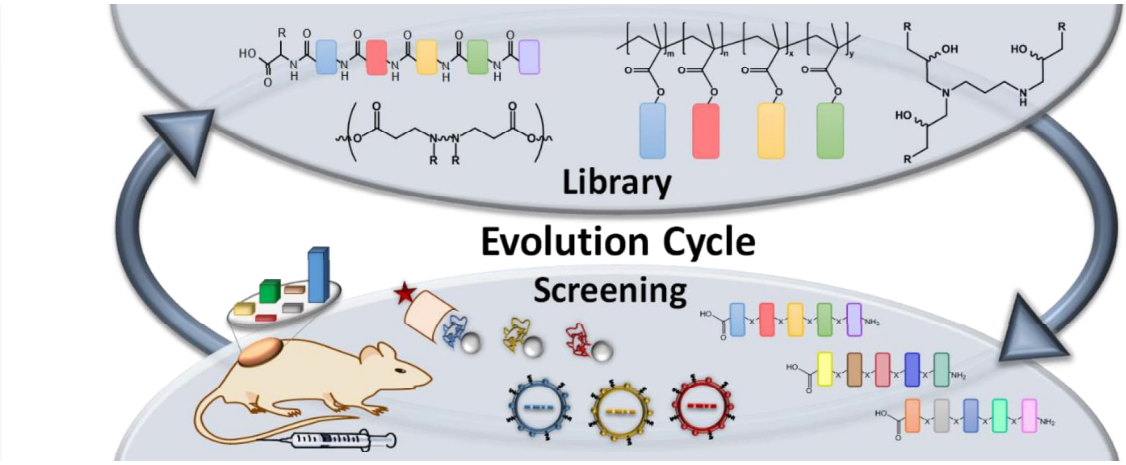

Keywords CRISPR Cas9; DNA; intracellular delivery; mRNA; polymer; siRNA; transfection;

Abbreviations ASGPR, asialoglycoprotein receptor; CART, charge-altering releasable transporters; CPP, cell-penetrating peptide; DET, diethylene triamine; eGFP, enhanced green fluorescent protein; mRNA, messenger RNA; OAA, oligoaminoamide; PACE, poly(amine-co-ester); PBAE, poly (β-amino ester); pCL, polycaprolactone; pDIPAMA, poly(2-diisopropylaminoethylmethacrylate); pDMAEMA, poly[(2-dimethylamino)ethyl methacrylate]; pDNA, plasmid DNA; PEG, polyethylene glycol; PEI, polyethylenimine; pHEMA, poly(2-hydroxyethyl methacrylate); pHPMA, poly[N-(2-hydroxypropyl) methacrylamide]; pLys, poly(L)lysine; PMO, phosphorodiamidate morpholino oligomer; pOEGMA, poly[oligo(ethylene glycol) monomethyl ether methacrylate]; pTMAEMA, poly[(2-trimethylamino)ethyl methacrylate]; siRNA, small interfering RNA; SPS, solid phase synthesis; Stp, succinoyl tetraethylene pentamine; TEP = TEPA, tetraethylene pentamine;

2.1 Introduction

Nucleic acid and/or protein macromolecule-based nanomedicines present an exciting avenue in medical care. Within the last three decades almost three-thousand gene therapy clinical trials have been performed, and at least nine gene therapy products reached medical market authorization, see [5] and http://www.abedia.com/wiley. Furthermore, at least eight oligonucleotide [10] and one siRNA [11, 22] drug products have been approved by the major medical agencies, and numerous clinical trials have reached advanced stages. All these macromolecular products depend on their successful intracellular delivery, which still appears as a critical bottleneck. It is not surprising that the current gene therapy products all are containing viral vectors or genetically modified cells. After a continuous struggle and refinement over thirty years, the development of effective retro/lentiviral vectors, adenovirus-associated viral (AAV) vectors or other viral vectors has paved the way towards approved medical drugs. In distinction, the marketed antisense agents (oligonucleotides) and RNA interference agents (siRNAs) all are synthetic nucleic acids. Here as well, advances in delivery chemistry have triggered the medical breakthrough [10, 81]. The design of lipid nanoparticles (LNPs) for delivery into hepatocytes [71] was the basis for the first marketed siRNA drug, Patisiran [22]. Recently, the design of asialoglycoprotein receptor (ASGPR) targeted, chemically completely modified siRNA conjugated with tri-(N-acetyl-galactosamine) ligand opened another way for liver-specific RNA interference therapy [82, 83]. Both LNPs and ASGPR-targeted siRNA conjugates are tested in advanced clinical studies where the target gene is located in liver hepatocytes. The medical efficacy of such nanomedicines is remarkable, considering that often only a small fraction (~1%) of active agent reaches the molecular target location [84], which usually is the cytosol, sometimes the nucleus of target cells. A further refinement of delivery carriers, especially for target tissues outside the liver, will have a tremendous impact on future nanomedicines.

Reasons for the slow progress in delivery of macromolecules are manifold. First of all, apart from recombinant proteins, macromolecular drugs present a new development challenge for pharmaceutical industry; synthetic and analytical tools had to be steadily developed to meet the requirement for macromolecule design at pharmaceutical grade and scale. Secondly, the different phases of extracellular and intracellular delivery demand bioresponsive actions of carriers, to alter their biophysical properties in a

dynamic (pH-, redox- or enzyme-sensitive) mode [45, 85-91]. Thirdly, recent experience tells that different macromolecular cargos (proteins, siRNA, mRNA, pDNA), often with different intracellular target sites, may require different carriers [13, 15, 92-95]. And fourth, the various different target organs and cells, and the different therapeutic modes (transient or permanent action) dictate different requirements to nanocarriers; optimization for ex vivo delivery into cultured cell most likely will not correlate with optimal in vivo delivery [96]. Reflecting all these hurdles, how can we optimize macromolecular drug delivery? Here we report on recent strategies to overcome the mentioned challenges, with the main focus on chemical evolution approaches toward optimized delivery of intracellularly active nucleic acid or protein therapeutics.

2.2 Chemical evolution of delivery nanoagents

Nature designed viruses as highly potent intracellular delivery agents, based on only four different nucleotides, twenty amino acids, in many cases also lipids and carbohydrates. With such a restricted chemical space of building blocks, and the requirement to assemble viruses under aqueous physiological in vivo conditions and disassemble them again under in vivo conditions ('assembly – disassembly paradox'), one might predict that synthetic nanoparticles generated under optimized chemical conditions utilizing numerous chemical building blocks might be far more effective. The impediment to design such optimized nanoparticles simply resides in the lack of knowledge about the perfect combination of building blocks. Random testing even of only a fraction of possible combinations of building blocks and their fast recycling would not result in optimized nanoagents within reasonable time. How did nature develop viruses and even more sophisticated, living structures? To our knowledge, the ingredients have been: i) defining structures in form of precise sequences, ii) storage (and reproduction) of this sequence information (via the genetic code), iii) subtle stochastic changes of this information with reproduction and time, and iv) a lot of time. It took natural evolution on earth several hundred million years to develop the first living organisms [97].

Artificial evolution strategies on an accelerated time scale are expected to be key measures for optimizing synthetic nanoagents. This may involve rational design of

building blocks based on a better understanding of the delivery process, combined with empirical screening of diverse chemical compound libraries, computational prediction by machine learning algorithms, virtual screening and, last but not least, storage of information on the precise molecular structure of the evolved nanoagents. In the following, examples of rational designs and evolution-based designs of different carrier types are presented, for illustrating the current stage of chemical evolution of delivery nanoagents.

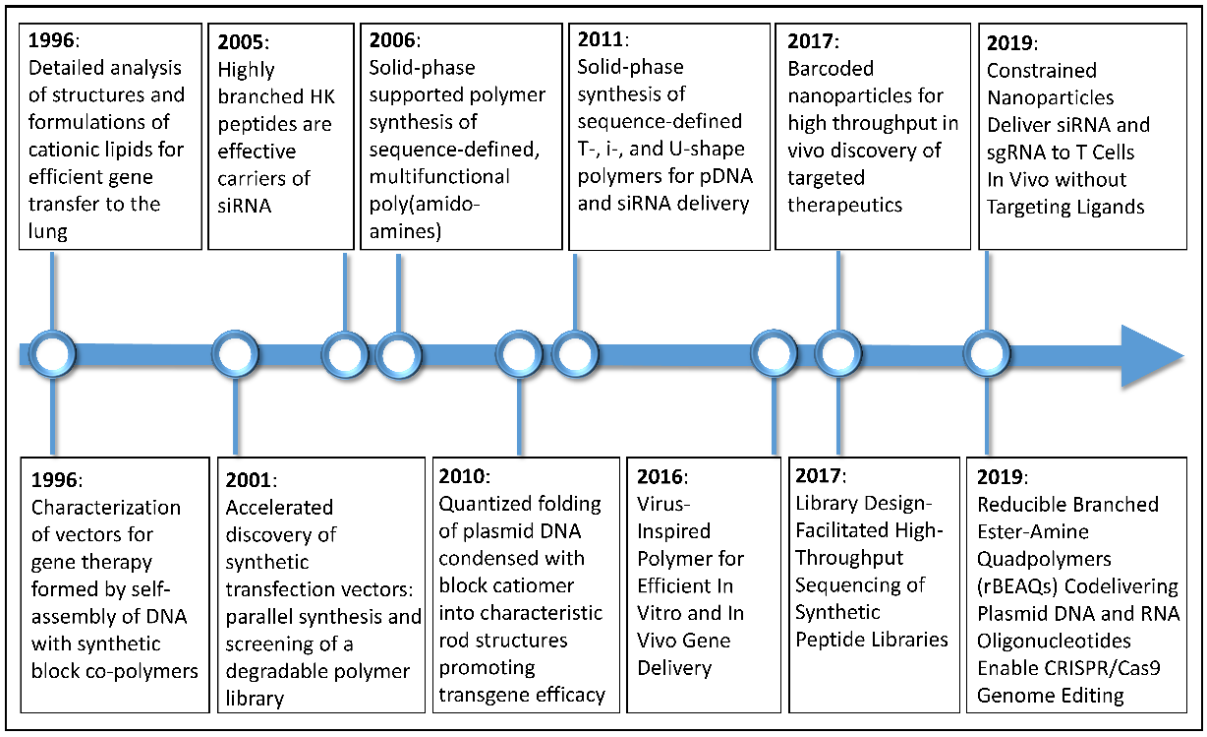

Figure 1. Schematic timeline of synthetic evolution strategies. Titles of representative reports which are discussed in the following sections and also can be found in the list of references.

2.2.1 Molecular conjugates

Initial efforts in intracellular delivery of RNA and DNA focused on transfection reagents such as poly(L)lysine (pLys), polyarginine, polyornithine, or DEAE-dextran [98-100]. These polycationic carriers can electrostatically bind, compact and protect the nucleic acid in form of nanoscaled polyplexes [6, 19]. Complexation of negatively charged nucleic acid with a small excess of carrier results in supercharged nanoparticles with positive surface charge, most convenient for enhanced cell interaction and nonspecific

intracellular uptake [101, 102]. Intracellular release from endocytic vesicles such as endolysosomes was identified as a critical delivery hurdle for the majority of carriers including polylysine [103], but less critical for endosomal cationizable carriers such as polyethylenimine (PEI) [104]. Several polycations were found to be toxic due to unspecific interaction with biomolecules [105, 106] and lack of degradability. These kinds of observations stimulated the search for biocompatible cationic backbones, which are more effective in intracellular release and biodegradability (see below).

A different direction in optimization has been the modification of basic carriers such as pLys with other delivery modules [107]. Modules can be receptor-binding targeting ligands, nanoparticle surface shielding domains, or lipid membrane-disturbing agents. To enhance endosomal escape into the cytosol, molecular conjugates with membrane-destabilizing peptides [58, 108, 109], or defective viral particles [110-112] were designed. To increase cellular receptor-specific uptake, molecular conjugates with targeting ligands were synthesized [113, 114]. Despite encouraging proof-of-concept studies, incorporation of ligands neither guarantees in vivo target specificity nor target receptor binding due to protein corona formation on the nanoparticle [115]. Thus, incorporation of hydrophilic surface shielding modules [116], including polyethylene glycol (PEG) [53, 117-124], poly[N-(2-hydroxypropyl) methacrylamide] (pHPMA) [125-127], hydroxyethyl starch [128], hyaluronic acid [129-131], or polysarcosine [132-134] often enhanced in vivo bioavailibility and also reduces toxic unspecific interactions. The mentioned delivery modules (compaction, shielding, targeting, endosomal escape) do not necessarily synergize [135]; for example, shielding may antagonize endolysosomal membrane destabilization. For this purpose, dynamic molecular conjugates and polyplexes were generated, which disassemble in specific (acidic, enzymatic or bioreducing) microenvironments [45, 88, 136-140]. In a nutshell, such carrier conjugates imitate virus-like cell entry processes [141, 142]. Encouraging therapeutic efficacies were demonstrated in several preclinical tumor models, such as described in [143-149]. Despite their high complexity, several of these molecular conjugate polyplexes reached the stage of application in human clinical studies [121, 150-152]. Nevertheless, conjugation of two or more macromolecules (polymers, proteins, peptides) usually presents a chemical challenging process with polydispersity in backbones and ill-defined conjugation sites or topologies; technical alternatives

include the design of high-precision polymers or defined lower molecular weight chemical entities.

2.2.2 Poly amino acid diblock polymers

In thoughtful and systematic studies, Kataoka and collaborators designed PEG-polycation block copolymers for chemical evolution of pDNA, siRNA and mRNA polyplexes. PEG blocks were found to significantly affect nanoparticle shape, condensation, and transcriptional availability of pDNA [153-156]. PEG-pLys packages the pDNA into rod structures, with a quantized length of pDNA folding by n times [153]. PEG shielding increased blood circulation time, but reduced transfection efficacy because of hampered cellular uptake. Systemic treatment with cRGD-targeted polyplexes with a rod length below 200 nm displayed antitumor efficacy against pancreatic cancer, whereas polyplexes with higher rod length, despite superior blood circulation, had negligible antitumor efficacy [154]. PEG-pLys with acid-labile linkage were applied to generate rod-shaped pDNA polyplexes, which under acidic conditions experience a removal of PEG from the polyplex and a dynamic change to compacted globules [155]. Further chemical evolution involved a series of PEG-pLys block copolymers with differing molecular weights of both pLys and PEG segments, for obtaining a refined understanding of pDNA packaging and gene transfer activity (see also section 3.1).

In order to replace pLys with more effective cationic delivery carriers, Kazunori Kataoka and colleagues amidated PEG-poly(aspartic acid) (pAsp) with various oligoethylenimines [157-160]. Diethylene triamine (DET) modified PEG-pAsp(DET) polyplexes showed a high biocompatibility and good diffusion into tissue as demonstrated in multi-cell spheroids [158]. For siRNA delivery, steroyl groups were introduced into pAsp(DET) [160]. Comparison of the various oligoamine side chains, an ‘even-odd rule’ (**Figure 2**) was established based on the differing pK values affecting endosomal buffering and escape. Polymers containing DET or tetraethylene pentamine (TEP) providing (after amidation) even units of protonatable aminoethanes showed best efficiency in pDNA transfections [161]. For mRNA delivery, this rule was unclear and was valid only for transfection levels at 12 hours (DET and TEP best); after 48 hours, the odd repeat triethylene tetramine (TET) displayed best transfection efficacy, followed by TEP [162]. For intravenous delivery of messenger RNA (mRNA),

the ω-terminus of the PEG-pAsp(TEP) block copolymer was provided with a cholesterol moiety to increase the polyplex stability by hydrophobic interaction. Upon intravenous injection, mRNA polyplexes showed enhanced blood circulation in comparison to Chol-free polyplexes. PEG-pAsp(TEP)-Chol based delivery of mRNA coding for the anti-angiogenic protein sFlt-1 inhibited growth of subcutaneous implanted pancreatic cancer in mice [163].

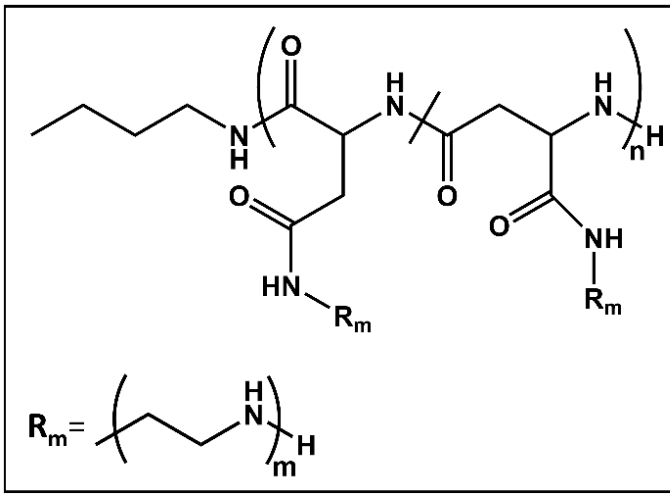

R_m	Number of protonated amines at	
	pH 7.4	pH 5.5
pAsp(EDA) m = 1	1	1
pAsp(DET) m = 2	1	2
pAsp(TET) m = 3	2	2
pAsp(TEP) m = 4	2	3

Figure 2. 'Even-odd rule'. Polyplexes from polymers with an even number of aminoethylene units in the side chains lead to higher endosomal buffer capacity (due to change of protonation between pH 7.4 and pH 5.5) and higher transfection efficiency than odd numbered ones [161].

2.2.3 Multi-block copolymer libraries

Based on the efficiency of reversible addition-fragmentation chain transfer (RAFT) polymerization [164, 165] multifunctional transfection block copolymers can be synthesized with good yields and low polydispersity. In this field, initial nucleic acid delivery studies were made with polymethacrylates [166-172] such as cationic poly[(2-dimethylamino)ethyl methacrylate] (pDMAEMA), or poly[(2-trimethylamino)ethyl methacrylate] (pTMAEMA), often prepared as co-blocks with hydrophilic pHPMA or PEG for improved biocompatibility and improved polyplex circulation in blood. A library of defined methacrylate polymers bearing pendant primary, secondary, and tertiary amino groups was synthesized using monomers (2-aminoethyl)-methacrylate, N-methyl-(2-aminoethyl)-methacrylate, or N,N-dimethyl-(2-aminoethyl)-methacrylate, respectively, in order to determine the effect of the amino substitution on pDNA

transfection [173]. Studies on cellular uptake and intracellular release suggested endosomal release effective via pore formation in lipid-membranes, where methacrylate-based polyplexes with a high primary amino group content mediated the best pDNA transfection, and polyplexes with tertiary amino groups the lowest pDNA transfection.

The group of Suzie Pun designed stabilized dual responsive nanoparticles for pDNA delivery *in vivo* [174]. The polyplexes were based on a ternary amphiphilic block copolymer containing a disulfide-linked hydrophobic polycaprolactone (pCL) block, a pH-sensitive tetraethylene pentamine (TEPA)-modified poly(glycidyl methacrylate) block, and a hydrophilic oligo(ethylene glycol) monomethyl ether methacrylate (OEGMA) block (**Figure 3A**). The pOEGMA block provides polyplex shielding in the blood circulation, the pCL block provides hydrophobic polyplex destabilization until intracellular disulfide cleavage, and the TEPA block endosomal cationization and endosomal escape. Subsequent work of the same lab optimized endosomal release of pDNA polyplexes by synthesizing VIPER (**Figure 3B**) [175]. This 'virus-inspired polymer for endosomal release' presents a methacrylate copolymer containing polycationic pDMAEMA for binding and compaction of DNA, a pOEGMA block for shielding, a pH-sensitive poly(2-diisopropylaminoethylmethacrylate) pDIPAMA block, and a neighboring poly(pyridyl disulfide ethyl methacrylate) pPDSEMA block. The latter activated disulfide block was coupled with lytic melittin peptides. Upon endosomal acidification the pDIPAMA block undergoes a transition from a hydrophobic to a hydrophilic phase, thus exposing the melittin peptides of the neighboring block in the endolysosomal compartment; this triggers endosomal membrane disruption and polyplex escape into the cell cytosol. Upon intratumoral administration VIPER facilitated pDNA delivery into KB tumors in mice. The carrier was also found effective for siRNA delivery and gene silencing in lung [176]. In further evolution, the same research lab successfully replaced melittin with other lytic peptides [177]. The endosomal responsiveness of pDIPAMA derivatives was utilized for nucleic acid delivery also by other investigators, for example in the design of siRNA micelleplexes for cancer immunotherapy by Yaping Li, Haijun Yu and collaborators [178, 179].

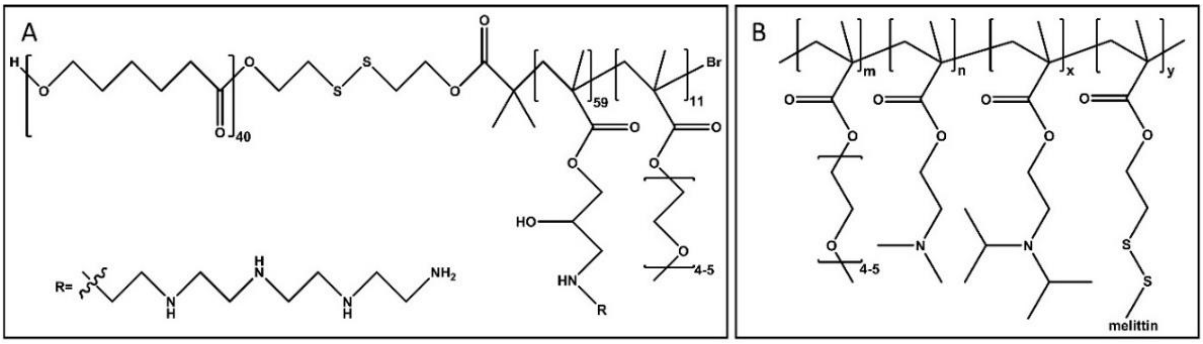

Figure 3. Block co-polymers based on methacrylate backbones. **(A)** OEGMA terminal triblock copolymer (PCL_{40}-SS-P(GMA-TEPA)$_{59}$-P(OEGMA)$_{11}$ [174]. **(B)** VIPER [175].

pDNA polyplexes may face the dilemma of insufficient stability in the blood circulation on the one hand, but at the same time limited release of pDNA from polycationic carriers inside the target cell. Therefore, in addition to chemically stable polymethacrylate polycations, also dynamic degradable analogues were synthesized. For example, Kwon and colleagues applied acid-degradable cationic ketal-linked methacrylamides, which were photo-polymerized in the presence of pDNA. Polyplexes under acidifying endosomal conditions lose the cationic groups of the polymethacrylate carrier, which enhances cargo pDNA release and pulmonary gene transfer after intratracheal delivery in mouse lung [180]. To address the 'polyplex dilemma' in a slightly different manner, Cheng et al [181] designed the pH-sensitive triblock copolymer p(PMA-PMBA)-b-p(OEGMA-DMAEMA), consisting of poly(propargyl methacrylate-graft-propyl-(4-methoxy-benzylidene)-amine)-block-poly(oligo(ethylene glycol) monomethyl ether methacrylate)-co-poly(2-(dimethylamino)ethyl methacrylate). The hydrophobic p(PMA-PMBA) domain enhances polyplex stability at physiological neutral pH. Upon endosomal acid-catalyzed cleavage of benzaldimines the domain undergoes a hydrophilic transition, thus enabling the release of pDNA. In comparison to the pH-stable analogue, *in vitro* gene transfer and also *in vivo* intraventricular gene transfer into brain was improved, although the *in vivo* efficiency remained moderate [181].

As a pioneer in methacrylate polyplexes [169-171], Wim Hennink and his team expanded the area and generated 'decationized polyplexes' as a completely novel class of methacrylate polyplexes [182-184]. These polyplexes were based on the terpolymer p(HPMA-DMAE-co-PDTEMA)-b-PEG, consisting of a PEG block and the

cationic block HPMA-DMAE (with pHPMA modified with dimethylaminoethyl carbonate at the hydroxyl group) containing 15% copolymerized N-(pyridyldithioethyl) methacrylamide (PDTMA). After pDNA polyplex formation with this polymer, the PDTMA units can be used for dithiol mediated crosslinkage into disulfide-stabilized polyplexes. By subsequent hydrolysis of the carbonate esters at pH 8.5, the cationic DMAE groups are removed. The resulting decationized pDNA polyplexes are stabilized by the formed disulfide crosslinks in the absence of polyelectrolyte interaction; they showed excellent biocompatibility, an enhanced residence time in blood circulation and increased accumulation in tumor. Analogous decationized polyplexes were also generated for siRNA delivery [185].

Evolution of nucleic acid carriers requires a focus on the specific selected target. The clinical breakthrough of cancer immunotherapy by chimeric antigen receptor (CAR) T cells raised interest in efficient *ex vivo* transfection of primary human T cells. With this focus, Pun and coworkers optimized methacrylate copolymers for pDNA and mRNA delivery into the Jurkat human T cell line and primary human T cells [186]. VIPER and several other linear, comb and sunflower pDMAEMA block copolymer architectures based on poly(2-hydroxyethyl methacrylate) (pHEMA) cores were evaluated. A subset of comb- and sunflower-shaped $pHEMA_{25}$-g-$pDMAEMA_{16}$ polymers were identified which can mediate transfection of Jurkat cells with efficiencies up to 50% with minimal toxicity. Transfection of both CD4+ and CD8+ primary human T cells with mRNA and pDNA were demonstrated with high viability and at efficiencies up to 25% and 18%, respectively.

2.2.4 Combinatorial chemistry libraries

More than two decades ago, Seng Cheng and colleagues published the result of the first large library screen of lipoplexes for gene transfer to the lung [187]. The study included several remarkable aspects: screening a huge number of cationic lipids; screening for the best formulation using the most authentic small animal model, which is the mouse lung *in vivo*; and discovery of the optimized formulation (containing lipid *#67*, a spermine – cholesterol derivative linked in T-shape configuration). This formulation was >100-fold more potent that previously tested lipoplexes. For development of novel cationic polymers with improved delivery and biocompatibility,

the initial screen focused on replacement of PLL with linear and hyperbranched poly (amino esters) [188, 189]. Short oligoethylenimines were converted by reaction with 1,4-butanediol diacrylate or 1,6-hexanediol diacrylate into degradable PEIs which are applied as transfection carriers *in vitro* and also *in vivo* [190-192]. Also, linear beta-amino ester polymers were produced via the same Michael addition starting from 4-aminobutanol [193]. The degradable PEI mimics showed favorable transfection activities. The team of Robert Langer developed a breakthrough concept, by generating large combinatorial libraries of biodegradable poly(β-amino esters) (PBAE), based on Michael addition of a series of primary or secondary amine monomers to several different diacrylates (**Figure 4A**) [194-196]. Such a large, 2350-member library was screened by a semi-automated high-throughput process for pDNA delivery, and 46 polymers were identified with higher transfection activity than the gold standard PEI [196]. A second generation library was generated containing 486 PBAEs which were characterized for biophysical and pDNA transfection properties [197]. Interestingly, the top nine polymers all contained amino alcohols as building blocks, and the three top polymers differed in structure by only one carbon. The two best polymers condensed pDNA to the smallest particle sizes of 71 and 79 nm.

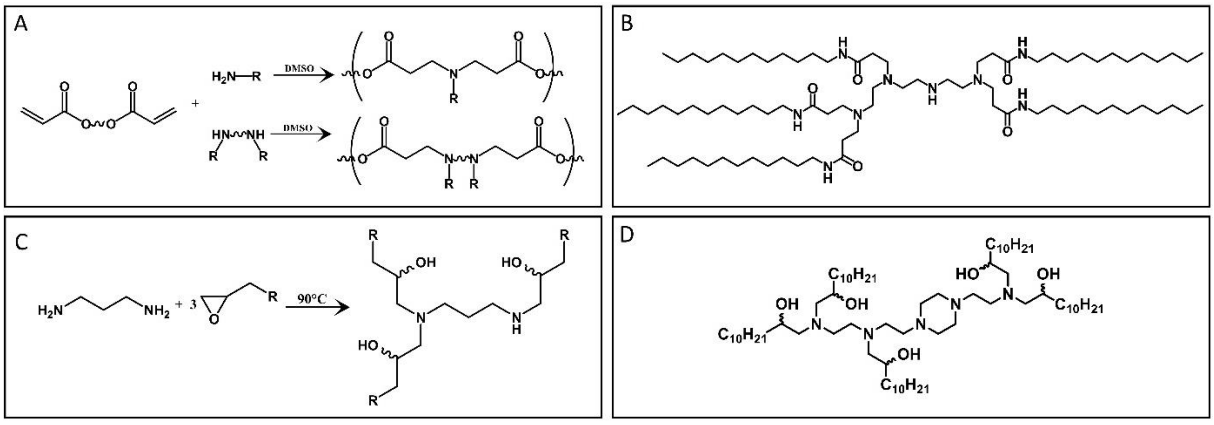

Figure 4. Lipidoids for siRNA delivery. **(A)** Combinatorial libraries of biodegradable poly(β-amino esters) via Michael addition of a series of primary or secondary amine monomers to several different diacrylate monomers [195]. **(B)** Lipidoid 98-N12-5 [198]. **(C)** Epoxide addition based libraries [199]. **(D)** Lipidoid C12-200 [199].

For siRNA delivery, Robert Langer, Daniel Anderson and colleagues designed an analogous Michael addition-based combinatorial library of over 1,200 structural diverse structures termed lipidoids [200]. These lipid-like structures were obtained by combinatorial Michael addition of lipidic acrylate esters or amides to various mono- to oligoamines. Lipidoid 98-N12-5, based on addition of five dodecylacrylamides to triethylentetramine (**Figure 4B**), performed best *in vitro*, and upon formulation with cholesterol and PEG-lipid, also mediated excellent *in vivo* gene silencing in liver hepatocytes of treated mice [198, 200]. A novel combinatorial library based on epoxide-addition chemistry (**Figure 4C**) yielded the highly potent lipidoid C12-200 (**Figure 4D**) which were able to mediate *in vivo* gene silencing in mouse liver at doses below 0.01 mg/kg [199, 201]. A subsequent high-throughput study of 1,536 structurally distinct nanoparticles with cationic cores and variable hydrophilic shells was performed by Daniel Siegwart and Anderson based on epoxide-functionalized hydrophilic block polymers that were combinatorially cross-linked with a diverse library of amines [202]. Cross-linkers with tertiary dimethylamine or piperazine groups and potential buffering capacity, as well as thin hydrophilic shells were favorable. Covalent cholesterol attachment to the polymeric carrier allowed for siRNA transfection to mouse liver hepatocytes *in vivo*.

The mentioned reports make clear that the cargo (pDNA or siRNA or other nucleic acids) as well as the specific application dictate the optimum nanocarrier, which needs to be identified by individual library screening. Consistently, using a library of low charge density poly(amine-co-ester) terpolymers generated by enzyme catalyzed polymerization, the Mark Saltzman lab demonstrated that different PACE polymers are required for optimized transfection of either pDNA, mRNA, or siRNA [95].

2.2.5 Sequence-defined macromolecules

Multifunctional molecular conjugates present a real challenge for precise chemical production. Nevertheless, their structure is by far exceeded in complexity, functionality, and high precision by natural macromolecules. The secret of natural proteins is their definition and information storage as (linear) sequences. Such sequences present virtual information, in nature stored on DNA or RNA templates, with this information translated into functional real structure by reading via the genetic code. For biomimetic

evolution of artificial macromolecular carriers, their definition as sequences is a key requirement. In short, sequences *per se* present perfectly defined information of an intangible construction plan in biomacromolecules, which can be stored on material templates (as in nature) or in digital virtual form (in artificial synthetic evolution). Execution of the construction plan may proceed in alternative ways; either by direct use of the digital code for artificial assembly by a chemical synthesizer into sequence-defined macromolecules; or via reading an artificial code from a real template by recognition with building block-loaded adapter molecules.

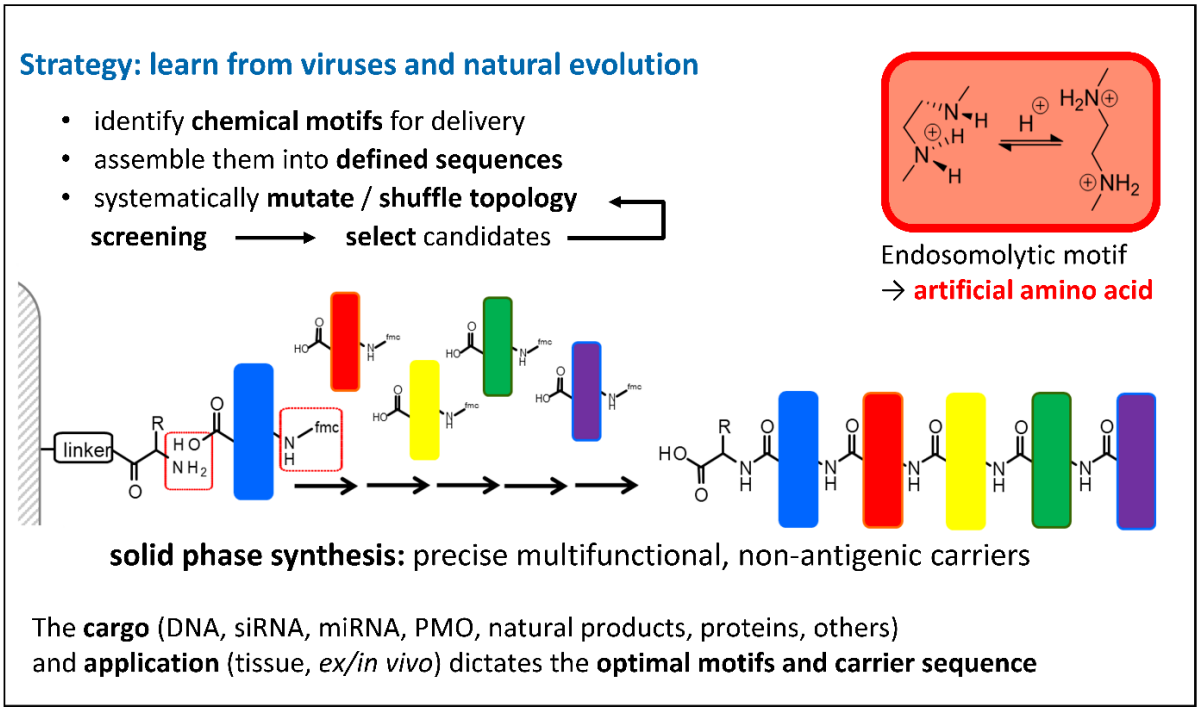

Figure 5. Chemical evolution strategy for optimizing sequence-defined nanocarriers. The endosomally cationizable diamino-ethane motif is displayed as example of a delivery motif which can be converted into an artificial amino acid and subsequently applied in the SPS sequence assembly.

Chemical synthesis of peptide and oligonucleotide sequences is well established, and the generation of precise sequence-defined artificial macromolecules is a recently emerging field [203-205]. We and others aimed at development of peptide-like chemical evolution strategies for intracellular macromolecule delivery (**Figure 5)**, where artificial amino acids with superior carrier properties would be integrated. Initial

evolution of sequence-defined transfection agents was based on standard peptides. First studies explored the requirements for nucleic acid binding by introducing the cationic amino acids lysine, arginines or ornithines [206, 207], disulfide-forming nanoparticle-stabilizing cysteines [208, 209], endosomal-buffering histidines [209-215] or membrane-destabilizing peptides [216, 217]. In their pioneering work, Christian Plank et al. [207] synthesized a series of branched oligocationic peptides and found that minimally six to eight cationic amino acids (arginine > lysine ~ ornithine) are required to condense pDNA into active gene delivery particles. The team of James Mixson systematically evaluated linear and branched peptide libraries containing lysines (for nucleic acid binding) and histidines (for endosomal buffering) in various ratios (e.g. HK, H2K, H3K) and numbers of branches (e.g. linear, four or eight branches). Addition of a histidine-rich tail, for example in peptide H2K4bT, significantly improved pDNA gene transfer activity, most likely by enhanced buffering capacity of the carrier [211]. Efficiencies were found to also depend on the target cells. In one study in combination with cationic liposomes, a linear HK peptide was found to transfect primary cells more effectively than the branched analogue [212]. Initial cellular uptake or size of the complexes could not explain the differences. Interestingly, a strong relation was found between the optimal type of HK carrier and the differing endocytic vesicle pH of different cell types. By altering the fraction of cationizable histidines, the endosomal pH of a cell may determine the amount of DNA released from the linear or branched HK polymer. In the primary cells in which the linear HK liposomes were the best carriers, the endolysosomes were highly acidic (pH of <5.0). Conversely, in cell lines where the branched HK liposomes were optimal, the pH of endolysosomes was above 6.0. These results with the HK liposome carriers were predictive of which cells could be transfected efficiently by the branched HK polymers alone. Whereas the linear HK polymers without liposomes were ineffective pDNA carriers in all tested cell cultures, the branched HK polymers without liposomes effectively transfected cells with a higher endosomal pH. For siRNA complexes, the H3K8b peptide was highly effective in gene silencing, whereas the effective pDNA carrier H2K4b was ineffective for siRNA [213].

In addition to natural amino acids, also artificial building blocks were introduced, such as triethylene tetramine or analogues developed by Zheng-Rong Lu and collaborators [218-220]. Fatty acids were also incorporated as lipophilic domains [219], such as in

the evolution of the PepFect cell-penetrating peptide series of Ulo Langel and colleagues [217, 221, 222]. Bradley Pentelute and coworkers introduced innovative technologies for peptide library synthesis including artificial 'non-canonical' amino acids for generation of xenopeptides and xenoproteins, and nano shotgun LC-MS/MS sequencing for high-throughput library screening [223-226]. The potency of their novel chemical evolution methodology was demonstrated by identification of xenoprotein interactors (**Figure 6A**) and or protein - protein interaction (PPI) inhibitors (**Figure 6B**) with far higher potency compared to previous conventional peptides. For innovative drug delivery, the Pentelute lab introduced several artificial macrocyclization technologies to improve peptide-based drugs, such as providing an enhanced transfer of a transportan-10 analogue or a BIM BH3 domain across the blood-brain-barrier [227]. To improve the intracellular delivery of splice-switching phosphorodiamidate morpholino oligonucleotides (PMOs), they conjugated PMOs with arginine-rich cell-penetrating peptides (CPPs) that had been first optimized by perfluoroaryl macrocyclization and bicyclization [228]. In addition, based on results with 64 PMO-CPP conjugates, machine learning algorithms were developed for computational prediction of suitable CPPs, and validated with seven novel CPP sequences that all proved to be effective [229]. Thus, empirical library screen and machine learning might synergize in a chemical evolution process.

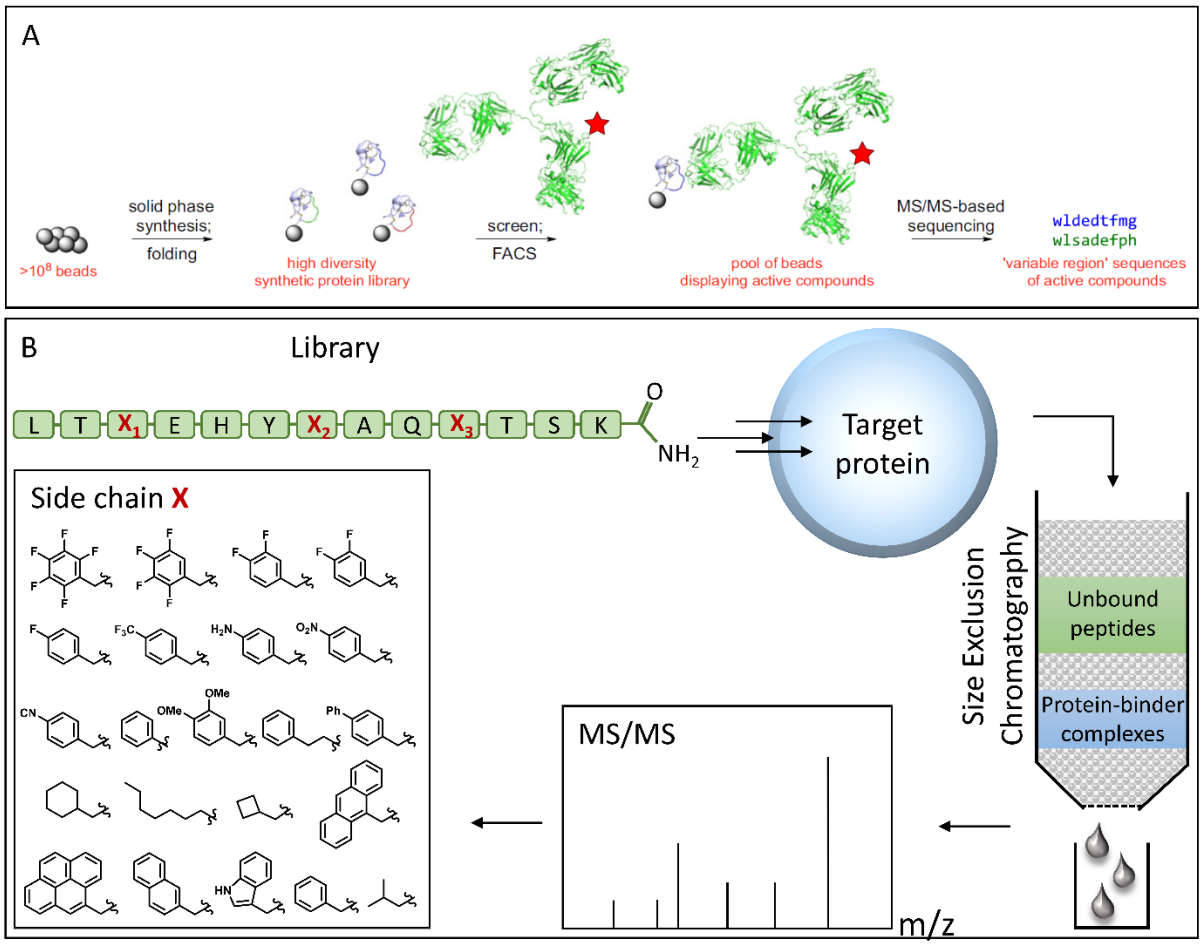

Figure 6. Synthetic artificial peptide libraries **(A)** for xenoprotein engineering, reproduced from [223] with permissions of *Proc. Natl. Acad. Sci. U. S. A.*; *D*-amino acids are in lowercase; **(B)** for identifying protein-protein interaction inhibitors, compare [224]; the example displays MDM2 binders identified from a third evolution library containing non-canonical amino acids.

Laura Hartmann, and Hans Börner [59, 230-234] adopted solid phase synthesis (SPS) for the sequence-defined alignment of completely unnatural chemical units. Instead of incorporating α-amino acids with standard protective groups, they performed alternating coupling of diamines (3,3'diamino-N-methyl-dipropylamine, or a bis (tBoc)-protected spermine, or a disulfide-containing unit) followed by succinic acid anhydride as dicarboxylic acid unit in each round of coupling. The resulting oligo(amidoamines) were applied for pDNA polyplex formation and thus, to our knowledge, present the first examples of completely artificial sequence-defined nanocarriers. Subsequently, to combine the known efficient transfection properties of PEI with the methodology of automated Fmoc peptide synthesis, David Schaffert and colleagues designed artificial oligo(aminoethylene) amino acids with amino-terminal Fmoc and internal tBoc

protective groups [60, 235, 236]. These artificial amino acids contain three to five repeats of the protonatable aminoethylenimine motif. The novel building blocks were assembled in combination with standard Fmoc and side chain protected α-amino acids by SPS into more than 1000 defined oligo(ethanamino)amide (OAA) sequences. Oligomer architectures included linear [60, 237], two-arm [60], three-arm [60, 238], four-arm [60, 236, 239] and comb architectures [240]. Branching points were provided by the two (α, ε) amines of lysine introduced as either via bis(Fmoc) lysine or Fmoc /Dde lysine , which after simultaneous or subsequent deprotection during synthesis can result in pseudo-symmetric or asymmetric branches. Optionally, lipo-oligoaminoamides were designed with i-shape, T-shape, or U-shape topology [60, 238, 241] by introducing bis (acyl)-modified lysines as hydrophobic polyplex stabilizating domains **(Figure 7)**. In several different topologies, terminal cysteines served for the stabilization of polyplexes by formation of bioreducible disulfide bridges. Due to the precision of the chemical design, simple open questions on structure –activity relationships were addressable. Testing the length of a linear sequence based on the building block Stp (succinyl TEP, containing three protonatable nitrogens per unit when integrated into the oligomer backbone) as requirement for pDNA compaction and gene transfer, an optimum length of 20 Stp units was identified, representing 61 protonable nitrogens and in total 100 nitrogens. pDNA transfection efficiency was about 5-fold higher and cytotoxicity about 10-fold lower as compared with the ‘gold standard’ linear PEI 22kDa, which contains around 500 (± 200) protonable nitrogens [237].

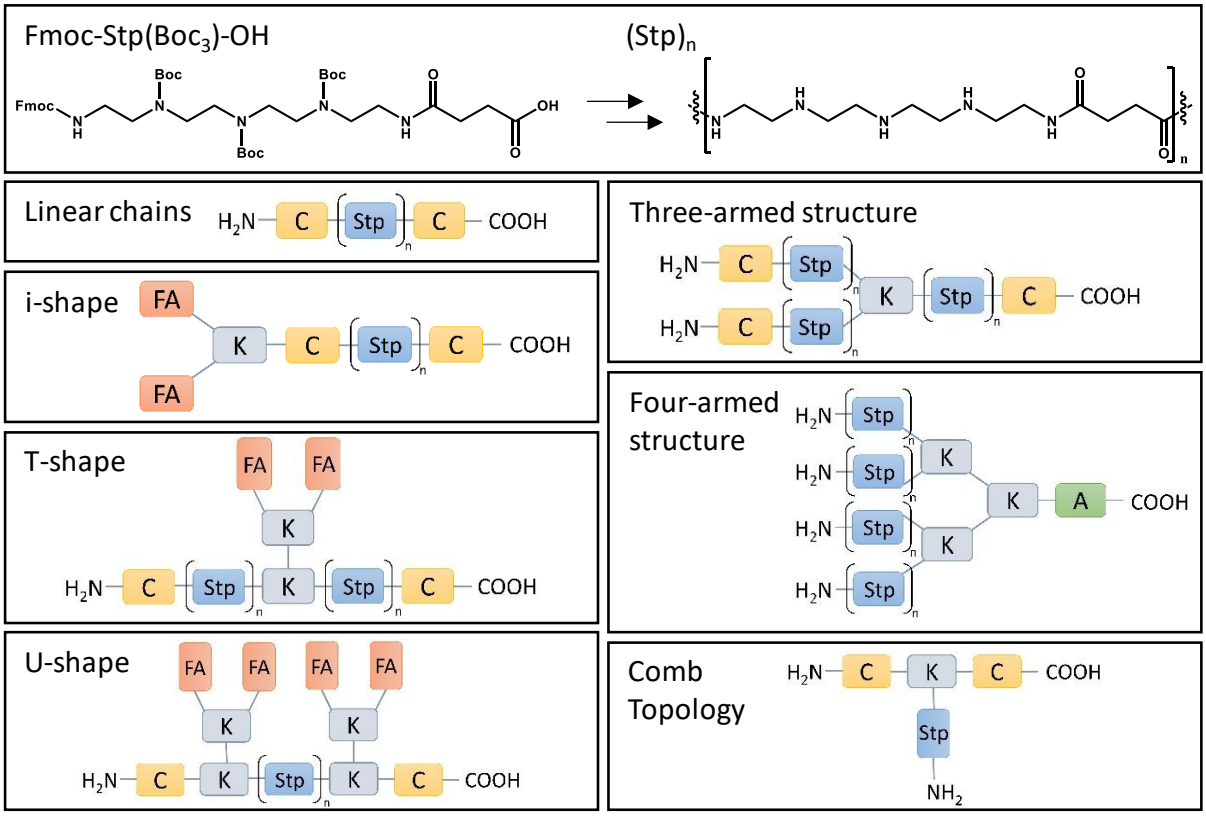

Figure 7. Protected artificial amino acid Fmoc-Stp(Boc_3)-OH and sequential assembly into Stp-based oligo(ethanamino)amide (OAA) sequences with different structural topologies [60, 236-240]. Stp, succinoyl tetraethylene pentamine; C, cysteine; K, lysine; A, alanine; FA, fatty acid.

For further optimization of pDNA carriers, the design of four-arms based on two branching lysines strongly reduced the number of coupling steps, and terminal cysteines increased polyplex stability and transfection efficiency. With regard to the total number of nitrogens, the type of selected polyamino acid played a more critical role than extending the length of arms beyond three building blocks. Units containing pentaethylene hexamine (Sph) were more effective than tetraethylene pentamine (Stp), which were more effective than triethylene tetramine (Gtt) building blocks [236]. A closer inspection of the total protonation capacity as well as the cationization pH confirmed independently the 'even-odd' rule which had been developed by Kataoka and colleagues (see section 2.2). Gtt and Sph with even numbered protonatable amino groups displayed higher total endolysosomal buffer capacity than the odd number analogue Stp. Within the relevant endolysosomal pH range, Gtt has a maximum buffer capacity at pH 5, and Stp a maximum around pH 7. Alternating incorporation of histidines increased the total buffer capacity with a more continuous cationization pH

profile and, especially for the ‘odd’ Stp building block, strongly enhanced gene transfer both in the *in vitro* and *in vivo* setting [239]. The even-odd rule was well applicable when comparing linear and comb topologies and their differing properties in pDNA complex formation, endosomal buffer capacity, cellular binding and intracellular uptake, and gene expression. In linear topologies, the two terminal amines of building blocks are consumed by amidation, this resulting in three (odd) or four (even) amines for Stp and Sph oligomers, respectively. Branched topology (with only one amine amidated) reverses properties, with four (even) and five (odd) protonatable amines for Stp and Sph. Consistently, the comb topology increased endosomal pH buffering for the Stp comb structures, but reduced endosomal buffering for the Sph comb structures. For both carriers, the combs mediated a higher overall cellular uptake in comparison to the linear topologies. In sum, Stp combs displayed a combined advantage in both buffering and cellular uptake and a strong (up to >100-fold) increase in pDNA transfection, whereas Sph combs mediated only a moderately (up to fourfold) enhanced transfection over the linear topology [240]. Incorporated Gtt building blocks enhance endosomal buffering but (due to lowest number of nitrogens) but display less pDNA binding; this could be compensated by incorporating cysteines which form polyplex-stabilizing disulfide cross-links [239].

Beyond pDNA compaction and core nanoassembly, incorporation of surface shielding and targeting domains was considered. Sequence-defined solid-phase-assisted assembly enables all-in-one synthesis of peptide or small-molecule targeting ligands attached to precise monodisperse PEG molecules and the nucleic-acid binding and endosomal buffering core OAA backbone. For example, monodisperse PEGylated two-arm oligomers with targeting ligands such as cRGD or B6 [242], folate [239, 243], c-Met binding peptide [244, 245], EGFR-binding peptide GE11 [246], or an IL-6 receptor binding peptide [247] were synthesized with defined uniform molecular weight, and receptor-mediated cellular uptake of polyplexes was confirmed resulting in enhanced gene transfer. By variation of the molecular weight of the PEG domain, its influence on biophysical and biological properties was elucidated. PEGylation was found to interfere with the endosomal escape function of the PEI-like OAA polyplexes, which is a limitation that also was previously detected for targeted, PEG-shielded PEI polyplexes [248, 249]. Importantly, enhancement of endosomal buffer capacity by

incorporation of histidines into the cationic OAA backbone compensated for this bottleneck [239, 243, 244].

PEGylation and incorporation of related hydrophilic domains affected also pDNA compaction; screening PEG domains from 12 to 72 ethylenoxide (EO) units demonstrated optimum compaction without PEG or 12 EO units, moderate compaction with 24 EO and lack of compaction with 48 or 72 EO repeat units [250]. In other studies similar low-molecular-weight PEG was found as favorable with ligand-PEG-shielded nanoparticles [251] or liposomes [252]. pDNA compaction was found as important requirement for intravenous systemic administration *in vivo* in mice in a HUH7 hepatocellular carcinoma xenograft model. pDNA gene transfer via a cMet binding peptide – $(EO)_{24}$ – (Stp/His)-Cys two-arm OAA was highly successful, but only if 1/3 of oligomers was substituted by an analogous PEG-free three-arm compacting oligomer. The formulation without or with compacting oligomer did not significantly differ in cell culture transfection [244].

Incorporation of tyrosine tripeptides at both ends of ligand-PEG-two arm oligoaminoamides was considered for nanoparticle stabilization by aromatic π-π stacking [243] also improved pDNA polyplex compaction. In a recent study, pDNA was compared with far smaller minicircle (MC) DNA in OAA formulations [253]. While the DNA type (number of base pairs) controlled the nanoparticle size, the carriers dominated the shape of polyplexes. c-Met-targeted, tyrosine tripeptide-containing OAA polyplexes presented compact structures with a rod size of 65–100nm for pDNA and 35–40nm for MC. As compared to their tyrosine-free pDNA analogues, the optimized MC nanostructure facilitated an ~200-fold enhanced gene transfer in c-Met-positive DU145 prostate carcinoma cells.

An alternative strategy for designing well-compacted surface-shielded polyplexes is the pre-formation of compacted pDNA core nanoparticles followed by post-modification with a shielding / targeting shell [254]. One recent example was the design of pDNA polyplexes with four-arm OAAs post-modified with acid-labile pHPMA. This enabled ‘deshielding’ in the endosomal environment, resulting in favorable gene transfer into tumor cells *in vitro* and *in vivo* [255]. Another example presents the disulfide-based modification of pDNA lipopolyplexes with a bidentate PEG–GE11 agent for EGF receptor-mediated gene transfer [256].

Optimization for other cargos such as small molecule drugs [257, 258], phosphorodiamidate morpholino oligomer (PMO), siRNA, mRNA, or proteins including Cas9/ sgRNA ribonucleoprotein (RNP) particles revealed significantly different requirements for nanocarriers as outlined in other sections. For example, in the evolution of siRNA carriers, polyplex stabilization by hydrophobic fatty acid domains was highly important (see section 3.2). PMO present a chemically different class of small, uncharged nucleic acid analogues that has already resulted in the exon-skipping drug Exondys, which is FDA-approved for treatment of Muscular Dystrophy. After screening a fatty acid lipo-OAA mini-library for small PMO molecules, Ulrich Lächelt and colleagues identified linolenic acid-containing oligomer PMO conjugates as most potent RNA slice-switching agents [259]. Far superior endosomal escape properties of the linolenic acid (containing three double bonds) over the analogous saturated stearic acid derivative appear as the most likely explanation for this non-predictable finding. Screening an analogous T-shaped lipo-OAA library for delivery of Cas9/sgRNA RNPs revealed a hydroxy-stearic acid (OHSteA) containing lipo-OAA as superior over analogues with unsaturated or saturated fatty acids without hydroxylation, displaying improved cellular uptake and endosomal release, an increased nuclear association and the highest CRISPR/Cas9 mediated gene knock-out [260].

Another example illustrating the advantage of sequence-defined artificial peptide-based evolution is the recent work by Sören Reinhard and colleagues [90]. He realized that the artificial Stp-based OAAs are not degradable by the lysosomal enzyme cathepsin B. A degradability of OAA nanocarriers in lysosomes however might be highly advantageous, blocking undesired cytotoxic lysosomal lytic activity of the nanocarrier. Designing a mini-library by inserting single natural *(L)* amino acids or dipeptides into a Stp backbone, followed by a library screen exposing to cathepsin B under endolysosomal conditions, resulted in the discovery of simple dipeptide cathepsin cleavage sites. Inserting for example *(L)*-RR into lipo-OAAs for intended lysosomal degradation resulted in siRNA nanocarriers with strongly reduced cytotoxicity as compared to their *(D)*-rr analogues.

A different assembly mode of sequence-defined macromolecular structures is the direct supramolecular assembly on a real template, as it happens in the natural evolutionary process. Such a DNA template-assisted synthesis was reported by David Liu and colleagues, where monomers were pre-arranged at a DNA template and

translated in an enzyme-free process into sequence-defined synthetic polymers [261]. In a recent study, the same group designed highly functionalized nucleic acid polymers (HFNAPs) assembled by ligase-mediated DNA-templated polymerization, starting with 32 building blocks that on a DNA backbone contain diverse side chains [262]. Repeated evolution cycles of polymer translation, selection and reverse translation, led to HFNAPs which can bind PCSK9 with high nM affinity.

2.2.6 Barcoded evolution of nanoagents *in vivo*

For chemical evolution of nanocarriers and their nucleic acid nanoparticles, analytical methods for high-throughput screening of compound libraries are of utmost importance, both *in vitro*, but even more *in vivo*. As reviewed above (section 2.5), Pentelute and coworkers applied nano shotgun LC-MS/MS sequencing as high-throughput method for screening compounds with defined unique molecular mass such as peptide analogues. Phage display library screening presents a commonly used molecular biology approach for fishing target-binding, phage-displayed peptides by panning the library to the desired target, followed by identifying the selected peptide via the phage-encoded nucleic acid sequence. This potent evolution strategy has been transferred into the chemistry field. For example, DNA-encoded chemical libraries [263, 264] have been generated by coupling chemical molecules to unique nucleic acid sequences (DNA barcodes). James Dahlman and colleagues [265] introduced DNA barcoding for high throughput screening and identification of suitable nanocarriers for *in vivo* delivery (**Figure 8)**. Single-stranded DNA barcodes were approximately 60 nucleotides long, terminally phosphorothioate–stabilized oligonucleotides, containing eight to ten central nucleotides as barcode and the 3’ and 5’ ends as adapter sequences for subsequent Illumina deep sequencing. Individual barcodes can be incorporated into the interior of different nanoparticles without affecting their activity. Upon simultaneous injection in a single mouse, the biodistribution of thirty different nanoparticles to eight tissue was monitored by deep sequencing [265, 266]. A follow-up paper analyzed differences of nucleic acid nanoparticle *in vivo* delivery between wild-type and Cav1 knockout mice; for this purpose, the authors optimized the barcode secondary structure, thereby making the DNA amplification much easier, and enabling concurrent ddPCR readouts [267]. In addition, the researchers made the following

important observation; by comparing delivery of 281 barcoded lipid nanoparticles (LNPs) to endothelial cells and macrophages *in vitro* and *in vivo*, the researcher found that *in vitro* delivery to immortalized mouse macrophages (RAWs) did not predict *in vivo* delivery to macrophages, and *in vitro* delivery to mouse aortic endothelial cells (iMAECs) did not predict *in vivo* delivery to endothelial cells of heart, lung, or bone marrow [96]. In many cases LNPs that performed well *in vivo* did not rank highly *in vitro* and thus would have been lost by an *in vitro* pre-screen; and LNPs top ranking *in vitro* did not perform well *in vivo*.

Beyond monitoring biodistribution only, in the next step the barcode-based system was further developed to measure functional delivery of hundreds barcoded LNPs within a single mouse. This novel strategy for *in vivo* evolution was termed 'Fast identification of nanoparticle delivery (FIND)' [268-270]. Functional delivery of RNA, such as Cre mRNA or specific siRNA, in the appropriate reporter mouse models (Lox-Stop-Lox-tdTomato mice or GFP mice, respectively) results in gene editing or gene silencing, which triggers induction/reduction of a reporter signal in the successfully transfected cells/organs. Successfully transfected cells can be isolated by cell sorting and analyzed for the barcoded bioactive LNPs. LNPs had been previously optimized to deliver Cas9 mRNA and sgRNA to hepatocytes. In their novel work, Sago et al [268] measured the functional mRNA delivery of more than 250 LNPs *in vivo* to multiple cell types. They identified two LNPs (7C2 and 7C3) with an altered tropism that efficiently deliver siRNA, mRNA, and single-guide RNA (sgRNA) to endothelial cells.

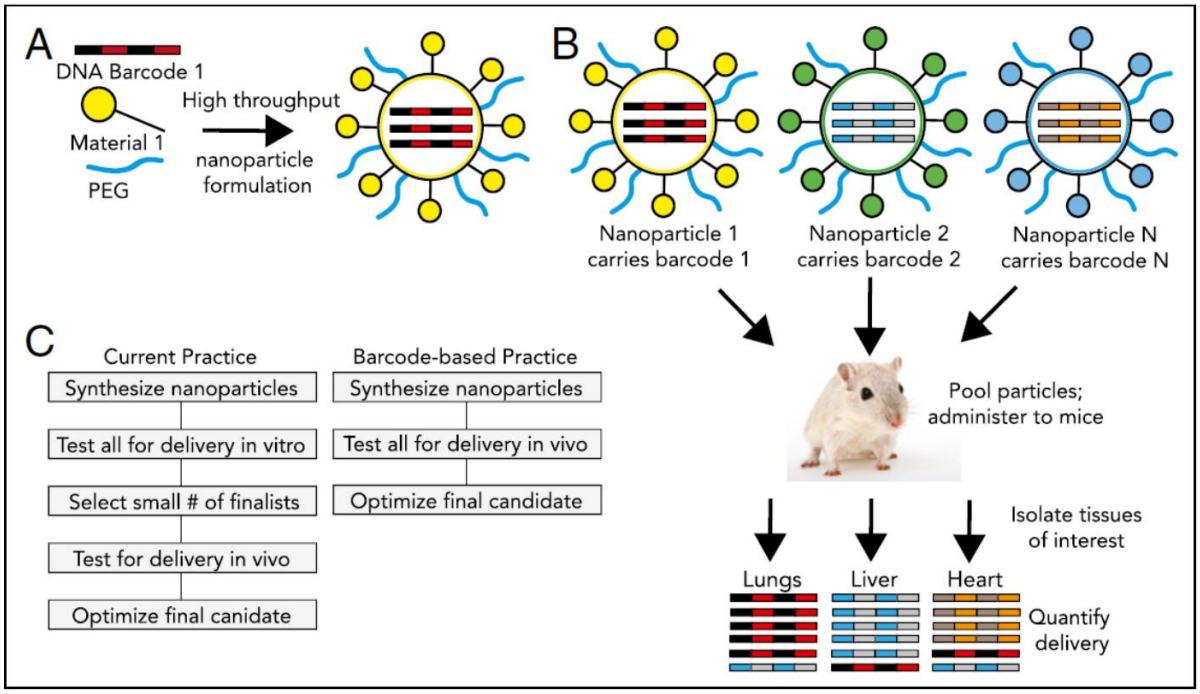

Figure 8. High throughput nanocarrier *in vivo* screening by DNA barcode sequences. DNA barcoded nanoparticles for high throughput *in vivo* nanoparticle delivery. **(A)** Nanoparticles carry individual DNA barcodes. **(B)** Each nanoparticle carries a distinct barcode. Particles are then pooled and administered simultaneously to mice. Tissues are then isolated, and delivery is quantified by sequencing the barcodes. In this example, nanoparticle 1 delivers to the lungs, nanoparticle 2 delivers to the liver, and nanoparticle N delivers to the heart. **(C)** The barcode-based practice enables multiplexed nanoparticle-distribution studies *in vivo*. Reproduced from Dahlman et al. [265] with permission of *Proc. Natl. Acad. Sci. U. S. A*.

By combining FIND with bioinformatics, *in vivo* RNA delivery was optimized in a directed evolution process. For example, Dahlman and coworkers identified LNP 'BM1' that delivers siRNA or sgRNA to bone marrow endothelial cells (BMECs). BMEC tropism was not related to the size of LNP, but changed with cholesterol content and PEG structure in the formulation [269]. Apparently, significant changes to vascular targeting can be made by simple changes in chemical composition instead of using active targeting ligands.

The same research group applied FIND to quantify *in vivo* delivery of 75 distinct mRNA LNPs to 28 cell types. They discovered that an LNP containing oxidized cholesterol delivers Cre mRNA for DNA editing into hepatic endothelial cells and Kupffer cells at low dose of 0.05 mg kg^{-1}, fivefold more potently than into hepatocytes. Cholesterol

oxidation on the hydrocarbon tail linked with sterol ring D outperformed cholesterol modifications on sterol ring B [270]. Most recently Dahlman's team applied 168 DNA-barcoded siGFP nanoparticles for identifying functional siRNA *in vivo* delivery to nine cell types in transgenic eGFP mice. Constrained lipid nanoparticles (cLNPs), containing an adamantly lipid, deliver siRNA and sgRNA to T lymphocytes at low doses and (in contrast to previously reported LNPs) do not preferentially target hepatocytes [271]. In sum, within a short period the barcode-based design has already proven as powerful strategy of chemical evolution towards optimized nanocarriers [272], providing solutions which would not have been predictable by rational design and classical screening. Provided that barcodes can be integrated from the interior of stable nanoparticles, and those would not expose or exchange nucleic acid barcodes with each other, the strategy could also be applied to polyplexes or other class of nanomaterials.

2.3 Optimizing for various macromolecular cargos

Delivery requirements of various macromolecular cargos are different **(Table 1)**, based on their different sizes, charges, chemical properties and different intracellular sites of action [13, 15, 92-95]. Conversely, different classes of nanocarriers offer characteristics which are more or less suitable for a given cargo. For standard cationic polymers [6, 15], polyplex formation is an entropy-driven process based on the electrostatic interaction between the multivalent polycationic polymer with the polyanionic nucleic acid cargo. A larger number of charges per polycationic carrier and also the polyanionic nucleic acid is favorable for stability of these polyelectrolyte complexes (PECs). Clear differences between large (pDNA, higher polyplex stability) and small (siRNA, lower polyplex stability) cargos can be seen. Covalent conjugates between siRNA and cationic polymers have been investigated to overcome the stability problem [273, 274].

In case of LNPs [71], hydrophobic lipid-lipid interactions, co-assembly of (mono/di)-cationic lipids into polycationic lipid micelles and liposomal structure dominate, resulting in incorporation and encapsulation of the nucleic acid cargo. Obviously electrostatic interactions are only partly responsible for LNP formation, therefore the

size of nucleic acid cargo is less influential, and formulations are also suitable for small cargos such as siRNA.

Lipopolyplexes present an intermediate class of nanomaterials based on lipid-conjugated polycations which self-assemble into larger polycationic micelles and electrostatically interact with negatively charged nucleic acid cargos. For all classes of carriers, optimization for a specific cargo type requires variation of the cationic domain (size, number of charges) and lipid domain of the carrier, optionally mixed lipid compositions (cationic lipid, cholesterol, phospholipid, PEG-lipid), N/P charge ratio and the formulation process.

Table 1. Differences in physicochemical properties of the different cargos and their requirements for delivery

Cargo	**Physicochemical properties**	**Requirements for delivery**
pDNA MC DNA	large (5-15 kbp) ds DNA, circular, bacterial vector backbone; minicircle (3-4 kbp) without backbone	Compaction into nanoparticle dimension, Protection against nucleases, Intranuclear delivery
siRNA	small (21-23 bp) ds RNA, can be partly/completely chemically modified to reduce innate immune responses and enhance biostability lower polyplex stability	Stable incorporation into nanoparticle or chemical conjugation to targeting unit, Cytosolic delivery, incorporation of guide strand into the RNA-induced silencing complex
mRNA	medium sized ss RNA, instable, can be partly modified to reduce immunogenicity and enhance stability	Synthetically modifications of the mRNA, binding to the translational machinery
Proteins	Variable in (medium) size, charge/ isoelectric point, hydrophilicity, stability, bioactivity	Extra/intracellular, various organelles, release in bioactive form; carriers need to be adjusted for every protein cargo

bp, base pairs; ds, double stranded; kbp, kilo base pairs; mRNA, messenger RNA; ss, single stranded [15, 93, 275, 276].

The main challenges for successful delivery of all types of cargo are the formation of stable nanoparticles with suitable size, protection of the cargo against destabilization by serum proteins and degradation, a delayed elimination from the blood circulation (renal clearance, liver and spleen uptake) and lack of inflammatory and immune responses. Nanoparticle shielding and targeting ligands were introduced, particle size and colloidal stability of nanoparticles variegated to obtain homing to target tissues, such as tumors via passive targeting and the enhanced permeation and retention (EPR effect) due to vascular leakage, or active transendothelial transport [277, 278]. Within target cells, successful intracellular transport, including endosomal escape, cargo release, cytosolic migration and optionally nuclear import have to be achieved [93, 275, 279]. In the following, chemical evolution-based optimization of nanocarriers is illustrated for the cargos pDNA, siRNA, mRNA, proteins and genome-editing nucleases.

2.3.1 pDNA delivery

A long-term experience with antitumoral pDNA polyplexes is largely based on targeted and surface shielded PEI conjugates. Tumoral delivery of therapeutic agents was enhanced by targeting ligands such as transferrin or EGF and included pDNA encoding TNF-α [143, 148, 280] or sodium iodide symporter (NIS) [149, 281], and tumor regressions were observed in mouse tumor models. In both therapeutic modality, gene transfer to a subpopulation of tumor target cells is sufficient, because the secreted TNF-α may react at neighboring cells (including endothelium), and also NIS enables targeted radionucleotide therapy with a strong by-stander effect on neighbouring untransfected tissue.

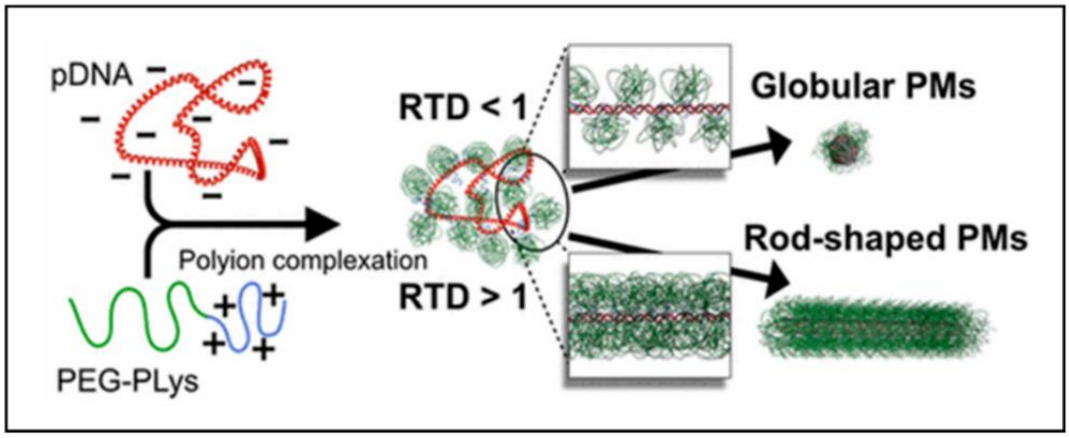

Figure. 9. PEG crowding as decisive factor in pDNA packaging into polyplexes. PM, polymer micelles; RTD, reduced tethering density. Reproduced from Takeda et al. [156] with permissions of American Chemical Society. Copyright 2017.

PEI is an effective pDNA transfection agent but displays significant, molecular-weight dependent cytotoxicity and low degradability. Kazunori Kataoka and colleagues had optimized biodegradable PEG-polyamino acid diblocks (see section 2.2) for pDNA compaction. They observed a higher *in vitro* gene expression with more extended rod-shaped nanoparticles than with compact globular shaped polyplexes [156]. However, a small polyplex size was important for *in vivo* efficiency [154]. The researchers applied a series of PEG-pLys block copolymers with various molecular weights of pLys and PEG segments for pDNA complexation. These studies showed that rod-shaped polyplexes formed when the tethered PEG chains covering pDNA in a pre-condensed state were dense enough to overlap each other (reduced tethering density (RTD) > 1) (see **Figure 9**), whereas globular polyplexes were obtained when PEG segments did not overlap (RTD < 1) [156]. The observations are consistent with related studies using other PEG-polycation polyplexes [282, 283]. Importantly, in a cell-free system the rod-shaped more extended nanoparticles mediated higher gene expression than the globular polyplexes [156].

The lab advanced the pDNA binding carrier structures by designing amidated PEG-poly(aspartic acid) (pAsp) derivatives with good buffering capacity in the endolysosomal range, yielding PEG-pAsp(DET) and PEG-pAsp(TEP) as most effective carriers [161]. For further optimization of *in vivo* delivery, the cyclic RGD peptide was installed as tumor targeting ligand, and cholesterol was attached to the other end of the nanocarrier for improved packaging by hydrophobic stabilization. The

latter step was critical for efficacy and enabled the use of high-molecular weight (20 kDa) PEG, which on the other hand improved polyplex blood circulation. The created cRGD-PEG-pAsp(DET)-cholesteryl polyplexes were tested in a subcutaneous BxPC3 pancreatic cancer xenograft mouse model, achieving improved accumulation at the tumor site. Potent tumor growth suppression was obtained by antiangiogenic sFlt-1 gene transfer [284]. The expression of soluble sFlt-1 exerts antiangiogenesis by trapping angiogenic molecules (VEGF); such a paracrine strategy by-passes the need of transfecting the majority of tumor target cells.

Jianjun Cheng and colleagues developed poly(glutamic acid vinyl-benzylester) pGlu(OBzV) into a library of cationic endosomolytic α-helical pDNA nanocarriers pGlu(OBz-X) [285]. For this purpose, the vinylgroups were oxidized to the benzaldehyde derivatives which were reductively aminated with a mini-library of 31 amines and oligoamines (see **Figure 10**). The nanocarriers were evaluated for pDNA delivery, with the top candidate outperforming the gold standard PEI by 12-fold. Subsequently the delivery system was also applied for Cas9 pDNA/sgRNA co-delivery [286].

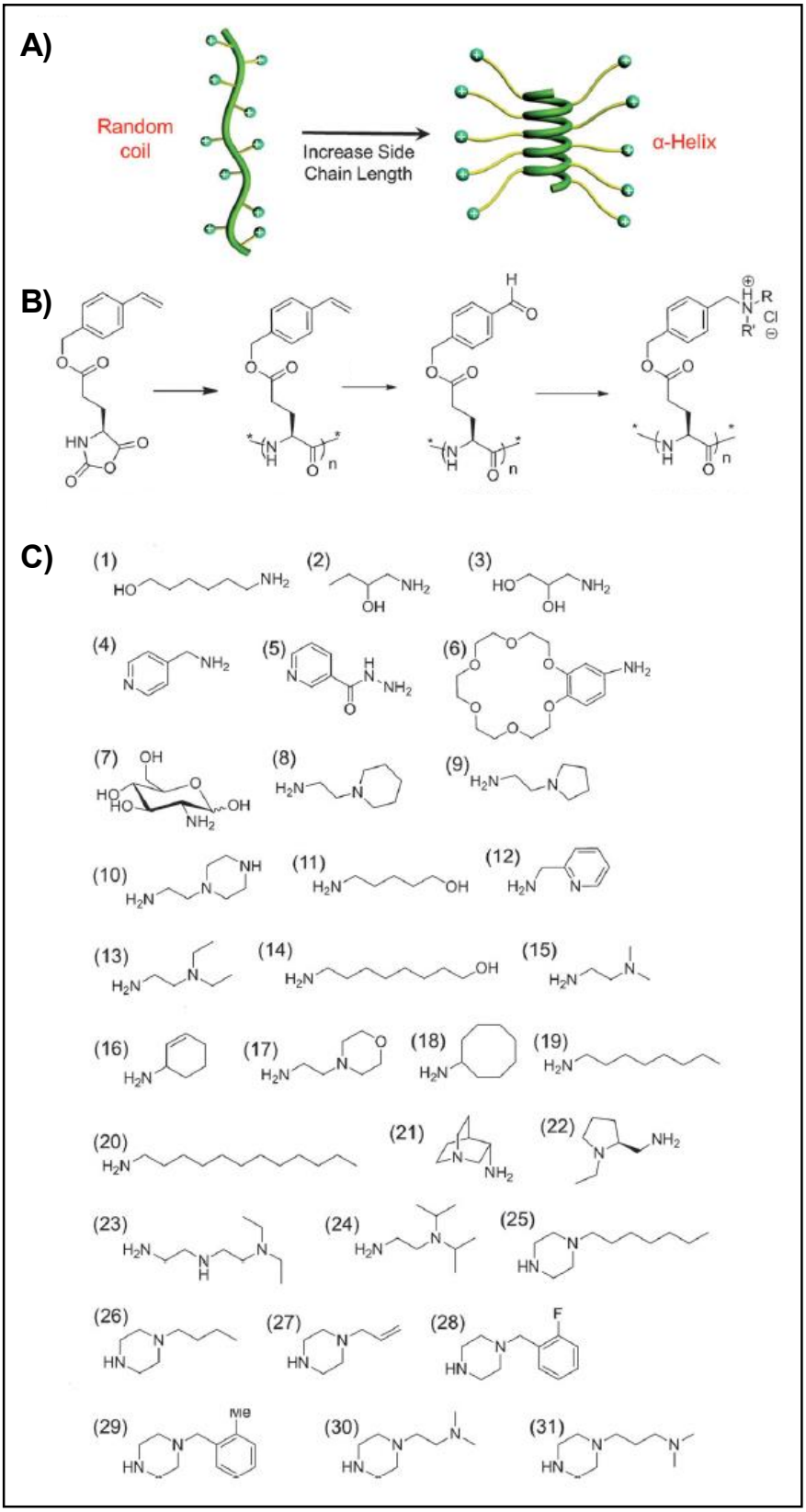

Figure 10. (A) Polypeptide with charged side chains and the random coil to helix transformation in response to elongated side chains. **(B)** Synthesis of polypeptides. **(C)** Amines used to synthesize pGlu(OBz-X). Reproduced from Gabrielson et al. [285] with permission. Copyright 2012 WILEY WILEY-VCH Verlag GmbH & Co. KGaA, Weinheim.

Jordan Green and coworkers extended the combinatorial design of poly(β-amino esters) (PBAEs, see section 2.4) for synthesis of multifunctional branched poly(ester amine) quadpolymers (BEAQs). Synthesis occurred via A2 + B2/B3 + C1 Michael addition, starting from small acrylate and amine monomers, followed by subsequent capping with amine-containing small molecules [287]. These BEAQs present advantages over previously reported linear PBAEs, particularly for volume-limited applications. A moderate degree of branching was favorable for effective pDNA transfer to retinal pigment epithelial cells. Structural properties, including good endosomal buffering capacity and sufficient tertiary amine content, correlated with gene transfer efficacy.

In optimizing sequence-defined OAAs (see section 2.5) for pDNA delivery, Petra Kos et al faced the dilemma between polyplex shielding and pDNA compaction. In their case, co-formulation of ligand-PEG-two-arm OAAs with PEG-free three-arms was critically required for polyplex stabilization and functional *in vivo* delivery into tumors [244]. Furthermore, the presence of a tumor–targeting ligand (such as c-Met binding peptide) as well as the presence of protonatable histidines in the carrier backbone was strictly necessary for the *in vivo* gene transfer. Based on this concept, c-Met targeted pDNA polyplexes were able to systemically deliver NIS pDNA into a subcutaneous HUH7 hepatocellular carcinoma xenograft in mice [245]. Functional NIS expression was detected using the diagnostic radioisotope iodide ^{123}I by scintigraphy. Three cycles of intravenous polyplex and therapeutic radioiodide administration retarded the tumor growth and prolonged the survival of mice.

By introducing the antitumoral cascade targeting ligand peptide I_6P_7, Rongqin Huang and collaborators generated glioma-targeted pDNA polyplexes [247]. The interleukin-6 peptide fragment I_6P_7 provides multiple functions, including blood-brain-barrier crossing, glioma-targeting, and direct tumor-inhibition by binding the IL-6 receptor without cellular activation. Intravenously applied I_6P_7-Stp-His/pDNA polyplexes were delivered into orthotopic U87 glioma in the mouse xenograft model; delivered pDNA encoding inhibitor of growth 4 (pING4) was successfully expressed in the glioma, which significantly prolonged the survival time of treated mice.

Nonviral pDNA carriers have also been developed for indications different from cancer. Zheng-Rong Lu and collaborators had optimized the cationizable lipopeptide like carrier ECO as pDNA and siRNA carrier (see also next section 3.2) in several chemical

evolution cycles by SPS. They applied ECO/pDNA nanoparticle for gene therapy of inherited retinal disorders by subretinal injection in genetic mouse models of Lebers' congenital amaurosis (LCA) [288] and Stargardt disease (STGD) [289], demonstrating therapeutic effects in these forms of blindness.

2.3.2 siRNA delivery

Small interfering RNA (siRNA, 2 nm helix diameter, 7 nm length, 21-23 base pairs) presents a far smaller double-stranded nucleic acid than pDNA. This opens a far broader range of formulation options, with small sizes of chemically modified small conjugates of free siRNA, unimolecular siRNA nanoplexes (with, for example, an only 1 nm thick coat), to various liposomal or polymer micelle formulations, which usually are in the size range of around 100 nm. Obviously, a greater flexibility provides an opportunity [57, 81, 290], but also a challenge for chemical evolution processes: should siRNA be chemically further minimized into drug-like molecules (to better diffuse into tissues)? Or should multiple siRNAs be formulated into larger virus-like delivery nanoparticles (to provide disease-focused localization) [291]? Quo vadis? Which direction to go? Irrespective of these challenging alternative choices, the siRNA drug concept has already proven to be a success story. Within two decades since discovery of the RNAi mechanism, the first siRNA drug product, Patisiran (Onpattro™) [22], reached the medical market in 2018, for therapy of hereditary transthyretin (TTR)-mediated amyloidosis (ATTR amyloidosis). Mutations in the TTR gene (producing a tetrameric protein, also called pre-albumin) result in tetramer destabilization, amyloid fibrils and plaques, and rapidly progressive, debilitating morbidity (polyneuropathy, cardiomyopathy) with high mortality. Patisiran contains siRNA directed against TTR mRNA formulated into 60 – 100 nm PEGylated LNPs. The design of LNPs for delivery is based on a long-term development by Cullis and collaborators [41, 71]. The formulation contains four lipidic excipients: cholesterol, distearyl phosphatidyl choline; DLin-MC3-DMA as special cationic lipid, consisting of a dimethylamino-propionic ester of a carba-analogue of di-linoleic acid glyceride; and the sheddable PEG derivative PEG2k-C-DMG. The cationic lipid DLin-MC3-DMA supports nucleic acid incorporation and endosomal membrane destabilization. The dimyristylated PEG agent stabilized the formulation but is gradually shed off in blood circulation; this triggers incorporation

of an apolipoprotein E corona [292], which results in targeted delivery to the LDL receptor and subsequent gene silencing in liver hepatocytes.

Alternative nanoformulations include siRNA conjugates with cholesterol [293], which enhanced the biodistribution to a series of tissues. More recently, conjugates with tri-(N-acetyl-galactosamine)-PEG ligand were designed for targeting the hepatocyte-specific asialoglycoprotein receptor (ASGPR); combined with complete chemical modification of siRNA backbone, upon administration via the subcutaneous route this opened another very potent way for liver-specific RNA interference therapy [82, 83]. ASGPR-targeted siRNA-PEG-GalNAc conjugates are currently evaluated in several advanced clinical studies with target genes being located in liver hepatocytes. The first subcutaneous siRNA-PEG-GalNAc conjugate product Givosiran, targeting aminolevulinic acid synthase 1 (ALAS1) for the treatment of acute hepatic porphyria, received market approval in November 2019. Gene silencing of ALAS1 reduces build-up of neurotoxic aminolevulinic acid (ALA) and porphobilinogen (PBG) metabolites [294].

Further chemical evolution of LNP formulation focused on higher potency at low doses, thus enhancing the biocompatibility at therapeutic dosage. By screening combinatorial libraries Daniel Anderson, Robert Langer and colleagues had identified cationic lipidoids such as 98-N12-5 [198, 200] or C12-200 [199, 201], which as part of siRNA LNP formulations were able to mediate *in vivo* gene silencing in mouse liver; in case of C12-200 efficient gene silencing was seen at doses below 10 µg/kg. Hideyoshi Harashima and coworkers invested efforts in optimizing pH-responsive cationic lipids as well as active targeting strategies beyond the liver [295, 296]. In recent work they systematically derivatized the hydrophilic head group and hydrophobic tails of YSK12-C4, a pH-sensitive cationic lipid that was previously developed in their laboratory. Studies revealed that hydrophilic head significantly affected the apparent pKa of the final LNP product, which is a key factor in both intrahepatic distribution and endosomal escape. In contrast, the hydrophobic tail strongly affected intrahepatic distribution without depending on apparent pKa. A structure-activity relationship study enabled the selection of a potent LNP composed of a pH-sensitive cationic lipid CL4H6 that showed efficient gene silencing at very low dose (50% silencing at 2.5 µg/kg), biodegradability and good biocompatibility. Compared to the previously developed LNPs, a superior efficiency for endosomal escape, cytosolic release and *in vivo* gene silencing was

observed [297]. Furthermore, the same research group developed tumor-targeted siRNA LNP formulations. They compared RGD peptide-modified lipid nanoparticles (RGD-LNPs) with analogous PEG-LNPs in a lung tumor metastasis model. Accumulation of PEG-LNPs in the tumor-bearing lung was lower than that for the RGD-LNPs. Intravenous administration of siRNA RGD-LNP induced gene silencing in the metastasized but not the normal lung. RGD-LNP of antiangiogenic siRNA against DLL4 greatly prolonged the survival of tumor mice [298].

Existing LNP and GalNAc conjugate technologies appear to be suitable for medical developments where the target cells are liver hepatocytes. For systemic targeting other tissues and organs, delivery technology still needs to be explored and optimized. As a significant step towards therapy, tumor-targeted siRNA polyplexes have already been evaluated in first clinical studies in cancer patients. The nanoparticles were based on transferrin-coated cyclodextrin-oligocation for active targeting the transferrin receptor. Complexes of siRNA against the M2 subunit of ribonucleotide reductase demonstrated gene silencing (and target protein reduction) in distant patient tumor tissue [152].

Zheng-Rong Lu and coworkers designed lipo-peptide like cationizable siRNA carriers with endosomal pH-dependent membrane disruptive capabilities, for the intracellular endosomal release of the internalized siRNA. These carriers consist of three domains: cationizable head, amino acid-based linkers including cysteines, histidines or lysines, and two terminal hydrophobic oleic acids. Initial studies (published between 2007 and 2009) identified (1-aminoethyl) iminobis [N-(oleoyl cysteinyl histinyl-1-aminoethyl) propionamide] (EHCO) as potent siRNA carrier, which upon attachment of bombesin or a RGD peptide via PEG spacers triggered receptor-mediated uptake and gene silencing in tumors *in vitro* and *in vivo* [219, 299, 300]. As published in 2013 [220], a new mini-library screen of SPS-prepared lipopeptides was performed to optimize the number of protonable amines and pKa of the cationic domain, the degree of unsaturation of the lipid tail, and the presence of histidines. The histidine-free carriers ECO (bis-oleic acid) and ECLn (bis-linolic acid) mediated the best siRNA silencing activity. Subsequently, ECO was successfully applied in RGD-PEG siRNA nanoformulations for therapeutic tumor-targeting. Intravenous injections of RGD-targeted ECO/sibeta3 nanoparticles reduced MDA-MB-231 breast tumor growth and metastasis [301]. Most recently, the system was used for therapeutic gene silencing of the onco-lncRNA DACR, resulting in reduced tumor growth [302].

In our own optimization of tumor receptor-targeted sequence-defined OAAs (compare section 2.5) for siRNA delivery, two different strategies were pursued. The first strategy aimed at generation of small unimolecular siRNA nanoplexes with a thin coat of ligand-PEG-OAA two arm molecules; nanoplex sizes increased only by 2 nm or 4 nm beyond free siRNA, depending on the length of PEG of 24 or 48 EO units, respectively [303]. Nanoplexes required stabilization by cysteine-based disulfide bridges within the OAA coat; furthermore, siRNA conjugation with an endosomal escape peptide (INF7) was strictly required for gene silencing efficacy. Folic acid (FolA) [303] or glutaminylated methotrexate [304] were used as targeting ligands. With the latter ligand, which also may act as intracellular dihydrofolate reductase inhibitor, antitumoral activity (50% cures of mice) was obtained after intratumoral administration of siRNA nanoplexes against spindle motor protein EG5 [304]. Systemic administration, however, was ineffective, as the nanoplexes were rapidly cleared via the kidney and could be recovered from the urine of treated mice.

As second strategy, for systemic administration, siRNA polyplexes of sizes around 100 nm were formulated by including non-PEGylated OAAs. For siRNA delivery, polyplex stabilization was required, either by defined cysteine-based disulfide cross-links and /or the incorporation of hydrophobic lipid domains [238]. Including terminal tyrosine tripeptide sequences for stabilization via π-π interaction resulted in further improvement [305]. A mini-library screen of lipo-OAAs for the effect of incorporated fatty acids on efficacy and biocompatibility revealed an impact on polyplex stability, endosomolytic activity and also cytotoxicity. The cytotoxicity issue was resolved by incorporation of designer cleavage sites into the lipo-OAA carrier, such as an SSBB disulfide building block between cationic and lipid domain, which are cleavable in the cytosol [306], or lysosomal cathepsin B cleavage sites for intended lysosomal degradation [90].

For incorporation of active targeting function, targeted combination polyplexes (TCPs) were generated [307]. In the siRNA polyplex formation, a targeted FolA-PEG two-arm or four-arm OAA was reacted with a non-PEGylated three-arm OAA. The reaction was performed by fast directed coupling of thionitrobenzoic acid (TNB) cysteine-modified OAA with the free terminal cysteine thiol groups of the other OAA via disulfide formation. In a variation of the strategies, Dian-Jang Lee et al designed targeted lipopolyplexes (TLPs) by combination of the targeted FolA-PEG two-arm with a T-

shaped lipo-OAA [308]. For both TCP and TLP, optimized combinations were tested *in vivo* and demonstrated gene silencing in a subcutaneous L1210 mouse leukemia model after intravenous administration.

Well-compacted surface-shielded siRNA lipopolyplexes were also formulated in an alternative mode, by pre-formation of compacted siRNA core complexes followed by post-modification with a PEG- targeting ligand shell. FolA, transferrin, or an EGFR binding peptide was immobilized via a cysteine-based linkage [309-311]. More recently, the strategy was expanded to the use of orthogonal, copper-free click chemistry. Lipo-OAAs were synthesized with a terminal azido function, and formulated siRNA lipoplexes were treated with DBCO-PEG-ligands. By these means, FolA-targeted siRNA nanoparticles were generated, which upon intravenous application presented tumor-targeted EG5 gene silencing and antitumoral action in combination with the antitumoral natural product pretubulysin [312]. Analogously, EGF receptor-targeted lipopolyplexes were formulated for EG5 siRNA/methotrexate co-delivery [313] or EG5 siRNA/pretubulysin co-delivery [314], demonstrating clear combination effects as tested in EGFR positive tumor cell cultures. As a novel type of combination therapy, a dual antitumoral conjugate of EG5 siRNA with the pro-apoptotic peptide KLK was designed [315]. For tumoral delivery, this bioreducible siRNA conjugate was formulated in a T-shaped azido-lipo-OAA and click-coated with DBCO-PEG-AP1 as ligand construct for targeting the IL4 receptor [315]. Both mitochondrial destabilization by cytosolic released KLK peptide and EG5 silencing triggered mitotic block was demonstrated.

An extension of this ‘chemical evolution’ screen for siRNA delivery carriers [316] addressed the question about a possible beneficial role of histidines. As reported above, histidines as endosomal buffering components had been found beneficial for pDNA delivery. However, histidines (which carry no charge at physiological pH), may also reduce polyplex stability. For pDNA polyplexes which (due to the far larger number of base pairs) are more stable than siRNA polyplexes, this usually does not present a problem. For example, pDNA/PEI polyplexes require >1M salt for dissociation, whereas PEI polyplexes of siRNA dissociate already with 0.5M sodium chloride [317]. For siRNA polyplex performance, incorporation of histidines can be a balancing act. Extra measures have to be taken for polyplex stabilization to counteract an unfavorable histidine effect. In case of T-shaped lipo-OAAs with a short cationizable Stp backbone

without and with incorporated histidines, the histidine-free carrier displayed a better gene silencing performance [315]. Analogous siRNA lipo-polyplexes formed with lipo-OAAs containing an extended Stp backbone (40 aminoethylene nitrogens) were found to be more stable, and incorporation of alternating histidines further improved gene silencing efficiency [318]. The observations are well consistent with published data. For siRNA carriers like ECO that contain only short cationic domains but lytic fatty acid domains, histidines might be dispensable, as reported by Lu and collaborators [220]. Histidines integrated into lipid-free larger cationic oligolysine peptides, such as the highly effective gene silencing H3K8b peptide, are required for endosomal escape activity [213].

2.3.3 mRNA delivery

Therapeutic mRNA delivery has become increasingly attractive in recent years. It has a great potential for addressing medical applications like immunotherapy, gene editing, regenerative medicine and vaccines [319, 320]. To improve the stability of the nucleic acid under physiological conditions and to decrease the immune response, synthetically modifications of the rather unstable mRNA are necessary. In addition, the development of efficient delivery carriers for mRNA is required to protect the cargo as well as for effective cellular uptake and cytosolic release [320]. The new therapeutic procedure offers new challenges and opportunities for the delivery of polymers. Because of the poor pharmacokinetic properties of mRNA, Rudolf Zentel and colleagues developed decationizable block copolymers containing disulfide-linked primary amines (**Figure 11A**) that form polyplexes with negatively charged mRNA. Different translation functionalities and polyplex structures were found depending on the composition of the block copolymers. They noted mRNA release of the nano-sized polyplexes in the reducing environment of the cytosol [321]. Christian Dohmen and collaborators evaluated cationic lipids and polymers formed with different defined oligoamines. They found that a modified PEI-like carrier with an (aminoethylene-aminopropylene-aminoethylene) sequence (**Figure 11B**) is more efficient than aminoethylene or aminopropylene based carriers, and leads to enhanced mRNA transfection [322].

Several researchers developed different degradable polymer-lipid nanoparticles for systemic delivery of mRNA to the lung [319, 320, 323]. James Kaczmarek et al formulated mRNA nanoparticles with degradable poly(β-amino ester)-lipid (PBAE-lipid) for functional delivery to the lungs. Through coformulation with lipid-PEG they obtained serum-stable nanoparticles with increased *in vitro* potency and most potent *in vivo* mRNA delivery to the lungs [323]. By means of polymer synthesis and nanoparticle formulation the potency of the degradable, polymeric nanoparticles can be increased. They also demonstrated the ability of particles to functionally deliver mRNA to pulmonary endothelial and immune cells by using Cre reporter gene mice [320]. Moreover, a combinatorial polyester library (**Figure 11C**) containing 480 distinct chemical structures was generated by Daniel Siegwart and coworkers with the aim to identify mRNA carriers. Surface shielding with 5% pluronic F127 improved the stability of mRNA polyplexes and enabled predominant lung gene transfer upon intravenous application in mice [319].

To enable tissue-selective mRNA delivery, novel ionizable amino-polyesters were designed by Piotr Kowalski et al (**Figure 11D**). Carriers were synthesized by ring opening polymerization of lactones with tertiary amino-alcohols and applied for mRNA formulation into LNPs. Effective mRNA expression in lung endothelium, liver hepatocytes, and splenic antigen presenting cells was found [324]. Standard LNPs as developed for the siRNA therapeutic Patisiran (see section 3.2) show effective hepatocyte delivery by LDL receptor mediated uptake; the small fraction (~1%) of cargo released into the cytosol is an early event (5-15 minutes after endocytosis [325, 326]). The efficiency on other tissues and cell types is highly variable. Recently, Arwyn Jones, Marianne Ashford and colleagues evaluated intracellular trafficking of mRNA LNPs in 30 different tumor cell lines, comparing highly transfecting cell lines with moderately or poorly transfecting cell lines [327]. High-transfecting cells showed rapid LNP uptake and trafficking through an organized endocytic pathway to lysosomes or rapid exocytosis was observed in well transfectable cells. Low-transfecting cells displayed slower endosomal trafficking of LNPs to lysosomes and defective endocytic organization and acidification. In line with [325, 326], efficient LNP transfection relies on an early and narrow endosomal escape window.

Wenfei Dong and collaborators generated stable polymeric nanoformulations by complexing mRNA with poly(N-isopropylacrylamide) (PNIPAM)-pLys–thiol (**Figure**

11E) and cRGD-PEG-pLys-thiol for systemic delivery to tumors. Thermo-responsive PNIPAM was incorporated for stabilization and mRNA protection during systemic circulation, redox-responsive disulfide linkages for extracellular stabilization and intracellular mRNA release. Furthermore, the PEG-conjugated cRGD ligand on the surface of the nanoformulation improved tumor accumulation and achieved potent gene expression of the loaded mRNA via integrin-facilitated cellular uptake [328].
Hydrophobic polyplex stabilization was also essential in the work of Kataoka and coworkers for optimizing systemic mRNA delivery by PEG-pAsp(TEP) block copolymers (**Figure 11F**). A cholesterol moiety had to be attached to the ω-terminus of the copolymer for enhanced blood retention upon intravenous administration. The i.v. administration of PEG-pAsp(TEP)-Chol polyplexes for the delivery of mRNA encoding the anti-angiogenic protein sFlt-1 resulted in a remarkable growth inhibition of pancreatic cancer in a subcutaneous inoculation mouse model [163].

Amphiphilic charge-altering releasable transporters (CARTs) are degradable materials for mRNA transfer and have been developed by Robert Waymouth and coworkers (**Figure 11G**). The step-economical synthesis of CARTs was achieved by an organocatalytic oligomerization. These transporters are capable of first building CART / mRNA complexes, protecting and delivering mRNA into cells. Subsequently CARTs undergo a degradative intramolecular rearrangement, degrading to neutral small molecules by controlled self-immolation, resulting in the release of mRNA into the cytoplasm and translation into protein [329]. Evolutionary optimization was possible using CART libraries incorporating different lipidic side groups. CART / mRNA complexes were demonstrated to successfully transfect lymphocytes *in vitro* and in mice *in vivo* [330]. Upon intratumoral injection, they can effectively trigger antitumor immune responses [331].

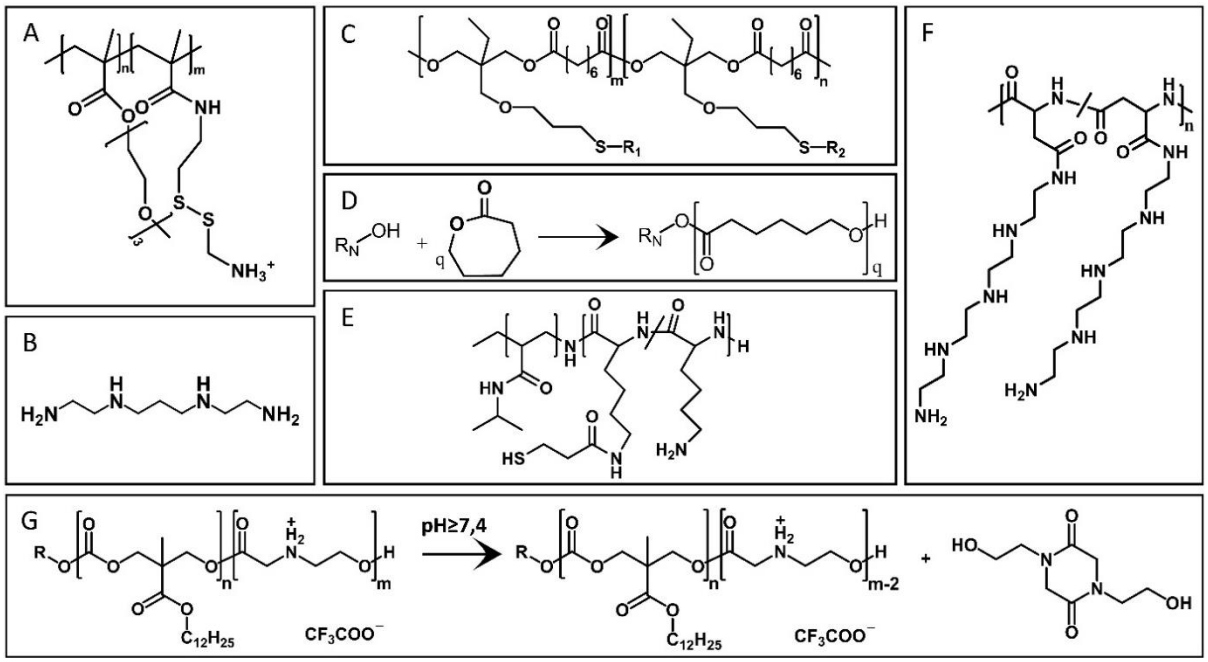

Figure 11. mRNA delivery carriers. **(A)** Reductive decationizable block copolymers [321]. **(B)** Ethylenimine-propylenimine-ethylenimine (EPE) sequence motif as superior building block [322]. **(C)** Functional and degradable poly(trimethylolpropane allyl ether-co-suberoyl chloride) library [319]. **(D)** Ring opening polymerization of lactones initiated by a tertiary amino-alcohol [324]. **(E)** PNIPAM pLys(SH) [328]. **(F)** PEG-pAsp(TEP) block copolymers [163]. **(G)** Biodegradation of a CART copolymer [329].

2.3.4 Intracellular protein delivery

Extracellularly active recombinant therapeutic proteins such as growth factors and antibodies have already captured a major fraction of the pharmaceutical market [332]. Delivery of proteins to intracellular target locations is a recent emerging task, fueled by developments of nanobodies with intracellular molecular targets or high-precision DNA endonucleases such as Cre recombinase, zinc finger nuclease, TALENs, or Cas9 protein for genome editing (see also section 3.5). In this novel research area, numerous different delivery approaches have been recently reported [333, 334]. These include physical incorporation into degradable hydrogels [335-339] or lipidic carriers, conjugation or complexation with polymers such as phenyl-biguanide modified [340] or phenyl-boronic acid modified [341] polycations (**Figure 12**), targeting ligands or other functional transduction domains [342-346], or covalent reversible recharging followed by electrostatic polycation complex formation [347-349]. In contrast to the previously discussed cargos DNA, siRNA, and mRNA, which are physicochemically uniform

within their compound class, protein cargos may very much differ in size, charge/ isoelectric point, hydrophilicity and stability. When screening libraries of sequence-defined OAA oligomers for delivery of different protein cargos (such as enhanced green fluorescent protein (eGFP), LacZ, RNase, or nanobodies), our own learning experience has been that different carriers or carrier concepts were best for the different protein cargos. In the nutshell, for every protein cargo an independent "chemical evolution search" for the most suitable nanocarrier has to be performed.

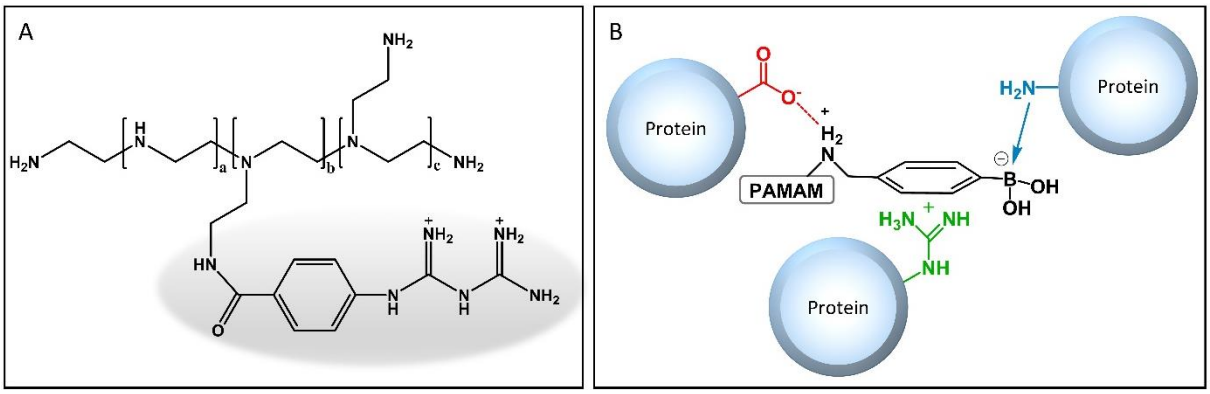

Figure 12. Polycationic protein carriers. **(A)** Phenyl-biguanidine-benzoic acid (PBGBA) modified branched PEI (25 kDa) containing in average 60 PBGBA per bPEI [340]. **(B)** Protein interactions with phenyl-boronic acid modified cationic G5 PAMAM dendrimer via nitrogen-boronate complexation, cation-π and ionic interactions enables dendrimer binding with either negatively or positively charged proteins [341].

A main delivery effort is the specific attachment of the protein formulation to the target cell, in order to trigger cellular uptake by endocytosis or related mechanisms. Subsequent release to the cytosol is the next challenge, followed by intracellular release at the target location (cytosol, nucleus) in bioactive form. Thus, in our work, proteins were bioreversibly conjugated with sequence-defined carriers. Optionally, linkers were used that are removed traceless under endosomal acidic conditions [350, 351]. Alternatively, redox-sensitive disulfide linkages were applied for bioreduction in the cytosol [352, 353].

Screening a sequence-defined oligoaminoamide (OAA) library for eGFP protein delivery presented a tetra oleoyl-modified protonatable OAA containing a folate-PEG domain for receptor targeting and nanoparticle shielding, and a protein disulfide

linkage, as the best intracellular eGFP delivery agent into folate receptor-expressing tumor cells [353] (**Figure 13A**). The formulation consisted of small worm-like nanomicelle rods with approximately 10 nm in diameter and 30 nm hydrodynamic diameter. Formulation of the bioreversible carrier conjugates with helper lipid resulted in formation of 50 nm proteoliposomes with similar protein delivery efficiency [354]. Replacing eGFP by antitumoral RNase A resulted in highly effective cytosolic delivery and the desired tumor cell killing.

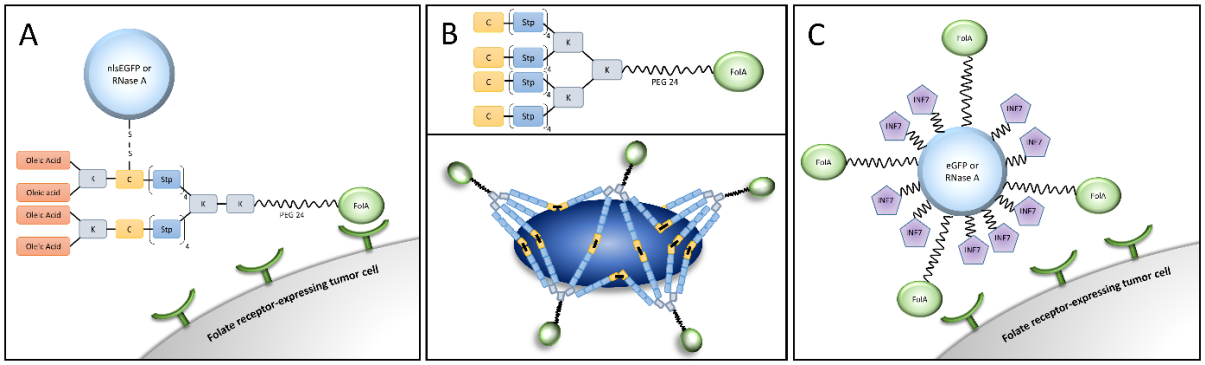

Figure 13. Protein delivery strategies by solid-phase synthesized nanocarriers. **(A)** Bioreversible protein disulfide linked lipo-OAA [353, 354]. **(B)** Folate-PEG linked four-arm OAAs for bioreversibly caging nanobody cargos [355]. **(C)** Traceless reversible protein conjugation with a targeting ligand (folate-PEG) and an endosomal escape peptide (INF7) [356].

Interestingly, when screening the library for intracellular delivery of very small (2 nm) nanobodies, the disulfide-linked lipo-OAA was not the most suitable delivery solution. Instead, a folate-PEG linked four-arm OAA containing a terminal cysteine on each arm (**Figure 13B**) was found as most effective, surprisingly without covalent linkage to the nanobody protein [355]. The very small size of the nanoplexes and the strict requirement of the cysteines on the carrier with disulfide forming capacity is consistent with bioreversible caging of the nanobodies within a disulfide cross-linked OAA net coating the nanobody. Nanoplexes were internalized via receptor-mediated endocytosis and partly released into the cytosol. Bioreductive cytosolic release of nanobodies was verified via intracellular staining of nanobody target proteins in living cells. **Figure 13C** illustrates the third protein delivery strategy as evaluated in our

group. In contrast to the other approaches, carrier-free delivery formulations of eGFP or RNase A were developed by direct, traceless reversible protein conjugation with folate-PEG targeting ligands and influenza-derived endosomal escape peptide (INF7) functionalization [356]. Folate ligand incorporation was required and sufficient for cellular uptake. For the smaller and basic RNase A protein, additional INF7 functionalization was required and sufficient for cytosolic delivery and potent cell killing; for the larger non-basic eGFP protein, cytosolic delivery was limited despite INF7 incorporation. In another complementary approach, Ulrich Lächelt and colleagues generated multifunctional hybrid nanosystems by coordinative self-assembly of His-tagged proteins (such as H_6-eGFP or H_6-transferrin), apoptotic peptides, or mitochondrial cytochrome c onto metal−organic frameworks (MOFs) [357]. Intracellular delivery and cell killing by the apoptotic cargos was observed.

In summary, on the one hand, the biochemical difference of proteins enables the exploration of many different delivery strategies; on the other hand, generic protein delivery solutions are futile, and individual protein cargos request individual optimizations by chemical evolution.

2.3.5 Delivery of genome-editing nucleases

Over the past several years great advances in precise genome modifying nucleases such as zinc finger nucleases (ZFN), transcription activator-like effector nucleases (TALEN), meganucleases (MN), or CRISPR Cas9 / sgRNA [7, 358] and others have opened a new era for genetic manipulation of model organisms [359] as well as the development of gene therapeutics [360-362]. For this purpose, nonviral vectors offer a broad and safer alternative to viral vectors, to overcome viral vector problems such as high occurrence of preexisting or induced immune response, or unintended sustained expression of programmable nucleases, which might lead to off-target cleavage. Transient expression profiles of nonviral vectors, which usually present a disadvantage for treatment of most genetic diseases, can be advantageously applied for transient expression of genome–modifying nucleases. Different intracellular delivery modalities for the genome-editing agents can be pursued: as gene expression constructs based on pDNA [363] or mRNA [362]; as recombinant protein, or as Cas9 protein/sgRNA ribonucleoprotein formulation [260, 361]. Especially, the easy design of the CRISPR-

associated protein 9 (Cas9) / single guide RNA (sgRNA) system has boosted genome editing strategies. CRISPR/Cas9 is considered to be an innovative tool for highly efficient genome engineering [361, 363, 364]. Therefore development of efficient and safe delivery technologies, as also reviewed in this ADDR issue [365-367], is of utmost importance.

Kam Leong, Jianjun Cheng and collaborators applied the cationic α-helical polypeptide poly(γ-4-((2-(piperidin-1-yl)ethyl)aminomethyl)benzyl-L-glutamate) which was developed out of a library screen (see **Figure 10**) for the co-delivery of sgRNA and pDNA expressing Cas9. PEGylated nanoparticles were obtained by including PEG-polythymidine$_{40}$ in the polyplex formulation. Single or multiplex gene editing was performed *in vitro* with an up to 47% efficiency. *In vivo* targeting gene deletion of polo-like kinase 1 (Plk1) suppressed the growth of HeLa tumors in mice and prolonged the animal survival rate [286].

Junjui Huang and colleagues developed a new strategy for the delivery of large pDNA coding for Cas9 and sgRNA for editing of two different genes (β-globin, rhomboid 5 homolog 1) by using PEI-β-cyclodextrin as cationic polymer to form nanocomplexes [363]. Zheng-Rong Lu and coworker optimized their bis (oleoyl-cysteine) oligoaminopeptide system ECO (see sections 3.1 and 3.2) by introducing triamino-triethylamine as a novel cationizable head group and optionally additional linker lysine or histidines. ECO and iECO (without any further linker amino acids) presented the most effective agents for intracellular delivery of pDNA expressing CRISPR/Cas9, resulting in genome editing [368].

Gleb Sukhorukov and colleagues reported on pDNA-based delivery of CRISPR Cas9 components, improved by polymeric and hybrid microcarriers made of degradable polymers coated by a biocompatible shell of silica [369]. Using a combinatorial design of poly(β-amino esters) (see section 2.4), Jordan Green and colleagues had developed branched ester-amine quadpolymers (BEAQs) for pDNA transfer (see section 3.1).To co-encapsulate and deliver Cas9 pDNA and sgRNA in the same biodegradable nanoparticle system, Green and collaborators extended the chemical evolution to the design of reducible BEAQs (rBEAQs), with a library varying the polymer branching, reducibility and hydrophobicity. These variations resulted in 40% Cas9-facilitated gene knockout in human embryonic kidney 293T cells, which also confirms the presence as well as the bioactivity of the two components in the same cell [370].

mRNA delivery enables high and transient expression of genome-modifying nucleases. Anthony Conway et al co-formulated LNPs with a novel ionizable lipid and mRNA encoding ZFNs. They achieved highly effective *in vivo* genome editing of several therapeutic gene targets such as the TTR or PCSK9 gene in hepatocytes [371]. Standard LNPs (see sections 2.4 and 3.2) preferably deliver nucleic acids (such as siRNA or mRNA) into liver hepatocytes. James Dahlman and coworkers applied their high-throughput barcode-based technology FIND (see section 2.6) to measure efficient LNP-based *in vivo* delivery mRNA and sgRNA into multiple organs. In this directed evolution process, they found more than 250 LNPs delivering mRNA to multiple cell types. They also identified two LNPs, 7C2 and 7C3, that efficiently deliver sgRNA and mRNA to endothelial cells. The LNP 7C3 was found to deliver Cas9 mRNA and sgRNA to splenic endothelial cells as efficiently as to hepatocytes, opening the opportunity for endothelial cell gene editing [268]. The team of Daniel Siegwart designed zwitterionic amino lipids nanoparticles for delivery of Cas9 mRNA plus sgRNAs. Co-delivery of Cas9 mRNA / LoxP sgRNA via an intravenous route resulted in rescued tdTomato fluorescent protein expression in the liver, lung, and kidneys of Lox-Stop-Lox tdTomato transgenic mice [372].

As the CRISPR-Cas9 protein activity is required only for the short period of the genome editing process, direct intracellular protein delivery into the cell nucleus is a further attractive option, preferable in form of an active Cas9 protein/sgRNA ribonucleoprotein complex. Delivery of protein cargos across cell membranes as well as endosome escape is a persistent challenge, which has to be met by strategies as outlined in section 3.4. Jennifer Doudna and colleagues designed CRISPR-Cas9 protein conjugates, harboring N-acetylgalactosamine (GalNac) trimers as targeting ligands to achieve effective ASGPR-mediated endocytosis into hepatocytes for liver-specific genome editing [373]. They could demonstrate gene editing in HepG2 cell culture when co-applied together with an endosomolytic peptide ppTG21.

David Liu and collaborators developed protein delivery for Cre recombinase, TALE, or Cas9 nuclease by conversion into negatively supercharged proteins followed by complexation with standard cationic liposomes. Supercharging was achieved by recombinant fusion with other negatively charged proteins or, in case of Cas9, by loading with the negatively charged sgRNA [374]. Subsequently the same research group applied bioreducible lipid carriers for improved intracellular release of the

ribonucleoprotein agent [375]. Yoo Kyung Kang et al followed a different approach for CRISPR Cas9 protein delivery. They conjugated Cas9 endonuclease covalently with cationic branched PEI, and subsequently used the cationic conjugate for complexation with sgRNA. The formed nanoparticles were applied for genome editing of methicillin-resistant Staphylococcus aureus (MRSA) [361].

Yuan Ping, Yijun Cheng and coworkers had generated effective carriers for intracellular protein delivery by modifying cationic amine-terminated polyamidoamine (PAMAM) generation 5 dendrimers with phenylboronic acid (PBA) residues (see also section 3.4). This modification has made it possible to bind with either negatively or positively charged proteins, assembling them into nanoparticles with potent cytosolic delivery, and maintaining the protein bioactivity after intracellular release. Amongst several protein cargos, they demonstrated efficient Cas9 protein/sgRNA co-delivery and gene editing [341]. Wenfu Zheng, Xingyu Jiang and colleagues reported on genome editing hybrid nanoparticles assembled from a core of gold nanoclusters modified with HIV tat peptide, Cas9 protein and sgRNA expressing pDNA, coated with a PEG-lipid shell. Using sgRNA targeting Polo-like kinase-1 (Plk1), a more than 70% down-regulation of Plk1 was observed in melanoma cells *in vitro* and a 75% suppression of melanoma growth in mice *in vivo* [376].

2.4 Conclusions

Extracellular and intracellular delivery of therapeutic nucleic acids or proteins has been the focus of numerous activities now already over 58 years, since first successful enhancement of poliovirus RNA delivery with basic proteins [377]. About three-thousand gene therapy clinical trials (see http://www.abedia.com/wiley [5]) have been performed, yielding at current stage nine gene therapy products. Numerous chemistry efforts resulted in one siRNA and at least eight synthetic oligonucleotides that were approved as drug products. Further nucleic acid products are in advanced clinical evaluation and will reach the market soon. In all these nanomedicine developments, efficient and safe transfer of the therapeutic nanoagent into the desired target tissues and cells of patients are still the most critical limitation and bottleneck.

Nature designed viruses as highly potent intracellular delivery agents, using a very limited tool-box of chemical building blocks assembled under physiological conditions.

We may learn from the elaborative mechanisms of viruses for infecting cells and might try to imitate them by generating ‘artificial viruses’. However, numerous different classes of viruses with widely different entry mechanisms exist. To paraphrase the quote from Richard Feynman ‘What I cannot create I do not understand’: being fascinated about viruses, does not mean to understand them and being able to create them. Viruses may be regarded as snapshots of natural evolution, and their diverse optimized processes may not be general applicable in an artificial setting. It might be more useful to learn from the general principles of natural evolution and adopt them to artificial synthetic designs and selection processes termed here as “chemical evolution”. In theory, refined synthetic nanocarriers designed from a far broader space of chemical building blocks and synthesized using a whole range of optimized chemical conditions might be more effective in delivery than natural viruses. We ‘simply’ lack the knowledge about their perfect construction plan.

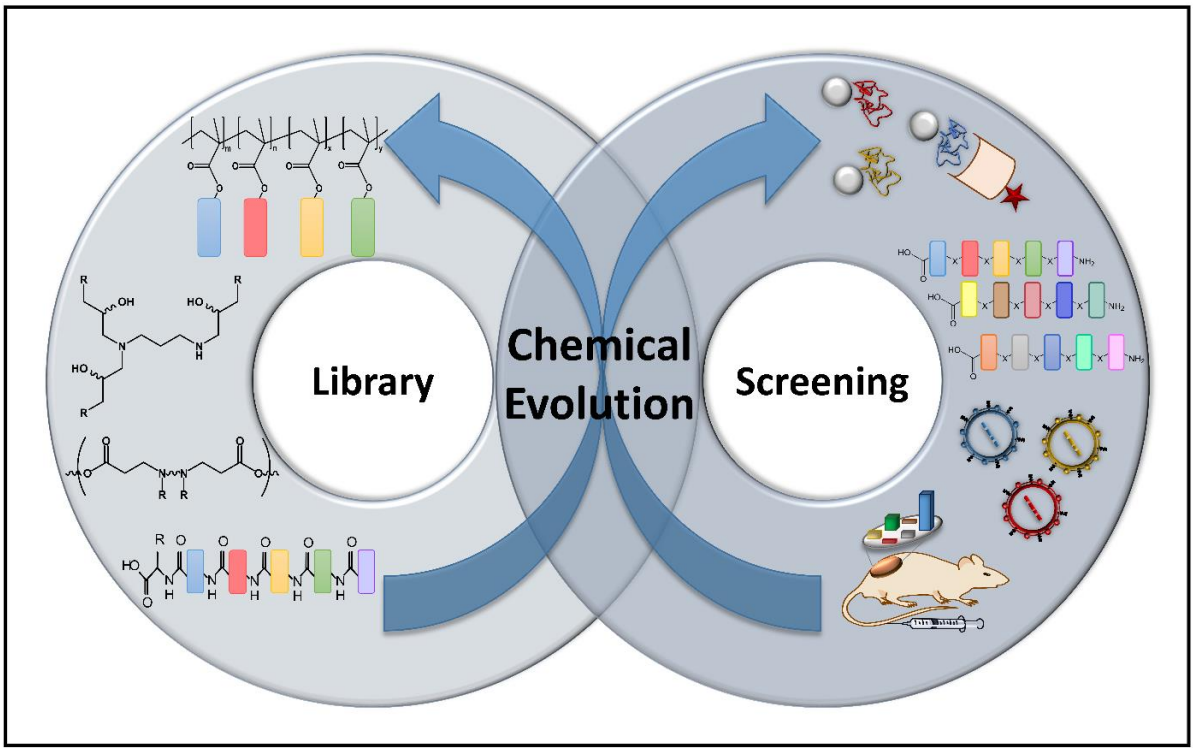

Figure 14. Chemical evolution of nanocarriers. Chemical libraries can be combinatorial or sequence-defined. Screening in appropriate *in vitro* or *in vivo* test models is supposed to (physically or functionally) enrich nanocarriers with favorable properties. Nanocarriers can be identified either directly (by sequence) or indirectly (by barcoding), providing input for the next evolution cycle.

General design principles for synthetic chemical evolution of nanocarriers (**Figure 14**) could be as follows:

i. Generation of libraries of chemical structures defined as retrievable 'Sequences', assembled from a set of chemical building blocks.
ii. Definition as 'Sequences' can be based on the actual sequence of subunits or on integrated (DNA or peptide) barcodes
iii. A 'Sequence' can be linear (as in natural nucleic acids and peptides) or might contain branching (such as in dendrons)
iv. 'Sequences' need to be retrievable in terms of structure identification (high-end analytics from genomics/proteomics) and regeneration of the structure (directed synthesis). The sequence information should be storable *in silico* or on a template (compare with the genetic code in natural evolution).
v. Libraries may be the result of random or designed small changes in sequence of building blocks ('mutations'), or rearrangement of previously found useful domains ('shuffling'). Analogous gene shuffling has been applied in natural and artificial evolution (just for example, note the abundant use of DNA binding zinc fingers in ~2800 human proteins [378]).
vi. Screening of the library has to be performed in appropriate test models, for identification and selection of most suitable nanocarrier candidates as starting point for the next refined library and next evolution cycle.
vii. Different macromolecular cargos (illustrated here for pDNA siRNA, mRNA, proteins, and genome–editing agents) may require different nanocarriers due to their different physicochemical properties and their different intracellular target sites and modes of action.
viii. The different therapeutic modes (transient or permanent action; low or high level of intervention required for therapeutic effects) as well as the various different target organs and cell types, may dictate different requirements to the nanocarrier. Optimization for *ex vivo* delivery into cultured cell most likely will not correlate with optimal *in vivo* delivery. Therefore, applying the most relevant screening model is of utmost importance. Keep in mind: even in the best case, you only get what you actually asked / screened for.

Chemical evolution may involve rational design of improved building blocks based on a better understanding of the delivery processes. It may be fueled by empirical

screening of diverse chemical compound libraries, computational prediction by machine learning algorithms, virtual screening. Chemical evolution can also be regarded as an evolution of knowledge. To illustrate this with one example of endosomal escape: in the early nineties, when this step was discovered to be ineffective in nonviral gene transfer, viral endosomolytic mechanisms were introduced to overcome this bottleneck [58, 379]. It also triggered the search for endosomolytic agents and the discovery that a simple cationizable polymer, PEI, can overcome the endosomal barrier via “The proton sponge: A trick to enter cells the viruses did not exploit“ [380, 381]. A refined molecular understanding of the aminoethylene protonation characteristics was developed and described as the “even-odd” effect [161] which pointed out that not every proton sponge might be applicable. Evolution continues with the notion that different intracellular endolysosomal sorting mechanisms in different cell types and tissues may strongly influence the selection of the most productive mechanism of cationizable nanocarriers [212, 327].

In conclusion, different chemical evolution strategies have already been pursued, as reported herein. Starting from rational design of multifunctional molecular conjugates and block copolymer libraries, screening of combinatorial chemistry libraries or sequence-defined peptide-like macromolecules has been performed, largely *ex vivo* in cell culture, but in part also in more relevant *in vivo* mouse models. DNA- or peptide-barcoded nanoagents, combined with high-end genomics / MS analytics for identification of nanocarriers, present encouraging options for future *in vivo* chemical evolution.

Acknowledgements

We greatly appreciate numerous inspiring discussions and comments by external and internal expert colleagues. We acknowledge the financial support of our research by the German Research Foundation (DFG) project-ID 201269156 SFB1032 subproject B4, SFB1066 project B5, DFG Excellence Cluster ‘Nanosystems Initiative Munich (NIM)’, and the UPGRADE (Unlocking Precision Gene Therapy) project from the European Union’s Horizon 2020 research and innovation programme under grant agreement No 825825. EW and Prof. Yuan Ping (Zhejiang University) appreciate the

award of the LMU Munich and Zhejiang University Partnership Fund for "Synthetic Delivery Carriers for Genome Editing“.

3 Lipoamino bundle LNPs for efficient mRNA transfection of dendritic cells and macrophages show high spleen selectivity

Franziska Haase,[1] Jana Pöhmerer,[1] Mina Yazdi,[1] Melina Grau,[1] Yanira Zeyn,[2] Ulrich Wilk,[1] Tobias Burghardt,[1] Miriam Höhn,[1] Christoph Hieber,[2] Matthias Bros,[2] Ernst Wagner,[1,3,4,] Simone Berger[1,3,4,]**

[1] Pharmaceutical Biotechnology, Department of Pharmacy, Ludwig-Maximilians-Universität Munich, Butenandtstrasse 5–13, 81377 Munich, Germany

[2] Department of Dermatology, University Medical Center of the Johannes Gutenberg University (JGU) Mainz, Langenbeckstrasse 1, 55131 Mainz, Germany

[3] Center for Nanoscience, Ludwig-Maximilians-Universität Munich, Geschwister-Scholl-Platz 1, 80539 Munich, Germany

[4] CNATM - Cluster for Nucleic Acid Therapeutics Munich, Germany

* Corresponding authors

This chapter is adapted from a research paper published in **European Journal of Pharmaceutics and Biopharmaceutics 2024, Volume 194, Pages 95-109 (ref.: [382]), Copyright Elsevier.**

Author contributions

The manuscript was written with collective contributions of all authors. F. Haase: conceptualization, writing, illustrations, review and editing; investigation, mRNA LNP formulation, physicochemical characterization, transfections, J. Pöhmerer and U. Wilk: in vivo experiments, M. Yazdi: FACS analysis and LNP formulation (eGFP), M. Grau: synthesis of the LAF-Stp carrier library, Y. Zeyn: eGFP expression studies, T. Burghardt: synthesis of OleA-carrier, M. Höhn: CLSM imaging, C. Hieber: conceptualization of eGFP expression studies, reviewing, M.Bros: conceptualization of eGFP expression studies, reviewing, E. Wagner: supervision, conceptualization, writing, reviewing, editing, S. Berger: supervision, transfections of immune cells, conceptualization, writing, reviewing, editing. All authors have thoroughly read and unanimously endorsed to the final published version of the manuscript.

Abstract

Messenger RNA (mRNA) is a powerful tool for nucleic acid-based therapies and vaccination, but efficient and specific delivery to target tissues remains a significant challenge. In this study, we demonstrate lipoamino xenopeptide carriers as components of highly efficient mRNA LNPs. These lipo-xenopeptides are defined as 2D sequences in different 3D topologies (bundles or different U-shapes). The polar artificial amino acid tetraethylene pentamino succinic acid (Stp) and various lipophilic tertiary lipoamino fatty acids (LAFs) act as ionizable amphiphilic units, connected in different ratios via bisamidated lysines as branching units. A series of more lipophilic LAF_4-Stp_1 carriers with bundle topology is especially well suited for efficient encapsulation of mRNA into LNPs, facilitated cellular uptake and strongly enhanced endosomal escape. These LNPs display improved, faster transfection kinetics compared to standard LNP formulations, with high potency in a variety of tumor cell lines (including N2a neuroblastoma, HepG2 and Huh7 hepatocellular, and HeLa cervical carcinoma cells), J774A.1 macrophages, and DC2.4 dendritic cells. High transfection levels were obtained even in the presence of serum at very low sub-microgram mRNA doses. Upon intravenous application of only 3 µg mRNA per mouse, *in vivo* mRNA expression is found with a high selectivity for dendritic cells and macrophages, resulting in a particularly high overall preferred expression in the spleen.

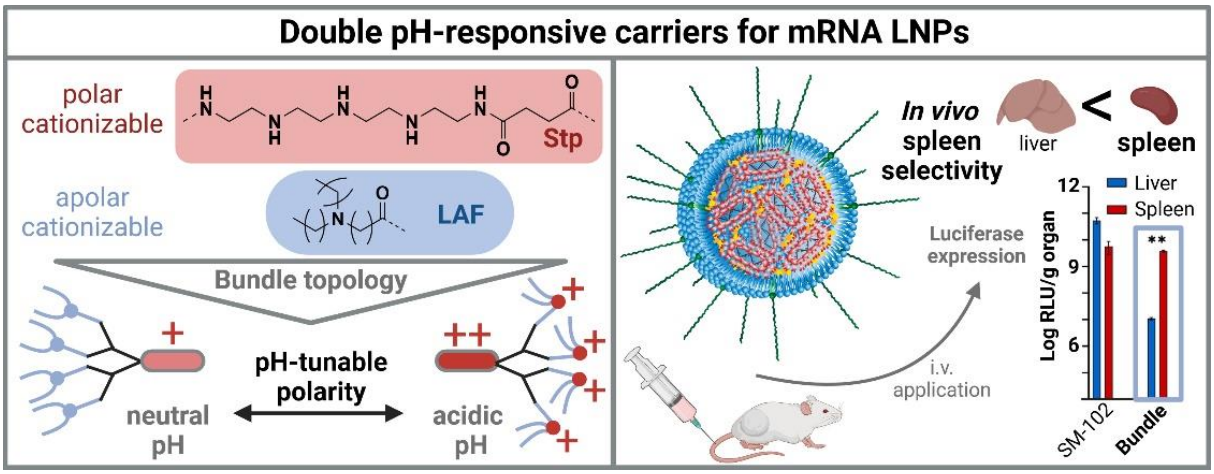

Keywords. mRNA, LNPs, xenopeptides, amino ethylene, lipoamino fatty acid, dendritic cells, macrophages, spleen.

3.1 Introduction

Over the last decades, lipid nanoparticles (LNPs) have evolved to become the most advanced nonviral platform for safe and highly effective nucleic acid delivery *in vivo*, since they can encapsulate and deliver a wide variety of therapeutic agents. The first FDA approved small-interfering RNA (siRNA) drug, Onpattro (Patisiran), is an LNP formulation that after intravenous application delivers siRNA into liver hepatocytes for the treatment of hereditary transthyretin amyloidosis [383]. More recently, messenger RNA (mRNA) LNPs have gained importance as intramuscularly applied vaccines in the context of the COVID-19 pandemic [384] and for other vaccination directions, such as antitumoral immunotherapy [385]. In addition, other work uses LNPs for the co-delivery of different nucleic acid molecules, such as CRISPR-Cas9 mRNA and single guide RNA to the liver, as evaluated in a recent clinical study for the treatment of transthyretin amyloidosis [386].

LNPs typically consist of four lipidic components: cholesterol, phospholipids, polyethylene glycol (PEG)-lipids, and cationizable lipids [387]. These components enable monodisperse particle formation and high encapsulation efficiency of nucleic acid, improve particle stability, and promote endosomal escape of nucleic acid after cellular uptake via endocytosis. The main focus in LNP research is the optimization of ionizable lipids since these are mainly responsible for efficient complexation of the negatively charged nucleic acid and endosomal escape after cellular uptake. Most recently, LNP optimization through variation of phospholipids, PEG lipids, replacement of cholesterol as well as ratio optimization of the individual components has come to the fore [388, 389]. For example, by replacing zwitterionic 1,2-distearoyl-sn-glycero-3-phosphocholine (DSPC) with anionic 1,2-distearoyl-sn-glycero-3-phosphoglycerol (DSPG) in Onpattro (Patisiran), the LNP surface charge can be switched from neutral to anionic and thus target the reticuloendothelial system (RES) [390]. Furthermore, the combination of appropriate helper lipids is crucial. By changing the head group of DOPC (1,2-dioleoyl-sn-glycero-3-phosphocholine) to ethanolamine (DOPE, 1,2-dioleoyl-sn-glycero-3-phosphoethanolamine), the LNP formulation containing cationic lipid DODAP (1,2-dioleoyl-3-dimethylammonium propane) facilitates a transition from the LDL (low density lipoprotein) receptor-mediated hepatocyte delivery via apolipoprotein E (ApoE) to predominant spleen targeting via complement receptors [391, 392]. Currently, the most advanced LNP formulations base on standard

cationizable lipids with a single positive charge or lipidoids with several positive charges [393, 394]. *In vivo,* the LNP composition dictates protein corona formation in the bloodstream, which in turn affects biodistribution and cellular uptake. Due to ApoE-mediated liver targeting and good blood perfusion, the liver represents an ideal organ for LNP delivery and a major site of drug metabolism [395]. In addition to that, the LNP composition influences the physico-chemical properties (particle size, charge, surface shielding), which enables organ-selective targeting in the absence of receptor targeting moieties. For example, particle size can be regulated by altering the PEG lipid concentration to reach hepatocytes by passing through liver fenestrae (100-160 nm depending on species) [396]. Further, negatively charged particles show high spleen preference as reported for lipoplexes [397]; and larger particle sizes, ranging from 200 to 500 nm, are beneficial for targeting splenic dendritic cells [398].

Despite the potent delivery of LNPs to the liver and the overall established medical usefulness of hepatocyte-directed nucleic acid therapies, it may be desirable to redirect the particles to other therapeutically relevant tissues. A new approach to minimize liver accumulation, is selective organ targeting (SORT). This method involves the addition of a fifth, “sorting” molecule to the lipid composition that determines the tissue-specific delivery and activity of the LNPs [399-401]. Most recently, peptide ligands specifically binding receptors/cell types were identified by *in vivo* phage peptide biopanning and conjugated to mRNA LNPs for photoreceptor targeting of the neutral retina after sub-retinal injection [402]. Additionally, there are strategies to address leukocytes; e.g., conjugation of a fusion protein, which addresses $\alpha_4\beta_7$ integrin expressed on gut-homing leukocytes, to the surface of the LNPs resulted in interferon γ silencing in the gut and therapeutic efficacy in experimental colitis [44]. Another approach is the design of new libraries of ionizable amino lipids based on ethanolamine, hydrazine, or hydroxylamine linkers for efficient siRNA delivery into leukocytes [403]. Library screening and evaluation with Fast Identification of Nanoparticle Delivery (FIND), a high-throughput DNA barcode-based *in vivo* LNP screening, facilitates the characterization of chemically distinct LNPs for efficient RNA delivery to T-lymphocytes or splenic immune cells *in vivo* via chemical targeting [404, 405]. Also, the additional incorporation of the bioactive phospholipid phosphatidylserine into LNPs promotes mRNA transfection efficiency in secondary lymphoid organs both *in vitro* and *in vivo* [406, 407].

A critical issue in successful nucleic acid delivery is the endosomal escape. Due to their ionizable character, LNPs are neutral at physiological pH, but become protonated in the acidic environment of endosomes. This aids in the fusion of their lipids with the endosomal membrane and facilitates nucleic acid delivery to the cytosol [408, 409]. Nevertheless, most of the cargo remains inactive by accumulation in late endosomes and lysosomes [387, 410]. There are several factors and limitations to endosomal escape that can hinder the efficiency of nanocarrier-mediated drug delivery, resulting in a cargo escape rate of only 1-2% [411, 412]. Overcoming these barriers is critical for the efficiency of therapeutic agents [84, 413].

The present study aimed at the evaluation of mRNA LNP formulations with improved intracellular cargo release. For this purpose, a small library of recently developed double pH-responsive lipo-xenopeptides [80] was evaluated as cationizable components in mRNA LNPs.

These sequence-defined xenopeptides were synthesized via solid phase-assisted peptide synthesis (SPPS). The double pH-responsiveness was implemented by combining cationizable polar aminoethylene units in form of the artificial amino acid succinoyl tetraethylene pentamine (Stp) [414], with cationizable apolar units in form of lipo amino fatty acids (LAFs) [80], yielding different 2D sequences and 3D topologies. These LAF-Stp carriers show a molecular chameleon character due to the pH-dependent switch in polarity and high endosomolytic activity. Selected library members were already found highly effective in standard mRNA lipopolyplexes [80]. To identify the best suitable LAF-Stp carriers for mRNA LNPs in comparison to standard ionizable lipids that contain only single tertiary amines (i.e., SM-102, and DLin-MC3-DMA) [384, 387, 415, 416], our multi-protonatable carriers with 6-10 protonatable amines were tested in different molar lipid, molar charge, and N/P ratios.

The LAF-Stp carriers formulated as LNPs turned out to be very potent, mediating high mRNA expression *in vitro* and *in vivo*, with an interesting specificity for the spleen as a central immune organ, displaying a far higher spleen/liver expression ratio than established standard SM-102 and DLin-MC3-DMA LNPs. All in all, our novel LAF-Stp carriers proved to be an interesting alternative to ionizable lipids in LNPs.

3.2 Materials and methods

3.2.1 Materials

Chemically modified CleanCap® FLuc mRNA (5moU), CleanCap® mCherry mRNA (5moU), and CleanCap® eGFP (5moU) encoding firefly luciferase, fluorescent protein mCherry, or enhanced green fluorescent protein (eGFP), respectively, were obtained from Trilink Biotechnologies (San Diego, CA, USA). EZ Cap™ Cy5 Firefly Luciferase mRNA (5-moUTP) was ordered from Apexbio Technology LLC (Houston, USA). Cholesterol was purchased from Sigma-Aldrich (Munich, Germany). 1,2-distearoyl-sn-glycero-3-phosphocholine (DSPC) and 1,2-dimyristoyl-rac-glycero-3-methoxypolyethylene glycol-2000 (DMG-PEG 2000) were obtained from Avanti Polar Lipids (Alabaster, AL, USA). The ionizable lipid DLin-MC3-DMA was ordered from MedChemExpress (Monmouth Junction, NJ, USA) and SM-102 from Biosynth Carbosynth (Staad, Switzerland). HEPES was purchased from Biomol (Hamburg, Germany), hydrazinium hydroxide, glucose, and disodium ethylenediaminetetraacetic acid (EDTA) from Merck (Darmstadt, Germany). Agarose BioReagent – low EEO was purchased from Sigma Aldrich (Munich, Germany), and GelRed 10,000× as well as ethanol absolute from VWR (Darmstadt, Germany).

Antibodies for flow cytometric analyses (immunostaining experiment, see section 2.6.3). eFl450-labeled anti-F4/80 (clone BM8), SB702-CD45 (30-F11), PE-CD32b (AT130-2), PE-Cy7-CD11c (N418), eFl506-CD3 (145-2C11), SB600-CD11b (M1/70), PE-CD11c (N418), PE-eFl610-Ly6G (1A8- L6g), and eFl780-FVD (for live/dead cell discrimination) were purchased from ThermoFisher (Waltham, MA, USA). APC-CD19 (1D3) was purchased from BD Biosciences (Franklin Lakes, NJ, USA).

All cell culture consumables were obtained from Faust Lab Science (Klettgau, Germany). Cell culture media, fetal bovine serum (FBS), antibiotics, trypsin/EDTA as well as paraformaldehyde (PFA) were purchased from Sigma Aldrich (Munich, Germany) and PAN-Biotech (Aidenbach, Germany). Cell culture 5× lysis buffer, and D-luciferin sodium salt were ordered from Promega (Mannheim, Germany); 6-(p-toluidino)-2-naphthalenesulfonyl chloride (TNS), β-mercaptoethanol, 3-(4,5-dimethylthiazol-2-yl)-2,5-diphenyiltetrazolium bromide (MTT), 4′,6-diamidino-2-phenylindole (DAPI), dithiothreitol (DTT), adenosine 5′-triphosphate (ATP) disodium

salt trihydrate, coenzyme A trilithium salt, bafilomycin A1, and protease and phosphatase inhibitor cocktail from Sigma-Aldrich (Munich, Germany).

Polypropylene syringe microreactors were obtained from Multisyntech (Witten, Germany). Fmoc-Stp(Boc)$_3$-OH was synthesized in house according to published protocols [80]. Fmoc-protected amino acids Fmoc-L-Lys(Dde)-OH and Fmoc-L-Lys(Fmoc)-OH, 2-chlorotritylchloride polystyrene resin, dimethylformamide and piperidine were acquired from Iris Biotech (Marktredwitz, Germany). Diisopropylethylamine (DIPEA), 1-hydroxybenzotriazole hydrate (HOBt), triton X-100, triisopropylsilane (TIS) were purchased from Sigma-Aldrich (Munich, Germany). (Benzotriazol-1-yloxy)-tripyrrolidinophosphonium hexafluorophosphate (PyBOP) was procured from Millipore (Oakville, Canada). Oleic acid was bought from ThermoFisher (Kandel, Germany). Trifluoroacetic acid was obtained from Acros Organics (Geel, Belgium). Sephadex G10 was acquired from GE Healthcare (Uppsala, Sweden).

3.2.2 Synthesis of cationizable carriers

The library of ionizable LAF-Stp carriers (**Table 1**) was synthesized by Melina Grau (Pharmaceutical Biotechnology, LMU Munich) via solid phase-assisted peptide synthesis (SPPS) as described in Thalmayr et al. [80]. The synthesis of OleA carrier ***1829*** was likewise carried out as described below, replacing the terminal LAF units with oleic acid (OleA) analogously as previously described [47, 60, 417].

Synthesis of OleA carrier *1829*

The OleA-Stp carrier with bundle topology, ***1829*** (**Figure 4**), was synthesized by Tobias Burghardt (Pharmaceutical Biotechnology, LMU Munich) via solid phase peptide synthesis (SPPS) analogously as described in Thalmayr et al. [80] but replacing LAF with oleic acid (OleA) as previously described [47, 417, 418].

A 2-chlorotritylchloride resin (1.56 mmol/g chloride) was loaded with Fmoc-Stp(Boc)$_3$-OH at a density of 0.1 µmol/mL. For this purpose, 750 mg of resin were added to a syringe reactor and pre-swollen for 20 min in dry DCM. The swollen resin was incubated with 0.1 eq. of the respective amino acid and 0.3 eq. DIPEA dissolved in dry DCM at RT for 1.5 h. The solution was discarded, and the resin was next treated with

capping solution consisting of 2 mL dry DCM, 1.5 mL MeOH, and 250 µL DIPEA at RT for 30 min. The fully capped resin was then washed thrice with DMF and thrice with DCM and dried overnight. The loading was determined based on the absorption of Fmoc [N-(9H-fluoren-9-ylmethyl)]-piperidine. Triplicates of 5-10 mg of the dry resin were weight into tubes and 1 mL of 20% (v/v) piperidine in DMF was added. The vessels were briefly vortex and incubated at RT for 90 min. The vessels were vortexed again and 25 µL of the supernatant were diluted with 975 µL DMF. The absorption was measured at 301 nm on a Genesys 10S UV-VIS spectrophotometer (Thermo Scientific; Dreieich, Germany) against DMF as blank. The resin loading was calculated as follows: amino acid loading [mmol/g] = (A_{301} × 1000) / (m[mg] × 7800 × D); D being the dilution factor. The pre-loaded resin in Fmoc-deprotected state was stored at 4 °C.

Prior to all manipulations, dry resins were swollen for 20 min in DCM. For general coupling steps, 4 eq. of the respective Fmoc-protected amino acid were dissolved in 1.5 mL DCM, and 8 eq. of DIPEA were added. The activating agents HOBt (4 eq.) and PyBOP (4 eq.) were dissolved in 1.5 mL DMF and then added as well. The solution was drawn up into the syringe reactor and the resin was incubated tor 1.5 h at RT under constant agitation. After the coupling step, the resin washed 3x with DMF and 3x with DCM and a Kaiser test (ninhydrin reaction to detect free amino groups) was performed as in-process-control to ensure reaction had occurred. Fmoc-deprotection was achieved by treating the resin 4x with 20% (v/v) piperidine in DMF for 10 min each. Next, the resin was washed 3x with DMF and 3x with DCM, and a Kaiser test was performed to ensure successful deprotection. Then the next amino acid was coupled as described above.

In case of ***1829***, at the two consecutive symmetrical branching points Fmoc-L-Lys(Fmoc)-OH was coupled. For the final fatty acid coupling, 5 eq. oleic acid were dissolved in 1.5 mL of 2% (v/v) triton X-100 in DCM, and 5 eq. DIPEA were added. The activating agents HOBt (5 eq.) and PyBOP (5 eq.) were dissolved in 1.5 mL DMF and then added as well. The fatty acid solution was drawn up into the syringe reactor enclosing as little air as possible. The syringe reactor was then covered in aluminum foil to protect the product from light and incubated for three days at RT under constant agitation. Afterwards, the resin was washed 5x with DMF and 5x with DCM. A Kaiser test was performed on a sample of the resin as in-process-control. The resin was dried overnight under reduced pressure.

Cleavage from the resin and whole deprotection was achieved by incubating the dry resin for 30 min with 2-3 mL of ice-cold cleavage solution consisting of DCM, TFA, TIS, and H_2O (v/v 60:35:2.5:2.5). During this time the syringe was covered in aluminum foil. Afterwards, the cleavage solution was drained into 40 mL ice-cold n-hexane. The resin was washed once with 3 mL DCM and this washing solution collected as well. From now on the crude product was constantly kept on ice. The vessel was vigorously mixed and then centrifuged for 15 min at 4000 rpm and at 4 °C. The upper phase was carefully pipetted off and the remaining lower phase was dried under nitrogen flow.

Purification and salt exchange of the crude product was carried out with size exclusion chromatography using a Sephadex G10 column (300 x 16 mm) and the Äktapurifier 10 FPLC system (GE Healthcare Biosciences AB (Uppsala, Sweden)) equipped with a P-900 solvent pump module, a UV-900 UV/Vis multi-wavelength detector, a pH/C-900 conductivity module and a Frac-900 automated faction collector and UNICORN 5.31 software. The residue was redissolved in 400 µL EtOH, and then diluted to 4 or 6 mL with mobile phase (0.01 M HCl/ACN, v/v 7:3). 2 mL were injected at a time and purified under isocratic conditions. Pure fractions were pooled, flash-frozen in liquid nitrogen and then freeze dried (Martin Christ Gefriertrocknungsanlagen (Osterode am Harz, Germany). The final product was analyzed by MALDI-TOF-MS on an Autoflex II mass spectrometer (Bruker Daltonics; Bremen, Germany) **(Figure 1)**.

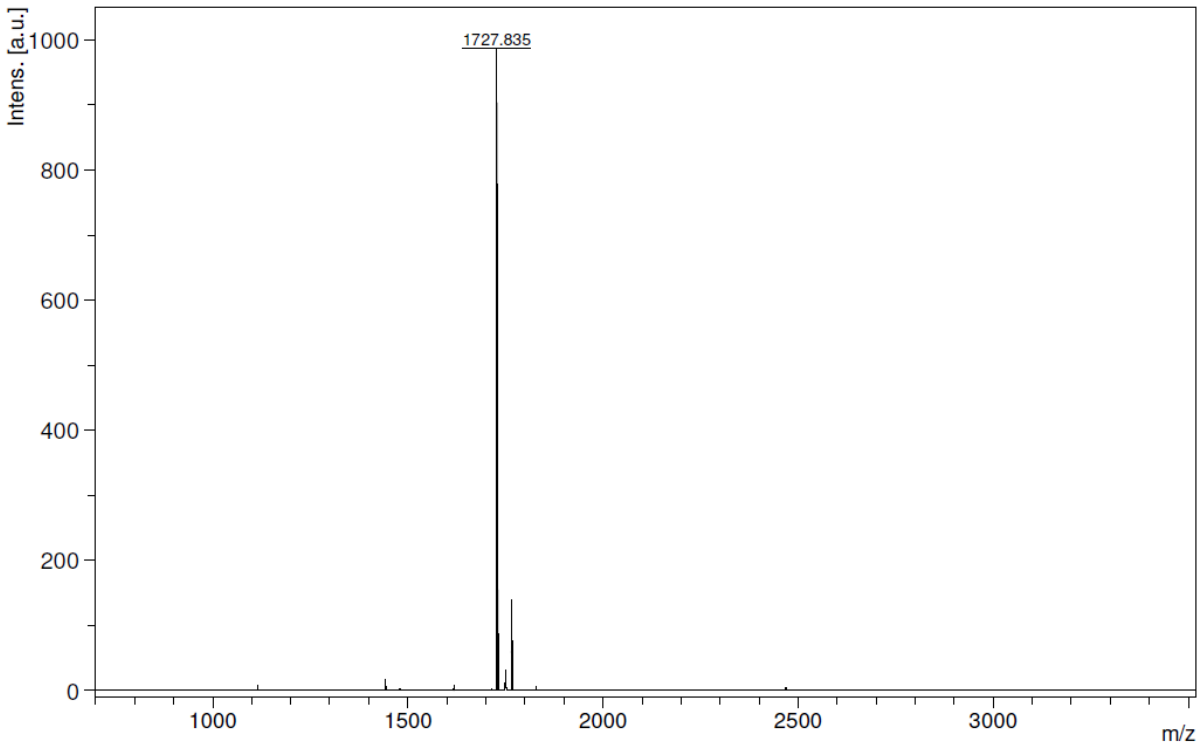

Figure. 1. MALDI-TOF-MS of OleA carrier *1829.* Calculated mass 1730.5 Da; found mass 1727.8 Da. Mass was measured by Tobias Burghardt (Pharmaceutical Biotechnology, LMU Munich).

Table 1. LAF-Stp carriers with bundle and U-shape topologies.

ID	sequence (N→C)	Stp/LAF ratio	protonatable amines
			with/without LAF
Bundles			
1613	K[K[12Oc)$_2$]$_2$-Stp	1:4	7 / 3
1621	K[K[8Oc)$_2$]$_2$-Stp	1:4	7 / 3
1713	K[K[12Oc)$_2$]$_2$-Stp$_2$	2:4	10 / 6
1730	K[K[8Oc)$_2$]$_2$-Stp$_2$	2:4	10 / 6
1752	K[K(12Bu)$_2$]$_2$-Stp	1:4	7 / 3
1753	K[K(16Bu)$_2$]$_2$-Stp	1:4	7 / 3
1754	K[K(12He)$_2$]$_2$-Stp	1:4	7 / 3
1755	K[K(14He)$_2$]$_2$-Stp	1:4	7 / 3
1762	K[K(10Oc)$_2$]$_2$-Stp	1:4	7 / 3
1829	K[K[OleA)$_2$]$_2$-Stp	-	3 / 3
U-shapes			
1611	K(12Oc)-Stp-K(12Oc)	1:2	6 / 4
1612	K(12Oc)$_2$-Stp-K(12Oc)-K(12Oc)	1:4	7 / 3
1620	K(8Oc)$_2$-Stp-K(8Oc)-K(8Oc)	1:4	7 / 3
1716	K(12Oc)$_2$-Stp-K[K(12Oc)$_2$]	1:4	7 / 3
1718	[K(12Oc)]$_2$-Stp-[K(12Oc)]$_2$	1:4	8 / 4
1720	K[K(12Oc)$_2$]-Stp-K[K(12Oc)$_2$]	1:4	8 / 4
1722	K(12Oc)$_2$-Stp$_2$-K(12Oc)-K(12Oc)	2:4	10 / 6

K, lysine; OleA, oleic acid; Stp, succinoyl tetraethylene pentamine; 12Bu, 16 Bu: LAF based on 4-aminobutanoic acid modified with two dodecyl chains or two hexadecyl chains; 12He, 14He: LAF based on 6-aminohexanoic acid and two dodecyl or tetradecyl chains; 8Oc, 10Oc, 12Oc: LAF based on 8-aminooctanoic acid and two octyl, decyl, or dodecyl chains, respectively. ***1829*** presents a OleA-based bundle control sequence. The number of protonatable amines includes Stp and N-terminal amino groups and is listed alternatively with and without lipophilic LAF tertiary amines that are not considered to be protonated at physiological pH. The synthesis of LAF-Stp carriers was performed by Melina Grau (Pharmaceutical Biotechnology, LMU Munich). OleA carrier ***1829*** was synthesized by Tobias Burghardt (Pharmaceutical Biotechnology, LMU Munich).

3.2.3 mRNA LNP formulation

LNPs were formulated by mixing an acidic aqueous phase containing mRNA with an EtOH phase containing ionizable and helper lipids (v/v 3:1) by rapid pipetting. The aqueous phase was prepared with mRNA in citrate buffer (10 mM, pH 4.0). The EtOH phase includes a mixture of cholesterol, 1,2-distearoyl-sn-glycero-3-phosphocholine (DSPC), 1,2-dimyristoyl-rac-glycero-3-methoxypolyethylene glycol-2000 (DMG-PEG 2000) and an ionizable lipid/carrier at predetermined molar and nitrogen/phosphate (N/P) ratios shown in **Table 2**. The N/P ratio represents the molar ratio of all protonatable nitrogens of the carrier to phosphates of the nucleic acid. All secondary amines of the Stp units, terminal amines, and the tertiary amines of the LAF units were considered in this N/P ratio calculation. The aqueous and EtOH solutions were rapidly mixed by pipetting for 30 sec and then incubated at room temperature (RT) for 10 min to allow LNP assembly. The formulated LNPs were diluted with HBG (20 mM of HEPES, 5% (w/v) glucose, pH 7.4) to a final ethanol concentration below 5% for *in vitro* experiments and dialyzed against HBG buffer in 1 kDa MWCO tubes at 4 °C for 2 h for subsequent *in vivo* studies. The final concentration of nucleic acid in the LNP solution was 3 µg/mL, unless indicated differently.

Table 2. Molar (mol%) and w/w (weight%) ratios of the lipids and ionizable carrier used in mRNA LNPs, and ratios between cationizable carrier to mRNA.

	ratios		ratios				
	Chol/DSPC/PEG DMG/ionizable carrier		w/w	N/P (ionizable carrier/mRNA)			
ID	molar [mol%]	w/w [weight%]	(total carrier/ mRNA)	N with LAF	N/P	N without LAF	N/P
Positive controls							
MC3	38.5/10/1.5/50	25.4/13.5/6.4/54.7	10		3	-	-
SM-102	38.5/10/1.5/50	24/12.7/6.1/57.2	22		6	-	-
Bundles							
1613	59.9/15.6/2.3/22.2	22.2/11.8/5.6/60.5	17	4+3	9	3	4.1
1621	59.9/15.6/2.3/22.2	24.5/13/6.2/56.3	16	4+3	9	3	4.1
1713	64.2/16.7/2.5/16.7	25.4/13.5/6.4/54.7	15	4+6	9	6	5.6
1730	64.2/16.7/2.5/16.7	27.5/14.6/6.9/51	14	4+6	9	6	5.6
1752	59.9/15.6/2.3/22.2	23.3/12.4/5.9/58.5	17	4+3	9	3	4.1
1753	59.9/15.6/2.3/22.2	21.2/11.2/5.3/62.3	18	4+3	9	3	4.1
1754	59.9/15.6/2.3/22.2	22.7/12.1/5.7/59.5	17	4+3	9	3	4.1
1755	59.9/15.6/2.3/22.2	21.7/11.5/5.5/61.4	18	4+3	9	3	4.1
1762	59.9/15.6/2.3/22.2	21.7/11.5/5.5/61.4	17	4+3	9	3	4.1
1829	46.2/12/1.8/40	16.9/9/4.3/69.9	23	0+3	9	3	9
U-shapes							
1611	57.8/15/2.2/25	27/14.3/6.8/51.9	14	2+4	9	4	6.3
1612	59.9/15.6/2.3/22.2	22.2/11.8/5.6/60.5	17	4+3	9	3	4.1
1620	59.9/15.6/2.3/22.2	24.5/13/6.2/56.3	16	4+3	9	3	4.1
1716	59.9/15.6/2.3/22.2	22.2/11.8/5.6/60.5	17	4+3	9	3	4.1
1718	61.6/16/2.4/20	23.2/12.3/5.9/58.6	17	4+4	9	4	4.7
1720	61.6/16/2.4/20	23.2/12.3/5.9/58.6	17	4+4	9	4	4.7
1722	64.2/16.7/2.5/16.7	25.4/13.5/6.4/54.7	15	4+6	9	6	5.6

The N/P ratio represents either the molar ratio of all protonatable nitrogens (LAF +Stp + any terminal amine) of the carrier to phosphates of the mRNA, or as an alternative N/P calculation

without considering the lipophilic tertiary LAF amines. LAF; lipoamino fatty acid; N, protonatable nitrogen; Stp, succinoyl tetraethylene pentamine.

3.2.4 Physicochemical characterization of LNPs

3.2.4.1 Particle size and zeta potential measurement

LNPs were formulated in HBG as described in section 2.3 at a concentration of 3 µg/mL FLuc mRNA. Measurements of size and zeta potential were performed with a Zetasizer Nano ZS (Malvern Instruments, Malvern, Worcestershire, U.K.) in a folded capillary cell (DTS1070) by dynamic and electrophoretic laser-light scattering (DLS, ELS). Size and polydispersity index were measured in 80 µL of the above described nanoparticle solutions using the following instrument settings: equilibration time 30 sec, temperature 25 °C, refractive index 1.330, viscosity 0.8872 mPa*s. Samples were measured three times with six sub runs per measurement. For measurement of the zeta potential, all samples were diluted to 800 µL with HBG directly before measurement. Parameters were identical to the size measurement apart from an equilibration time of 60 sec. Three measurements with 15 sub runs lasting 10 sec each were performed, and zeta potentials were calculated by the Smoluchowski equation.

3.2.4.2 Agarose gel shift assay

A 1% (w/v) agarose gel was prepared by dissolving agarose in 1x TBE buffer (trizma base 10.8 g, boric acid 5.5 g, disodium EDTA 0.75 g, in 1 L of water) and heating it up to 100 °C. Then, 1x GelRed was added, and the agarose solution was poured in the electrophoresis chamber and left for 40 min at RT to form a gel. mRNA LNPs were prepared as described above (see section 2.3) containing 60 ng of FLuc mRNA in 20 µL of HBG. 4 µL of loading buffer (6 mL glycerol, 1.2 mL 0.5 M EDTA, 2.8 mL H_2O, 0.02 g bromophenol blue) was added to each sample before filling it into the gel pockets. Electrophoresis was performed in 1x TBE buffer at 120 V for 70 min.

3.2.4.3 TNS dye binding assay

For the TNS assay, 20 mM citric acid/NaOH buffer (with 150 mM NaCl; pH 3.0, 3.5, 4.0, 4.5, 5.0, 5.5), 20 mM sodium dihydrogen phosphate/NaOH buffer (with 150 mM NaCl; pH 6.0, 6.4, 6.8, 7.2, 7.6, 8.0), and 20 mM Tris/HCl buffer (with 150 mM NaCl; pH 8.5, 9.0, 9.5, 10.0) were prepared. TNS was dissolved at 0.6 mM in water as a stock solution. In a black 96-well plate, 2 µL of the TNS solution, 12 µL of the LNP

solution containing 250 ng of FLuc mRNA in 20 µL of HBG and 186 µL of each of the buffers above were mixed. After shaking the incubation mixture (400 rpm, 10 min), the fluorescence of the TNS was measured using a Spark Tecan microplate reader (Spectrafluor Plus, Tecan, Männedorf, Switzerland) at an excitation wavelength of 360 nm and an emission wavelength of 465 nm. The apparent pKa of the surface was calculated as the pH at which the LNP showed 50% of the maximum fluorescence.

3.2.4.4 RiboGreen assay

mRNA encapsulation efficiency [ee(%)] was measured using QUANT-iT™ RiboGreen RNA Assay-Kit (ThermoFisher Scientific). LNPs were formulated in HBG as described in section 2.3). In a black 96-well plate, 40 µL of HBG buffer (blank) or LNP solution were added to 210 µL of 1x TE buffer (10 mM Tris-HCl, 1 mM EDTA, pH 7.5 in RNase-free water) per well. 50 µL of the obtained solutions was added to either 50 µL 1x TE buffer for non-lysed LNPs or 50 µL triton/1x TE buffer (2% (v/v) triton X-100 in TE buffer) for lysed LNPs. 96-well plates were incubated for 10 min at 37 °C to ensure complete lysis of triton incubated LNPs and afterwards cooled down for 5 min at RT. RiboGreen reagent was diluted 1:100 in 1x TE buffer and 100 µL were added to each well. After 5 min incubation, the fluorescent signal was measured in duplicates in a Spark Tecan microplate reader (Spectrafluor Plus, Tecan, Männedorf, Switzerland) at 485/535 nm excitation/emission wavelength. After subtracting the blank measurement, the encapsulation efficiency (in percent) was calculated with following equation:

$$ee(\%) = (1 - \left(\frac{mean\ emission_{\ non-lysed\ LNPs}}{mean\ emission_{\ lysed\ LNPs}}\right)) * 100$$

3.2.5 *In vitro* characterization

3.2.5.1 Cell culture

The murine neuroblastoma cell line Neuro2A (N2a) (ATCC, American Type Culture Collection Manassas, Virginia, USA), the human adenocarcinoma cell line HeLa (DSMZ, German Collection of Microorganisms and Cell Cultures GmbH, Braunschweig, Germany), and HeLa-Gal8-mRuby3 cells (stably expressing Galectin8-mRuby3 fusion protein) [419-421] were cultured in Dulbecco's modified Eagle's medium (DMEM)-low glucose (1 g/L glucose). Human hepatocellular carcinoma cell

lines Huh7 and HepG2 were cultured in Dulbecco's Modified Eagle Medium (DMEM)/Nutrient Mixture F12-Ham. The murine dendritic cell (DC)-like cell line DC2.4 (Merck Millipore, Darmstadt, Germany) was grown in Iscove's Modified Dulbecco's Medium (IMDM). The murine macrophage (MAC) model cell line J-774A.1 (DSMZ, German Collection of Microorganisms and Cell Cultures GmbH, Braunschweig, Germany) was cultured in DMEM-high glucose (4.5 g/L glucose). All cell culture media were supplemented with 10% (v/v) FBS, 4 mM of stable L-glutamine, 100 U/mL of penicillin, 100 µg/mL of streptomycin, and in case of DC2.4 cells, additionally with 50 µM of β-mercaptoethanol. The cell lines were cultured at 37 °C and 5% CO_2 in an incubator at a relative humidity of 95%.

3.2.5.2 Cellular transfection efficiency of FLuc mRNA LNPs determined via luciferase reporter assay

One day prior to mRNA delivery, 10,000 N2a, 8000 Huh7, 8000 HepG2, 8000 HeLa, 5000 DC2.4, and 10,000 J774A.1 cells/well were seeded in 96-well plates. Before the treatment, cell culture medium was replaced by 80 µL of fresh medium containing 10% (v/v) FBS. LNPs were added in 20 µl HBG buffer, unless indicated differently. mRNA LNP treatments were performed in triplicate in 96-well plates. The transfection efficiency of LNPs was evaluated for different doses of FLuc mRNA per well. HBG buffer was used as negative control. Dlin-MC3-DMA (as used in Patisiran) and SM-102 (as used in the Moderna COVID-19 vaccine) LNPs served as positive controls for mRNA LNPs. After 24 h incubation at 37 °C, the medium was removed, and cells were treated with 100 µL of 0.5x cell culture lysis buffer (Promega). Prior to measurement of luciferase activity, plates were incubated for 1 h at RT. Luciferase activity was measured in 35 µL cell lysate for 10 sec in a Centro LB 960 plate reader luminometer (Berthold Technologies, Bad Wildbad, Germany) after addition of 100 µL/well of LAR buffer (20 mM glycylglycine; 1 mM $MgCl_2$; 0.1 mM EDTA; 3.3 mM DTT; 0.55 mM ATP; 0.27 mM coenzyme A, pH 8-8.5) supplemented with 5% (v/v) of a mixture of 10 mM luciferin and 29 mM glycylglycine. When the measured values overshot the detector limit of the plate reader luminometer, the cell lysate was 10- or 100-fold diluted in PBS (phosphate buffered saline; 136.9 mM NaCl, 2.7 mM KCl, 8.1 mM Na_2HPO_4, 1.5 mM KH_2PO_4) and mixed thoroughly before measurement. Transfection efficiency was presented as relative light units (RLU) per well. Transfections of DC2.4, and J774A.1

cells were performed by Dr. Simone Berger (Pharmaceutical Biotechnology, LMU Munich).

3.2.5.3 Viability of transfected cells assessed via MTT assay

Transfections were performed as described above (see section 2.5.2). At 24 h after transfection, 10 µL MTT (5 mg/mL) were added to each well, reaching a final concentration of 0.5 mg/mL. After incubation for 2 h at 37 °C and 5% CO_2, the supernatant was removed, and the plates were stored at -80 °C for at least 1 h. Then, the purple formazan product was dissolved in 100 µL DMSO by constant shaking for 30 min at 37 °C. Quantification was done photometrically using a spark Tecan microplate reader (Spectrafluor Plus, Tecan, Männedorf, Switzerland). Absorbance was measured at wavelength λ = 590 nm with background correction at λ = 630 nm. Experiments were carried out in triplicates. Relative metabolic activity normalized to control wells (HBG-treated cells) was calculated by the equation: $[A]_{test}/[A]_{control}$. Transfections of DC2.4, and J774A.1 cells were performed by Dr. Simone Berger (Pharmaceutical Biotechnology, LMU Munich).

3.2.5.4 Cellular transfection efficiency of mRNA LNPs determined by flow cytometry

mRNA LNP treatments were performed in triplicate in 96-well plates. N2a cells were seeded 24 h prior to transfection (10,000 cells/well). On the next day, the medium was replaced with 80 µL of fresh pre-warmed medium containing 10% (v/v) FBS. The LNPs were prepared as described in section 2.3, and volumes of 20 or 5 µL of LNP solution containing 60 or 15 ng mCherry mRNA were added per well. HBG buffer was added to reach a final volume of 100 µL per well. 20 µL HBG buffer per well was used as negative control. After 24 h of treatment, cells were trypsinized and resuspended in PBS solution containing 10% (v/v) FBS (FACS buffer) for flow cytometric evaluation. All samples were analyzed by flow cytometry using a CytoFLEX S Flow Cytometer (Beckman Coulter, Brea, CA, USA). Before measurement, 1 ng/µL 4′,6-diamidino-2-phenylindole (DAPI) was added to discriminate between viable and dead cells. The cellular fluorescence was assayed by excitation of DAPI at 405 nm and detection of emission at 450 nm. Only viable cells were considered. Gates were set compared to control measurements with HBG buffer-treated cells. The percentage of mCherry positive cells represented efficient mRNA transfection. Flow cytometry data were analyzed using FlowJo™ v10.8 flow cytometric analysis software by FlowJo, LLC

(Becton, Dickinson and Company, U.S.). The cellular mCherry expression was assayed by excitation at 561 nm, the detection of emission at 610 nm for mCherry. Only isolated viable cells were evaluated. The transfection efficiency was determined as the percentage of mCherry positive cells. Flow cytometry measurements were performed in collaboration with Mina Yazdi (Pharmaceutical Biotechnology, LMU Munich).

3.2.5.5 Confocal laser scanning microscopy (CLSM)

HeLa-Gal8-mRuby3 cells [419-421] (18,000 per well) were seeded into ibidi µ-slide 8-well chamber slides (Ibidi GmbH, Germany) and cultured overnight at 37 °C. LNPs were formulated as described in section 2.3 at a total mRNA concentration of 6.75 µg/mL, whereby 80% of Fluc mRNA and 20% of Cy5-labelled Fluc mRNA were mixed. Medium was changed before transfection, and 20 µL of LNP solution was added to the cells to a final volume of 300 µL per well. After incubation at 37 °C for 4 h, cells were washed twice with PBS, fixed with 4% (w/v) paraformaldehyde in PBS for 45 min at RT in the dark and washed with PBS again. Nuclei were stained with DAPI (1 µg/mL in PBS) for 20 min at RT in the dark. After removal of the staining solution, cells were washed twice with PBS and stored in 300 µL fresh PBS. Imaging was performed by Miriam Höhn (Pharmaceutical Biotechnology, LMU Munich) with a Leica-TCS-SP8 CLSM equipped with an HC PL APO 63 x 1.4 objective and images were processed with the LAS X software from Leica.

3.2.5.6 Bafilomycin A1 assay

N2a cells were seeded in 96-well plates as described above (see section 2.5.2) one day prior to transfection. Medium was changed to either fresh medium or medium supplemented with bafilomycin A1 (BafA1) (0.1 µg/µL in DMSO) to reach a final concentration of 200 nM BafA1 after LNP addition and then incubated for 2 h. LNPs were formed as described in section 2.3 at a concentration of 3 µg/mL mRNA and transfected with 20 µL per well. Cells were incubated for 4 h and then lysed. Luciferase activity was measured as described above (see section 2.5.2). Transfections were performed in triplicates.

3.2.5.7 Serum dilution assay

One day prior to transfection, N2a, Huh7, DC2.4, and J774A.1 cells were seeded in 96-well plates as described above (see section 2.5.2). Medium was replaced with 80

µL fresh medium containing 10% (v/v) FBS before the treatment. LNPs were formulated as described above (see section 2.3) at a final mRNA concentration of 3 µg/mL. Directly before transfection, LNPs were diluted appropriately with FBS, and 20 µL of each dilution was added to the cells at indicated mRNA doses ranging from 0.15 to 30 ng/well. As a control, HBG-diluted LNPs were transfected at an mRNA dose of 30 ng per well. Read-out was performed at 24 h after transfection via a luciferase reporter assay as described above (see section 2.5.2). Transfections were carried out in triplicates. Transfections of DC2.4, and J774A.1 cells were performed by Dr. Simone Berger (Pharmaceutical Biotechnology, LMU Munich).

3.2.6 *In vivo* activity of mRNA LNPs in mice

3.2.6.1 In vivo application of mRNA LNPs

In vivo experiments were performed according to the guidelines of the German Animal Welfare Act and were approved by the animal experiments ethical committee of the Government of Upper Bavaria (accreditation number Gz. ROB-55.2-2532.Vet_02-19-20). For the evaluation of luciferase expression (section 2.6.2), N2a cells (10^6 cells in 150 µL PBS) were inoculated subcutaneously into the left flank of 6-week-old female A/J mice (Envigo RMS GmbH, Düsseldorf, Germany). For the immunostaining experiment (section 2.6.3), tumor-free 6-week-old female A/J mice were used. Mice were randomly divided into groups of three (tumor-bearing mice) or five (tumor-free mice), respectively, and were housed in isolated ventilated cages under specific pathogen-free conditions with a 12 h day/night interval, and food and water ad libitum. Weight and general well-being were monitored continuously. Tumor size was measured with a caliper and determined by the formula: $\frac{a*b^2}{2}$ (a = longest side of the tumor; b = widest side vertical to a). When tumors reached a size of 250-500 mm^3, LNPs formulated with FLuc mRNA were injected intravenously via the tail vein at a dose of 3 µg mRNA in 150 µL injection volume per mouse. The same application (3 µg mRNA; 150 µL HBG; i.v.) was done in the tumor-free 6-week-old mice with eGFP mRNA LNP formulations. At 6 h post LNP injections, blood samples were taken for evaluation of plasma parameters, and the mice were euthanized. The organs (lungs, liver, spleen, kidneys, heart, muscle (biceps femoris), brain, and tumor) were dissected and washed with PBS. The luciferase or eGFP expression, respectively, were

determined as described below. The in vivo study was performed by Jana Pöhmerer and Ulrich Wilk (Pharmaceutical Biotechnology, LMU Munich).

3.2.6.2 Ex vivo luciferase reporter assay of organs and tumors

Organs and tumor tissues were homogenized in Luciferase Cell Culture Lysis Reagent 1x, supplemented with 1% (v/v) protease and phosphatase inhibitor cocktail using a tissue and cell homogenizer (FastPrep®-24, MP Biomedicals, USA). Then, the samples were frozen overnight at -80 °C to ensure full lysis. In a next step, the samples were thawed and centrifuged for 10 min at maximum speed (~ 13,000 rpm) and 4 °C. Luciferase activity in 25 µL supernatant was measured in a Centro LB 960 plate reader luminometer (Berthold Technologies, Bad Wildbad, Germany) for 10 sec as described above (see section 2.5.2). Luciferase activity is presented as relative light units (RLU) per gram (g) tumor or organ. Measurements of organs were carried out by Jana Pöhmerer and Ulrich Wilk (Pharmaceutical Biotechnology, LMU Munich).

3.2.6.3 Ex vivo immunostaining

Preparation of single cell suspensions from dissected organs. Spleens were mashed through a 40 µM cell strainer (Greiner Bio-One, Frickenhausen, Germany) with a pestle to produce a single-cell suspension. Spleen cells (2×10^6 in 500 µL) were resuspended in medium (IMDM containing 5% (v/v) FBS, 2 mM L-glutamine, 100 U/mL penicillin, 100 µg/mL streptomycin, and 50 µM β-mercaptoethanol), placed in FACS tubes and kept overnight in the incubator (37 °C, 7.5% CO_2). Liver dissociation was performed to yield murine liver non-parenchymal cells (NPCs) following a previously described method [422]. Briefly, an enzyme-dependent dissociation mixture was pre-incubated for 15 min at 37 °C (Liver Dissociation Kit; Miltenyi Biotec, Bergisch-Gladbach, Germany). The liver tissue was dissected into small pieces and transferred into prepared C tubes (Miltenyi Biotec). The C tubes were subjected to a gentle MACS Dissociator using program m_liver_03. The resulting cell suspension was incubated under continuous shaking for 30 min at 37 °C, followed by another round of gentle MACS-mediated cell dissociation (m_liver_04). Subsequently, liver NPCs were enriched by using density centrifugation with 30% Histodenz-HBSS (both from Sigma-Aldrich). To obtain lung cell suspensions, the Lung Dissociation Kit (Miltenyi Biotec) was used, following the manufacturer's protocol. The experiments and analysis were carried out by Yanira Zeyn (Department of Dermatology, University Medical Center, JGU Mainz).

Flow cytometry and gating strategy. To stain cells, cells were washed in antibody incubation buffer containing PBS, 2% (v/v) FBS, and 0.5 mM EDTA. Subsequently, the samples were incubated with Fc receptor blocking antibody (clone 2.4-G2) for 15 min at 4 °C. Afterwards, the samples were incubated with fluorescence-labeled antibodies (*see section 2.1*) for 20 min at 4 °C. Then, cells were washed with PBS and incubated with eFl780-FVD to identify living cells. Samples were measured using an Attune NxT flow cytometer, and data were analyzed by using Attune NxT software, both by ThermoFisher. Gating was performed according to the strategies described in **Figure 2** and **3.** Measurements were done by Yanira Zeyn (Department of Dermatology, University Medical Center, JGU Mainz).

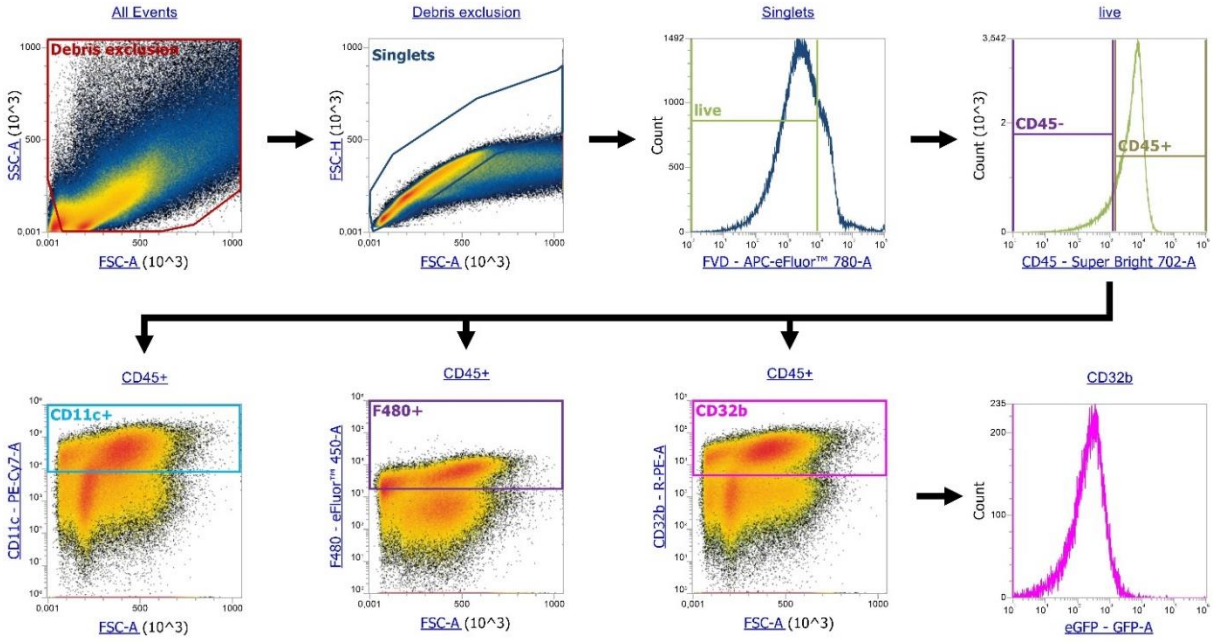

Figure 2. Gating strategy of liver NPC (non-parenchymal cells). Debris and doublets were excluded from further analysis. Then, FVD^- and $CD45^+$ cell population (living immune cells) was discriminated into $F4/80^+$ (KC, Kupffer cells), $CD11c^+$ (DC, dendritic cells), and $CD32b^+$ (LSEC, liver sinusoidal endothelial cells). For each cell population the eGFP MFI (mean fluorescence intensity) or percentage of $eGFP^+$ cells was used as readout. Measurements were performed by Yanira Zeyn (Department of Dermatology, University Medical Center, JGU Mainz).

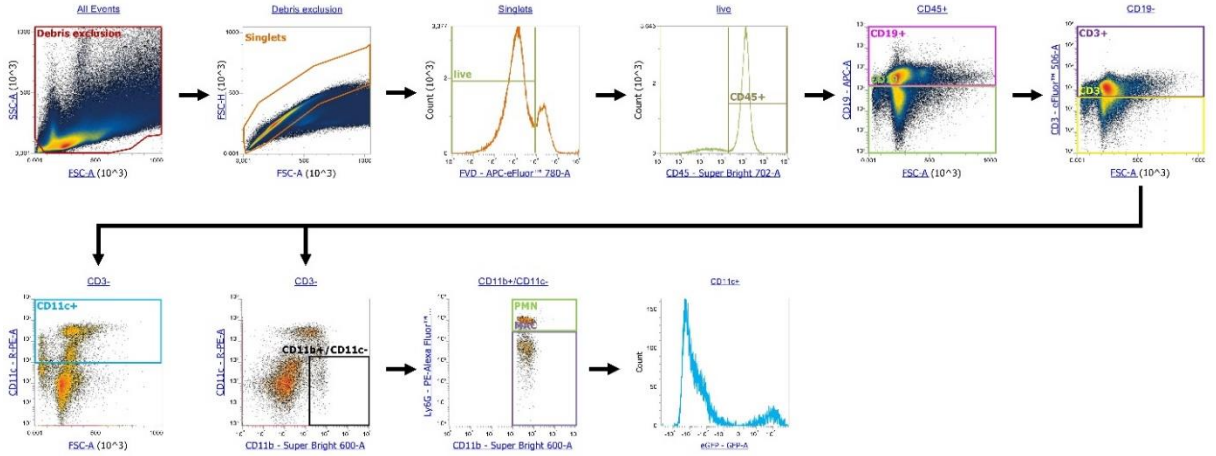

Figure 3. Gating strategy for cells of spleen and lungs. After exclusion of debris and doublets from further analysis, cells were gated for FVD$^-$ and CD45$^+$ cell populations (living immune cells). Next, B cells were defined as CD19$^+$. CD19$^-$ fraction was further discriminated in CD3$^+$ (T cells), and CD3$^-$ fractions. CD3$^-$ cells were gated for CD11c$^+$ (DCs) and CD11b$^+$/CD11$^-$. The CD11b$^+$/CD11$^-$ fraction was further discriminated by Ly6G$^+$ (PMN, polymorphonuclear leukocytes/neutrophils), and Ly6G$^-$ fractions (macrophages). For each cell population, the eGFP MFI (mean fluorescence intensity) or percentage of eGFP$^+$ cells was used as readout. Measurements were carried out by Yanira Zeyn (Department of Dermatology, University Medical Center, JGU Mainz).

3.2.7 Statistical analysis

All data were analyzed at least in triplicates and presented as arithmetic mean ± standard deviation (SD), if not otherwise stated. In order to analyze statistical significances, an unpaired Student's two-tailed t-test with Welch's correction, or an ordinary one-way ANOVA (multiple comparison, Tukey test), respectively, were carried out using GraphPad Prism^{TM} 9.5.1. Statistical significance was indicated by p values ≤0.05. The indication "ns" was used to display non-significant differences (p >0.05).

3.3 Results and discussion

3.3.1 mRNA LNP formulation with novel ionizable LAF-Stp carriers

Recently, novel LAF-Stp carriers for nucleic acid delivery were generated by a sequence-defined combination of succinoyl tetraethylene pentamine (Stp) units as cationizable polar domain and lipo amino fatty acids (LAF) as cationizable lipidic domain, containing a central tertiary amine between hydrocarbon chains [80]. The LAFs were generated by reductive amination of different amino fatty acids with fatty aldehydes of various lengths. By this, the position of the tertiary amine was shifted within the LAF molecule, resulting in different LAF types. In the displayed LAF nomenclature, the carbon chain lengths of the terminal alkyl chains are indicated by digits (8, 12, 14, 16), and the amino fatty acids of the LAF building block by two-letter abbreviations (Bu, He, Oc) (**Scheme 1A**). Lysines connect the polar (Stp) and apolar (LAF) units into diverse topologies, for example bundles (N-terminal branched lipophilic domains), and U-shapes with hydrophilic center and lipophilic ends at the N- and C-terminus (**Scheme 1B, Table 1**). The hydrophilic/lipophilic balance within the carriers was varied by the adjustment of the ratio of Stp to LAF units. Lipophilic tertiary LAF amino groups of the LAF-Stp carriers are commonly not protonated at physiological pH, therefore the protonatable nitrogens are listed alternatively with and without consideration of lipophilic tertiary amines of the LAF units (**Table 1**).

So far, the LAF-Stp carriers were used in lipopolyplexes for pDNA, mRNA, and siRNA delivery [80]. In the current study their use as cationizable lipidic component within mRNA LNPs should be investigated. Hereto, a subset of the LAF-Stp carrier library was selected. The more lipophilic LAF-Stp carriers with only one polar Stp unit per molecule and an Stp/LAF ratio of 1:4 (bundle or U-shape topology) were considered to be most suitable for LNP formulations. For comparison, cationizable lipids DLin-MC3-DMA (MC3, as used in the Patisiran formulation) and SM-102 (as used in the Moderna COVID-19 vaccine) were included as commercially available gold standards. As a further control, the OleA-Stp bundle structure ***1829*** (**Figure 4, Table 1**) was synthesized as analog to LAF-Stp bundle ***1621***. Here, the LAF units were substituted by standard oleic acid. Since oleic acid is known to be efficient in lipo-oligomers [60] and ionizable lipids for LNP formulation and nucleic acid delivery [423], it was

considered as a suitable control motif. All LAF-Stp carriers used in the current study were synthesized and characterized as described in Thalmayr et al [80].

Scheme 1. LAF-Stp carriers as cationizable lipids for LNP formulations.

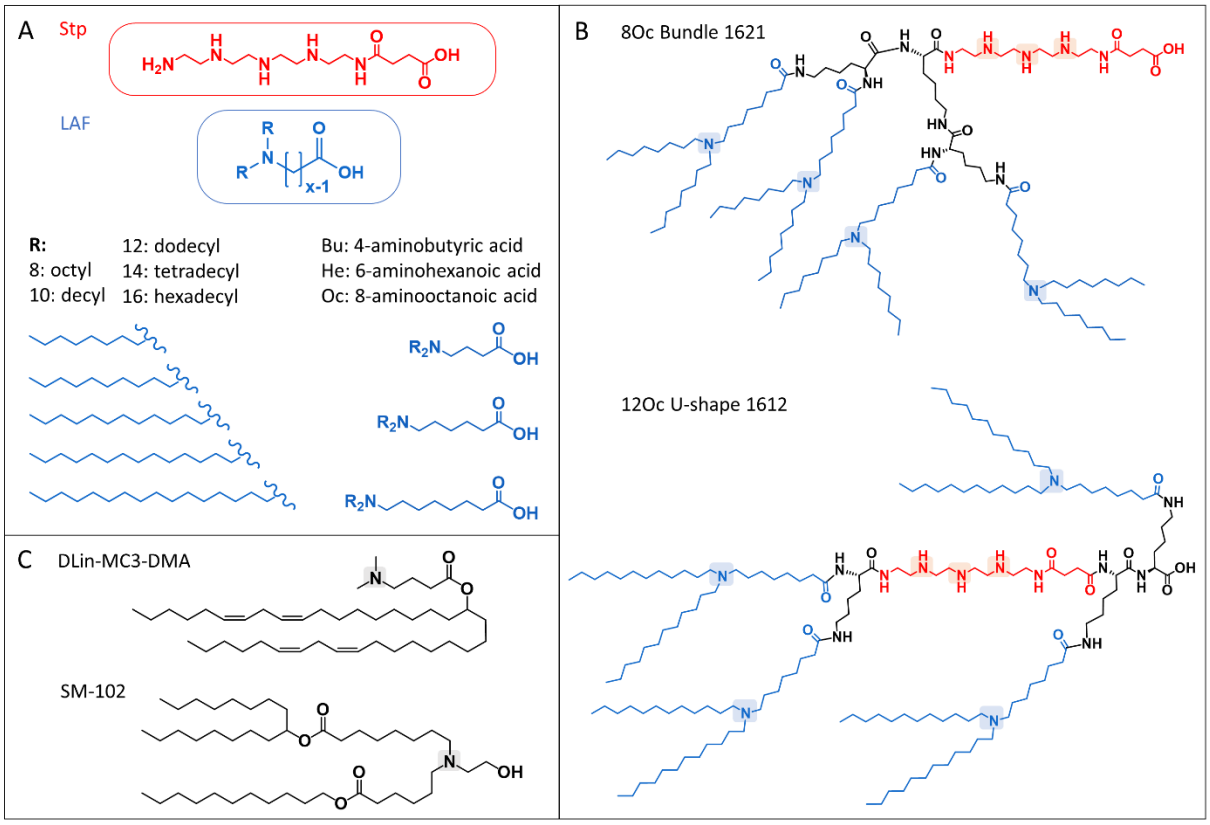

(A) Succinoyl-tetraethylene pentamine (Stp; red) and LAF (blue) as building blocks for mRNA LNP carriers. Different LAFs comprise ω-amino fatty acids of different carbon backbone length (Bu, He, Oc) with amines disubstituted with alky chains of different carbon lengths (8, 10, 12, 14, 16). By this variation, the position of the tertiary amine can be shifted within the LAF lipidic acid, resulting in different LAF types. **(B)** Different topologies of LAF-Stp carriers, exemplarily shown for sequences of 8Oc bundle ***1621*** and 12Oc U-shape ***1612***. The synthesis of LAF-Stp carriers was performed by Melina Grau (Pharmaceutical Biotechnology, LMU Munich). **(C)** Commercially available gold standards DLin-MC3-DMA and SM-102.

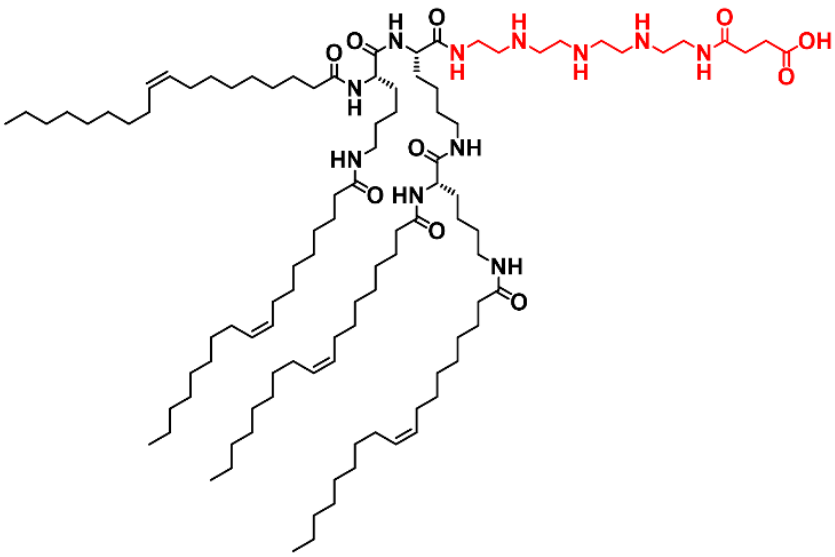

Figure 4. OleA-Stp bundle carrier ***1829***. Synthesis of OleA carrier ***1829*** was done by Tobias Burghardt (Pharmaceutical Biotechnology, LMU Munich).

LNPs were prepared by flash mixing (rapid pipetting) of the acidic aqueous phase (citrate buffer 10 mM, pH 4.0) containing FLuc mRNA with the ethanolic lipid phase composed of cholesterol, DSPC, PEG-DMG, and an ionizable carrier or lipid (**Scheme 2A**). LNPs were formulated at different molar and weight/weight (w/w) lipid ratios (**Scheme 2B**). **Table 2** also lists the N/P ratio, which corresponds to the molar ratio of all protonatable nitrogens of the carrier (secondary amines of Stp, tertiary amine of LAF, N-terminal amines) to negatively charged mRNA phosphates. All novel cationizable LAF-Stp carriers contain at least six amines, whereas DLin-MC3-DMA and SM-102 contain only one tertiary amine. At an identical N/P ratio, this would result in LAF-Stp LNPs with a strongly reduced total lipid/mRNA mass ratio compared to the DLin-MC3-DMA and SM-102 LNPs. Hence, the N/P ratio of LAF-Stp carriers was raised to 9 and similar w/w ratios of cholesterol/DSPC/PEG DMG/ionizable carrier were used as in the state-of-the-art formulations, resulting in different molar ratios of lipids (**Scheme 2B**). As mentioned above, not all LAF-Stp amines are protonated at physiological pH. Hence, an additional alternative calculation of the N/P ratio is provided in **Table 2**, without considering the lipophilic tertiary LAF amines (N/P ratio only including secondary amines of Stp and N-terminal amines). For additional information, the total lipids+carrier / mRNA ratio in weight% is presented in **Table 2**.

Scheme 2. mRNA LNP formulations.

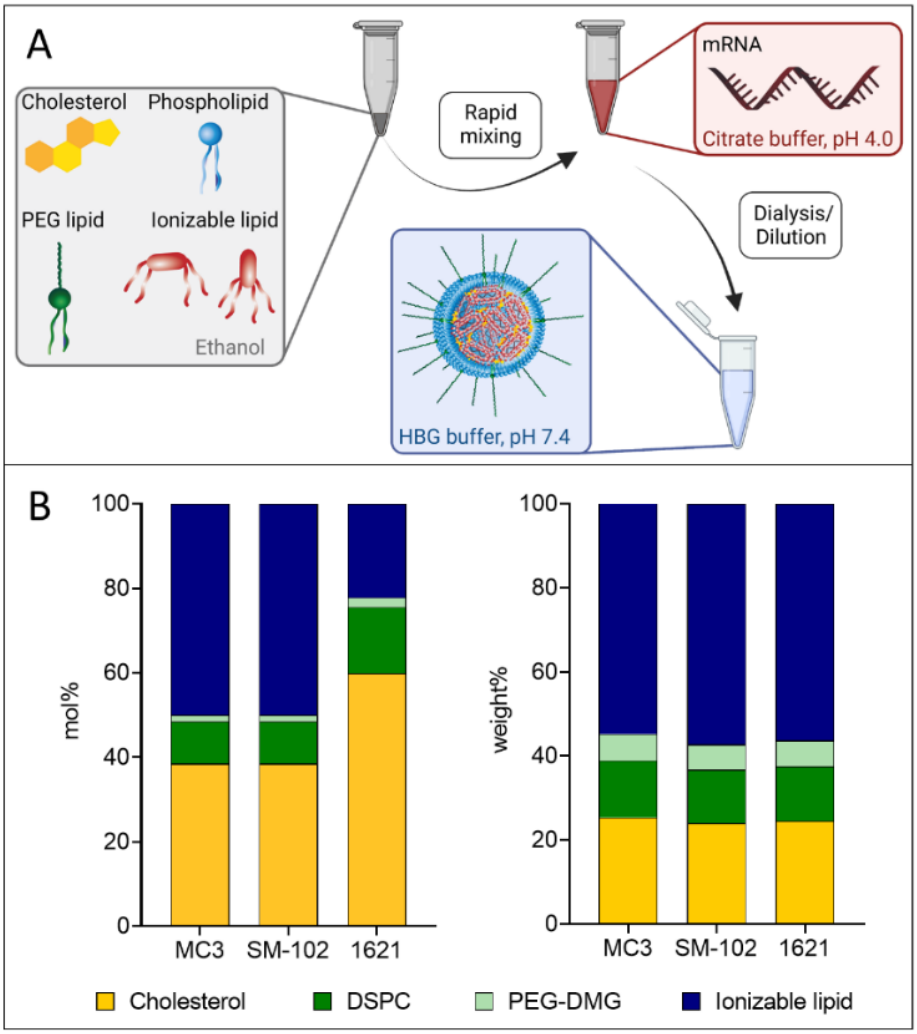

(A) LNPs were formulated by flash mixing an ethanol phase of cholesterol, phospholipids, PEG lipids and cationizable lipids (or LAF-Stp carriers) with an aqueous phase of mRNA using rapid pipetting, followed by dilution or dialysis with HBG buffer. **(B)** Molar and weight ratios of standard LNPs (MC3; SM-102,) and LAF-Stp LNPs (exemplarily shown for ***1621***).

3.3.2 Physicochemical characterization of mRNA LNPs

To figure out the requirements on the LAF-Stp carriers for LNP formulation, particles were physicochemically characterized regarding size distribution, zeta potential apparent surface pK_a, mRNA encapsulation efficiency, and stability of corresponding LNP formulations. DLS and ELS measurements revealed defined, homogeneous nanoparticles with hydrodynamic diameters of around 120–200 nm and an almost neutral zeta potential for the mRNA LNPs formulated with the novel LAF carriers, by

this exhibiting comparable particle properties like the standard LNPs formulated with DLin-MC3-DMA and SM-102 (**Figure 5**). Only in the case of U-shape ***1620*** (8Oc, Stp/LAF = 1:4), nanoparticle formation was problematic, resulting in larger particles with a z-average >270 nm. Moreover, the tested LAF-Stp LNPs successfully encapsulated mRNA (encapsulation efficiency ee ≥80%, except ***1613***), as determined via RiboGreen assay (**Table 3**). This was confirmed by a gel shift assay (**Figure 6**).

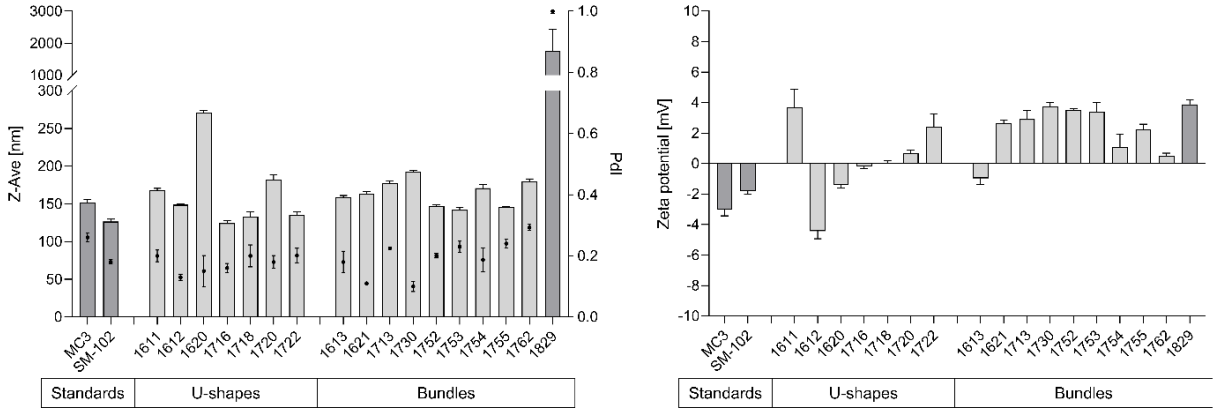

Figure 5. Particle characterization by dynamic and electrophoretic light scattering. Physicochemical characterization of mRNA LNPs formed with different LAF-Stp carriers (N/P 9) in comparison to standard LNPs DLin-MC3-DMA (N/P 3) and SM-102 (N/P 6) containing 3 µg/mL FLuc mRNA, regarding particle size (Z-Ave), polydispersity index (PdI), and zeta potential in indicated molar ratios (LNP compositions see **Table 2**). Data are presented as mean ± SD (n=3). Statistical analysis was done by unpaired Student's two-tailed t-test with Welch's correction; GraphPad Prism™ 9.5.1. Significance between ***1621*** and ***1829***: * $p \leq 0.05$.

Table 3. mRNA encapsulation efficiency (ee) in LNPs at N/P 9, determined by the RiboGreen assay.

LAF-Stp carrier	ee [%]
1611	93.6
1612	92.5
1613	78.9
1621	97.7
1716	100
1720	94.1
1752	90.0
1755	97.5

For LNP compositions, see **Table 2**.

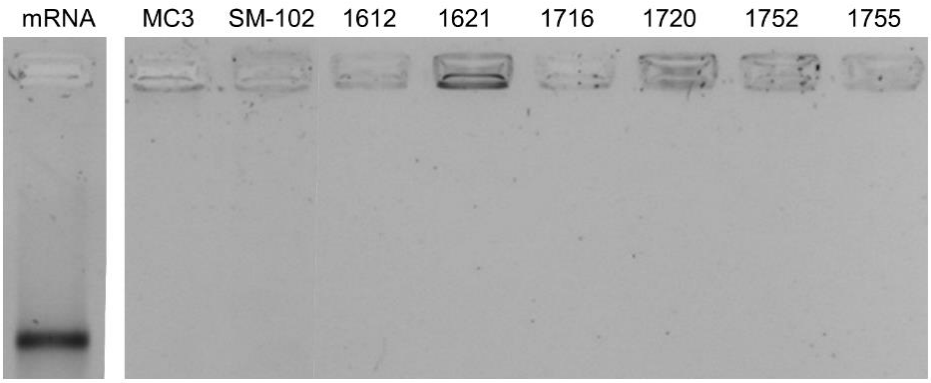

Figure 6. Agarose gelshift assay of FLuc mRNA LNPs formed with LAF-Stp carriers of different topologies containing different LAF motifs at N/P 9 in comparison to standard LNPs (DLin-MC3-DMA, SM-102), and free mRNA. LNP compositions see **Table 2**.

Additionally, the apparent surface pK_a of selected LNP formulations was determined by a TNS dye binding assay (**Table 4**). According to literature, the optimal pK_a of the LNP's surface is in the range of 6.2 to 6.5, resulting in neutral particles at physiological pH and positively charged particles in acidic endosomes, by this promoting endosomal disruption [387]. The results of the TNS dye binding assay were in accordance with the trend in zeta potential for the evaluated carriers, as 12Oc U-shape ***1612*** had the lowest apparent surface pK_a (pK_a = 5.1) and the lowest zeta potential of <-4 mV, followed by ***1613*** and ***1716***. Bundle ***1621*** seemed to be most beneficial with an apparent pK_a of 6.4 (**Table 4**).

Table 4. TNS dye binding assay for the surface pKa determination of mRNA LNPs at N/P 9.

LAF-Stp carrier	pKa
1612	5.1
1613	5.4
1621	6.4
1716	5.5

For LNP compositions, see **Table 2**.

The replacement of LAF by oleic acid strongly affected particle formation. Comparing 8Oc bundle ***1621*** with its OleA analog ***1829***, lack of aqueous solubility and aggregation in case of the latter was a severe issue (160 vs 1760 nm; **Figure 5**). Therefore, ***1829*** was excluded from further physicochemical and biological characterization.

Bundles were additionally characterized at N/P 18. Compared to N/P 9, significantly increased particle sizes were obtained at this N/P ratio, except for 12Oc bundle ***1613*** (**Figure 7**). Noteworthy, 8Oc bundle ***1621*** still formed monodisperse particles, yet size increased by 25 nm at the higher N/P ratio.

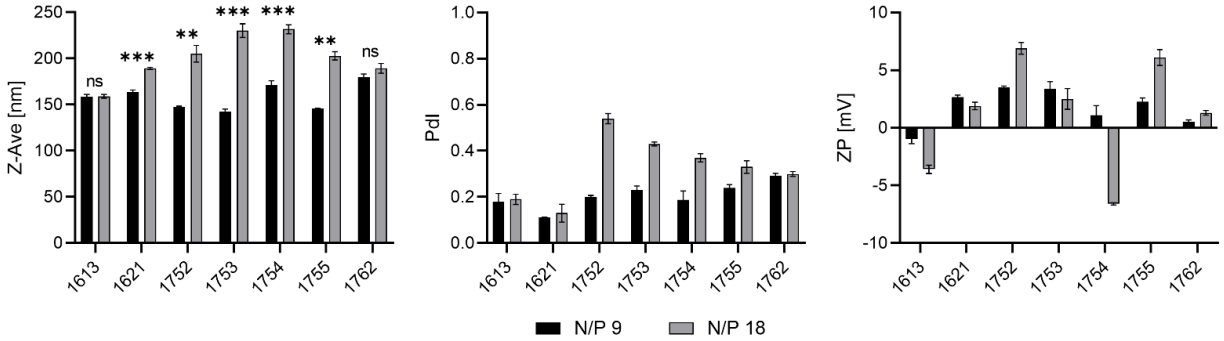

Figure 7. Physicochemical characterization of mRNA LNPs by dynamic and electrophoretic light scattering. mRNA LNPs formed with bundle carriers in N/P9 and N/P18 containing 3 µg/mL FLuc mRNA (LNP compositions see **Table 2**) were evaluated regarding particle size (Z-Ave), polydispersity index (PdI) and zeta potential (ZP). Data are presented as mean ± SD out of triplicates. Statistical analysis was done by unpaired Student's two-tailed t-test with Welch's correction; GraphPad Prism™ 9.5.1. Significant differences between N/P 9 and 18: ** $p \leq 0.01$; *** $p \leq 0.001$; ns, statistically not significant.

3.3.3 Biological evaluation of LAF-Stp carriers in mRNA LNPs

The LAF-Stp carriers were tested for their capability to deliver mRNA LNPs to three different tumor cell lines (N2a, HepG2, and Huh7) using a luciferase reporter assay (**Figure 8**). A standard luciferase mRNA dose (250 ng/well) [417] and a fourfold lower dose (62.5 ng/well) were chosen. Lipidic carriers with a Stp/LAF ratio of 1:4 (**Figure 8**) were significantly more efficient than more hydrophilic carriers with a Stp/LAF ratio of 1:2 or 2:4 (**Figure 9**). High luciferase expression for several LAF-Stp carriers as well as carrier- and cell line-dependent differences in luciferase expression were observed.

In N2a cells (**Figure 8A**), all LAF-Stp carriers outperformed DLin-MC3-DMA LNPs. LAF-Stp bundle ***1621*** (8Oc, Stp/LAF = 1:4) even outperformed SM-102 LNPs with 5-fold higher RLU values. ***1621*** analogs ***1752*** (12Bu) and ***1755*** (14He) as well as U-shape carriers ***1716*** (8Oc, Stp/LAF = 1:4) and ***1720*** (12Oc, Stp/LAF = 1:4) showed similar luciferase expression levels as SM-102. In HepG2 cells (**Figure 8B**), all carriers were comparable or superior to DLin-MC3-DMA, with SM-102 LNPs providing the highest transfection activity. In Huh7 cells (**Figure 8C**), ***1755*** and SM-102 containing LNPs ranked top. Also, bundle carriers ***1621*** (8Oc) and its LAF analogs ***1752*** (12Bu) and ***1754*** (12He) could reach high expression levels (10-fold higher than DLin-MC3-DMA). Noteworthy, LAF 8Oc bundle ***1621*** reached six log units higher RLU values than its OleA analog ***1829*** (**Figure 9**). This emphasizes the benefit of the cationizable LAF motif over a standard OleA fatty acid for mRNA transfection.

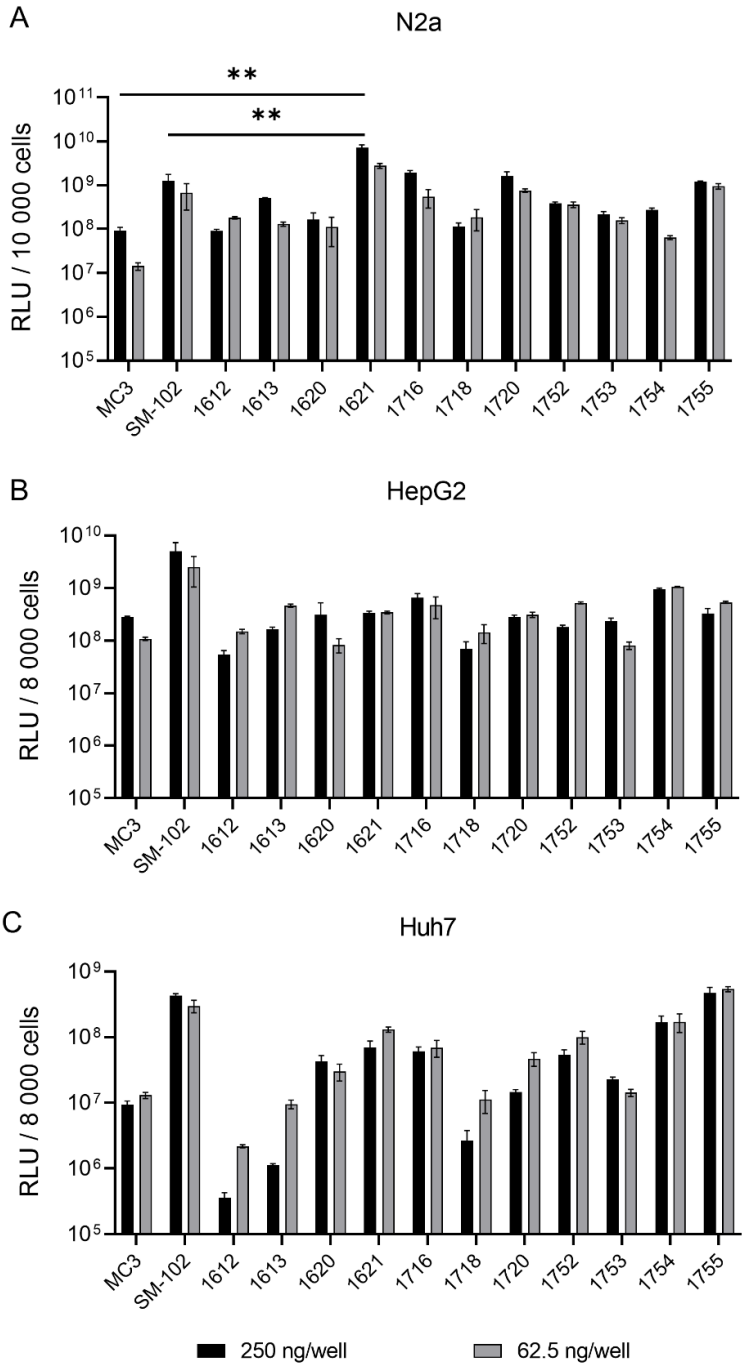

Figure 8. Luciferase expression induced by mRNA LNPs in different tumor cell lines. N2a **(A)**, HepG2 **(B),** and Huh7 **(C)** cells were transfected with mRNA LNPs at 250 ng and 62.5 ng FLuc mRNA per well. LNPs were prepared at N/P 9 and at different molar ratios and were compared to DLin-MC3-DMA (MC3, N/P 3) and SM-102 (N/P 6) LNPs serving as gold standards (LNP compositions see **Table 2**). Luciferase activity was measured 24 h after transfection and is shown as RLU values (n=3; mean ± SD) after background subtraction (HBG-treated control cells). Statistical analysis was done by unpaired Student's two-tailed t-test with Welch's correction; GraphPad Prism™ 9.5.1. Significant differences of 1621 vs MC3 and SM-102 at 250 ng mRNA/well: ** $p \leq 0.01$.

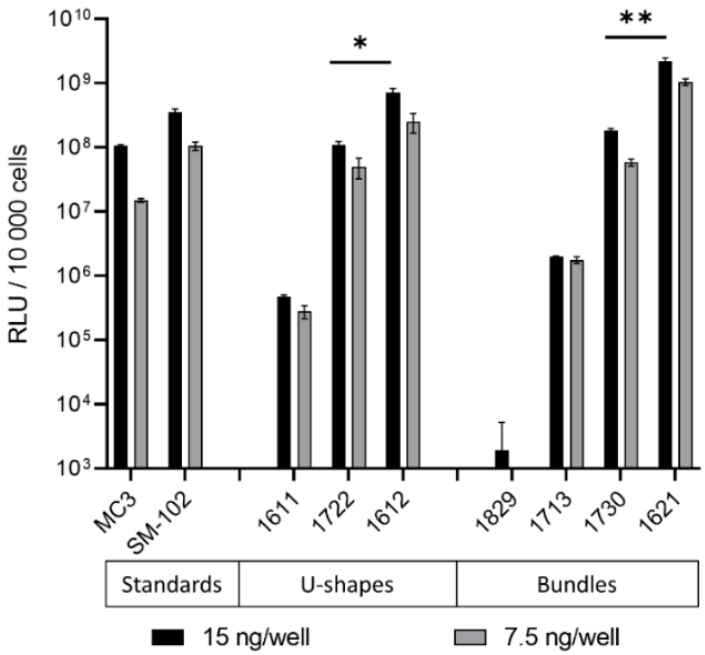

Figure 9. Luciferase activity in N2a cells after transfection with mRNA LNPs at 15 ng and 7.5 ng FLuc mRNA per well. LNPs were prepared at N/P 9 and different molar ratios and compared to DLin-MC3-DMA (MC3, N/P 3) and SM-102 (N/P 6) LNPs serving as gold standards (LNP compositions see **Table 2**). Luciferase activity was measured at 24 h after transfection (n=3, mean ± SD) and is shown as RLU values after background subtraction (HBG-treated control cells). Statistical analysis was done by unpaired Student's two-tailed t-test with Welch's correction; GraphPad Prism™ 9.5.1. Significant differences between Stp/LAF ratios of 2:4 (U-***1722***; B-***1730***) and 1:4 (U-***1612***; B-***1621***) at an mRNA dose of 15 ng/well: * $p \leq 0.05$; ** $p \leq 0.01$.

mRNA that encodes for fluorescent mCherry reporter protein and flow cytometry was utilized to assess the transfection efficiency at the cellular level (**Figure 10**). Hereby, the mean fluorescence intensity (MFI) correlates with mCherry protein expression of the total cell population. Carriers that mediated high luciferase expression also displayed high mCherry expression in almost 100% of cells, even at a low mRNA dose of 15 ng/well. The top-performing structures identified in the luciferase activity assay (8Oc bundle ***1621***, and 12Oc U-shape ***1716***) also proved to be the most effective carriers in the flow cytometry study. They outperformed the gold standards DLin-MC3-DMA and SM-102 regardless of the applied mRNA dose. Only for ***1612*** and ***1755***, a discrepancy between the mean fluorescence intensity and the results of the luciferase activity assay was observed. 12Oc U-shape ***1612*** was highly efficient with almost 100% transfected cells, but performed less effective in the luciferase reporter assay.

Compared to 8Oc bundle ***1621***, 12Oc analog ***1613*** yielded <90% mCherry positive cells, which also matched with the lower MFI and RLU values.

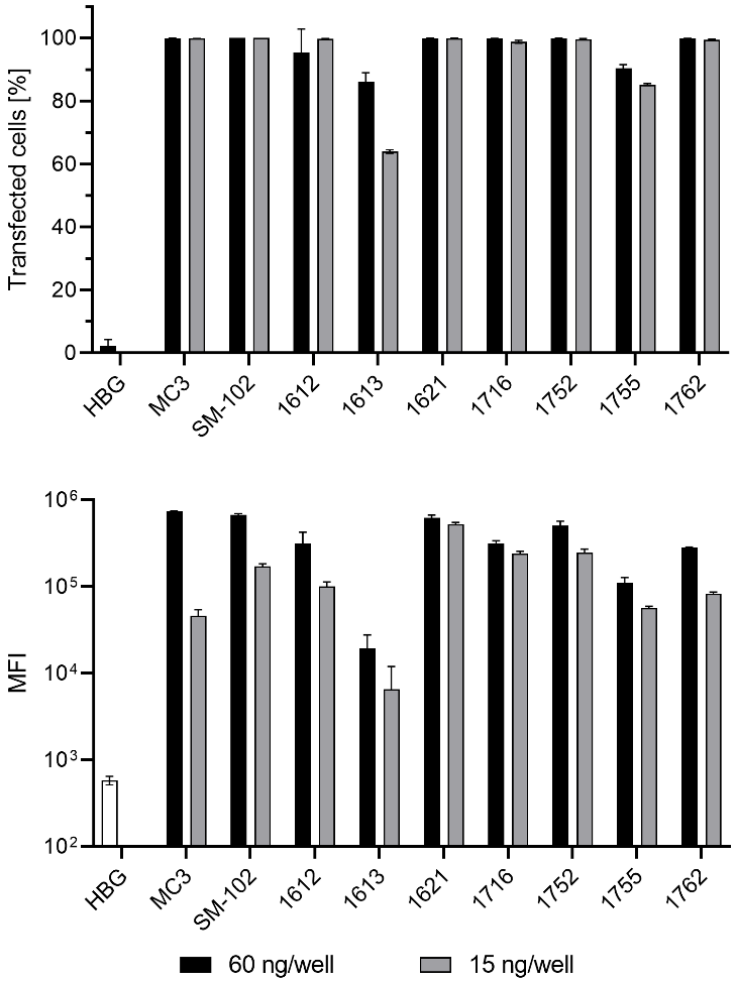

Figure 10. Transfection efficiency of mRNA LNPs in N2a cells as assessed by flow cytometry. (A) Transfection of 60 ng and 15 ng mCherry mRNA per well. LNPs were prepared at N/P 9 and at different molar ratios and were compared to DLin-MC3-DMA (MC3, N/P 3), and SM-102 (N/P 6) LNPs serving as positive controls (LNP compositions see **Table 2**). mCherry expression was measured 24 h after transfection (n=3; mean + SD) and is determined by the percentage of cells expressing mCherry protein 24 h post treatment. Flow cytometry measurements were performed together with Mina Yazdi (Pharmaceutical Biotechnology, LMU Munich).

The bundle carriers with different LAF motifs were further tested at an additional N/P ratio of 18 in two different cell lines (N2a, HeLa) at low mRNA concentrations of 15 ng/well (**Figure 11A**). In N2a cells, all bundles, except 12Oc carrier ***1613***, could reach RLU levels as high as SM-102 and clearly outperformed DLin-MC3-DMA up to sixfold. In HeLa cells, terminal alkyl chains consisting of dodecyl and hexadecyl were less favorable. Nevertheless, 12Oc ***1613*** was at least comparable to SM-102, and 16Bu ***1753*** showed even higher RLU values. All other bundles reached even higher expression levels than SM-102.

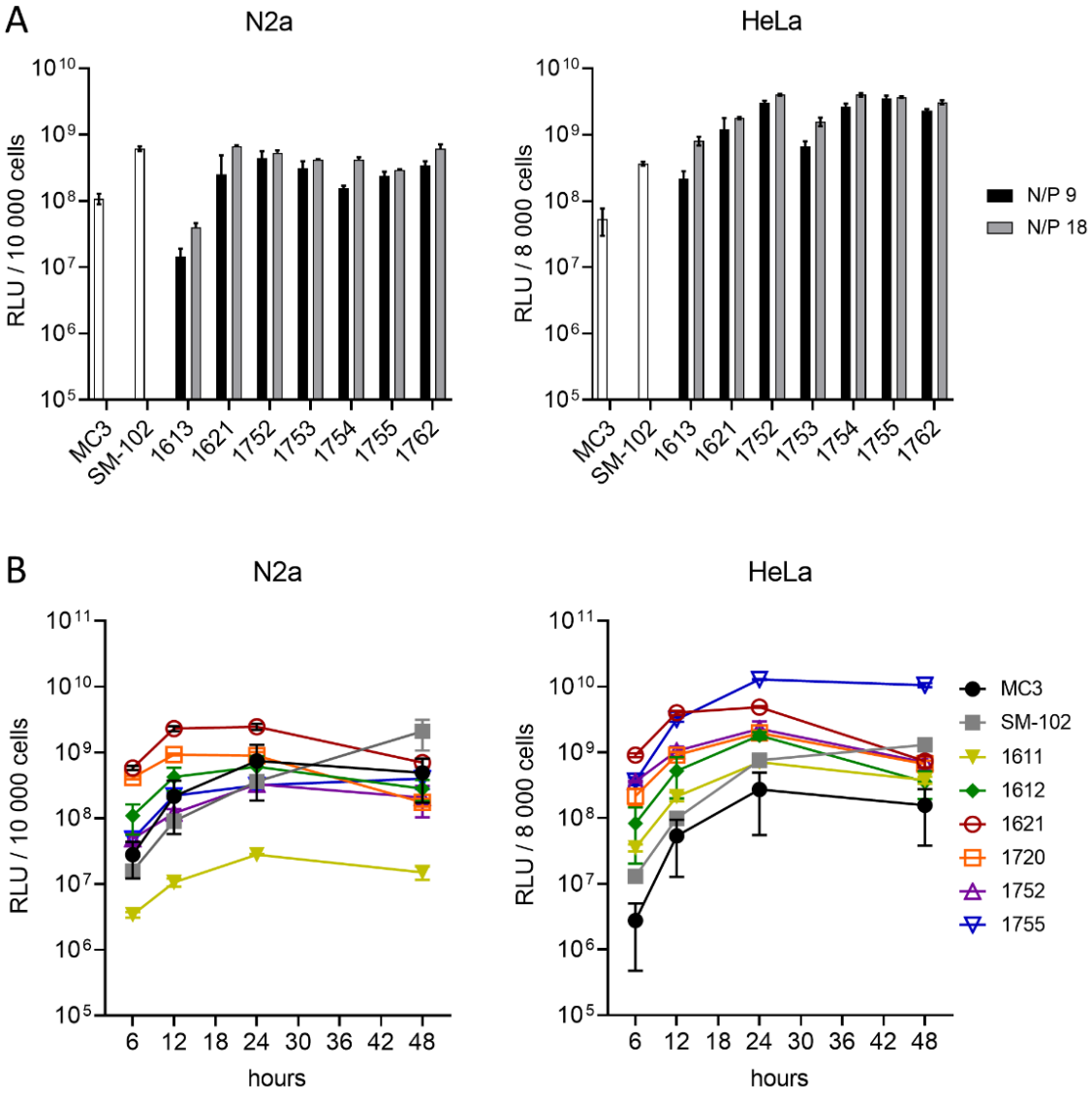

Figure 11. Luciferase expression induced by mRNA LNPs in N2a (left) and HeLa cells (right). (A) Transfection of 15 ng FLuc mRNA per well. LNPs were prepared at N/P 9 and N/P 18 and at different molar ratios and were compared to DLin-MC3-DMA (MC3, N/P 3) and SM-

102 (N/P 6) LNPs serving as gold standards (LNP compositions see **Table 2**). Luciferase activity was measured 24 h after transfection and is shown as RLU values (n=3; mean ± SD) after background subtraction (HBG-treated control cells). **(B)** Transfection kinetics. Time-dependent luciferase expression after transfection of 60 ng FLuc mRNA per well on N2a and Hela cells. LNPs were prepared at N/P 9 and at different molar ratios and were compared to DLin-MC3-DMA (MC3, N/P 3) and SM-102 (N/P 6) LNPs serving as gold standards (LNP compositions see **Table 2**). Luciferase activity was measured 6, 12, 24, and 48 h after transfection and is shown as RLU values (n=3; mean ± SD) after background subtraction (HBG-treated control cells).

To figure out the best time point for the detection of reporter mRNA expression, the transfection kinetics of a selection of LAF-Stp carriers with different topologies and LAF domains was evaluated (**Figure 11B**) in two different cell lines (N2a, HeLa). Generally, the highest transfection efficiencies were reached after 24 h of incubation, except for SM-102 being most efficient after 48 h. Nevertheless, the LAF-Stp carriers, especially those with an Stp/LAF ratio of 1:4 (8Oc bundle ***1621***, 12Oc U-shapes ***1612*** and ***1720***), showed remarkably fast transfection kinetics. At 6 h post transfection, they already reached at least 10-fold higher RLU levels than SM-102 in both cell lines. They could outperform the gold standards DLin-MC3-DMA and SM-102 by far. Especially 8Oc bundle ***1621*** maintained high transfection efficiency after 12-24 h in both cell lines, and 14He bundle ***1755*** showed the highest mRNA expression in HeLa cells after 24 and 48 h overall. 12Oc U-shape ***1611*** (Stp/LAF = 1:2) was only moderately efficient. All in all, the LAF-Stp carriers displayed faster transfection kinetics than DLin-MC3-DMA and SM-102 and were superior at early time points (e.g., ***1621*** vs SM-102 at 6 h: 37-fold higher RLU values, ** p = 0.0020 in N2a cells, and 70-fold higher RLU values, ** p = 0.0017 in HeLa cells).

In addition to N2a and Huh7 cells, a selection of carriers was tested in the DC-like cell line DC2.4 and in the macrophage model cell line J774A.1 using different low mRNA concentrations. Only best performing carriers with a Stp/LAF ratio of 1:4, different topologies and LAF motifs were chosen. Biological evaluation was carried out using a luciferase reporter assay (**Figure 12**), and cytotoxicity was assessed by measuring the metabolic activity of transfected cells via an MTT assay (**Figure 13**). High luciferase expression was observed for several LAF-Stp carriers. At the highest concentration (30 ng/well), the difference between the carriers did not stand out as much as at lower

concentrations. Especially for the best performing LAF-Stp carrier ***1621*** (8Oc, Stp/LAF = 1:4), very high luciferase expression was observed even at the lowest dose (3 ng/well) in all cell lines. DLin-MC3-DMA was outperformed by far in N2a, DC2.4 and J774A.1 cells. Especially in immune cells (DC2.4 and J774A.1), there did not appear to be any significant dose dependency for ***1621***, as 30 and 3 ng/well yielded similar RLU levels. ***1621*** analog ***1755*** (14He) showed comparable levels of transfection efficiency to SM-102 in N2a, Huh7 and J774A.1 cells, whereas it was less efficient in DC2.4 cells. Dose reduction maintained high transfection efficiencies but reduced toxicity, which was observed at higher doses (30 ng/well) (**Figure 13**).

In terms of cytotoxicity, the critical dose was cell line-dependent. In N2a cells, relatively high mRNA doses of 30 ng/well were still well tolerated, whereas in Huh7, DC2.4 and J774A.1 cells a reduced dose of 15 ng/well was required. Especially LAF-Stp U-shapes showed rather high cytotoxicity at higher mRNA dose compared to bundle carriers in tumor cell lines (N2a, Huh7). It can be assumed that mechanisms for effective mRNA delivery, such as destabilization of the lipid membrane, may cause toxic effects. Nevertheless, this can be managed by lowering the mRNA dose and choosing a suitable carrier.

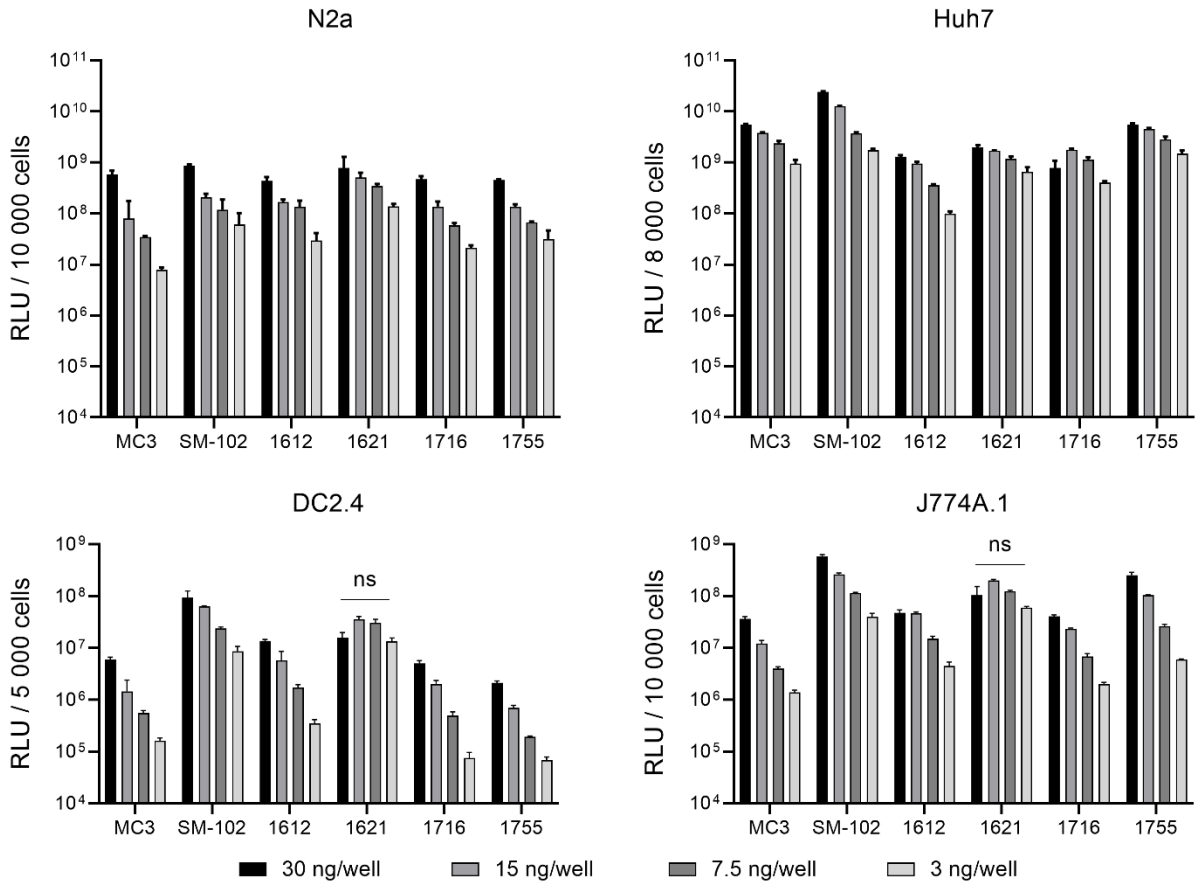

Figure 12. Luciferase expression induced by mRNA LNPs in N2a, Huh7, DC2.4 and J774A.1 cells. Cells were transfected with mRNA LNPs at FLuc mRNA doses of 30, 15, 7.5, and 3 ng/well. LNPs were prepared at N/P 9 at different molar ratios and were compared to DLin-MC3-DMA (MC3, N/P 3) and SM-102 (N/P 6) LNPs serving as gold standards (LNP compositions see **Table 2**). Luciferase activity was measured at 24 h after transfection and is shown as RLU values (n=3; mean + SD) after background subtraction of HBG-treated control cells. Statistical analysis was done by unpaired Student's two-tailed t-test with Welch's correction; GraphPad Prism™ 9.5.1. Statistical differences for 1621 LNPs at highest vs lowest applied mRNA dose: ns, not significant. Transfections of DC2.4 and J774A.1 cells were performed and measured by Dr. Simone Berger (Pharmaceutical Biotechnology, LMU Munich).

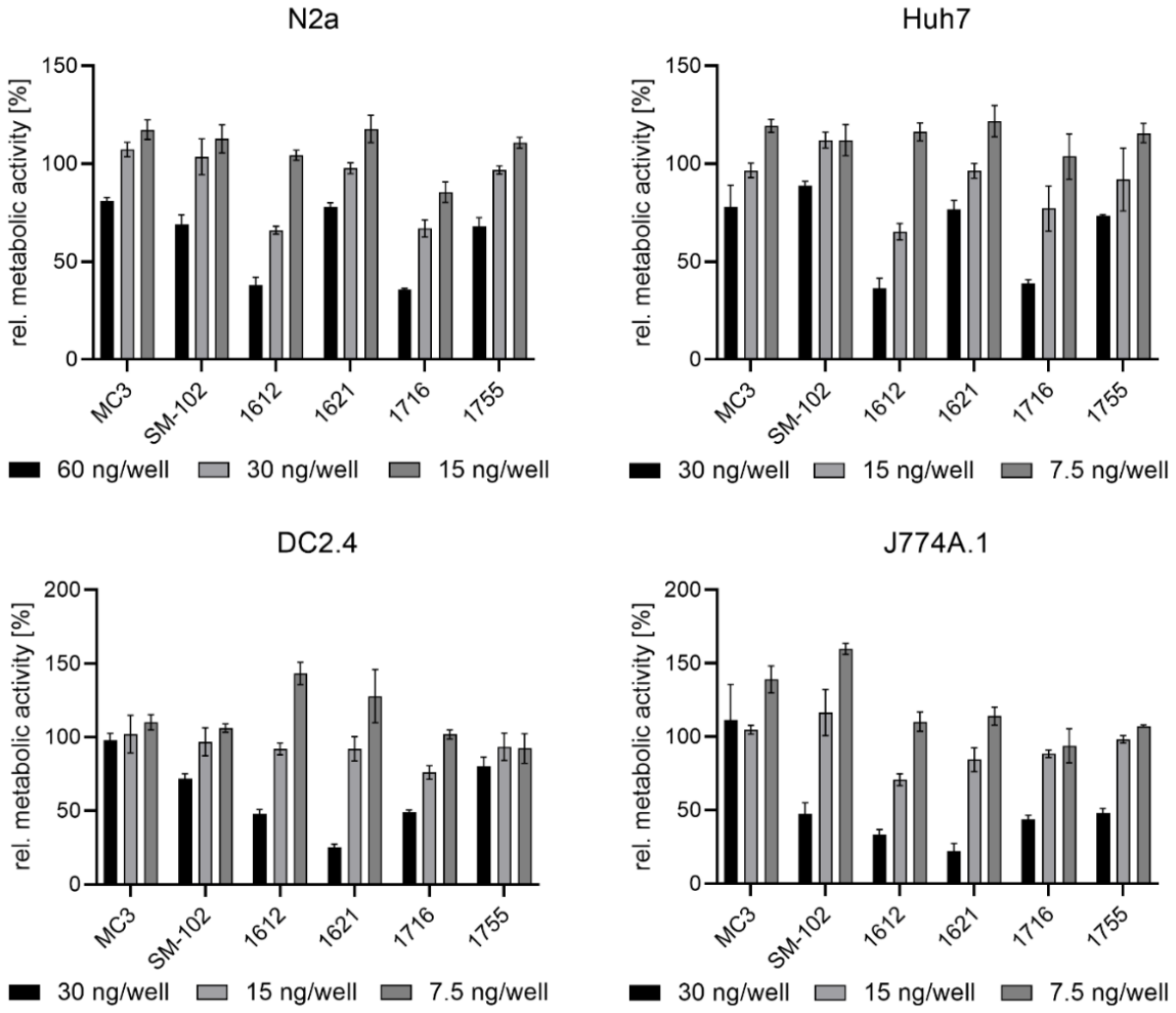

Figure 13. Metabolic activity of different cell lines (N2a, Huh7, DC2.4, J774A.1) transfected with FLuc mRNA LNPs at the indicated mRNA doses/well, determined via MTT assay at 24 h after transfection. Metabolic activity is presented in relation to HBG-treated control cells (n=3; mean ± SD). LNP compositions see **Table 2.** Transfections of DC2.4 and J774A.1 cells were performed and measured by Dr. Simone Berger (Pharmaceutical Biotechnology, LMU Munich).

3.3.4 Mechanistic studies on endosomal escape of mRNA LNPs

To gain a better understanding of the delivery process of LAF-Stp LNPs, mechanistic studies on the endosomal escape were carried out. Only carriers with a preferable Stp/LAF ratio of 1:4, different topologies and LAF motifs were evaluated. Due to the pH-dependent reversibly protonatable LAF building blocks and the previously described fast transfection kinetics (**Figure 11B**) of the LAF-Stp carriers, a fast

endocytosis upon destabilizing effects on the endosomal membrane was expected. The following evidence supports this hypothesis. Intracellular uptake of Cy5-labeled mRNA LNPs into endolysosomal vesicles and destabilization/disruption of endosomal membranes was monitored by CLSM at 4 h after transfection of HeLa cells that stably expressed the Galectin-8 mRuby3 fusion protein (HeLa-Gal8-mRuby3) [419-421] (**Figure 14A**). When endosomes are disrupted, the Gal8-mRuby3 protein interacts with the glycans present on the inner surface of the endosomal membranes, leading to green-fluorescent spots. As observed in HBG-treated control cells, the cells exhibited a dispersed cytosolic pattern of Gal8-mRuby3 distribution in the cytosol, when endosomal membrane destabilization was not present. All LAF-Stp carriers predominantly facilitated cellular uptake of the corresponding mRNA LNP through endocytosis, as visualized by Cy5-labeled mRNA (red dots), and mediated endosomal membrane destabilization, resulting in membrane disruption (green dots). Certain LAF-Stp carriers exhibited more notable cellular internalization than others. Especially for the 8Oc bundle carrier ***1621*** and 12Oc U-shape ***1716***, cellular internalization via endocytosis was most pronounced as indicated by large, partly overlapping Gal8 and mRNA positive areas (yellow). 8Oc bundle ***1621*** was most effective in promoting endocytosis with a greater quantity of endosomal mRNA (red dots) compared to the other carriers. LAF-Stp carriers showed higher endosomal escape after 4 h than standard LNPs DLin-MC3-DMA and SM-102. At that early time point and relatively low mRNA dose (135 ng/300 µL medium per well), both the mRNA uptake and the endosomal disruption mediated by the standard formulations was hardly detectable. This is in accordance with the results of the transfection kinetic studies (**Figure 11B**), where the standard formulations (DLin-MC3-DMA and SM-102) showed slower transfection kinetics and needed longer incubation times to reach high transfection rates than LAF-Stp LNPs.

Furthermore, the pH-dependence of endosomolytic activity was evaluated in a bafilomycin A1 (BafA1) assay in N2a cells (**Figure 14B**). BafA1 specifically hinders endosomal acidification by inhibition of the endosomal proton pump (vacuolar H^+ ATPase). When cells were treated with BafA1 prior to transfection, the transfection efficiencies of the mRNA LNPs were significantly decreased. Especially the standard LNPs showed a strong BafA1 effect, resulting in a massive decrease in RLU values (52-fold for DLin-MC3-DMA, 144-fold for SM-102). Also for the LAF-Stp U-shapes, a

BafA1 effect was visible, but less distinctive (12-fold for ***1612***, and 22-fold for ***1716***). In the case of bundles, the BafA1 effect was less pronounced; the RLU values decreased only by sevenfold for ***1755*** (14He) and by approx. threefold for ***1621*** (8Oc).

In summary, the results of the BafA1 assay indicate that endosomal acidification was crucial for efficient mRNA delivery in the case of U-shaped LAF-Stp carriers, such as ***1612*** and ***1716***, and especially for the standard DLin-MC3-DMA and SM-102 LNPs (**Figure 14B**). However, it was not absolutely necessary for 8Oc bundle ***1621***, which also showed the highest amount of cytosolic mRNA release and endosomal destabilization in the CSLM images (**Figure 14A**). Here, fast endosomal escape seemed to be mediated largely regardless of endosomal acidification. Possibly, in addition to endocytosis into acidifying endosomes, other uptake mechanisms may exist, such as fast passage through various lipid membranes at neutral pH, which would be consistent with the fast kinetics of mRNA expression already after 4 h.

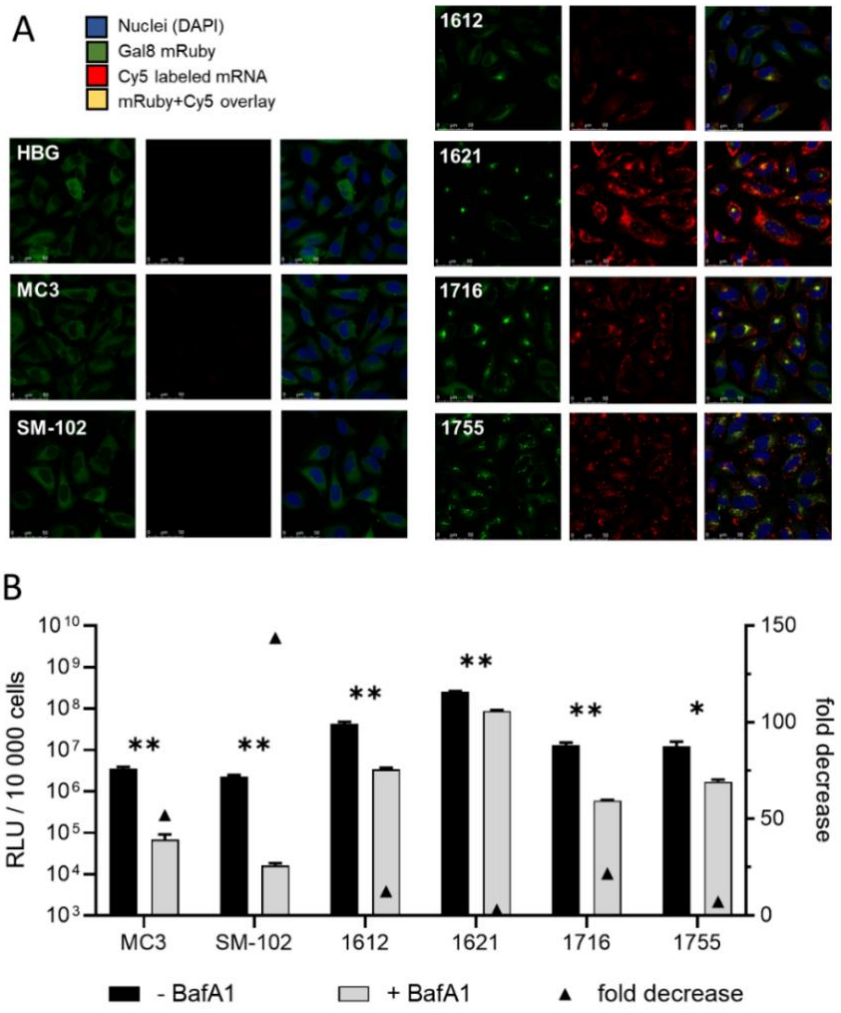

Figure 14. Mechanistic studies. (A) Rupture of endosomes in HeLa Gal8-mRuby3 cells (green) transfected with LNPs containing 135 ng/well mRNA (20% Cy5-labelled; red) after 4 h as assessed by CLSM. The nuclei were stained with DAPI (blue). CLSM images were captured by Miriam Höhn (Pharmaceutical Biotechnology, LMU Munich) **(B)** Influence of endosomal protonation on mRNA LNP transfection efficiency using bafilomycin A1 (BafA1) as an H^+-ATPase inhibitor. Transfection of 60 ng FLuc mRNA per well of N2a cells untreated ("-BafA1", black) or treated with 200 nM BafA1 ("+BafA1", grey) 2 h before transfection. LNPs were prepared at N/P 9 and at different molar ratios and were compared to MC3, N/P 3 and SM-102, N/P 6 LNPs serving as gold standards (LNP compositions see **Table 2**). Luciferase activity was measured 4 h after transfection and is shown as RLU values (n=3; mean + SD) after background subtraction (HBG-treated control cells). Statistical analysis was done by unpaired Student's two-tailed t-test with Welch's correction; GraphPad Prism™ 9.5.1. Significance between "-BafA1" and "+BafA1": * $p \leq 0.05$; ** $p \leq 0.01$.

3.3.5 Screen of mRNA LNPs in presence of full serum

The translation from *in vitro* to the *in vivo* setting poses several challenges since *in vitro* models cannot accurately mimic the physiological environment. When LNPs are administered intravenously (i.v.), they come into contact with various blood components such as plasma proteins, which adsorb onto the nanoparticle surface and can affect their cellular interaction [424, 425]. Thus, the transfection efficiency of mRNA LNPs was evaluated in the presence of serum in four different cell lines (N2a, Huh7, DC2.4, and J774A.1) as a pre-screening for *in vivo* studies. Additionally, the mRNA dose was further titrated down to 150 pg/well.

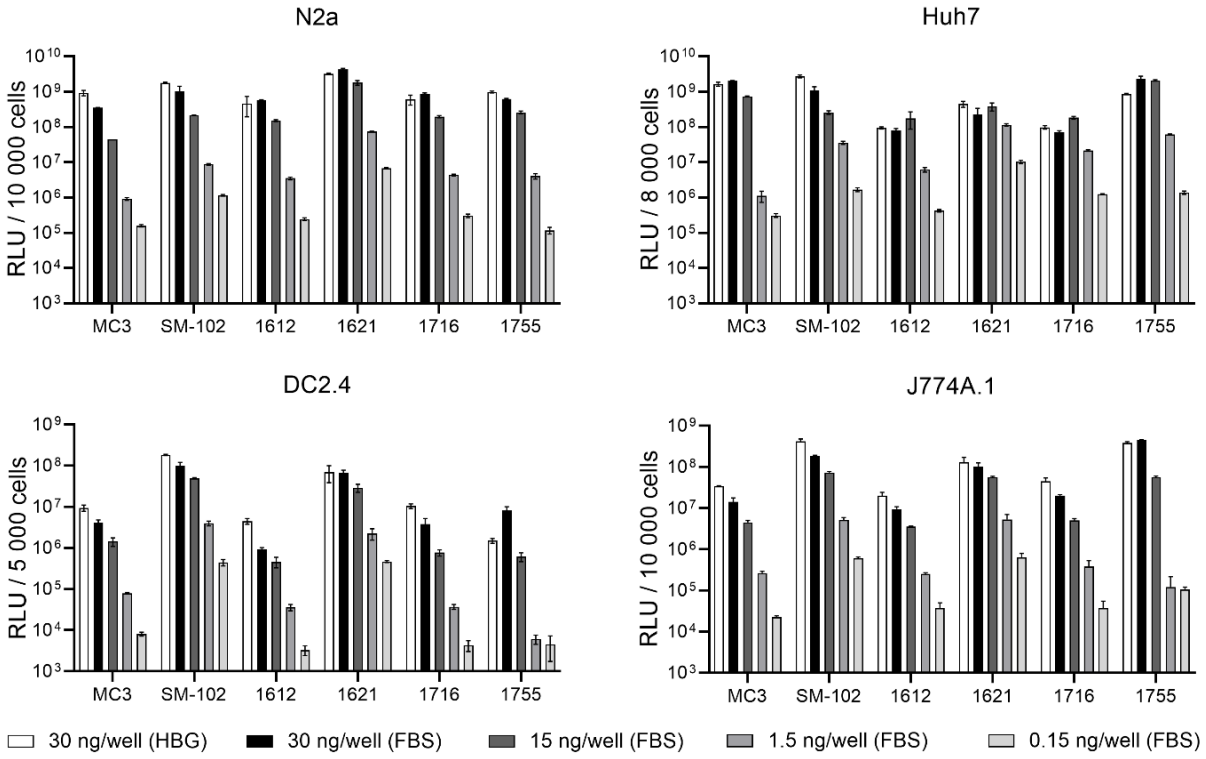

Figure 15. Luciferase activity after transfection with mRNA LNPs in the presence of high serum in different cell lines. Transfection efficiency of fetal bovine serum (FBS)-diluted mRNA LNPs at the indicated FLuc mRNA doses in N2a, Huh7, DC2.4, and J774A.1 cells in comparison to LNPs diluted in HBG (30 ng/well). Prior to transfection, LNPs were diluted in serum or HBG (30 ng/well containing 50% serum or HBG, 15 ng/well containing 75% serum, 1.5 ng/well containing 97.5% serum, and 0.15 ng/well containing 99.75% serum) and then transfected in standard 10% FBS containing cell culture medium. Luciferase activity was evaluated at 24 h after transfection (n=3; mean ± SD). DLin-MC3-DMA (MC3), N/P 3; SM-102, N/P 6; ***1612***, ***1621***, ***1716*** and ***1755***, N/P 9 (LNP compositions see **Table 2**). Transfections of DC2.4 and J774A.1 cells were performed and measured by Dr. Simone Berger (Pharmaceutical Biotechnology, LMU Munich).

Generally, in all cell lines incubation in full (up to 99%) serum resulted in a comparable transfection efficiency as obtained in standard 10% FBS containing cell culture medium (**Figure 15**). All tested LAF-Stp carriers were highly active in the presence of serum at higher mRNA doses. Especially 8Oc bundle ***1621*** was extremely efficient, outperforming DLin-MC3-DMA by far and showing high RLU values in all cell lines comparable (DC2.4, J774A.1) or superior (N2a, Huh7) to SM-102. Noteworthy, at the very low mRNA dose of 150 pg/well, ***1621*** reached around one log unit higher RLU

levels than SM-102 in N2a and Huh7 cells. 14He bundle ***1755*** was very potent and even superior to ***1621*** at higher mRNA doses (30 and 15 ng/well), particularly in Huh7 and J774A.1 cells. U-shapes (***1612, 1716***) were inferior to bundles in the presence of full serum and showed lower transfection efficiency.

3.3.6 *In vivo* application of mRNA LNPs

In sum, cell culture experiments identified bundles such as ***1621*** and its LAF analogs as most effective and superior to U-shape carriers (**Figures 8, 10-12, 15**). Nevertheless, to evaluate one representative of each topology class, U-shape ***1612*** and bundle ***1621*** were chosen for intravenous application of 3 µg FLuc mRNA per mouse in an N2a tumor model. LNPs were dialyzed against HBG for 2 h to completely remove residual ethanol for *in vivo* studies. At 6 h post injection, organs were retrieved; the quantitated luciferase expression per gram organ is shown in **Figure 16**. No visible toxicity was observed; standard plasma parameter (ALT, alanine transaminase; AST, aspartate aminotransferase; Crea, creatinine; BUN, blood urea nitrogen) are displayed in **Figure 17**. The well-established SM-102 LNPs mediated maximal expression in the liver by being >10-fold higher than DLin-MC3-DMA LNPs and >100-fold higher than the LAF-Stp LNPs. SM-102 LNPs also mediated the highest expression in the subcutaneous N2a tumors. However, despite their far lower potency in the liver and tumor, 12Oc U-shape ***1612*** and 8Oc bundle ***1621*** LNPs elicited RLU values as high as DLin-MC3-DMA and SM-102 in the spleen, thereby showing a much higher spleen selectivity. In the case of ***1612***, luciferase activity per gram organ in the spleen was 60-fold higher than in the liver ($p \leq 0.05$), and for ***1621*** even 350-fold ($p \leq 0.01$).

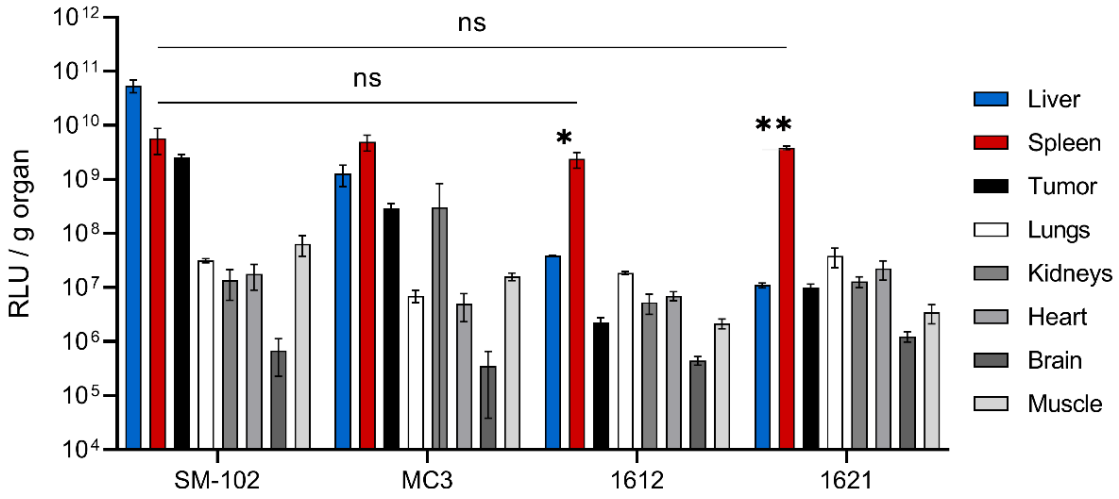

Figure 16. Luciferase expression of mRNA LNPs in different organs. N2a tumor-bearing A/J mice were intravenously injected with LNP formulations containing 3 µg FLuc mRNA in 150 µL HBG per mouse. LNPs were prepared at N/P ratios 3 (DLin-MC3-DMA, MC3), 6 (SM-102), or 9 (1612, 1621) at different molar ratios (LNP compositions see **Table 2**). Luciferase activity in RLU was determined *ex vivo* per gram (g) organ at 6 h post injection (n=3; mean ± SD). Statistical analysis was done by unpaired Student's two-tailed t-test with Welch's correction; GraphPad Prism™ 9.5.1. Significance between liver and spleen expression: * $p \leq 0.05$ for ***1612***, ** $p \leq 0.01$ for ***1621***. Significance between SM-102 and ***1612*** or ***1621***, in spleen expression: ns, statistically not significant. The in vivo study was performed by Jana Pöhmerer and Ulrich Wilk (Pharmaceutical Biotechnology, LMU Munich).

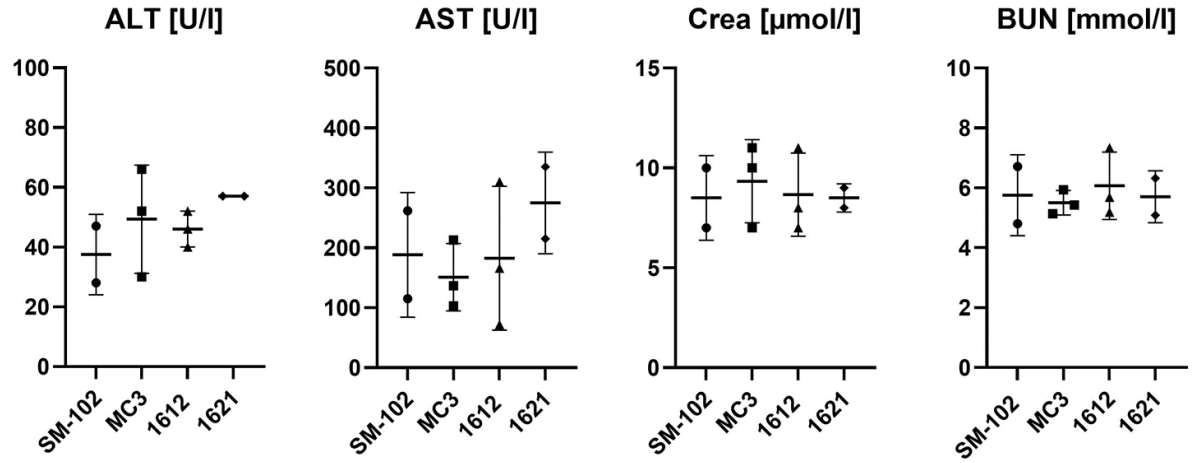

Figure 17. Evaluation of standard plasma parameters after intravenously applied FLuc mRNA LNPs in N2A tumor-bearing A/J mice. Administration as described for **Figure 16**. Blood samples were taken at 6 h after injection. 3 µg FLuc mRNA; DLin-MC3-DMA (MC3, N/P 3), SM-102 (N/P 6), ***1612*** and ***1621*** (N/P 9); SM-102 (n=2), DLin-MC3-DMA (MC3, n=3), ***1612***

(n=3), ***1621*** (n=2). The evaluation of standard plasma parameters was performed by Jana Pöhmerer (Pharmaceutical Biotechnology, LMU Munich).
ALT, alanine transaminase; AST, aspartate aminotransferase; Crea, creatinine; BUN, blood urea nitrogen.

Based on their high transfection activity in the spleen, SM-102 and ***1621*** LNPs were applied for eGFP mRNA delivery in tumor-free A/J mice to delineate cell type-specific transfection efficacies of immune cells within the liver, the spleen, and the lungs (**Figure 18**). Standard plasma parameter (ALT, AST, Crea, BUN) are displayed in **Figure 19**, and demonstrated good biocompatibility of the LNPs.

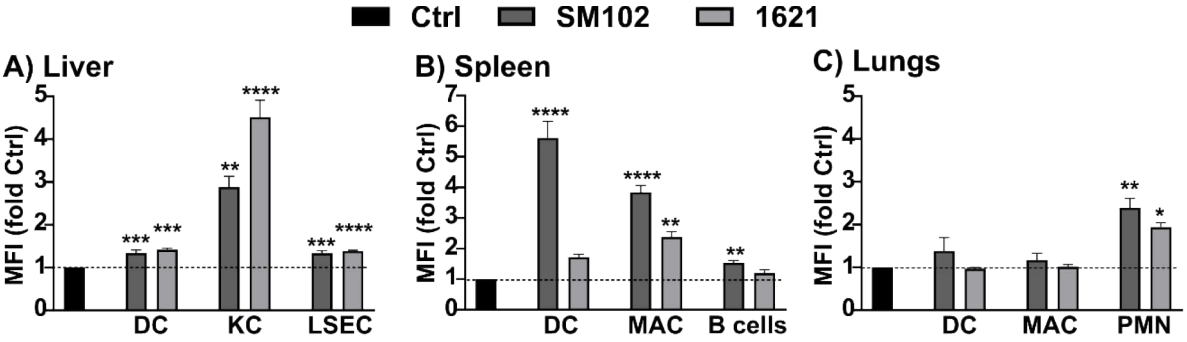

Figure 18. eGFP expression in immune cells of liver, spleen, and lungs at 6 h after intravenous administration of LNP formulations containing 3 µg eGFP mRNA in 150 µL HBG per mouse (n=5; mean + SEM). SM-102 (N/P 6); ***1621*** (N/P 9); LNP compositions see **Table 2**. Gating was performed according to the gating strategies displayed in **Figure 2** and **3**. eGFP expression presented as mean fluorescence intensity (MFI) was normalized to HBG-treated controls (Ctrl). Statistical analysis was done by one-way ANOVA, Tukey test; GraphPad Prism™ 9.5.1. Significant differences vs Ctrl: * $p \leq 0.05$; ** $p \leq 0.01$; *** $p \leq 0.001$; **** $p \leq 0.0001$. DC, dendritic cells; MAC, macrophages; KC, Kupffer cells; B cells; PMN, polymorphonuclear leukocytes/neutrophils; and LSEC, liver sinusoidal endothelial cell. The experiments and analysis were carried out by Yanira Zeyn (Department of Dermatology, University Medical Center, JGU Mainz).

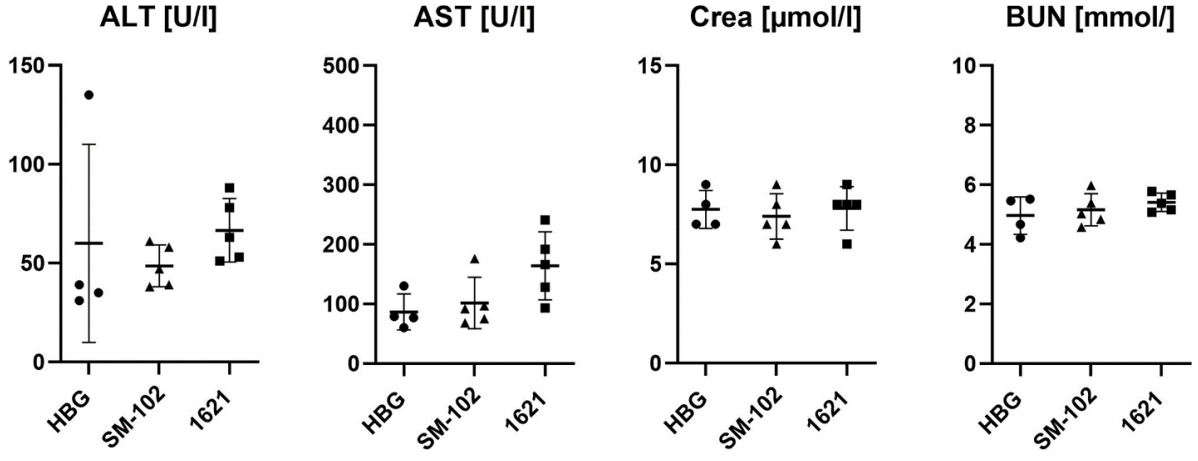

Figure 19. Evaluation of standard plasma parameters after intravenously applied eGFP mRNA LNPs in tumor-free A/J mice. Administration as described for **Figure 18**. Blood samples were taken at 6 h after injection. 3 µg eGFP mRNA; SM-102 (N/P 6), ***1621*** (N/P 9); HBG (n=4), SM-102 (n=5), ***1621*** (n=5). The evaluation of standard plasma parameters was performed by Jana Pöhmerer (Pharmaceutical Biotechnology, LMU Munich).
ALT, alanine transaminase; AST, aspartate aminotransferase; Crea, creatinine; BUN, blood urea nitrogen.

Expression within splenic and liver dendritic cells (DCs) was found for both LNPs, with SM-102 highest in spleen DCs. ***1621*** displayed highest expression in liver macrophages (Kupffer cells, KCs), whereas SM-102 transfected more spleen macrophages (MACs). Both formulations showed moderate expression levels in liver sinusoidal endothelial cells (LSECs; liver) and B-cells (spleen). In the lungs, eGFP gene expression in DCs and MACs was insignificant within the range of assay sensitivity (MFI) for both LNPs, whereas a moderate expression could be detected for both LNPs in polymorphonuclear neutrophils (PMNs). In other immune cell types, no eGFP expression was monitored (*data not shown*).

It should be noted that the evaluated immune cell types represent only a marginal fraction of the total cell population of the distinct organs (<4-5%). Thus, the results of eGFP expression obtained on the single cell level cannot be directly compared with the results of the *ex vivo* luciferase activity assay of the whole organ (**Figure 16**). For example, the apparent discrepancy of a slightly higher eGFP expression of ***1621*** LNPs in liver immune cells (**Figure 18A**) despite an approx. 100-fold higher luciferase expression of SM-102 LNPs in the liver (**Figure 16**) can be explained by the different

assay. In contrast to the *ex vivo* luciferase reporter assay, eGFP expression was only recorded for immune cells, and hepatocytes and other non-immune cells were not analyzed. As known from previous work, SM-102 mRNA LNPs express highly in liver hepatocytes, and to some extent also in liver immune cells, whereas the eGFP expression signal of ***1621*** LNPs reflects predominant transfection of immune cells and not hepatocytes. This hypothesis could be supported by looking at the eGFP expression in CD45 (lymphocyte common antigen)-negative (i.e., non-immune cells) vs CD45-positive cells (i.e., immune cells) in the liver (**Figure 20**), which was slightly higher in non-immune cells for SM-102 than for ***1621***. SM-102 may transfect at low extent both $CD45^-$ hepatocytes (**Figure 20**, left panel), albeit below statistical significance, and $CD45^+$ immune cells (**Figure 20**, right panel). However, since hepatocytes account for about 95% of all liver cells, even low transfection of this cell population may account at large part for the strong luciferase signal of this organ (**Figure 16**). Since ***1621*** transfected the quantitatively minor $CD45^+$ liver-resident immune cell population at similar extent as SM-102 (**Figure 20**, right panel), the overall much lower luciferase activity in livers of ***1621***-treated mice might be due to an inability of ***1621*** to transfect hepatocytes *in vivo* (**Figure 20**, left panel).

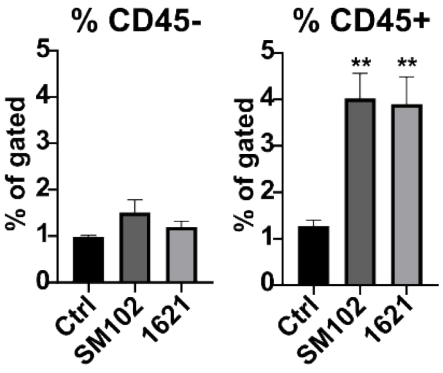

Figure 20. eGFP expression of CD45-negative ($CD45^-$) vs CD45-positive cells ($CD45^+$) in the liver at 6 h after intravenous administration of LNP formulations containing 3 µg eGFP mRNA in 150 µL HBG per mouse (n=5; mean + SEM). Data are presented as percentage of eGFP-positive cells within the $CD45^{-/+}$ populations. Statistical analysis was done by one-way ANOVA, Tukey test; GraphPad Prism™ 9.5.1. Significant differences vs Ctrl (HBG-treated mice): ** $p \leq 0.01$. The experiments and analysis were carried out by Yanira Zeyn (Department of Dermatology, University Medical Center, JGU Mainz).

3.4 Conclusion

A chemical evolution design of xenopeptides, defined in a precise 2D sequence and 3D architecture made of LAFs, Stp, and α,ε-amido-linked lysines, identified new potent mRNA carriers. Here, we demonstrate the high potential of this novel LAF-Stp class as cationizable carriers in mRNA LNP formulations. We identified LAF 8Oc carrier ***1621*** with a Stp/LAF ratio of 1:4 and bundle 3D topology as the most efficient carrier, with impressive dynamics of re-distribution from the lipidic to the aqueous phase by 100-fold upon endosomal acidification [80][426]. The incorporation of the LAF building block provided efficient nanoparticle formation, cellular uptake, and potent endosomal escape even in the presence of serum, resulting in fast and high reporter expression kinetics at very low mRNA doses (150 pg/well) in antigen-presenting cells and tumor cell lines. Upon intravenous administration of 3 µg mRNA per mouse, LAF-Stp mRNA LNPs exerted predominant mRNA expression in the spleen, far higher compared to other organs such as the liver, which was observed as the main organ of reporter expression by established standard mRNA LNPs (DLin-MC3-DMA and SM-102). Cellular analysis of eGFP mRNA expression in liver, lungs, and spleen revealed reporter expression in dendritic cells, macrophages, Kupffer cells, liver sinusoidal endothelial cells, and neutrophils.

Current LNP library formulation was performed by simple flash mixing of standard ethanol/pH 4 citrate buffer solutions at small scale. LNP characteristics can be further refined by standardized formulation procedures including microfluidics [427]. Additionally, optimizing ratios of helper lipids, PEG-lipids and ligand targeting of LNPs could help in ‘chemical and biological targeting’, to modulate organ selectivity and efficacy [400, 428, 429].

Conflict of Interest

Declarations of interest: none

Acknowledgements

The authors acknowledge support by the German Research Foundation (DFG) SFB1032 (project-ID 201269156) sub-project B4 (to E.W.), SFB1066 subproject B15

(to M.B.), and BMBF Cluster for Future ‘CNATM - Cluster for Nucleic Acid Therapeutics Munich’ (to E.W.). We thank *i)* Dr. Yi Lin and Prof. Ulrich Lächelt for providing the HeLa-Gal8-mRuby3 cells, *ii)* Johanna Seidl and Ricarda Steffens (both Pharmaceutical Biotechnology, LMU Munich) for support in LAF synthesis, *iii)* Carolina Medina-Montano and Evelyn Montermann (both Department of Dermatology, University Medical Center of the JGU Mainz) for their help in the immunostaining experiment, and *iv)* Wolfgang Rödl, Olga Brück, and Markus Kovac (all Pharmaceutical Biotechnology, LMU Munich) for their practical support.

The Graphical Abstract as well as Scheme 2A were created with BioRender.com.

4 Summary

Within the past years, the interest in nucleic acid-based therapies has raised across various medicinal fields, from gene therapy and cancer treatment, to vaccine development. In contrast to viral vectors, nonviral gene delivery with different carrier systems, including polyplexes, lipoplexes and LNPs, has emerged as a promising alternative, offering a safer and more precise approach without any structural limitations. Despite their potential, nonviral carriers still require enhancement in different regards, including an appropriate size, sufficient stability outside cells, and efficient cellular uptake and endosomal escape inside target cells in accordance with the particular cargo and application field. Chemical evolution, as an optimization strategy, can help to enhance the efficiency by the synthesis of a sequence defined nanocarrier library, high-throughput screenings of the carriers, and subsequently by selected and specific structure modification. The inclusion of statistical analysis and machine learning techniques can accelerate and facilitate the formulation optimization and improve the efficiency of this development process. Consequently, apparently unlimited modifications can be systemically applied to these artificial carriers to specifically enhance their efficiency in nucleic acid-based applications.

In the thesis, a library of novel, precise and sequence defined carriers synthesized via SPPS, was applied for the development of efficient mRNA delivery in LNPs. Within the carriers, a cationizable polar aminoethylene unit, in the form of the synthetic amino acid Stp, was linked via lysines with cationizable apolar LAF units for a double pH-responsive character. These precisely designed cationizable carriers with specific sequences and architecture, comprising bundle and U-shape topologies, led to the development of very potent mRNA delivery system. Further structural variations of LAF-Stp carriers based on the variation of the number of Stp and LAF units inside the single molecule and the incorporation of different LAF types (8Oc, 12Oc, 12Bu, 16Bu, 12He, 14He, 10Oc). Notably, these LAF-Stp carriers demonstrated a molecular chameleon-like behavior, characterized by a pH-dependent polarity switch and significant endosomolytic activity.

This novel LAF-Stp class exhibited remarkable potential as cationizable carriers combined with carefully selected helper lipids (cholesterol, DSPC, PEG-DMG) and molar and N/P ratios in mRNA LNP formulations. Especially the combination of Stp with four LAF domains inside the ionizable lipid facilitated monodisperse and stable nanoparticle formation, high cellular uptake, and efficient endosomal escape, compared to its OleA analog. LAF-Stp carriers in LNPs resulted in rapid transfection kinetics, in comparison to gold standard ionizable lipids (DLin-MC3-DMA and SM-102), and very high transfection levels at remarkably low mRNA doses in tumor and antigen-presenting cells, even in the presence of full serum.

When intravenously administered to mice, the LAF-Stp mRNA LNPs displayed mainly mRNA expression in the spleen, surpassing expression levels observed in other organs such as the liver, which is typically the primary tissue for common gold standard LNPs. Detailed cellular analysis showed cell type specific eGFP mRNA expression in dendritic cells, macrophages, Kupffer cells, liver sinusoidal endothelial cells, and neutrophils. Through these comprehensive screenings of the synthesized library, 8Oc bundle carrier ***1621*** with a hydrophilic/lipophilic balance of 1:4 was identified as most efficient.

Overall, these results revealed how small structural modifications, including alterations in topology, variations in the type of LAF or adjustments to the hydrophilic/lipophilic balance, inside the cationizable lipid of the LNP, lead to significant changes in physicochemical particle characteristics and mRNA expression both, *in vitro* and *in vivo*. Nevertheless, these newly developed LAF-Stp carriers are highly potent as cationizable lipids in LNPs for mRNA delivery. These findings suggest the potential of LAF-Stp carriers as suitable and promising candidates for further advancements in nucleic acid-based therapeutic development.

6 Appendix

Abbreviations

AAV	Adenovirus-associated virus
ACN	Acetonitrile
ApoE	Apolipoprotein E
ASGPR	Asialoglycoprotein receptor
ATP	Adenosine 5′-triphosphate
BafA1	Bafilomycin A1
CART	Charge-altering releasable transporters
CRISPR	Clustered, regularly interspaced, short palindromic repeats
Cas	CRISPR-associated
CLSM	Confocal laser scanning microscopy
COVID-19	Coronavirus disease 2019
CPP	Cell-penetrating peptide
Cy5	Cyanine 5
Da	Dalton
DAPI	4′,6-diamidino-2-phenylindole
DBCO	Dibenzo cyclooctyne
DC2.4	Immortalized murine dendritic cells
DCM	Dichloromethane
Dde	4,4-Dimethyl-2,6-dioxocyclohexylidene)ethyl protecting group
DET	Diethylene triamine
DIPEA	N,N-Diisopropylethylamine
DLS	Dynamic light scattering
DMEM	Dulbecco‘s modified Eagle‘s medium
DMF	N,N-Dimethylformamide
DMSO	Dimethyl sulfoxide
DODAP	1,2-dioleoyl-3-dimethylammonium propane
DoE	Design of experiments
DOPC	1,2-dioleoyl-sn-glycero-3-phosphocholine
DOPE	1,2-dioleoyl-sn-glycero-3-phosphoethanolamine
DSPC	1,2-distearoyl-sn-glycero-3-phosphocholine
DSPG	1,2-distearoyl-sn-glycero-3-phosphoglycerol

DTT	Dithiothreitol
EDTA	Ethylenediaminetetraacetic acid
eGFP	Enhanced green fluorescent protein
ELS	Electrophoretic light scattering
EPR	Enhanced permeability and retention
EtOH	Ethanol
FBS	Fetal bovine serum
FDA	Food and Drug Administration
FIND	Fast Identification of Nanoparticle Delivery
FLuc	Firefly luciferase
Fmoc	Fluorenylmethoxycarbonyl
HBG	Hepes-buffered glucose
HCl	Hydrochloric acid
HeLa	Human cervix carcinoma cell line
HEPES	N-(2-hydroxethyl) piperazine-N-(2-ethansulfonic acid)
HepG2	Human hepatocellular carcinoma cell line
HOBt	1-Hydroxybenzotriazole
Huh7	Human hepatocellular carcinoma cell line
IMDM	Iscove's Modified Dulbecco's Medium
J774A.1	Murine macrophage cell line
KC	Kupffer cells
KCl	Potassium chloride
kDa	Kilodalton
LAF	Lipoamino fatty acid
LDL	Low density lipoprotein
LNP	Lipid nanoparticle
LSEC	Liver sinusoidal endothelial cells
MAC	Murine macrophage
MALDI	Matrix-assisted laser desorption/ionization
MeOH	Methanol
MFI	Mean fluorescence intensity
mM	Millimolar
mRNA	Messenger RNA
MS	Mass spectrometry

MTT	3-(4,5-dimethylthiazol-2-yl)-2,5-diphenyltetrazolium bromide
mV	Millivolt
MWCO	Molecular weight cut-off
N/P	Nitrogen to phosphate ratio
N2a	Murine adherent neuroblastoma cell line
NaCl	Sodium chloride
NaOH	Sodium hydroxide
nm	Nanometer
NPCs	Non-parenchymal cells
ns	not significant
OAA	Oligoaminoamide
OleA	Oleic acid
PACE	Poly(amine-co-ester)
PBAE	Poly (β-amino ester)
PBS	Phosphate buffered saline
pCL	Polycaprolactone
PDI	Polydispersity index
pDIPAMA	Poly(2-diisopropylaminoethylmethacrylate)
pDMAEMA	Poly[(2-dimethylamino)ethyl methacrylate];
pDNA	Plasmid desoxyribonucleic acid
PEG	Polyethylene glycol
PEG-DMG	1,2-dimyristoyl-rac-glycero-3-methoxypolyethylene glycol-2000
PEI	Polyethylenimine
pHEMA	Poly(2-hydroxyethyl methacrylate)
pHPMA	Poly[N-(2-hydroxypropyl) methacrylamide]
pKa	-log10 Ka (acid dissociation constant)
pLys	Poly(L)lysine
PMN	Polymorphonuclear leukocytes/neutrophils
PMO	Phosphorodiamidate morpholino oligomer
pOEGMA	Poly[oligo(ethylene glycol) monomethyl ether methacrylate]
pTMAEMA	Poly[(2-trimethylamino)ethyl methacrylate]
PyBOP	(Benzotriazol-1-yloxy)-tripyrrolidinophosphonium hexafluorophosphate
QbD	Quality by design
RES	reticuloendothelial system

RLU	Relative light units
RNA	Ribonucleic acid
rpm	Rounds per minute
RT	Room temperature
SD	Standard deviation
sgRNA	single guide RNA
siRNA	Small interfering RNA
SORT	Selective organ targeting
SPPS	Solid-phase peptide synthesis
Stp	Succinyl-tetraethylene pentaamine
TBE	Tris-boric acid-EDTA buffer
TEP	TEPA, tetraethylene pentamine
TFA	Trifluoroacetic acid
TIS	Triisopropylsilane
TNS	6-(p-Toluidino)-2-naphthalenesulfonyl chloride
TOF	Time of flight
Tris	Tris(hydroxymethyl)aminomethan

7 References

[1] J.D. Watson, F.H.C. Crick, Molecular Structure of Nucleic Acids: A Structure for Deoxyribose Nucleic Acid, Nature, 171 (1953) 737-738.
[2] M.H.F. Wilkins, A.R. Stokes, H.R. Wilson, Molecular Structure of Nucleic Acids: Molecular Structure of Deoxypentose Nucleic Acids, Nature, 171 (1953) 738-740.
[3] T. Friedmann, R. Roblin, Gene therapy for human genetic disease?, Science, 175 (1972) 949-955.
[4] W. Sun, Q. Shi, H. Zhang, K. Yang, Y. Ke, Y. Wang, L. Qiao, Advances in the techniques and methodologies of cancer gene therapy, Discov Med, 27 (2019) 45-55.
[5] S.L. Ginn, A.K. Amaya, I.E. Alexander, M. Edelstein, M.R. Abedi, Gene therapy clinical trials worldwide to 2017: An update, J Gene Med, 20 (2018) e3015.
[6] U. Lächelt, E. Wagner, Nucleic Acid Therapeutics Using Polyplexes: A Journey of 50 Years (and Beyond), Chemical Reviews, 115 (2015) 11043-11078.
[7] J.A. Doudna, E. Charpentier, Genome editing. The new frontier of genome engineering with CRISPR-Cas9, Science, 346 (2014) 1258096.
[8] C.A. Lino, J.C. Harper, J.P. Carney, J.A. Timlin, Delivering CRISPR: a review of the challenges and approaches, Drug Deliv, 25 (2018) 1234-1257.
[9] J.A. Kulkarni, D. Witzigmann, S.B. Thomson, S. Chen, B.R. Leavitt, P.R. Cullis, R. van der Meel, The current landscape of nucleic acid therapeutics, Nature Nanotechnology, 16 (2021) 630-643.
[10] C.A. Stein, D. Castanotto, FDA-Approved Oligonucleotide Therapies in 2017, Mol Ther, 25 (2017) 1069-1075.
[11] R. Titze-de-Almeida, C. David, S.S. Titze-de-Almeida, The Race of 10 Synthetic RNAi-Based Drugs to the Pharmaceutical Market, Pharm Res, 34 (2017) 1339-1363.
[12] S.M. Hammond, A. Aartsma-Rus, S. Alves, S.E. Borgos, R.A.M. Buijsen, R.W.J. Collin, G. Covello, M.A. Denti, L.R. Desviat, L. Echevarría, C. Foged, G. Gaina, A. Garanto, A.T. Goyenvalle, M. Guzowska, I. Holodnuka, D.R. Jones, S. Krause, T. Lehto, M. Montolio, W. Van Roon-Mom, V. Arechavala-Gomeza, Delivery of oligonucleotide-based therapeutics: challenges and opportunities, EMBO Mol Med, 13 (2021) e13243.
[13] A.K. Blakney, G. Yilmaz, P.F. McKay, C.R. Becer, R.J. Shattock, One Size Does Not Fit All: The Effect of Chain Length and Charge Density of Poly(ethylene imine) Based Copolymers on Delivery of pDNA, mRNA, and RepRNA Polyplexes, Biomacromolecules, 19 (2018) 2870-2879.
[14] F. Freitag, E. Wagner, Optimizing synthetic nucleic acid and protein nanocarriers: The chemical evolution approach, Adv Drug Deliv Rev, 168 (2021) 30-54.
[15] L. Peng, E. Wagner, Polymeric Carriers for Nucleic Acid Delivery: Current Designs and Future Directions, Biomacromolecules, 20 (2019) 3613-3626.
[16] J.D. Torres-Vanegas, J.C. Cruz, L.H. Reyes, Delivery Systems for Nucleic Acids and Proteins: Barriers, Cell Capture Pathways and Nanocarriers, Pharmaceutics, 13 (2021).
[17] B.B. Mendes, J. Conniot, A. Avital, D. Yao, X. Jiang, X. Zhou, N. Sharf-Pauker, Y. Xiao, O. Adir, H. Liang, J. Shi, A. Schroeder, J. Conde, Nanodelivery of nucleic acids, Nature Reviews Methods Primers, 2 (2022) 24.
[18] C. Chen, Z. Yang, X. Tang, Chemical modifications of nucleic acid drugs and their delivery systems for gene-based therapy, Med Res Rev, 38 (2018) 829-869.
[19] P.L. Felgner, Y. Barenholz, J.P. Behr, S.H. Cheng, P. Cullis, L. Huang, J.A. Jessee, L. Seymour, F. Szoka, A.R. Thierry, E. Wagner, G. Wu, Nomenclature for synthetic gene delivery systems, Hum Gene Ther, 8 (1997) 511-512.
[20] L. Schoenmaker, D. Witzigmann, J.A. Kulkarni, R. Verbeke, G. Kersten, W. Jiskoot, D.J.A. Crommelin, mRNA-lipid nanoparticle COVID-19 vaccines: Structure and stability, Int J Pharm, 601 (2021) 120586.
[21] R. Verbeke, I. Lentacker, S.C. De Smedt, H. Dewitte, The dawn of mRNA vaccines: The COVID-19 case, J Control Release, 333 (2021) 511-520.

[22] D. Adams, A. Gonzalez-Duarte, W.D. O'Riordan, C.C. Yang, M. Ueda, A.V. Kristen, I. Tournev, H.H. Schmidt, T. Coelho, J.L. Berk, K.P. Lin, G. Vita, S. Attarian, V. Planté-Bordeneuve, M.M. Mezei, J.M. Campistol, J. Buades, T.H. Brannagan, 3rd, B.J. Kim, J. Oh, Y. Parman, Y. Sekijima, P.N. Hawkins, S.D. Solomon, M. Polydefkis, P.J. Dyck, P.J. Gandhi, S. Goyal, J. Chen, A.L. Strahs, S.V. Nochur, M.T. Sweetser, P.P. Garg, A.K. Vaishnaw, J.A. Gollob, O.B. Suhr, Patisiran, an RNAi Therapeutic, for Hereditary Transthyretin Amyloidosis, N Engl J Med, 379 (2018) 11-21.
[23] J.D. Gillmore, E. Gane, J. Taubel, J. Kao, M. Fontana, M.L. Maitland, J. Seitzer, D. O'Connell, K.R. Walsh, K. Wood, J. Phillips, Y. Xu, A. Amaral, A.P. Boyd, J.E. Cehelsky, M.D. McKee, A. Schiermeier, O. Harari, A. Murphy, C.A. Kyratsous, B. Zambrowicz, R. Soltys, D.E. Gutstein, J. Leonard, L. Sepp-Lorenzino, D. Lebwohl, CRISPR-Cas9 In Vivo Gene Editing for Transthyretin Amyloidosis, N Engl J Med, 385 (2021) 493-502.
[24] I.M.S. Degors, C. Wang, Z.U. Rehman, I.S. Zuhorn, Carriers Break Barriers in Drug Delivery: Endocytosis and Endosomal Escape of Gene Delivery Vectors, Accounts of Chemical Research, 52 (2019) 1750-1760.
[25] B. Winkeljann, D.C. Keul, O.M. Merkel, Engineering poly- and micelleplexes for nucleic acid delivery – A reflection on their endosomal escape, Journal of Controlled Release, 353 (2023) 518-534.
[26] R. Duncan, S.C. Richardson, Endocytosis and intracellular trafficking as gateways for nanomedicine delivery: opportunities and challenges, Molecular pharmaceutics, 9 (2012) 2380-2402.
[27] N. Nayerossadat, T. Maedeh, P.A. Ali, Viral and nonviral delivery systems for gene delivery, Adv Biomed Res, 1 (2012) 27.
[28] Y. Zhang, A. Satterlee, L. Huang, In vivo gene delivery by nonviral vectors: overcoming hurdles?, Mol Ther, 20 (2012) 1298-1304.
[29] P. Zhang, E. Wagner, History of Polymeric Gene Delivery Systems, Top Curr Chem (Cham), 375 (2017) 26.
[30] V.A. Bloomfield, DNA condensation by multivalent cations, Biopolymers, 44 (1997) 269-282.
[31] N. Hoshyar, S. Gray, H. Han, G. Bao, The effect of nanoparticle size on in vivo pharmacokinetics and cellular interaction, Nanomedicine (Lond), 11 (2016) 673-692.
[32] J.E. Zuckerman, C.H. Choi, H. Han, M.E. Davis, Polycation-siRNA nanoparticles can disassemble at the kidney glomerular basement membrane, Proc Natl Acad Sci U S A, 109 (2012) 3137-3142.
[33] E.C. Dreaden, L.A. Austin, M.A. Mackey, M.A. El-Sayed, Size matters: gold nanoparticles in targeted cancer drug delivery, Ther Deliv, 3 (2012) 457-478.
[34] S.A. Kulkarni, S.S. Feng, Effects of particle size and surface modification on cellular uptake and biodistribution of polymeric nanoparticles for drug delivery, Pharm Res, 30 (2013) 2512-2522.
[35] A.B. de Barros, A. Tsourkas, B. Saboury, V.N. Cardoso, A. Alavi, Emerging role of radiolabeled nanoparticles as an effective diagnostic technique, EJNMMI Res, 2 (2012) 39.
[36] H. Maeda, Toward a full understanding of the EPR effect in primary and metastatic tumors as well as issues related to its heterogeneity, Adv Drug Deliv Rev, 91 (2015) 3-6.
[37] S.F. Dowdy, Overcoming cellular barriers for RNA therapeutics, Nat Biotechnol, 35 (2017) 222-229.
[38] S.A. Smith, L.I. Selby, A.P.R. Johnston, G.K. Such, The Endosomal Escape of Nanoparticles: Toward More Efficient Cellular Delivery, Bioconjugate Chemistry, 30 (2019) 263-272.
[39] S.F. Dowdy, R.L. Setten, X.S. Cui, S.G. Jadhav, Delivery of RNA Therapeutics: The Great Endosomal Escape!, Nucleic Acid Ther, 32 (2022) 361-368.
[40] S.F. Dowdy, Endosomal escape of RNA therapeutics: How do we solve this rate-limiting problem?, Rna, 29 (2023) 396-401.
[41] S.C. Semple, A. Akinc, J. Chen, A.P. Sandhu, B.L. Mui, C.K. Cho, D.W.Y. Sah, D. Stebbing, E.J. Crosley, E. Yaworski, I.M. Hafez, J.R. Dorkin, J. Qin, K. Lam, K.G. Rajeev,

K.F. Wong, L.B. Jeffs, L. Nechev, M.L. Eisenhardt, M. Jayaraman, M. Kazem, M.A. Maier, M. Srinivasulu, M.J. Weinstein, Q. Chen, R. Alvarez, S.A. Barros, S. De, S.K. Klimuk, T. Borland, V. Kosovrasti, W.L. Cantley, Y.K. Tam, M. Manoharan, M.A. Ciufolini, M.A. Tracy, A. de Fougerolles, I. MacLachlan, P.R. Cullis, T.D. Madden, M.J. Hope, Rational design of cationic lipids for siRNA delivery, Nat Biotech, 28 (2010) 172-176.
[42] M. Ogris, P. Steinlein, S. Carotta, S. Brunner, E. Wagner, DNA/polyethylenimine transfection particles: influence of ligands, polymer size, and PEGylation on internalization and gene expression, AAPS PharmSci, 3 (2001) E21.
[43] V.C. Vetter, E. Wagner, Targeting nucleic acid-based therapeutics to tumors: Challenges and strategies for polyplexes, J Control Release, 346 (2022) 110-135.
[44] N. Dammes, M. Goldsmith, S. Ramishetti, J.L.J. Dearling, N. Veiga, A.B. Packard, D. Peer, Conformation-sensitive targeting of lipid nanoparticles for RNA therapeutics, Nat Nanotechnol, 16 (2021) 1030-1038.
[45] S. Hager, E. Wagner, Bioresponsive polyplexes - chemically programmed for nucleic acid delivery, Expert Opin Drug Deliv, 15 (2018) 1067-1083.
[46] J. Luo, J. Schmaus, M. Cui, E. Hörterer, U. Wilk, M. Höhn, M. Däther, S. Berger, T. Benli-Hoppe, L. Peng, E. Wagner, Hyaluronate siRNA nanoparticles with positive charge display rapid attachment to tumor endothelium and penetration into tumors, J Control Release, 329 (2021) 919-933.
[47] S. Berger, A. Krhač Levačić, E. Hörterer, U. Wilk, T. Benli-Hoppe, Y. Wang, Ö. Öztürk, J. Luo, E. Wagner, Optimizing pDNA Lipo-polyplexes: A Balancing Act between Stability and Cargo Release, Biomacromolecules, 22 (2021) 1282-1296.
[48] K. Negron, N. Khalasawi, B. Lu, C.Y. Ho, J. Lee, S. Shenoy, H.Q. Mao, T.H. Wang, J. Hanes, J.S. Suk, Widespread gene transfer to malignant gliomas with In vitro-to-In vivo correlation, J Control Release, 303 (2019) 1-11.
[49] K.A. Whitehead, J. Matthews, P.H. Chang, F. Niroui, J.R. Dorkin, M. Severgnini, D.G. Anderson, In vitro-in vivo translation of lipid nanoparticles for hepatocellular siRNA delivery, ACS Nano, 6 (2012) 6922-6929.
[50] M.P. Monopoli, C. Åberg, A. Salvati, K.A. Dawson, Biomolecular coronas provide the biological identity of nanosized materials, Nature Nanotechnology, 7 (2012) 779-786.
[51] A. Tomak, S. Cesmeli, B.D. Hanoglu, D. Winkler, C. Oksel Karakus, Nanoparticle-protein corona complex: understanding multiple interactions between environmental factors, corona formation, and biological activity, Nanotoxicology, 15 (2021) 1331-1357.
[52] H. Li, Y. Wang, Q. Tang, D. Yin, C. Tang, E. He, L. Zou, Q. Peng, The protein corona and its effects on nanoparticle-based drug delivery systems, Acta Biomater, 129 (2021) 57-72.
[53] M. Ogris, S. Brunner, S. Schüller, R. Kircheis, E. Wagner, PEGylated DNA/transferrin-PEI complexes: reduced interaction with blood components, extended circulation in blood and potential for systemic gene delivery, Gene Ther, 6 (1999) 595-605.
[54] J.S. Suk, Q. Xu, N. Kim, J. Hanes, L.M. Ensign, PEGylation as a strategy for improving nanoparticle-based drug and gene delivery, Adv Drug Deliv Rev, 99 (2016) 28-51.
[55] S. Schöttler, G. Becker, S. Winzen, T. Steinbach, K. Mohr, K. Landfester, V. Mailänder, F.R. Wurm, Protein adsorption is required for stealth effect of poly(ethylene glycol)- and poly(phosphoester)-coated nanocarriers, Nat Nanotechnol, 11 (2016) 372-377.
[56] C. Weber, M. Voigt, J. Simon, A.K. Danner, H. Frey, V. Mailänder, M. Helm, S. Morsbach, K. Landfester, Functionalization of Liposomes with Hydrophilic Polymers Results in Macrophage Uptake Independent of the Protein Corona, Biomacromolecules, 20 (2019) 2989-2999.
[57] E. Wagner, Polymers for siRNA delivery: inspired by viruses to be targeted, dynamic, and precise, Acc Chem Res, 45 (2012) 1005-1013.
[58] E. Wagner, C. Plank, K. Zatloukal, M. Cotten, M.L. Birnstiel, Influenza virus hemagglutinin HA-2 N-terminal fusogenic peptides augment gene transfer by transferrin-polylysine-DNA complexes: toward a synthetic virus-like gene-transfer vehicle, Proc.Natl.Acad.Sci.U.S.A, 89 (1992) 7934-7938.

[59] L. Hartmann, E. Krause, M. Antonietti, H.G. Borner, Solid-phase supported polymer synthesis of sequence-defined, multifunctional poly(amidoamines), Biomacromolecules., 7 (2006) 1239-1244.
[60] D. Schaffert, C. Troiber, E.E. Salcher, T. Frohlich, I. Martin, N. Badgujar, C. Dohmen, D. Edinger, R. Klager, G. Maiwald, K. Farkasova, S. Seeber, K. Jahn-Hofmann, P. Hadwiger, E. Wagner, Solid-phase synthesis of sequence-defined T-, i-, and U-shape polymers for pDNA and siRNA delivery, Angew Chem Int Ed Engl, 50 (2011) 8986-8989.
[61] S. Morys, E. Wagner, U. Lächelt, From Artificial Amino Acids to Sequence-Defined Targeted Oligoaminoamides, Methods Mol Biol, 1445 (2016) 235-258.
[62] M. Tavares Luiz, J. Santos Rosa Viegas, J. Palma Abriata, F. Viegas, F. Testa Moura de Carvalho Vicentini, M.V. Lopes Badra Bentley, M. Chorilli, J. Maldonado Marchetti, D.R. Tapia-Blácido, Design of experiments (DoE) to develop and to optimize nanoparticles as drug delivery systems, European Journal of Pharmaceutics and Biopharmaceutics, 165 (2021) 127-148.
[63] S. Adam, D. Suzzi, C. Radeke, J.G. Khinast, An integrated Quality by Design (QbD) approach towards design space definition of a blending unit operation by Discrete Element Method (DEM) simulation, Eur J Pharm Sci, 42 (2011) 106-115.
[64] M. Rawal, A. Singh, M.M. Amiji, Quality-by-Design Concepts to Improve Nanotechnology-Based Drug Development, Pharm Res, 36 (2019) 153.
[65] L. Gurba-Bryśkiewicz, W. Maruszak, D.A. Smuga, K. Dubiel, M. Wieczorek, Quality by Design (QbD) and Design of Experiments (DOE) as a Strategy for Tuning Lipid Nanoparticle Formulations for RNA Delivery, Biomedicines, 11 (2023).
[66] N.P. S, P. Colombo, G. Colombo, M.R. D, Design of experiments (DoE) in pharmaceutical development, Drug Dev Ind Pharm, 43 (2017) 889-901.
[67] A.A. Metwally, A.A. Nayel, R.M. Hathout, In silico prediction of siRNA ionizable-lipid nanoparticles In vivo efficacy: Machine learning modeling based on formulation and molecular descriptors, Front Mol Biosci, 9 (2022) 1042720.
[68] R. Mashima, S. Takada, Lipid Nanoparticles: A Novel Gene Delivery Technique for Clinical Application, Curr Issues Mol Biol, 44 (2022) 5013-5027.
[69] P.R. Cullis, L.D. Mayer, M.B. Bally, T.D. Madden, M.J. Hope, Generating and loading of liposomal systems for drug-delivery applications, Advanced Drug Delivery Reviews, 3 (1989) 267-282.
[70] R. Tenchov, R. Bird, A.E. Curtze, Q. Zhou, Lipid Nanoparticles─From Liposomes to mRNA Vaccine Delivery, a Landscape of Research Diversity and Advancement, ACS Nano, 15 (2021) 16982-17015.
[71] P.R. Cullis, M.J. Hope, Lipid Nanoparticle Systems for Enabling Gene Therapies, Mol Ther, 25 (2017) 1467-1475.
[72] C. Hald Albertsen, J.A. Kulkarni, D. Witzigmann, M. Lind, K. Petersson, J.B. Simonsen, The role of lipid components in lipid nanoparticles for vaccines and gene therapy, Adv Drug Deliv Rev, 188 (2022) 114416.
[73] X. Hou, T. Zaks, R. Langer, Y. Dong, Lipid nanoparticles for mRNA delivery, Nature Reviews Materials, 6 (2021) 1078-1094.
[74] T.S. Zimmermann, A.C.H. Lee, A. Akinc, B. Bramlage, D. Bumcrot, M.N. Fedoruk, J. Harborth, J.A. Heyes, L.B. Jeffs, M. John, A.D. Judge, K. Lam, K. McClintock, L.V. Nechev, L.R. Palmer, T. Racie, I. Röhl, S. Seiffert, S. Shanmugam, V. Sood, J. Soutschek, I. Toudjarska, A.J. Wheat, E. Yaworski, W. Zedalis, V. Koteliansky, M. Manoharan, H.-P. Vornlocher, I. MacLachlan, RNAi-mediated gene silencing in non-human primates, Nature, 441 (2006) 111-114.
[75] M. Jayaraman, S.M. Ansell, B.L. Mui, Y.K. Tam, J. Chen, X. Du, D. Butler, L. Eltepu, S. Matsuda, J.K. Narayanannair, K.G. Rajeev, I.M. Hafez, A. Akinc, M.A. Maier, M.A. Tracy, P.R. Cullis, T.D. Madden, M. Manoharan, M.J. Hope, Maximizing the potency of siRNA lipid nanoparticles for hepatic gene silencing in vivo, Angew Chem Int Ed Engl, 51 (2012) 8529-8533.

[76] Y. Eygeris, M. Gupta, J. Kim, G. Sahay, Chemistry of Lipid Nanoparticles for RNA Delivery, Accounts of Chemical Research, 55 (2022) 2-12.
[77] C.B. Roces, G. Lou, N. Jain, S. Abraham, A. Thomas, G.W. Halbert, Y. Perrie, Manufacturing Considerations for the Development of Lipid Nanoparticles Using Microfluidics, Pharmaceutics, 12 (2020).
[78] M. Maeki, S. Uno, A. Niwa, Y. Okada, M. Tokeshi, Microfluidic technologies and devices for lipid nanoparticle-based RNA delivery, J Control Release, 344 (2022) 80-96.
[79] M. Puccetti, A. Schoubben, S. Giovagnoli, M. Ricci, Biodrug Delivery Systems: Do mRNA Lipid Nanoparticles Come of Age?, Int J Mol Sci, 24 (2023).
[80] S. Thalmayr, M. Grau, L. Peng, J. Pöhmerer, U. Wilk, P. Folda, M. Yazdi, E. Weidinger, T. Burghardt, M. Höhn, E. Wagner, S. Berger, Molecular Chameleon Carriers for Nucleic Acid Delivery: The Sweet Spot between Lipoplexes and Polyplexes, Adv. Mater., 35 (2023) 2211105.
[81] M. Egli, M. Manoharan, Re-Engineering RNA Molecules into Therapeutic Agents, Accounts of chemical research, 52 (2019) 1036-1047.
[82] J.K. Nair, H. Attarwala, A. Sehgal, Q. Wang, K. Aluri, X. Zhang, M. Gao, J. Liu, R. Indrakanti, S. Schofield, P. Kretschmer, C.R. Brown, S. Gupta, J.L.S. Willoughby, J.A. Boshar, V. Jadhav, K. Charisse, T. Zimmermann, K. Fitzgerald, M. Manoharan, K.G. Rajeev, A. Akinc, R. Hutabarat, M.A. Maier, Impact of enhanced metabolic stability on pharmacokinetics and pharmacodynamics of GalNAc-siRNA conjugates, Nucleic Acids Res, 45 (2017) 10969-10977.
[83] D.J. Foster, C.R. Brown, S. Shaikh, C. Trapp, M.K. Schlegel, K. Qian, A. Sehgal, K.G. Rajeev, V. Jadhav, M. Manoharan, S. Kuchimanchi, M.A. Maier, S. Milstein, Advanced siRNA Designs Further Improve In Vivo Performance of GalNAc-siRNA Conjugates, Mol Ther, 26 (2018) 708-717.
[84] A. Wittrup, J. Lieberman, Knocking down disease: a progress report on siRNA therapeutics, Nat Rev Genet, 16 (2015) 543-552.
[85] D. Oupicky, V. Diwadkar, Stimuli-responsive gene delivery vectors, Curr.Opin.Mol Ther, 5 (2003) 345-350.
[86] E. Wagner, Programmed drug delivery: nanosystems for tumor targeting, Expert Opin Biol Ther, 7 (2007) 587-593.
[87] M. Sun, K. Wang, D. Oupicky, Advances in Stimulus-Responsive Polymeric Materials for Systemic Delivery of Nucleic Acids, Advanced healthcare materials, 7 (2018).
[88] D.J. Peeler, D.L. Sellers, S.H. Pun, pH-Sensitive Polymers as Dynamic Mediators of Barriers to Nucleic Acid Delivery, Bioconjug Chem, 30 (2019) 350-365.
[89] H. Hatakeyama, H. Akita, K. Kogure, M. Oishi, Y. Nagasaki, Y. Kihira, M. Ueno, H. Kobayashi, H. Kikuchi, H. Harashima, Development of a novel systemic gene delivery system for cancer therapy with a tumor-specific cleavable PEG-lipid, Gene Ther, 14 (2007) 68-77.
[90] S. Reinhard, Y. Wang, S. Dengler, E. Wagner, Precise Enzymatic Cleavage Sites for Improved Bioactivity of siRNA Lipo-Polyplexes, Bioconjug Chem, 29 (2018) 3649-3657.
[91] P.M. Klein, E. Wagner, Bioreducible polycations as shuttles for therapeutic nucleic acid and protein transfection, Antioxid Redox Signal, 21 (2014) 804-817.
[92] A. Kwok, S.L. Hart, Comparative structural and functional studies of nanoparticle formulations for DNA and siRNA delivery, Nanomedicine, 7 (2011) 210-219.
[93] C. Scholz, E. Wagner, Therapeutic plasmid DNA versus siRNA delivery: common and different tasks for synthetic carriers, J Control Release, 161 (2012) 554-565.
[94] C. Goncalves, S. Akhter, C. Pichon, P. Midoux, Intracellular Availability of pDNA and mRNA after Transfection: A Comparative Study among Polyplexes, Lipoplexes, and Lipopolyplexes, Molecular pharmaceutics, 13 (2016) 3153-3163.
[95] A.C. Kauffman, A.S. Piotrowski-Daspit, K.H. Nakazawa, Y. Jiang, A. Datye, W.M. Saltzman, Tunability of Biodegradable Poly(amine- co-ester) Polymers for Customized Nucleic Acid Delivery and Other Biomedical Applications, Biomacromolecules, 19 (2018) 3861-3873.

[96] K. Paunovska, C.D. Sago, C.M. Monaco, W.H. Hudson, M.G. Castro, T.G. Rudoltz, S. Kalathoor, D.A. Vanover, P.J. Santangelo, R. Ahmed, A.V. Bryksin, J.E. Dahlman, A Direct Comparison of in Vitro and in Vivo Nucleic Acid Delivery Mediated by Hundreds of Nanoparticles Reveals a Weak Correlation, Nano Lett, 18 (2018) 2148-2157.
[97] A.C. Allwood, M.R. Walter, B.S. Kamber, C.P. Marshall, I.W. Burch, Stromatolite reef from the Early Archaean era of Australia, Nature, 441 (2006) 714-718.
[98] A. Vaheri, J.S. Pagano, Infectious poliovirus RNA: a sensitive method of assay 2, Virology, 27 (1965) 434-436.
[99] J.H. McCutchan, J.S. Pagano, Enchancement of the infectivity of simian virus 40 deoxyribonucleic acid with diethylaminoethyl-dextran, J Natl Cancer Inst, 41 (1968) 351-357.
[100] F.E. Farber, J.L. Melnick, J.S. Butel, Optimal conditions for uptake of exogenous DNA by Chinese hamster lung cells deficient in hypoxanthine-guanine phosphoribosyltransferase, Biochim.Biophys.Acta, 390 (1975) 298-311.
[101] K.A. Mislick, J.D. Baldeschwieler, Evidence for the role of proteoglycans in cation-mediated gene transfer, Proc.Natl.Acad.Sci.U.S.A, 93 (1996) 12349-12354.
[102] I. Kopatz, J.S. Remy, J.P. Behr, A model for non-viral gene delivery: through syndecan adhesion molecules and powered by actin, The journal of gene medicine, 6 (2004) 769-776.
[103] M. Cotten, F. Langle-Rouault, H. Kirlappos, E. Wagner, K. Mechtler, M. Zenke, H. Beug, M.L. Birnstiel, Transferrin-polycation-mediated introduction of DNA into human leukemic cells: stimulation by agents that affect the survival of transfected DNA or modulate transferrin receptor levels, Proc.Natl.Acad.Sci.U.S.A, 87 (1990) 4033-4037.
[104] S.M. Zou, P. Erbacher, J.S. Remy, J.P. Behr, Systemic linear polyethylenimine (L-PEI)-mediated gene delivery in the mouse, J.Gene Med., 2 (2000) 128-134.
[105] O.M. Merkel, R. Urbanics, P. Bedocs, Z. Rozsnyay, L. Rosivall, M. Toth, T. Kissel, J. Szebeni, In vitro and in vivo complement activation and related anaphylactic effects associated with polyethylenimine and polyethylenimine-graft-poly(ethylene glycol) block copolymers, Biomaterials, 32 (2011) 4936-4942.
[106] C. Plank, K. Mechtler, F.C. Szoka, Jr., E. Wagner, Activation of the complement system by synthetic DNA complexes: a potential barrier for intravenous gene delivery, Hum Gene Ther, 7 (1996) 1437-1446.
[107] E. Wagner, M. Ogris, W. Zauner, Polylysine-based transfection systems utilizing receptor-mediated delivery, Adv Drug Deliv Rev, 30 (1998) 97-113.
[108] M. Meyer, A. Philipp, R. Oskuee, C. Schmidt, E. Wagner, Breathing life into polycations: functionalization with pH-responsive endosomolytic peptides and polyethylene glycol enables siRNA delivery, J Am Chem Soc, 130 (2008) 3272-3273.
[109] J.G. Schellinger, J.A. Pahang, R.N. Johnson, D.S. Chu, D.L. Sellers, D.O. Maris, A.J. Convertine, P.S. Stayton, P.J. Horner, S.H. Pun, Melittin-grafted HPMA-oligolysine based copolymers for gene delivery, Biomaterials, 34 (2013) 2318-2326.
[110] E. Wagner, K. Zatloukal, M. Cotten, H. Kirlappos, K. Mechtler, D.T. Curiel, M.L. Birnstiel, Coupling of adenovirus to transferrin-polylysine/DNA complexes greatly enhances receptor-mediated gene delivery and expression of transfected genes, Proc.Natl.Acad.Sci.U.S.A, 89 (1992) 6099-6103.
[111] R.J. Cristiano, L.C. Smith, M.A. Kay, B.R. Brinkley, S.L. Woo, Hepatic gene therapy: efficient gene delivery and expression in primary hepatocytes utilizing a conjugated adenovirus-DNA complex 139, Proc Natl Acad Sci U S A, 90 (1993) 11548-11552.
[112] W. Zauner, D. Blaas, E. Kuechler, E. Wagner, Rhinovirus-mediated endosomal release of transfection complexes, J Virol., 69 (1995) 1085-1092.
[113] G.Y. Wu, C.H. Wu, Receptor-mediated gene delivery and expression in vivo 738, J Biol Chem, 262 (1988) 14621-14624.
[114] E. Wagner, M. Zenke, M. Cotten, H. Beug, M.L. Birnstiel, Transferrin-polycation conjugates as carriers for DNA uptake into cells, Proc.Natl.Acad.Sci.U.S.A, 87 (1990) 3410-3414.
[115] M. Tonigold, J. Simon, D. Estupinan, M. Kokkinopoulou, J. Reinholz, U. Kintzel, A. Kaltbeitzel, P. Renz, M.P. Domogalla, K. Steinbrink, I. Lieberwirth, D. Crespy, K. Landfester,

V. Mailander, Pre-adsorption of antibodies enables targeting of nanocarriers despite a biomolecular corona, Nat Nanotechnol, 13 (2018) 862-869.
[116] R. Laga, R. Carlisle, M. Tangney, K. Ulbrich, L.W. Seymour, Polymer coatings for delivery of nucleic acid therapeutics, J Control Release, 161 (2012) 537-553.
[117] R. Kircheis, S. Schuller, S. Brunner, M. Ogris, K.H. Heider, W. Zauner, E. Wagner, Polycation-based DNA complexes for tumor-targeted gene delivery in vivo, The journal of gene medicine, 1 (1999) 111-120.
[118] I.K. Park, T.H. Kim, Y.H. Park, B.A. Shin, E.S. Choi, E.H. Chowdhury, T. Akaike, C.S. Cho, Galactosylated chitosan-graft-poly(ethylene glycol) as hepatocyte-targeting DNA carrier, J Control Release, 76 (2001) 349-362.
[119] T. Blessing, M. Kursa, R. Holzhauser, R. Kircheis, E. Wagner, Different strategies for formation of pegylated EGF-conjugated PEI/DNA complexes for targeted gene delivery, Bioconjug Chem, 12 (2001) 529-537.
[120] M. Kursa, G.F. Walker, V. Roessler, M. Ogris, W. Roedl, R. Kircheis, E. Wagner, Novel Shielded Transferrin-Polyethylene Glycol-Polyethylenimine/DNA Complexes for Systemic Tumor-Targeted Gene Transfer, Bioconjug.Chem., 14 (2003) 222-231.
[121] M.W. Konstan, P.B. Davis, J.S. Wagener, K.A. Hilliard, R.C. Stern, L.J. Milgram, T.H. Kowalczyk, S.L. Hyatt, T.L. Fink, C.R. Gedeon, S.M. Oette, J.M. Payne, O. Muhammad, A.G. Ziady, R.C. Moen, M.J. Cooper, Compacted DNA nanoparticles administered to the nasal mucosa of cystic fibrosis subjects are safe and demonstrate partial to complete cystic fibrosis transmembrane regulator reconstitution, Hum Gene Ther, 15 (2004) 1255-1269.
[122] T. Merdan, K. Kunath, H. Petersen, U. Bakowsky, K.H. Voigt, J. Kopecek, T. Kissel, PEGylation of poly(ethylene imine) affects stability of complexes with plasmid DNA under in vivo conditions in a dose-dependent manner after intravenous injection into mice, Bioconjug.Chem., 16 (2005) 785-792.
[123] O.M. Merkel, D. Librizzi, A. Pfestroff, T. Schurrat, K. Buyens, N.N. Sanders, S.C. De Smedt, M. Behe, T. Kissel, Stability of siRNA polyplexes from poly(ethylenimine) and poly(ethylenimine)-g-poly(ethylene glycol) under in vivo conditions: effects on pharmacokinetics and biodistribution measured by Fluorescence Fluctuation Spectroscopy and Single Photon Emission Computed Tomography (SPECT) imaging, J Control Release, 138 (2009) 148-159.
[124] A. Taschauer, W. Polzer, F. Alioglu, M. Billerhart, S. Decker, T. Kittelmann, E. Geppl, S. Elmenofi, M. Zehl, E. Urban, H. Sami, M. Ogris, Peptide-Targeted Polyplexes for Aerosol-Mediated Gene Delivery to CD49f-Overexpressing Tumor Lesions in Lung, Molecular therapy. Nucleic acids, 18 (2019) 774-786.
[125] K.D. Fisher, K. Ulbrich, V. Subr, C.M. Ward, V. Mautner, D. Blakey, L.W. Seymour, A versatile system for receptor-mediated gene delivery permits increased entry of DNA into target cells, enhanced delivery to the nucleus and elevated rates of transgene expression, Gene Ther., 7 (2000) 1337-1343.
[126] R.C. Carlisle, T. Etrych, S.S. Briggs, J.A. Preece, K. Ulbrich, L.W. Seymour, Polymer-coated polyethylenimine/DNA complexes designed for triggered activation by intracellular reduction, The journal of gene medicine, 6 (2004) 337-344.
[127] R.N. Johnson, D.S. Chu, J. Shi, J.G. Schellinger, P.M. Carlson, S.H. Pun, HPMA-oligolysine copolymers for gene delivery: optimization of peptide length and polymer molecular weight, J Control Release, 155 (2011) 303-311.
[128] M. Noga, D. Edinger, R. Klager, S.V. Wegner, J.P. Spatz, E. Wagner, G. Winter, A. Besheer, The effect of molar mass and degree of hydroxyethylation on the controlled shielding and deshielding of hydroxyethyl starch-coated polyplexes, Biomaterials, 34 (2013) 2530-2538.
[129] M. Hornof, F.M. de la, M. Hallikainen, R.H. Tammi, A. Urtti, Low molecular weight hyaluronan shielding of DNA/PEI polyplexes facilitates CD44 receptor mediated uptake in human corneal epithelial cells, J Gene Med., 10 (2008) 70-80.
[130] T. Ito, C. Yoshihara, K. Hamada, Y. Koyama, DNA/polyethyleneimine/hyaluronic acid small complex particles and tumor suppression in mice, Biomaterials, 31 (2010) 2912-2918.

[131] T. Sato, M. Nakata, Z. Yang, Y. Torizuka, S. Kishimoto, M. Ishihara, In vitro and in vivo gene delivery using chitosan/hyaluronic acid nanoparticles: Influences of molecular mass of hyaluronic acid and lyophilization on transfection efficiency, The journal of gene medicine, 19 (2017).
[132] P. Heller, A. Birke, D. Huesmann, B. Weber, K. Fischer, A. Reske-Kunz, M. Bros, M. Barz, Introducing PeptoPlexes: Polylysine-block-Polysarcosine Based Polyplexes for Transfection of HEK 293T Cells, Macromolecular bioscience, 14 (2014) 1380-1395.
[133] P. Heller, D. Hobernik, U. Lachelt, M. Schinnerer, B. Weber, M. Schmidt, E. Wagner, M. Bros, M. Barz, Combining reactive triblock copolymers with functional cross-linkers: A versatile pathway to disulfide stabilized-polyplex libraries and their application as pDNA vaccines, J Control Release, 258 (2017) 146-160.
[134] P.M. Klein, K. Klinker, W. Zhang, S. Kern, E. Kessel, E. Wagner, M. Barz, Efficient Shielding of Polyplexes Using Heterotelechelic Polysarcosines, Polymers, 10 (2018).
[135] J. Chen, K. Wang, J. Wu, H. Tian, X. Chen, Polycations for Gene Delivery: Dilemmas and Solutions, Bioconjug Chem, 30 (2019) 338-349.
[136] G.F. Walker, C. Fella, J. Pelisek, J. Fahrmeir, S. Boeckle, M. Ogris, E. Wagner, Toward synthetic viruses: endosomal pH-triggered deshielding of targeted polyplexes greatly enhances gene transfer in vitro and in vivo, Mol Ther, 11 (2005) 418-425.
[137] C. Fella, G.F. Walker, M. Ogris, E. Wagner, Amine-reactive pyridylhydrazone-based PEG reagents for pH-reversible PEI polyplex shielding, Eur.J Pharm.Sci, 34 (2008) 309-320.
[138] V. Knorr, M. Ogris, E. Wagner, An acid sensitive ketal-based polyethylene glycol-oligoethylenimine copolymer mediates improved transfection efficiency at reduced toxicity, Pharm Res, 25 (2008) 2937-2945.
[139] J.A. Wolff, D.B. Rozema, Breaking the Bonds: Non-viral Vectors Become Chemically Dynamic, Mol Ther, 16 (2008) 8-15.
[140] D.B. Rozema, A.V. Blokhin, D.H. Wakefield, J.D. Benson, J.C. Carlson, J.J. Klein, L.J. Almeida, A.L. Nicholas, H.L. Hamilton, Q. Chu, J.O. Hegge, S.C. Wong, V.S. Trubetskoy, C.M. Hagen, E. Kitas, J.A. Wolff, D.L. Lewis, Protease-triggered siRNA delivery vehicles, J Control Release, 209 (2015) 57-66.
[141] E. Wagner, Strategies to improve DNA polyplexes for in vivo gene transfer: will "artificial viruses" be the answer?, Pharm.Res., 21 (2004) 8-14.
[142] T. Luo, H. Liang, R. Jin, Y. Nie, Virus-inspired and mimetic designs in non-viral gene delivery, J Gene Med, 21 (2019) e3090.
[143] R. Kircheis, E. Ostermann, M.F. Wolschek, C. Lichtenberger, C. Magin-Lachmann, L. Wightman, M. Kursa, E. Wagner, Tumor-targeted gene delivery of tumor necrosis factor-alpha induces tumor necrosis and tumor regression without systemic toxicity, Cancer Gene Ther, 9 (2002) 673-680.
[144] R.M. Schiffelers, A. Ansari, J. Xu, Q. Zhou, Q. Tang, G. Storm, G. Molema, P.Y. Lu, P.V. Scaria, M.C. Woodle, Cancer siRNA therapy by tumor selective delivery with ligand-targeted sterically stabilized nanoparticle, Nucleic Acids Res., 32 (2004) e149.
[145] A. Ndoye, G. Dolivet, A. Hogset, A. Leroux, A. Fifre, P. Erbacher, K. Berg, J.P. Behr, F. Guillemin, J.L. Merlin, Eradication of p53-mutated head and neck squamous cell carcinoma xenografts using nonviral p53 gene therapy and photochemical internalization, Mol.Ther., 13 (2006) 1156-1162.
[146] A. Shir, M. Ogris, W. Roedl, E. Wagner, A. Levitzki, EGFR-homing dsRNA activates cancer-targeted immune response and eliminates disseminated EGFR-overexpressing tumors in mice, Clinical cancer research : an official journal of the American Association for Cancer Research, 17 (2011) 1033-1043.
[147] G. Abourbeh, A. Shir, E. Mishani, M. Ogris, W. Rodl, E. Wagner, A. Levitzki, PolyIC GE11 polyplex inhibits EGFR-overexpressing tumors, IUBMB life, 64 (2012) 324-330.
[148] B. Su, A. Cengizeroglu, K. Farkasova, J.R. Viola, M. Anton, J.W. Ellwart, R. Haase, E. Wagner, M. Ogris, Systemic TNFalpha gene therapy synergizes with liposomal doxorubicine in the treatment of metastatic cancer, Mol Ther, 21 (2013) 300-308.

[149] K.A. Schmohl, A. Gupta, G.K. Grunwald, M. Trajkovic-Arsic, K. Klutz, R. Braren, M. Schwaiger, P.J. Nelson, M. Ogris, E. Wagner, J.T. Siveke, C. Spitzweg, Imaging and targeted therapy of pancreatic ductal adenocarcinoma using the theranostic sodium iodide symporter (NIS) gene, Oncotarget, 8 (2017) 33393-33404.
[150] S. Schreiber, E. Kampgen, E. Wagner, D. Pirkhammer, J. Trcka, H. Korschan, A. Lindemann, R. Dorffner, H. Kittler, F. Kasteliz, Z. Kupcu, A. Sinski, K. Zatloukal, M. Buschle, W. Schmidt, M. Birnstiel, R.E. Kempe, T. Voigt, H.A. Weber, H. Pehamberger, R. Mertelsmann, E.B. Brocker, K. Wolff, G. Stingl, Immunotherapy of metastatic malignant melanoma by a vaccine consisting of autologous interleukin 2-transfected cancer cells: outcome of a phase I study, Hum.Gene Ther, 10 (1999) 983-993.
[151] K. Anwer, M.N. Barnes, J. Fewell, D.H. Lewis, R.D. Alvarez, Phase-I clinical trial of IL-12 plasmid/lipopolymer complexes for the treatment of recurrent ovarian cancer, Gene Ther, 17 (2010) 360-369.
[152] M.E. Davis, J.E. Zuckerman, C.H. Choi, D. Seligson, A. Tolcher, C.A. Alabi, Y. Yen, J.D. Heidel, A. Ribas, Evidence of RNAi in humans from systemically administered siRNA via targeted nanoparticles, Nature, 464 (2010) 1067-1070.
[153] K. Osada, H. Oshima, D. Kobayashi, M. Doi, M. Enoki, Y. Yamasaki, K. Kataoka, Quantized folding of plasmid DNA condensed with block catiomer into characteristic rod structures promoting transgene efficacy, J Am Chem Soc, 132 (2010) 12343-12348.
[154] A. Dirisala, K. Osada, Q. Chen, T.A. Tockary, K. Machitani, S. Osawa, X. Liu, T. Ishii, K. Miyata, M. Oba, S. Uchida, K. Itaka, K. Kataoka, Optimized rod length of polyplex micelles for maximizing transfection efficiency and their performance in systemic gene therapy against stroma-rich pancreatic tumors, Biomaterials, 35 (2014) 5359-5368.
[155] T.A. Tockary, K. Osada, Y. Motoda, S. Hiki, Q. Chen, K.M. Takeda, A. Dirisala, S. Osawa, K. Kataoka, Rod-to-Globule Transition of pDNA/PEG-Poly(l-Lysine) Polyplex Micelles Induced by a Collapsed Balance Between DNA Rigidity and PEG Crowdedness, Small (Weinheim an der Bergstrasse, Germany), 12 (2016) 1193-1200.
[156] K.M. Takeda, K. Osada, T.A. Tockary, A. Dirisala, Q. Chen, K. Kataoka, Poly(ethylene glycol) Crowding as Critical Factor To Determine pDNA Packaging Scheme into Polyplex Micelles for Enhanced Gene Expression, Biomacromolecules, 18 (2017) 36-43.
[157] K. Miyata, N. Nishiyama, K. Kataoka, Rational design of smart supramolecular assemblies for gene delivery: chemical challenges in the creation of artificial viruses, Chem. Soc. Rev., 41 (2012) 2562-2574.
[158] M. Han, Y. Bae, N. Nishiyama, K. Miyata, M. Oba, K. Kataoka, Transfection study using multicellular tumor spheroids for screening non-viral polymeric gene vectors with low cytotoxicity and high transfection efficiencies, J Control Release, 121 (2007) 38-48.
[159] K. Miyata, M. Oba, M. Nakanishi, S. Fukushima, Y. Yamasaki, H. Koyama, N. Nishiyama, K. Kataoka, Polyplexes from poly(aspartamide) bearing 1,2-diaminoethane side chains induce pH-selective, endosomal membrane destabilization with amplified transfection and negligible cytotoxicity, Journal of the American Chemical Society, 130 (2008) 16287-16294.
[160] H.J. Kim, A. Ishii, K. Miyata, Y. Lee, S. Wu, M. Oba, N. Nishiyama, K. Kataoka, Introduction of stearoyl moieties into a biocompatible cationic polyaspartamide derivative, PAsp(DET), with endosomal escaping function for enhanced siRNA-mediated gene knockdown, J Control Release, 145 (2010) 141-148.
[161] H. Uchida, K. Miyata, M. Oba, T. Ishii, T. Suma, K. Itaka, N. Nishiyama, K. Kataoka, Odd-even effect of repeating aminoethylene units in the side chain of N-substituted polyaspartamides on gene transfection profiles, J Am Chem Soc, 133 (2011) 15524-15532.
[162] H. Uchida, K. Itaka, T. Nomoto, T. Ishii, T. Suma, M. Ikegami, K. Miyata, M. Oba, N. Nishiyama, K. Kataoka, Modulated protonation of side chain aminoethylene repeats in N-substituted polyaspartamides promotes mRNA transfection, J Am Chem Soc, 136 (2014) 12396-12405.
[163] S. Uchida, H. Kinoh, T. Ishii, A. Matsui, T.A. Tockary, K.M. Takeda, H. Uchida, K. Osada, K. Itaka, K. Kataoka, Systemic delivery of messenger RNA for the treatment of

pancreatic cancer using polyplex nanomicelles with a cholesterol moiety, Biomaterials, 82 (2016) 221-228.
[164] C. Boyer, V. Bulmus, T.P. Davis, V. Ladmiral, J. Liu, S. Perrier, Bioapplications of RAFT polymerization, Chem Rev, 109 (2009) 5402-5436.
[165] M.H. Stenzel, RAFT polymerization: an avenue to functional polymeric micelles for drug delivery, Chem Commun (Camb), (2008) 3486-3503.
[166] M.A. Wolfert, E.H. Schacht, V. Toncheva, K. Ulbrich, O. Nazarova, L.W. Seymour, P.R. Dash, D. Oupicky, Characterization of vectors for gene therapy formed by self-assembly of DNA with synthetic block co-polymers 724, Hum Gene Ther, 7 (1996) 2123-2133.
[167] N. Murthy, J. Campbell, N. Fausto, A.S. Hoffman, P.S. Stayton, Bioinspired pH-Responsive Polymers for the Intracellular Delivery of Biomolecular Drugs, Bioconjug.Chem., 14 (2003) 412-419.
[168] K.A. Howard, P.R. Dash, M.L. Read, K. Ward, L.M. Tomkins, O. Nazarova, K. Ulbrich, L.W. Seymour, Influence of hydrophilicity of cationic polymers on the biophysical properties of polyelectrolyte complexes formed by self-assembly with DNA, Biochim.Biophys.Acta, 1475 (2000) 245-255.
[169] J.Y. Cherng, W.P. van de, H. Talsma, D.J. Crommelin, W.E. Hennink, Effect of size and serum proteins on transfection efficiency of poly ((2-dimethylamino)ethyl methacrylate)-plasmid nanoparticles 809, Pharm.Res., 13 (1996) 1038-1042.
[170] P. van de Wetering, J.Y. Cherng, H. Talsma, D.J. Crommelin, W.E. Hennink, 2-(Dimethylamino)ethyl methacrylate based (co)polymers as gene transfer agents 1031, J.Control Release, 53 (1998) 145-153.
[171] F.J. Verbaan, C. Oussoren, C.J. Snel, D.J. Crommelin, W.E. Hennink, G. Storm, Steric stabilization of poly(2-(dimethylamino)ethyl methacrylate)-based polyplexes mediates prolonged circulation and tumor targeting in mice, J.Gene Med., 6 (2004) 64-75.
[172] M. Barz, M. Tarantola, K. Fischer, M. Schmidt, R. Luxenhofer, A. Janshoff, P. Theato, R. Zentel, From defined reactive diblock copolymers to functional HPMA-based self-assembled nanoaggregates, Biomacromolecules, 9 (2008) 3114-3118.
[173] A.K. Trutzschler, T. Bus, M. Reifarth, J.C. Brendel, S. Hoeppener, A. Traeger, U.S. Schubert, Beyond Gene Transfection with Methacrylate-Based Polyplexes-The Influence of the Amino Substitution Pattern, Bioconjug Chem, 29 (2018) 2181-2194.
[174] H. Wei, L.R. Volpatti, D.L. Sellers, D.O. Maris, I.W. Andrews, A.S. Hemphill, L.W. Chan, D.S. Chu, P.J. Horner, S.H. Pun, Dual responsive, stabilized nanoparticles for efficient in vivo plasmid delivery, Angew Chem Int Ed Engl, 52 (2013) 5377-5381.
[175] Y. Cheng, R.C. Yumul, S.H. Pun, Virus-Inspired Polymer for Efficient In Vitro and In Vivo Gene Delivery, Angew Chem Int Ed Engl, 55 (2016) 12013-12017.
[176] D.P. Feldmann, Y. Cheng, R. Kandil, Y. Xie, M. Mohammadi, H. Harz, A. Sharma, D.J. Peeler, A. Moszczynska, H. Leonhardt, S.H. Pun, O.M. Merkel, In vitro and in vivo delivery of siRNA via VIPER polymer system to lung cells, J Control Release, 276 (2018) 50-58.
[177] D.J. Peeler, S.N. Thai, Y. Cheng, P.J. Horner, D.L. Sellers, S.H. Pun, pH-sensitive polymer micelles provide selective and potentiated lytic capacity to venom peptides for effective intracellular delivery, Biomaterials, 192 (2019) 235-244.
[178] T. Wang, D. Wang, H. Yu, M. Wang, J. Liu, B. Feng, F. Zhou, Q. Yin, Z. Zhang, Y. Huang, Y. Li, Intracellularly Acid-Switchable Multifunctional Micelles for Combinational Photo/Chemotherapy of the Drug-Resistant Tumor, ACS Nano, 10 (2016) 3496-3508.
[179] W. Wang, M. Saeed, Y. Zhou, L. Yang, D. Wang, H. Yu, Non-viral gene delivery for cancer immunotherapy, The journal of gene medicine, 21 (2019) e3092.
[180] I.K. Ko, A. Ziady, S. Lu, Y.J. Kwon, Acid-degradable cationic methacrylamide polymerized in the presence of plasmid DNA as tunable non-viral gene carrier, Biomaterials, 29 (2008) 3872-3881.
[181] Y. Cheng, D.L. Sellers, J.Y. Tan, D.J. Peeler, P.J. Horner, S.H. Pun, Development of switchable polymers to address the dilemma of stability and cargo release in polycationic nucleic acid carriers, Biomaterials, 127 (2017) 89-96.

[182] L. Novo, E.V. van Gaal, E. Mastrobattista, C.F. van Nostrum, W.E. Hennink, Decationized crosslinked polyplexes for redox-triggered gene delivery, J Control Release, 169 (2013) 246-256.
[183] L. Novo, L.Y. Rizzo, S.K. Golombek, G.R. Dakwar, B. Lou, K. Remaut, E. Mastrobattista, C.F. van Nostrum, W. Jahnen-Dechent, F. Kiessling, K. Braeckmans, T. Lammers, W.E. Hennink, Decationized polyplexes as stable and safe carrier systems for improved biodistribution in systemic gene therapy, J Control Release, 195 (2014) 162-175.
[184] L. Novo, E. Mastrobattista, C.F. van Nostrum, W.E. Hennink, Targeted decationized polyplexes for cell specific gene delivery, Bioconjug Chem, 25 (2014) 802-812.
[185] L. Novo, K.M. Takeda, T. Petteta, G.R. Dakwar, J.B. van den Dikkenberg, K. Remaut, K. Braeckmans, C.F. van Nostrum, E. Mastrobattista, W.E. Hennink, Targeted decationized polyplexes for siRNA delivery, Molecular pharmaceutics, 12 (2015) 150-161.
[186] B.R. Olden, Y. Cheng, J.L. Yu, S.H. Pun, Cationic polymers for non-viral gene delivery to human T cells, J Control Release, 282 (2018) 140-147.
[187] E.R. Lee, J. Marshall, C.S. Siegel, C. Jiang, N.S. Yew, M.R. Nichols, J.B. Nietupski, R.J. Ziegler, M.B. Lane, K.X. Wang, N.C. Wan, R.K. Scheule, D.J. Harris, A.E. Smith, S.H. Cheng, Detailed analysis of structures and formulations of cationic lipids for efficient gene transfer to the lung, Human gene therapy, 7 (1996) 1701-1717.
[188] Y.B. Lim, S.O. Han, H.U. Kong, Y. Lee, J.S. Park, B. Jeong, S.W. Kim, Biodegradable polyester, poly[alpha-(4-aminobutyl)-L-glycolic acid], as a non-toxic gene carrier, Pharm Res, 17 (2000) 811-816.
[189] Y.B. Lim, S.M. Kim, H. Suh, J.S. Park, Biodegradable, endosome disruptive, and cationic network-type polymer as a highly efficient and nontoxic gene delivery carrier, Bioconjug Chem, 13 (2002) 952-957.
[190] M.L. Forrest, J.T. Koerber, D.W. Pack, A degradable polyethylenimine derivative with low toxicity for highly efficient gene delivery, Bioconjug.Chem., 14 (2003) 934-940.
[191] J. Kloeckner, S. Bruzzano, M. Ogris, E. Wagner, Gene carriers based on hexanediol diacrylate linked oligoethylenimine: effect of chemical structure of polymer on biological properties, Bioconjug Chem, 17 (2006) 1339-1345.
[192] V. Russ, H. Elfberg, C. Thoma, J. Kloeckner, M. Ogris, E. Wagner, Novel degradable oligoethylenimine acrylate ester-based pseudodendrimers for in vitro and in vivo gene transfer, Gene Ther, 15 (2008) 18-29.
[193] A. Akinc, D.G. Anderson, D.M. Lynn, R. Langer, Synthesis of poly(beta-amino ester)s optimized for highly effective gene delivery, Bioconjug.Chem., 14 (2003) 979-988.
[194] D.M. Lynn, D.G. Anderson, D. Putnam, R. Langer, Accelerated discovery of synthetic transfection vectors: parallel synthesis and screening of a degradable polymer library, J.Am.Chem.Soc., 123 (2001) 8155-8156.
[195] A. Akinc, D.M. Lynn, D.G. Anderson, R. Langer, Parallel synthesis and biophysical characterization of a degradable polymer library for gene delivery, J.Am.Chem Soc., 125 (2003) 5316-5323.
[196] D.G. Anderson, D.M. Lynn, R. Langer, Semi-Automated Synthesis and Screening of a Large Library of Degradable Cationic Polymers for Gene Delivery, Angew.Chem.Int.Ed Engl., 42 (2003) 3153-3158.
[197] D.G. Anderson, A. Akinc, N. Hossain, R. Langer, Structure/property studies of polymeric gene delivery using a library of poly(beta-amino esters), Mol Ther, 11 (2005) 426-434.
[198] A. Akinc, M. Goldberg, J. Qin, J.R. Dorkin, C. Gamba-Vitalo, M. Maier, K.N. Jayaprakash, M. Jayaraman, K.G. Rajeev, M. Manoharan, V. Koteliansky, I. Rohl, E.S. Leshchiner, R. Langer, D.G. Anderson, Development of Lipidoid-siRNA Formulations for Systemic Delivery to the Liver, Mol Ther, 17 (2009) 872-879.
[199] K.T. Love, K.P. Mahon, C.G. Levins, K.A. Whitehead, W. Querbes, J.R. Dorkin, J. Qin, W. Cantley, L.L. Qin, T. Racie, M. Frank-Kamenetsky, K.N. Yip, R. Alvarez, D.W. Sah, A. de Fougerolles, K. Fitzgerald, V. Koteliansky, A. Akinc, R. Langer, D.G. Anderson, Lipid-like

materials for low-dose, in vivo gene silencing, Proc Natl Acad Sci U S A, 107 (2010) 1864-1869.
[200] A. Akinc, A. Zumbuehl, M. Goldberg, E.S. Leshchiner, V. Busini, N. Hossain, S.A. Bacallado, D.N. Nguyen, J. Fuller, R. Alvarez, A. Borodovsky, T. Borland, R. Constien, A. de Fougerolles, J.R. Dorkin, J.K. Narayanannair, M. Jayaraman, M. John, V. Koteliansky, M. Manoharan, L. Nechev, J. Qin, T. Racie, D. Raitcheva, K.G. Rajeev, D.W. Sah, J. Soutschek, I. Toudjarska, H.P. Vornlocher, T.S. Zimmermann, R. Langer, D.G. Anderson, A combinatorial library of lipid-like materials for delivery of RNAi therapeutics, Nat.Biotechnol., 26 (2008) 561-569.
[201] K.P. Mahon, K.T. Love, K.A. Whitehead, J. Qin, A. Akinc, E. Leshchiner, I. Leshchiner, R. Langer, D.G. Anderson, Combinatorial approach to determine functional group effects on lipidoid-mediated siRNA delivery, Bioconjug Chem, 21 (2010) 1448-1454.
[202] D.J. Siegwart, K.A. Whitehead, L. Nuhn, G. Sahay, H. Cheng, S. Jiang, M. Ma, A. Lytton-Jean, A. Vegas, P. Fenton, C.G. Levins, K.T. Love, H. Lee, C. Cortez, S.P. Collins, Y.F. Li, J. Jang, W. Querbes, C. Zurenko, T. Novobrantseva, R. Langer, D.G. Anderson, Combinatorial synthesis of chemically diverse core-shell nanoparticles for intracellular delivery, Proc Natl Acad Sci U S A, 108 (2011) 12996-13001.
[203] J.F. Lutz, M. Ouchi, D.R. Liu, M. Sawamoto, Sequence-controlled polymers, Science, 341 (2013) 1238149.
[204] S.C. Solleder, R.V. Schneider, K.S. Wetzel, A.C. Boukis, M.A.R. Meier, Recent Progress in the Design of Monodisperse, Sequence-Defined Macromolecules, Macromolecular rapid communications, 38 (2017).
[205] S. Celasun, D. Remmler, T. Schwaar, M.G. Weller, F. Du Prez, H.G. Borner, Digging into the Sequential Space of Thiolactone Precision Polymers: A Combinatorial Strategy to Identify Functional Domains, Angew Chem Int Ed Engl, 58 (2019) 1960-1964.
[206] M.S. Wadhwa, D.L. Knoell, A.P. Young, K.G. Rice, Targeted gene delivery with a low molecular weight glycopeptide carrier, Bioconjug Chem, 6 (1995) 283-291.
[207] C. Plank, M.X. Tang, A.R. Wolfe, F.C. Szoka, Jr., Branched cationic peptides for gene delivery: role of type and number of cationic residues in formation and in vitro activity of DNA polyplexes, Hum.Gene Ther., 10 (1999) 319-332.
[208] D.L. McKenzie, K.Y. Kwok, K.G. Rice, A potent new class of reductively activated peptide gene delivery agents, J.Biol.Chem., 275 (2000) 9970-9977.
[209] M. Stevenson, V. Ramos-Perez, S. Singh, M. Soliman, J.A. Preece, S.S. Briggs, M.L. Read, L.W. Seymour, Delivery of siRNA mediated by histidine-containing reducible polycations, J Control Release, 130 (2008) 46-56.
[210] Q.R. Chen, L. Zhang, S.A. Stass, A.J. Mixson, Branched co-polymers of histidine and lysine are efficient carriers of plasmids, Nucleic Acids Res., 29 (2001) 1334-1340.
[211] Q. Leng, A.J. Mixson, Modified branched peptides with a histidine-rich tail enhance in vitro gene transfection, Nucleic Acids Res, 33 (2005) e40.
[212] Q.R. Chen, L. Zhang, P.W. Luther, A.J. Mixson, Optimal transfection with the HK polymer depends on its degree of branching and the pH of endocytic vesicles, Nucleic Acids Res., 30 (2002) 1338-1345.
[213] Q. Leng, P. Scaria, J. Zhu, N. Ambulos, P. Campbell, A.J. Mixson, Highly branched HK peptides are effective carriers of siRNA, The journal of gene medicine, 7 (2005) 977-986.
[214] Q. Leng, S.T. Chou, P.V. Scaria, M.C. Woodle, A.J. Mixson, Increased tumor distribution and expression of histidine-rich plasmid polyplexes, The journal of gene medicine, 16 (2014) 317-328.
[215] Q. Leng, A.J. Mixson, The neuropilin-1 receptor mediates enhanced tumor delivery of H2K polyplexes, The journal of gene medicine, 18 (2016) 134-144.
[216] T.B. Wyman, F. Nicol, O. Zelphati, P.V. Scaria, C. Plank, F.C. Szoka, Jr., Design, synthesis, and characterization of a cationic peptide that binds to nucleic acids and permeabilizes bilayers, Biochemistry, 36 (1997) 3008-3017.
[217] K. Ezzat, S.E. Andaloussi, E.M. Zaghloul, T. Lehto, S. Lindberg, P.M. Moreno, J.R. Viola, T. Magdy, R. Abdo, P. Guterstam, R. Sillard, S.M. Hammond, M.J. Wood, A.A.

Arzumanov, M.J. Gait, C.I. Smith, M. Hallbrink, U. Langel, PepFect 14, a novel cell-penetrating peptide for oligonucleotide delivery in solution and as solid formulation, Nucleic Acids Res, 39 (2011) 5284-5298.
[218] X.L. Wang, R. Jensen, Z.R. Lu, A novel environment-sensitive biodegradable polydisulfide with protonatable pendants for nucleic acid delivery, J.Control Release, 120 (2007) 250-258.
[219] X.L. Wang, S. Ramusovic, T. Nguyen, Z.R. Lu, Novel polymerizable surfactants with pH-sensitive amphiphilicity and cell membrane disruption for efficient siRNA delivery, Bioconjug Chem, 18 (2007) 2169-2177.
[220] A.S. Malamas, M. Gujrati, C.M. Kummitha, R. Xu, Z.R. Lu, Design and evaluation of new pH-sensitive amphiphilic cationic lipids for siRNA delivery, J Control Release, 171 (2013) 296-307.
[221] T. Lehto, R. Abes, N. Oskolkov, J. Suhorutsenko, D.M. Copolovici, I. Mager, J.R. Viola, O.E. Simonson, K. Ezzat, P. Guterstam, E. Eriste, C.I. Smith, B. Lebleu, A. Samir El, U. Langel, Delivery of nucleic acids with a stearylated (RxR)4 peptide using a non-covalent co-incubation strategy, J Control Release, 141 (2010) 42-51.
[222] S.E. Andaloussi, T. Lehto, I. Mager, K. Rosenthal-Aizman, Oprea, II, O.E. Simonson, H. Sork, K. Ezzat, D.M. Copolovici, K. Kurrikoff, J.R. Viola, E.M. Zaghloul, R. Sillard, H.J. Johansson, F. Said Hassane, P. Guterstam, J. Suhorutsenko, P.M. Moreno, N. Oskolkov, J. Halldin, U. Tedebark, A. Metspalu, B. Lebleu, J. Lehtio, C.I. Smith, U. Langel, Design of a peptide-based vector, PepFect6, for efficient delivery of siRNA in cell culture and systemically in vivo, Nucleic Acids Res, 39 (2011) 3972-3987.
[223] Z.P. Gates, A.A. Vinogradov, A.J. Quartararo, A. Bandyopadhyay, Z.N. Choo, E.D. Evans, K.H. Halloran, A.J. Mijalis, S.K. Mong, M.D. Simon, E.A. Standley, E.D. Styduhar, S.Z. Tasker, F. Touti, J.M. Weber, J.L. Wilson, T.F. Jamison, B.L. Pentelute, Xenoprotein engineering via synthetic libraries, Proc Natl Acad Sci U S A, 115 (2018) E5298-e5306.
[224] F. Touti, Z.P. Gates, A. Bandyopadhyay, G. Lautrette, B.L. Pentelute, In-solution enrichment identifies peptide inhibitors of protein-protein interactions, Nature chemical biology, 15 (2019) 410-418.
[225] B.L. Pentelute, L. Wang, Editorial overview: Chemistry for biopolymers to investigate and even move beyond nature, Current opinion in chemical biology, 34 (2016) v-vi.
[226] A.A. Vinogradov, Z.P. Gates, C. Zhang, A.J. Quartararo, K.H. Halloran, B.L. Pentelute, Library Design-Facilitated High-Throughput Sequencing of Synthetic Peptide Libraries, ACS combinatorial science, 19 (2017) 694-701.
[227] C.M. Fadzen, J.M. Wolfe, C.F. Cho, E.A. Chiocca, S.E. Lawler, B.L. Pentelute, Perfluoroarene-Based Peptide Macrocycles to Enhance Penetration Across the Blood-Brain Barrier, J Am Chem Soc, 139 (2017) 15628-15631.
[228] J.M. Wolfe, C.M. Fadzen, R.L. Holden, M. Yao, G.J. Hanson, B.L. Pentelute, Perfluoroaryl Bicyclic Cell-Penetrating Peptides for Delivery of Antisense Oligonucleotides, Angew Chem Int Ed Engl, 57 (2018) 4756-4759.
[229] J.M. Wolfe, C.M. Fadzen, Z.N. Choo, R.L. Holden, M. Yao, G.J. Hanson, B.L. Pentelute, Machine Learning To Predict Cell-Penetrating Peptides for Antisense Delivery, ACS central science, 4 (2018) 512-520.
[230] L. Hartmann, S. Häfele, R. Peschka-Süss, M. Antonietti, H.G. Börner, Sequence Positioning of Disulfide Linkages to Program the Degradation of Monodisperse Poly(amidoamines), Macromolecules, 40 (2007) 7771-7776.
[231] L. Hartmann, S. Hafele, R. Peschka-Suss, M. Antonietti, H.G. Borner, Tailor-Made Poly(amidoamine)s for Controlled Complexation and Condensation of DNA, Chemistry., 14 (2008) 2025-2033.
[232] L. Hartmann, H.G. Börner, Precision Polymers: Monodisperse, Monomer-Sequence-Defined Segments to Target Future Demands of Polymers in Medicine, Advanced Materials, 21 (2009) 3425-3431.
[233] L. Hartmann, Polymers for Control Freaks: Sequence-Defined Poly(amidoamine)s and Their Biomedical Applications, Macromolecular Chemistry and Physics, 212 (2011) 8-13.

[234] S.A. Hill, C. Gerke, L. Hartmann, Recent Developments in Solid-Phase Strategies towards Synthetic, Sequence-Defined Macromolecules, Chemistry, an Asian journal, 13 (2018) 3611-3622.
[235] D. Schaffert, N. Badgujar, E. Wagner, Novel Fmoc-polyamino acids for solid-phase synthesis of defined polyamidoamines, Organic letters, 13 (2011) 1586-1589.
[236] E.E. Salcher, P. Kos, T. Frohlich, N. Badgujar, M. Scheible, E. Wagner, Sequence-defined four-arm oligo(ethanamino)amides for pDNA and siRNA delivery: Impact of building blocks on efficacy, J Control Release, 164 (2012) 380-386.
[237] C. Scholz, P. Kos, L. Leclercq, X. Jin, H. Cottet, E. Wagner, Correlation of length of linear oligo(ethanamino) amides with gene transfer and cytotoxicity, ChemMedChem, 9 (2014) 2104-2110.
[238] T. Frohlich, D. Edinger, R. Klager, C. Troiber, E. Salcher, N. Badgujar, I. Martin, D. Schaffert, A. Cengizeroglu, P. Hadwiger, H.P. Vornlocher, E. Wagner, Structure-activity relationships of siRNA carriers based on sequence-defined oligo (ethane amino) amides, J Control Release, 160 (2012) 532-541.
[239] U. Lachelt, P. Kos, F.M. Mickler, A. Herrmann, E.E. Salcher, W. Rodl, N. Badgujar, C. Brauchle, E. Wagner, Fine-tuning of proton sponges by precise diaminoethanes and histidines in pDNA polyplexes, Nanomedicine, 10 (2014) 35-44.
[240] C. Scholz, P. Kos, E. Wagner, Comb-like oligoaminoethane carriers: change in topology improves pDNA delivery, Bioconjug Chem, 25 (2014) 251-261.
[241] D. Schaffert, C. Troiber, E. Wagner, New Sequence-Defined Polyaminoamides with Tailored Endosomolytic Properties for Plasmid DNA Delivery, Bioconjug Chem, 23 (2012) 1157-1165.
[242] I. Martin, C. Dohmen, C. Mas-Moruno, C. Troiber, P. Kos, D. Schaffert, U. Lachelt, M. Teixido, M. Günther, H. Kessler, E. Giralt, E. Wagner, Solid-phase-assisted synthesis of targeting peptide-PEG-oligo(ethane amino)amides for receptor-mediated gene delivery, Organic & Biomolecular Chemistry, 10 (2012) 3258-3268.
[243] D. He, K. Muller, A. Krhac Levacic, P. Kos, U. Lachelt, E. Wagner, Combinatorial Optimization of Sequence-Defined Oligo(ethanamino)amides for Folate Receptor-Targeted pDNA and siRNA Delivery, Bioconjug Chem, 27 (2016) 647-659.
[244] P. Kos, U. Lachelt, A. Herrmann, F.M. Mickler, M. Doblinger, D. He, A. Krhac Levacic, S. Morys, C. Brauchle, E. Wagner, Histidine-rich stabilized polyplexes for cMet-directed tumor-targeted gene transfer, Nanoscale, 7 (2015) 5350-5362.
[245] S. Urnauer, S. Morys, A. Krhac Levacic, A.M. Muller, C. Schug, K.A. Schmohl, N. Schwenk, C. Zach, J. Carlsen, P. Bartenstein, E. Wagner, C. Spitzweg, Sequence-defined cMET/HGFR-targeted Polymers as Gene Delivery Vehicles for the Theranostic Sodium Iodide Symporter (NIS) Gene, Mol Ther, 24 (2016) 1395-1404.
[246] P. Kos, U. Lachelt, D. He, Y. Nie, Z. Gu, E. Wagner, Dual-targeted polyplexes based on sequence-defined peptide-PEG-oligoamino amides, Journal of pharmaceutical sciences, 104 (2015) 464-475.
[247] S. Wang, S. Reinhard, C. Li, M. Qian, H. Jiang, Y. Du, U. Lachelt, W. Lu, E. Wagner, R. Huang, Antitumoral Cascade-Targeting Ligand for IL-6 Receptor-Mediated Gene Delivery to Glioma, Mol Ther, 25 (2017) 1556-1566.
[248] G.F. Walker, C. Fella, J. Pelisek, J. Fahrmeir, S. Boeckle, M. Ogris, E. Wagner, Toward synthetic viruses: endosomal pH-triggered deshielding of targeted polyplexes greatly enhances gene transfer in vitro and in vivo, Mol Ther, 11 (2005) 418-425.
[249] D. Schaffert, M. Kiss, W. Rodl, A. Shir, A. Levitzki, M. Ogris, E. Wagner, Poly(I:C)-mediated tumor growth suppression in EGF-receptor overexpressing tumors using EGF-polyethylene glycol-linear polyethylenimine as carrier, Pharm Res, 28 (2011) 731-741.
[250] S. Morys, A. Krhac Levacic, S. Urnauer, S. Kempter, S. Kern, J.O. Radler, C. Spitzweg, U. Lachelt, E. Wagner, Influence of Defined Hydrophilic Blocks within Oligoaminoamide Copolymers: Compaction versus Shielding of pDNA Nanoparticles, Polymers, 9 (2017).

[251] J.M. Williford, M.M. Archang, I. Minn, Y. Ren, M. Wo, J. Vandermark, P.B. Fisher, M.G. Pomper, H.Q. Mao, Critical Length of PEG Grafts on lPEI/DNA Nanoparticles for Efficient in Vivo Delivery, ACS Biomater Sci Eng, 2 (2016) 567-578.
[252] J.F. Stefanick, J.D. Ashley, T. Kiziltepe, B. Bilgicer, A systematic analysis of peptide linker length and liposomal polyethylene glycol coating on cellular uptake of peptide-targeted liposomes, ACS Nano, 7 (2013) 2935-2947.
[253] A.K. Levacic, S. Morys, S. Kempter, U. Lachelt, E. Wagner, Minicircle Versus Plasmid DNA Delivery by Receptor-Targeted Polyplexes, Hum Gene Ther, 28 (2017) 862-874.
[254] M. Ogris, G. Walker, T. Blessing, R. Kircheis, M. Wolschek, E. Wagner, Tumor-targeted gene therapy: strategies for the preparation of ligand-polyethylene glycol-polyethylenimine/DNA complexes, J Control Release, 91 (2003) 173-181.
[255] L. Beckert, L. Kostka, E. Kessel, A. Krhac Levacic, H. Kostkova, T. Etrych, U. Lachelt, E. Wagner, Acid-labile pHPMA modification of four-arm oligoaminoamide pDNA polyplexes balances shielding and gene transfer activity in vitro and in vivo, European journal of pharmaceutics and biopharmaceutics : official journal of Arbeitsgemeinschaft fur Pharmazeutische Verfahrenstechnik e.V, 105 (2016) 85-96.
[256] S. Morys, S. Urnauer, C. Spitzweg, E. Wagner, EGFR Targeting and Shielding of pDNA Lipopolyplexes via Bivalent Attachment of a Sequence-Defined PEG Agent, Macromolecular bioscience, 18 (2018).
[257] I. Truebenbach, S. Kern, D.M. Loy, M. Hohn, J. Gorges, U. Kazmaier, E. Wagner, Combination Chemotherapy of L1210 Tumors in Mice with Pretubulysin and Methotrexate Lipo-Oligomer Nanoparticles, Molecular pharmaceutics, 16 (2019) 2405-2417.
[258] I. Truebenbach, J. Gorges, J. Kuhn, S. Kern, E. Baratti, U. Kazmaier, E. Wagner, U. Lächelt, Sequence-Defined Oligoamide Drug Conjugates of Pretubulysin and Methotrexate for Folate Receptor Targeted Cancer Therapy, Macromol Biosci, 17 (2017).
[259] J. Kuhn, P.M. Klein, N. Al Danaf, J.Z. Nordin, S. Reinhard, D.M. Loy, M. Höhn, S. El Andaloussi, D.C. Lamb, E. Wagner, Y. Aoki, T. Lehto, U. Lächelt, Supramolecular Assembly of Aminoethylene-Lipopeptide PMO Conjugates into RNA Splice-Switching Nanomicelles, Advanced Functional Materials, 0 1906432.
[260] J. Kuhn, Y. Lin, A. Krhac Levacic, N. Al Danaf, L. Peng, M. Höhn, D.C. Lamb, E. Wagner, U. Lächelt, Delivery of Cas9/sgRNA Ribonucleoprotein Complexes via Hydroxystearyl Oligoamino Amides, Bioconjug Chem, 31 (2020) 729-742.
[261] J. Niu, R. Hili, D.R. Liu, Enzyme-free translation of DNA into sequence-defined synthetic polymers structurally unrelated to nucleic acids, Nature chemistry, 5 (2013) 282-292.
[262] Z. Chen, P.A. Lichtor, A.P. Berliner, J.C. Chen, D.R. Liu, Evolution of sequence-defined highly functionalized nucleic acid polymers, Nature chemistry, 10 (2018) 420-427.
[263] Y. Li, R. De Luca, S. Cazzamalli, F. Pretto, D. Bajic, J. Scheuermann, D. Neri, Versatile protein recognition by the encoded display of multiple chemical elements on a constant macrocyclic scaffold, Nature chemistry, 10 (2018) 441-448.
[264] D. Neri, R.A. Lerner, DNA-Encoded Chemical Libraries: A Selection System Based on Endowing Organic Compounds with Amplifiable Information, Annual review of biochemistry, 87 (2018) 479-502.
[265] J.E. Dahlman, K.J. Kauffman, Y. Xing, T.E. Shaw, F.F. Mir, C.C. Dlott, R. Langer, D.G. Anderson, E.T. Wang, Barcoded nanoparticles for high throughput in vivo discovery of targeted therapeutics, Proc Natl Acad Sci U S A, 114 (2017) 2060-2065.
[266] M.P. Lokugamage, C.D. Sago, J.E. Dahlman, Testing thousands of nanoparticles in vivo using DNA barcodes, Current opinion in biomedical engineering, 7 (2018) 1-8.
[267] C.D. Sago, M.P. Lokugamage, G.N. Lando, N. Djeddar, N.N. Shah, C. Syed, A.V. Bryksin, J.E. Dahlman, Modifying a Commonly Expressed Endocytic Receptor Retargets Nanoparticles in Vivo, Nano Lett, 18 (2018) 7590-7600.
[268] C.D. Sago, M.P. Lokugamage, K. Paunovska, D.A. Vanover, C.M. Monaco, N.N. Shah, M. Gamboa Castro, S.E. Anderson, T.G. Rudoltz, G.N. Lando, P. Munnilal Tiwari, J.L. Kirschman, N. Willett, Y.C. Jang, P.J. Santangelo, A.V. Bryksin, J.E. Dahlman, High-

throughput in vivo screen of functional mRNA delivery identifies nanoparticles for endothelial cell gene editing, Proc Natl Acad Sci U S A, 115 (2018) E9944-e9952.
[269] C.D. Sago, M.P. Lokugamage, F.Z. Islam, B.R. Krupczak, M. Sato, J.E. Dahlman, Nanoparticles That Deliver RNA to Bone Marrow Identified by in Vivo Directed Evolution, J Am Chem Soc, 140 (2018) 17095-17105.
[270] K. Paunovska, A.J. Da Silva Sanchez, C.D. Sago, Z. Gan, M.P. Lokugamage, F.Z. Islam, S. Kalathoor, B.R. Krupczak, J.E. Dahlman, Nanoparticles Containing Oxidized Cholesterol Deliver mRNA to the Liver Microenvironment at Clinically Relevant Doses, Advanced materials (Deerfield Beach, Fla.), 31 (2019) e1807748.
[271] M.P. Lokugamage, C.D. Sago, Z. Gan, B.R. Krupczak, J.E. Dahlman, Constrained Nanoparticles Deliver siRNA and sgRNA to T Cells In Vivo without Targeting Ligands, Adv Mater, 31 (2019) e1902251.
[272] K. Paunovska, D. Loughrey, C.D. Sago, R. Langer, J.E. Dahlman, Using Large Datasets to Understand Nanotechnology, Advanced materials (Deerfield Beach, Fla.), 31 (2019) e1902798.
[273] M. Meyer, C. Dohmen, A. Philipp, D. Kiener, G. Maiwald, C. Scheu, M. Ogris, E. Wagner, Synthesis and Biological Evaluation of a Bioresponsive and Endosomolytic siRNA−Polymer Conjugate, Molecular pharmaceutics, 6 (2009) 752-762.
[274] D.B. Rozema, D.L. Lewis, D.H. Wakefield, S.C. Wong, J.J. Klein, P.L. Roesch, S.L. Bertin, T.W. Reppen, Q. Chu, A.V. Blokhin, J.E. Hagstrom, J.A. Wolff, Dynamic PolyConjugates for targeted in vivo delivery of siRNA to hepatocytes, Proc.Natl.Acad.Sci U.S.A, 104 (2007) 12982-12987.
[275] R.K. Thapa, M.O. Sullivan, Gene delivery by peptide-assisted transport, Current opinion in biomedical engineering, 7 (2018) 71-82.
[276] M.S. Draz, B.A. Fang, P. Zhang, Z. Hu, S. Gu, K.C. Weng, J.W. Gray, F.F. Chen, Nanoparticle-mediated systemic delivery of siRNA for treatment of cancers and viral infections, Theranostics, 4 (2014) 872-892.
[277] H. Maeda, The enhanced permeability and retention (EPR) effect in tumor vasculature: the key role of tumor-selective macromolecular drug targeting, Adv Enzyme Regul, 41 (2001) 189-207.
[278] S. Sindhwani, A.M. Syed, J. Ngai, B.R. Kingston, L. Maiorino, J. Rothschild, P. MacMillan, Y. Zhang, N.U. Rajesh, T. Hoang, J.L.Y. Wu, S. Wilhelm, A. Zilman, S. Gadde, A. Sulaiman, B. Ouyang, Z. Lin, L. Wang, M. Egeblad, W.C.W. Chan, The entry of nanoparticles into solid tumours, Nat Mater, 19 (2020) 566-575.
[279] S. Brunner, E. Furtbauer, T. Sauer, M. Kursa, E. Wagner, Overcoming the nuclear barrier: cell cycle independent nonviral gene transfer with linear polyethylenimine or electroporation, Mol Ther, 5 (2002) 80-86.
[280] E. Wagner, R. Kircheis, G.F. Walker, Targeted nucleic acid delivery into tumors: new avenues for cancer therapy, Biomedicine & pharmacotherapy = Biomedecine & pharmacotherapie, 58 (2004) 152-161.
[281] K. Klutz, D. Schaffert, M.J. Willhauck, G.K. Grunwald, R. Haase, N. Wunderlich, C. Zach, F.J. Gildehaus, R. Senekowitsch-Schmidtke, B. Goke, E. Wagner, M. Ogris, C. Spitzweg, Epidermal growth factor receptor-targeted (131)I-therapy of liver cancer following systemic delivery of the sodium iodide symporter gene, Mol Ther, 19 (2011) 676-685.
[282] J. DeRouchey, G.F. Walker, E. Wagner, J.O. Radler, Decorated rods: a "bottom-up" self-assembly of monomolecular DNA complexes, J Phys Chem B, 110 (2006) 4548-4554.
[283] J. DeRouchey, C. Schmidt, G.F. Walker, C. Koch, C. Plank, E. Wagner, J.O. Radler, Monomolecular assembly of siRNA and poly(ethylene glycol)-peptide copolymers, Biomacromolecules., 9 (2008) 724-732.
[284] Z. Ge, Q. Chen, K. Osada, X. Liu, T.A. Tockary, S. Uchida, A. Dirisala, T. Ishii, T. Nomoto, K. Toh, Y. Matsumoto, M. Oba, M.R. Kano, K. Itaka, K. Kataoka, Targeted gene delivery by polyplex micelles with crowded PEG palisade and cRGD moiety for systemic treatment of pancreatic tumors, Biomaterials, 35 (2014) 3416-3426.

[285] N.P. Gabrielson, H. Lu, L. Yin, D. Li, F. Wang, J. Cheng, Reactive and bioactive cationic alpha-helical polypeptide template for nonviral gene delivery, Angew Chem Int Ed Engl, 51 (2012) 1143-1147.
[286] H.X. Wang, Z. Song, Y.H. Lao, X. Xu, J. Gong, D. Cheng, S. Chakraborty, J.S. Park, M. Li, D. Huang, L. Yin, J. Cheng, K.W. Leong, Nonviral gene editing via CRISPR/Cas9 delivery by membrane-disruptive and endosomolytic helical polypeptide, Proc Natl Acad Sci U S A, 115 (2018) 4903-4908.
[287] D.R. Wilson, Y. Rui, K. Siddiq, D. Routkevitch, J.J. Green, Differentially Branched Ester Amine Quadpolymers with Amphiphilic and pH-Sensitive Properties for Efficient Plasmid DNA Delivery, Molecular pharmaceutics, 16 (2019) 655-668.
[288] D. Sun, B. Sahu, S. Gao, R.M. Schur, A.M. Vaidya, A. Maeda, K. Palczewski, Z.R. Lu, Targeted Multifunctional Lipid ECO Plasmid DNA Nanoparticles as Efficient Non-viral Gene Therapy for Leber's Congenital Amaurosis, Molecular therapy. Nucleic acids, 7 (2017) 42-52.
[289] D. Sun, R.M. Schur, A.E. Sears, S.Q. Gao, A. Vaidya, W. Sun, A. Maeda, T. Kern, K. Palczewski, Z.R. Lu, Non-viral Gene Therapy for Stargardt Disease with ECO/pRHO-ABCA4 Self-Assembled Nanoparticles, Mol Ther, 28 (2020) 293-303.
[290] Y. Dong, D.J. Siegwart, D.G. Anderson, Strategies, design, and chemistry in siRNA delivery systems, Adv Drug Deliv Rev, 144 (2019) 133-147.
[291] E. Wagner, Biomaterials in RNAi therapeutics: quo vadis?, Biomaterials Science, 1 (2013) 804-809.
[292] A. Akinc, W. Querbes, S. De, J. Qin, M. Frank-Kamenetsky, K.N. Jayaprakash, M. Jayaraman, K.G. Rajeev, W.L. Cantley, J.R. Dorkin, J.S. Butler, L. Qin, T. Racie, A. Sprague, E. Fava, A. Zeigerer, M.J. Hope, M. Zerial, D.W. Sah, K. Fitzgerald, M.A. Tracy, M. Manoharan, V. Koteliansky, A. Fougerolles, M.A. Maier, Targeted delivery of RNAi therapeutics with endogenous and exogenous ligand-based mechanisms, Mol Ther, 18 (2010) 1357-1364.
[293] J. Soutschek, A. Akinc, B. Bramlage, K. Charisse, R. Constien, M. Donoghue, S. Elbashir, A. Geick, P. Hadwiger, J. Harborth, M. John, V. Kesavan, G. Lavine, R.K. Pandey, T. Racie, K.G. Rajeev, I. Rohl, I. Toudjarska, G. Wang, S. Wuschko, D. Bumcrot, V. Koteliansky, S. Limmer, M. Manoharan, H.P. Vornlocher, Therapeutic silencing of an endogenous gene by systemic administration of modified siRNAs, Nature, 432 (2004) 173-178.
[294] P.R. de Paula Brandão, S.S. Titze-de-Almeida, R. Titze-de-Almeida, Leading RNA Interference Therapeutics Part 2: Silencing Delta-Aminolevulinic Acid Synthase 1, with a Focus on Givosiran, Mol Diagn Ther, 24 (2020) 61-68.
[295] I.A. Khalil, Y. Yamada, H. Harashima, Optimization of siRNA delivery to target sites: issues and future directions, Expert Opin Drug Deliv, 15 (2018) 1053-1065.
[296] Y. Sato, H. Matsui, R. Sato, H. Harashima, Neutralization of negative charges of siRNA results in improved safety and efficient gene silencing activity of lipid nanoparticles loaded with high levels of siRNA, J Control Release, 284 (2018) 179-187.
[297] Y. Sato, K. Hashiba, K. Sasaki, M. Maeki, M. Tokeshi, H. Harashima, Understanding structure-activity relationships of pH-sensitive cationic lipids facilitates the rational identification of promising lipid nanoparticles for delivering siRNAs in vivo, J Control Release, 295 (2019) 140-152.
[298] Y. Sakurai, T. Hada, A. Kato, Y. Hagino, W. Mizumura, H. Harashima, Effective Therapy Using a Liposomal siRNA that Targets the Tumor Vasculature in a Model Murine Breast Cancer with Lung Metastasis, Molecular therapy oncolytics, 11 (2018) 102-108.
[299] X.L. Wang, R. Xu, X. Wu, D. Gillespie, R. Jensen, Z.R. Lu, Targeted systemic delivery of a therapeutic siRNA with a multifunctional carrier controls tumor proliferation in mice, Mol Pharm., 6 (2009) 738-746.
[300] X.-L. Wang, R. Xu, Z.-R. Lu, A peptide-targeted delivery system with pH-sensitive amphiphilic cell membrane disruption for efficient receptor-mediated siRNA delivery, Journal of Controlled Release, 134 (2009) 207-213.

[301] J.G. Parvani, M.D. Gujrati, M.A. Mack, W.P. Schiemann, Z.R. Lu, Silencing beta3 Integrin by Targeted ECO/siRNA Nanoparticles Inhibits EMT and Metastasis of Triple-Negative Breast Cancer, Cancer research, 75 (2015) 2316-2325.
[302] A.M. Vaidya, Z. Sun, N. Ayat, A. Schilb, X. Liu, H. Jiang, D. Sun, J. Scheidt, V. Qian, S. He, H. Gilmore, W.P. Schiemann, Z.R. Lu, Systemic Delivery of Tumor-Targeting siRNA Nanoparticles against an Oncogenic LncRNA Facilitates Effective Triple-Negative Breast Cancer Therapy, Bioconjug Chem, 30 (2019) 907-919.
[303] C. Dohmen, D. Edinger, T. Frohlich, L. Schreiner, U. Lachelt, C. Troiber, J. Radler, P. Hadwiger, H.P. Vornlocher, E. Wagner, Nanosized Multifunctional Polyplexes for Receptor-Mediated SiRNA Delivery, ACS nano, 6 (2012) 5198-5208.
[304] D.J. Lee, E. Kessel, D. Edinger, D. He, P.M. Klein, L. Voith von Voithenberg, D.C. Lamb, U. Lachelt, T. Lehto, E. Wagner, Dual antitumoral potency of EG5 siRNA nanoplexes armed with cytotoxic bifunctional glutamyl-methotrexate targeting ligand, Biomaterials, 77 (2016) 98-110.
[305] C. Troiber, D. Edinger, P. Kos, L. Schreiner, R. Klager, A. Herrmann, E. Wagner, Stabilizing effect of tyrosine trimers on pDNA and siRNA polyplexes, Biomaterials, 34 (2013) 1624-1633.
[306] P.M. Klein, S. Reinhard, D.J. Lee, K. Muller, D. Ponader, L. Hartmann, E. Wagner, Precise redox-sensitive cleavage sites for improved bioactivity of siRNA lipopolyplexes, Nanoscale, 8 (2016) 18098-18104.
[307] D.J. Lee, D. He, E. Kessel, K. Padari, S. Kempter, U. Lachelt, J.O. Radler, M. Pooga, E. Wagner, Tumoral gene silencing by receptor-targeted combinatorial siRNA polyplexes, J Control Release, 244 (2016) 280-291.
[308] D.J. Lee, E. Kessel, T. Lehto, X. Liu, N. Yoshinaga, K. Padari, Y.C. Chen, S. Kempter, S. Uchida, J.O. Rädler, M. Pooga, M.T. Sheu, K. Kataoka, E. Wagner, Systemic Delivery of Folate-PEG siRNA Lipopolyplexes with Enhanced Intracellular Stability for In Vivo Gene Silencing in Leukemia, Bioconjug Chem, 28 (2017) 2393-2409.
[309] K. Muller, P.M. Klein, P. Heissig, A. Roidl, E. Wagner, EGF receptor targeted lipo-oligocation polyplexes for antitumoral siRNA and miRNA delivery, Nanotechnology, 27 (2016) 464001.
[310] K. Muller, E. Kessel, P.M. Klein, M. Hohn, E. Wagner, Post-PEGylation of siRNA Lipo-oligoamino Amide Polyplexes Using Tetra-glutamylated Folic Acid as Ligand for Receptor-Targeted Delivery, Molecular pharmaceutics, 13 (2016) 2332-2345.
[311] W. Zhang, K. Muller, E. Kessel, S. Reinhard, D. He, P.M. Klein, M. Hohn, W. Rodl, S. Kempter, E. Wagner, Targeted siRNA Delivery Using a Lipo-Oligoaminoamide Nanocore with an Influenza Peptide and Transferrin Shell, Advanced healthcare materials, 5 (2016) 1493-1504.
[312] P.M. Klein, S. Kern, D.J. Lee, J. Schmaus, M. Hohn, J. Gorges, U. Kazmaier, E. Wagner, Folate receptor-directed orthogonal click-functionalization of siRNA lipopolyplexes for tumor cell killing in vivo, Biomaterials, 178 (2018) 630-642.
[313] B. Steinborn, I. Truebenbach, S. Morys, U. Lachelt, E. Wagner, W. Zhang, Epidermal growth factor receptor targeted methotrexate and small interfering RNA co-delivery, The journal of gene medicine, 20 (2018) e3041.
[314] I. Truebenbach, W. Zhang, Y. Wang, S. Kern, M. Hohn, S. Reinhard, J. Gorges, U. Kazmaier, E. Wagner, Co-delivery of pretubulysin and siEG5 to EGFR overexpressing carcinoma cells, Int J Pharm, 569 (2019) 118570.
[315] J. Luo, M. Höhn, S. Reinhard, D.M. Loy, P.M. Klein, E. Wagner, IL4-Receptor-Targeted Dual Antitumoral Apoptotic Peptide—siRNA Conjugate Lipoplexes, Advanced Functional Materials, 0 1900697.
[316] J. Luo, E. Wagner, Y. Wang, Artificial peptides for antitumoral siRNA delivery, J Mater Chem B, 8 (2020) 2020-2031.
[317] A. Zintchenko, A. Philipp, A. Dehshahri, E. Wagner, Simple modifications of branched PEI lead to highly efficient siRNA carriers with low toxicity, Bioconjug Chem, 19 (2008) 1448-1455.

[318] Y. Wang, J. Luo, I. Truebenbach, S. Reinhard, P.M. Klein, M. Höhn, S. Kern, S. Morys, D.M. Loy, E. Wagner, W. Zhang, Double Click-Functionalized siRNA Polyplexes for Gene Silencing in Epidermal Growth Factor Receptor-Positive Tumor Cells, ACS Biomater Sci Eng, 6 (2020) 1074-1089.
[319] Y. Yan, H. Xiong, X. Zhang, Q. Cheng, D.J. Siegwart, Systemic mRNA Delivery to the Lungs by Functional Polyester-based Carriers, Biomacromolecules, 18 (2017) 4307-4315.
[320] J.C. Kaczmarek, K.J. Kauffman, O.S. Fenton, K. Sadtler, A.K. Patel, M.W. Heartlein, F. DeRosa, D.G. Anderson, Optimization of a Degradable Polymer-Lipid Nanoparticle for Potent Systemic Delivery of mRNA to the Lung Endothelium and Immune Cells, Nano Lett, 18 (2018) 6449-6454.
[321] L. Nuhn, L. Kaps, M. Diken, D. Schuppan, R. Zentel, Reductive Decationizable Block Copolymers for Stimuli-Responsive mRNA Delivery, Macromolecular rapid communications, 37 (2016) 924-933.
[322] A. Jarzebinska, T. Pasewald, J. Lambrecht, O. Mykhaylyk, L. Kummerling, P. Beck, G. Hasenpusch, C. Rudolph, C. Plank, C. Dohmen, A Single Methylene Group in Oligoalkylamine-Based Cationic Polymers and Lipids Promotes Enhanced mRNA Delivery, Angew Chem Int Ed Engl, 55 (2016) 9591-9595.
[323] J.C. Kaczmarek, A.K. Patel, K.J. Kauffman, O.S. Fenton, M.J. Webber, M.W. Heartlein, F. DeRosa, D.G. Anderson, Polymer-Lipid Nanoparticles for Systemic Delivery of mRNA to the Lungs, Angew Chem Int Ed Engl, 55 (2016) 13808-13812.
[324] P.S. Kowalski, U. Capasso Palmiero, Y. Huang, A. Rudra, R. Langer, D.G. Anderson, Ionizable Amino-Polyesters Synthesized via Ring Opening Polymerization of Tertiary Amino-Alcohols for Tissue Selective mRNA Delivery, Adv Mater, (2018) e1801151.
[325] J. Gilleron, W. Querbes, A. Zeigerer, A. Borodovsky, G. Marsico, U. Schubert, K. Manygoats, S. Seifert, C. Andree, M. Stoter, H. Epstein-Barash, L. Zhang, V. Koteliansky, K. Fitzgerald, E. Fava, M. Bickle, Y. Kalaidzidis, A. Akinc, M. Maier, M. Zerial, Image-based analysis of lipid nanoparticle-mediated siRNA delivery, intracellular trafficking and endosomal escape, Nature biotechnology, 31 (2013) 638-646.
[326] A. Wittrup, A. Ai, X. Liu, P. Hamar, R. Trifonova, K. Charisse, M. Manoharan, T. Kirchhausen, J. Lieberman, Visualizing lipid-formulated siRNA release from endosomes and target gene knockdown, Nat Biotechnol, 33 (2015) 870-876.
[327] E.J. Sayers, S.E. Peel, A. Schantz, R.M. England, M. Beano, S.M. Bates, A.S. Desai, S. Puri, M.B. Ashford, A.T. Jones, Endocytic Profiling of Cancer Cell Models Reveals Critical Factors Influencing LNP-Mediated mRNA Delivery and Protein Expression, Mol Ther, 27 (2019) 1950-1962.
[328] Q. Chen, R. Qi, X. Chen, X. Yang, S. Wu, H. Xiao, W. Dong, A Targeted and Stable Polymeric Nanoformulation Enhances Systemic Delivery of mRNA to Tumors, Mol Ther, 25 (2017) 92-101.
[329] C.J. McKinlay, J.R. Vargas, T.R. Blake, J.W. Hardy, M. Kanada, C.H. Contag, P.A. Wender, R.M. Waymouth, Charge-altering releasable transporters (CARTs) for the delivery and release of mRNA in living animals, Proceedings of the National Academy of Sciences, 114 (2017) E448-E456.
[330] C.J. McKinlay, N.L. Benner, O.A. Haabeth, R.M. Waymouth, P.A. Wender, Enhanced mRNA delivery into lymphocytes enabled by lipid-varied libraries of charge-altering releasable transporters, Proc Natl Acad Sci U S A, 115 (2018) E5859-e5866.
[331] O.A.W. Haabeth, T.R. Blake, C.J. McKinlay, A.A. Tveita, A. Sallets, R.M. Waymouth, P.A. Wender, R. Levy, Local Delivery of Ox40l, Cd80, and Cd86 mRNA Kindles Global Anticancer Immunity, Cancer research, 79 (2019) 1624-1634.
[332] H.A. Lagasse, A. Alexaki, V.L. Simhadri, N.H. Katagiri, W. Jankowski, Z.E. Sauna, C. Kimchi-Sarfaty, Recent advances in (therapeutic protein) drug development, F1000Research, 6 (2017) 113.
[333] X. Liu, F. Wu, Y. Ji, L. Yin, Recent Advances in Anti-cancer Protein/Peptide Delivery, Bioconjug Chem, 30 (2019) 305-324.

[334] Y.W. Lee, D.C. Luther, J.A. Kretzmann, A. Burden, T. Jeon, S. Zhai, V.M. Rotello, Protein Delivery into the Cell Cytosol using Non-Viral Nanocarriers, Theranostics, 9 (2019) 3280-3292.
[335] K.H. Bae, M. Kurisawa, Emerging hydrogel designs for controlled protein delivery, Biomater Sci, 4 (2016) 1184-1192.
[336] J. Dai, W. Long, Z. Liang, L. Wen, F. Yang, G. Chen, A novel vehicle for local protein delivery to the inner ear: injectable and biodegradable thermosensitive hydrogel loaded with PLGA nanoparticles, Drug development and industrial pharmacy, 44 (2018) 89-98.
[337] T. Jiang, S. Shen, T. Wang, M. Li, B. He, R. Mo, A Substrate-Selective Enzyme-Catalysis Assembly Strategy for Oligopeptide Hydrogel-Assisted Combinatorial Protein Delivery, Nano Lett, 17 (2017) 7447-7454.
[338] M.C. Koetting, J.F. Guido, M. Gupta, A. Zhang, N.A. Peppas, pH-responsive and enzymatically-responsive hydrogel microparticles for the oral delivery of therapeutic proteins: Effects of protein size, crosslinking density, and hydrogel degradation on protein delivery, J Control Release, 221 (2016) 18-25.
[339] A. Matsumoto, M. Tanaka, H. Matsumoto, K. Ochi, Y. Moro-Oka, H. Kuwata, H. Yamada, I. Shirakawa, T. Miyazawa, H. Ishii, K. Kataoka, Y. Ogawa, Y. Miyahara, T. Suganami, Synthetic "smart gel" provides glucose-responsive insulin delivery in diabetic mice, Science advances, 3 (2017) eaaq0723.
[340] C. Yu, E. Tan, Y. Xu, J. Lv, Y. Cheng, A Guanidinium-Rich Polymer for Efficient Cytosolic Delivery of Native Proteins, Bioconjug Chem, 30 (2019) 413-417.
[341] C. Liu, T. Wan, H. Wang, S. Zhang, Y. Ping, Y. Cheng, A boronic acid-rich dendrimer with robust and unprecedented efficiency for cytosolic protein delivery and CRISPR-Cas9 gene editing, Science advances, 5 (2019) eaaw8922.
[342] S.R. Schwarze, A. Ho, A. Vocero-Akbani, S.F. Dowdy, In vivo protein transduction: delivery of a biologically active protein into the mouse, Science, 285 (1999) 1569-1572.
[343] R.K. June, K. Gogoi, A. Eguchi, X.S. Cui, S.F. Dowdy, Synthesis of a pH-Sensitive Nitrilotriacetic Linker to Peptide Transduction Domains To Enable Intracellular Delivery of Histidine Imidazole Ring-Containing Macromolecules, Journal of the American Chemical Society, 132 (2010) 10680-10682.
[344] N. Nischan, H.D. Herce, F. Natale, N. Bohlke, N. Budisa, M.C. Cardoso, C.P. Hackenberger, Covalent attachment of cyclic TAT peptides to GFP results in protein delivery into live cells with immediate bioavailability, Angew Chem Int Ed Engl, 54 (2015) 1950-1953.
[345] A.F.L. Schneider, A.L.D. Wallabregue, L. Franz, C.P.R. Hackenberger, Targeted Subcellular Protein Delivery Using Cleavable Cyclic Cell-Penetrating Peptides, Bioconjug Chem, 30 (2019) 400-404.
[346] Y. Kawaguchi, S. Ise, Y. Azuma, T. Takeuchi, K. Kawano, T.K. Le, J. Ohkanda, S. Futaki, Dipicolylamine/Metal Complexes that Promote Direct Cell-Membrane Penetration of Octaarginine, Bioconjug Chem, 30 (2019) 454-460.
[347] Y. Lee, S. Fukushima, Y. Bae, S. Hiki, T. Ishii, K. Kataoka, A protein nanocarrier from charge-conversion polymer in response to endosomal pH, J Am Chem Soc, 129 (2007) 5362-5363.
[348] Y. Lee, T. Ishii, H. Cabral, H.J. Kim, J.H. Seo, N. Nishiyama, H. Oshima, K. Osada, K. Kataoka, Charge-conversional polyionic complex micelles-efficient nanocarriers for protein delivery into cytoplasm, Angew Chem Int Ed Engl, 48 (2009) 5309-5312.
[349] A. Tao, G.L. Huang, K. Igarashi, T. Hong, S. Liao, F. Stellacci, Y. Matsumoto, T. Yamasoba, K. Kataoka, H. Cabral, Polymeric Micelles Loading Proteins through Concurrent Ion Complexation and pH-Cleavable Covalent Bonding for In Vivo Delivery, Macromolecular bioscience, (2019) e1900161.
[350] K. Maier, E. Wagner, Acid-labile traceless click linker for protein transduction, J Am Chem Soc, 134 (2012) 10169-10173.
[351] X. Liu, P. Zhang, D. He, W. Rodl, T. Preiss, J.O. Radler, E. Wagner, U. Lachelt, pH-Reversible Cationic RNase A Conjugates for Enhanced Cellular Delivery and Tumor Cell Killing, Biomacromolecules, 17 (2016) 173-182.

[352] K. Maier, I. Martin, E. Wagner, Sequence Defined Disulfide-Linked Shuttle for Strongly Enhanced Intracellular Protein Delivery, Molecular pharmaceutics, 9 (2012) 3560-3568.
[353] P. Zhang, D. He, P.M. Klein, X. Liu, R. Röder, M. Döblinger, E. Wagner, Enhanced Intracellular Protein Transduction by Sequence Defined Tetra-Oleoyl Oligoaminoamides Targeted for Cancer Therapy, Advanced Functional Materials, 25 (2015) 6627-6636.
[354] P. Zhang, B. Steinborn, U. Lachelt, S. Zahler, E. Wagner, Lipo-Oligomer Nanoformulations for Targeted Intracellular Protein Delivery, Biomacromolecules, 18 (2017) 2509-2520.
[355] R. Roder, J. Helma, T. Preiss, J.O. Radler, H. Leonhardt, E. Wagner, Intracellular Delivery of Nanobodies for Imaging of Target Proteins in Live Cells, Pharm Res, 34 (2017) 161-174.
[356] X. Liu, P. Zhang, W. Rodl, K. Maier, U. Lachelt, E. Wagner, Toward Artificial Immunotoxins: Traceless Reversible Conjugation of RNase A with Receptor Targeting and Endosomal Escape Domains, Molecular pharmaceutics, 14 (2017) 1439-1449.
[357] R. Roder, T. Preiss, P. Hirschle, B. Steinborn, A. Zimpel, M. Hohn, J.O. Radler, T. Bein, E. Wagner, S. Wuttke, U. Lachelt, Multifunctional Nanoparticles by Coordinative Self-Assembly of His-Tagged Units with Metal-Organic Frameworks, J Am Chem Soc, 139 (2017) 2359-2368.
[358] M. Nishiga, L.S. Qi, J.C. Wu, Therapeutic genome editing in cardiovascular diseases, Adv Drug Deliv Rev, 168 (2021) 147-157.
[359] A. Zarei, V. Razban, S.E. Hosseini, S.M.B. Tabei, Creating cell and animal models of human disease by genome editing using CRISPR/Cas9, The journal of gene medicine, 21 (2019) e3082.
[360] X. Xu, T. Wan, H. Xin, J. Wu, Y. Ping, Delivery of CRISPR/Cas9 for Therapeutic Genome Editing, The journal of gene medicine, (2019) e3107.
[361] Y.K. Kang, K. Kwon, J.S. Ryu, H.N. Lee, C. Park, H.J. Chung, Nonviral Genome Editing Based on a Polymer-Derivatized CRISPR Nanocomplex for Targeting Bacterial Pathogens and Antibiotic Resistance, Bioconjug Chem, 28 (2017) 957-967.
[362] H.X. Zhang, Y. Zhang, H. Yin, Genome Editing with mRNA Encoding ZFN, TALEN, and Cas9, Mol Ther, 27 (2019) 735-746.
[363] Z. Zhang, T. Wan, Y. Chen, Y. Chen, H. Sun, T. Cao, Z. Songyang, G. Tang, C. Wu, Y. Ping, F.J. Xu, J. Huang, Cationic Polymer-Mediated CRISPR/Cas9 Plasmid Delivery for Genome Editing, Macromolecular rapid communications, 40 (2019) e1800068.
[364] X. Chen, Y. Chen, H. Xin, T. Wan, Y. Ping, Near-infrared optogenetic engineering of photothermal nanoCRISPR for programmable genome editing, Proceedings of the National Academy of Sciences, 117 (2020) 2395-2405.
[365] C.F. Xu, G.J. Chen, Y.L. Luo, Y. Zhang, G. Zhao, Z.D. Lu, A. Czarna, Z. Gu, J. Wang, Rational designs of in vivo CRISPR-Cas delivery systems, Adv Drug Deliv Rev, 168 (2021) 3-29.
[366] H. Tang, X. Zhao, X. Jiang, Synthetic multi-layer nanoparticles for CRISPR-Cas9 genome editing, Adv Drug Deliv Rev, 168 (2021) 55-78.
[367] T. Wan, Y. Ping, Delivery of genome-editing biomacromolecules for treatment of lung genetic disorders, Adv Drug Deliv Rev, 168 (2021) 196-216.
[368] D. Sun, Z. Sun, H. Jiang, A.M. Vaidya, R. Xin, N.R. Ayat, A.L. Schilb, P.L. Qiao, Z. Han, A. Naderi, Z.R. Lu, Synthesis and Evaluation of pH-Sensitive Multifunctional Lipids for Efficient Delivery of CRISPR/Cas9 in Gene Editing, Bioconjug Chem, 30 (2019) 667-678.
[369] A.S. Timin, A.R. Muslimov, K.V. Lepik, O.S. Epifanovskaya, A.I. Shakirova, U. Mock, K. Riecken, M.V. Okilova, V.S. Sergeev, B.V. Afanasyev, B. Fehse, G.B. Sukhorukov, Efficient gene editing via non-viral delivery of CRISPR-Cas9 system using polymeric and hybrid microcarriers, Nanomedicine, 14 (2018) 97-108.
[370] Y. Rui, D.R. Wilson, K. Sanders, J.J. Green, Reducible Branched Ester-Amine Quadpolymers (rBEAQs) Codelivering Plasmid DNA and RNA Oligonucleotides Enable CRISPR/Cas9 Genome Editing, ACS applied materials & interfaces, 11 (2019) 10472-10480.

[371] A. Conway, M. Mendel, K. Kim, K. McGovern, A. Boyko, L. Zhang, J.C. Miller, R.C. DeKelver, D.E. Paschon, B.L. Mui, P.J.C. Lin, Y.K. Tam, C. Barbosa, T. Redelmeier, M.C. Holmes, G. Lee, Non-viral Delivery of Zinc Finger Nuclease mRNA Enables Highly Efficient In Vivo Genome Editing of Multiple Therapeutic Gene Targets, Molecular Therapy, 27 (2019) 866-877.
[372] J.B. Miller, S. Zhang, P. Kos, H. Xiong, K. Zhou, S.S. Perelman, H. Zhu, D.J. Siegwart, Non-Viral CRISPR/Cas Gene Editing In Vitro and In Vivo Enabled by Synthetic Nanoparticle Co-Delivery of Cas9 mRNA and sgRNA, Angew Chem Int Ed Engl, 56 (2017) 1059-1063.
[373] R. Rouet, B.A. Thuma, M.D. Roy, N.G. Lintner, D.M. Rubitski, J.E. Finley, H.M. Wisniewska, R. Mendonsa, A. Hirsh, L. de Onate, J. Compte Barron, T.J. McLellan, J. Bellenger, X. Feng, A. Varghese, B.A. Chrunyk, K. Borzilleri, K.D. Hesp, K. Zhou, N. Ma, M. Tu, R. Dullea, K.F. McClure, R.C. Wilson, S. Liras, V. Mascitti, J.A. Doudna, Receptor-Mediated Delivery of CRISPR-Cas9 Endonuclease for Cell-Type-Specific Gene Editing, J Am Chem Soc, 140 (2018) 6596-6603.
[374] J.A. Zuris, D.B. Thompson, Y. Shu, J.P. Guilinger, J.L. Bessen, J.H. Hu, M.L. Maeder, J.K. Joung, Z.Y. Chen, D.R. Liu, Cationic lipid-mediated delivery of proteins enables efficient protein-based genome editing in vitro and in vivo, Nature biotechnology, 33 (2015) 73-80.
[375] M. Wang, J.A. Zuris, F. Meng, H. Rees, S. Sun, P. Deng, Y. Han, X. Gao, D. Pouli, Q. Wu, I. Georgakoudi, D.R. Liu, Q. Xu, Efficient delivery of genome-editing proteins using bioreducible lipid nanoparticles, Proc Natl Acad Sci U S A, 113 (2016) 2868-2873.
[376] P. Wang, L. Zhang, Y. Xie, N. Wang, R. Tang, W. Zheng, X. Jiang, Genome Editing for Cancer Therapy: Delivery of Cas9 Protein/sgRNA Plasmid via a Gold Nanocluster/Lipid Core-Shell Nanocarrier, Advanced science (Weinheim, Baden-Wurttemberg, Germany), 4 (2017) 1700175.
[377] C.E. Smull, E.H. Ludwig, Enhancement of the plaque forming capacity of poliovirus ribonucleic acid with basic proteins, J.Bacteriol., 84 (1962) 1035-1040.
[378] C. Andreini, L. Banci, I. Bertini, A. Rosato, Counting the zinc-proteins encoded in the human genome, Journal of proteome research, 5 (2006) 196-201.
[379] D.T. Curiel, S. Agarwal, E. Wagner, M. Cotten, Adenovirus enhancement of transferrin-polylysine-mediated gene delivery, Proc.Natl.Acad.Sci.U.S.A, 88 (1991) 8850-8854.
[380] O. Boussif, F. Lezoualc'h, M.A. Zanta, M.D. Mergny, D. Scherman, B. Demeneix, J.P. Behr, A versatile vector for gene and oligonucleotide transfer into cells in culture and in vivo: polyethylenimine, Proc.Natl.Acad.Sci.U.S.A, 92 (1995) 7297-7301.
[381] J.P. Behr, The proton sponge: A trick to enter cells the viruses did not exploit, Chimia, 51 (1997) 34-36.
[382] F. Haase, J. Pöhmerer, M. Yazdi, M. Grau, Y. Zeyn, U. Wilk, T. Burghardt, M. Höhn, C. Hieber, M. Bros, E. Wagner, S. Berger, Lipoamino bundle LNPs for efficient mRNA transfection of dendritic cells and macrophages show high spleen selectivity, European Journal of Pharmaceutics and Biopharmaceutics, 194 (2024) 95-109.
[383] D. Adams, A. Gonzalez-Duarte, W.D. O'Riordan, C.C. Yang, M. Ueda, A.V. Kristen, I. Tournev, H.H. Schmidt, T. Coelho, J.L. Berk, K.P. Lin, G. Vita, S. Attarian, V. Planté-Bordeneuve, M.M. Mezei, J.M. Campistol, J. Buades, T.H. Brannagan, 3rd, B.J. Kim, J. Oh, Y. Parman, Y. Sekijima, P.N. Hawkins, S.D. Solomon, M. Polydefkis, P.J. Dyck, P.J. Gandhi, S. Goyal, J. Chen, A.L. Strahs, S.V. Nochur, M.T. Sweetser, P.P. Garg, A.K. Vaishnaw, J.A. Gollob, O.B. Suhr, Patisiran, an RNAi Therapeutic, for Hereditary Transthyretin Amyloidosis, N. Engl. J. Med., 379 (2018) 11-21.
[384] L. Schoenmaker, D. Witzigmann, J.A. Kulkarni, R. Verbeke, G. Kersten, W. Jiskoot, D.J.A. Crommelin, mRNA-lipid nanoparticle COVID-19 vaccines: Structure and stability, Int. J. Pharm., 601 (2021) 120586.
[385] S. Bevers, S.A.A. Kooijmans, E. Van de Velde, M.J.W. Evers, S. Seghers, J.J.J.M. Gitz-Francois, N.C.H. van Kronenburg, M.H.A.M. Fens, E. Mastrobattista, L. Hassler, H. Sork, T. Lehto, K.E. Ahmed, S. El Andaloussi, K. Fiedler, K. Breckpot, M. Maes, D. Van Hoorick, T. Bastogne, R.M. Schiffelers, S. De Koker, mRNA-LNP vaccines tuned for systemic

immunization induce strong antitumor immunity by engaging splenic immune cells, Mol. Ther., 30 (2022) 3078-3094.
[386] J.D. Gillmore, E. Gane, J. Taubel, J. Kao, M. Fontana, M.L. Maitland, J. Seitzer, D. O'Connell, K.R. Walsh, K. Wood, J. Phillips, Y. Xu, A. Amaral, A.P. Boyd, J.E. Cehelsky, M.D. McKee, A. Schiermeier, O. Harari, A. Murphy, C.A. Kyratsous, B. Zambrowicz, R. Soltys, D.E. Gutstein, J. Leonard, L. Sepp-Lorenzino, D. Lebwohl, CRISPR-Cas9 In Vivo Gene Editing for Transthyretin Amyloidosis, N. Engl. J. Med., 385 (2021) 493-502.
[387] P.R. Cullis, M.J. Hope, Lipid Nanoparticle Systems for Enabling Gene Therapies, Mol. Ther., 25 (2017) 1467-1475.
[388] S.T. LoPresti, M.L. Arral, N. Chaudhary, K.A. Whitehead, The replacement of helper lipids with charged alternatives in lipid nanoparticles facilitates targeted mRNA delivery to the spleen and lungs, J. Controlled Release, 345 (2022) 819-831.
[389] D. Bi, D.M. Unthan, L. Hu, J. Bussmann, K. Remaut, M. Barz, H. Zhang, Polysarcosine-based lipid formulations for intracranial delivery of mRNA, Journal of Controlled Release, 356 (2023) 1-13.
[390] R. Pattipeiluhu, G. Arias-Alpizar, G. Basha, K.Y.T. Chan, J. Bussmann, T.H. Sharp, M.A. Moradi, N. Sommerdijk, E.N. Harris, P.R. Cullis, A. Kros, D. Witzigmann, F. Campbell, Anionic Lipid Nanoparticles Preferentially Deliver mRNA to the Hepatic Reticuloendothelial System, Adv Mater, 34 (2022) e2201095.
[391] S. Kimura, I.A. Khalil, Y.H.A. Elewa, H. Harashima, Novel lipid combination for delivery of plasmid DNA to immune cells in the spleen, J. Controlled Release, 330 (2021) 753-764.
[392] S. Kimura, H. Harashima, On the mechanism of tissue-selective gene delivery by lipid nanoparticles, J Control Release, 362 (2023) 797-811.
[393] A. Akinc, M. Goldberg, J. Qin, J.R. Dorkin, C. Gamba-Vitalo, M. Maier, K.N. Jayaprakash, M. Jayaraman, K.G. Rajeev, M. Manoharan, V. Koteliansky, I. Röhl, E.S. Leshchiner, R. Langer, D.G. Anderson, Development of lipidoid-siRNA formulations for systemic delivery to the liver, Mol. Ther., 17 (2009) 872-879.
[394] K.A. Whitehead, J.R. Dorkin, A.J. Vegas, P.H. Chang, O. Veiseh, J. Matthews, O.S. Fenton, Y. Zhang, K.T. Olejnik, V. Yesilyurt, D. Chen, S. Barros, B. Klebanov, T. Novobrantseva, R. Langer, D.G. Anderson, Degradable lipid nanoparticles with predictable in vivo siRNA delivery activity, Nat. Commun., 5 (2014) 4277.
[395] X. Yan, F. Kuipers, L.M. Havekes, R. Havinga, B. Dontje, K. Poelstra, G.L. Scherphof, J.A. Kamps, The role of apolipoprotein E in the elimination of liposomes from blood by hepatocytes in the mouse, Biochem Biophys Res Commun, 328 (2005) 57-62.
[396] K. Lam, P. Schreiner, A. Leung, P. Stainton, S. Reid, E. Yaworski, P. Lutwyche, J. Heyes, Optimizing Lipid Nanoparticles for Delivery in Primates, Advanced Materials, 35 (2023) 2211420.
[397] L.M. Kranz, M. Diken, H. Haas, S. Kreiter, C. Loquai, K.C. Reuter, M. Meng, D. Fritz, F. Vascotto, H. Hefesha, C. Grunwitz, M. Vormehr, Y. Husemann, A. Selmi, A.N. Kuhn, J. Buck, E. Derhovanessian, R. Rae, S. Attig, J. Diekmann, R.A. Jabulowsky, S. Heesch, J. Hassel, P. Langguth, S. Grabbe, C. Huber, O. Tureci, U. Sahin, Systemic RNA delivery to dendritic cells exploits antiviral defence for cancer immunotherapy, Nature, 534 (2016) 396-401.
[398] K. Sasaki, Y. Sato, K. Okuda, K. Iwakawa, H. Harashima, mRNA-Loaded Lipid Nanoparticles Targeting Dendritic Cells for Cancer Immunotherapy, Pharmaceutics, 14 (2022).
[399] Q. Cheng, T. Wei, L. Farbiak, L.T. Johnson, S.A. Dilliard, D.J. Siegwart, Selective organ targeting (SORT) nanoparticles for tissue-specific mRNA delivery and CRISPR-Cas gene editing, Nat Nanotechnol, 15 (2020) 313-320.
[400] S.A. Dilliard, Q. Cheng, D.J. Siegwart, On the mechanism of tissue-specific mRNA delivery by selective organ targeting nanoparticles, Proc Natl Acad Sci U S A, 118 (2021).
[401] S.A. Dilliard, Y. Sun, M.O. Brown, Y.C. Sung, S. Chatterjee, L. Farbiak, A. Vaidya, X. Lian, X. Wang, A. Lemoff, D.J. Siegwart, The interplay of quaternary ammonium lipid structure and protein corona on lung-specific mRNA delivery by selective organ targeting (SORT) nanoparticles, J Control Release, 361 (2023) 361-372.

[402] M. Herrera-Barrera, R.C. Ryals, M. Gautam, A. Jozic, M. Landry, T. Korzun, M. Gupta, C. Acosta, J. Stoddard, R. Reynaga, W. Tschetter, N. Jacomino, O. Taratula, C. Sun, A.K. Lauer, M. Neuringer, G. Sahay, Peptide-guided lipid nanoparticles deliver mRNA to the neural retina of rodents and nonhuman primates, Sci Adv, 9 (2023) eadd4623.
[403] S. Ramishetti, I. Hazan-Halevy, R. Palakuri, S. Chatterjee, S. Naidu Gonna, N. Dammes, I. Freilich, L. Kolik Shmuel, D. Danino, D. Peer, A Combinatorial Library of Lipid Nanoparticles for RNA Delivery to Leukocytes, Adv. Mater., 32 (2020) e1906128.
[404] M.P. Lokugamage, C.D. Sago, Z. Gan, B.R. Krupczak, J.E. Dahlman, Constrained Nanoparticles Deliver siRNA and sgRNA to T Cells In Vivo without Targeting Ligands, Adv. Mater., 31 (2019) e1902251-e1902251.
[405] H. Ni, M.Z.C. Hatit, K. Zhao, D. Loughrey, M.P. Lokugamage, H.E. Peck, A.D. Cid, A. Muralidharan, Y. Kim, P.J. Santangelo, J.E. Dahlman, Piperazine-derived lipid nanoparticles deliver mRNA to immune cells in vivo, Nat. Comm., 13 (2022) 4766.
[406] C. Lotter, C.L. Alter, J.S. Bolten, P. Detampel, C.G. Palivan, T. Einfalt, J. Huwyler, Incorporation of phosphatidylserine improves efficiency of lipid based gene delivery systems, Eur J Pharm Biopharm, 172 (2022) 134-143.
[407] S. Luozhong, Z. Yuan, T. Sarmiento, Y. Chen, W. Gu, C. McCurdy, W. Gao, R. Li, S. Wilkens, S. Jiang, Phosphatidylserine Lipid Nanoparticles Promote Systemic RNA Delivery to Secondary Lymphoid Organs, Nano Lett, 22 (2022) 8304-8311.
[408] A. Spadea, M. Jackman, L. Cui, S. Pereira, M.J. Lawrence, R.A. Campbell, M. Ashford, Nucleic Acid-Loaded Lipid Nanoparticle Interactions with Model Endosomal Membranes, ACS Applied Materials & Interfaces, 14 (2022) 30371-30384.
[409] C. Qiu, F. Xia, J. Zhang, Q. Shi, Y. Meng, C. Wang, H. Pang, L. Gu, C. Xu, Q. Guo, J. Wang, Advanced Strategies for Overcoming Endosomal/Lysosomal Barrier in Nanodrug Delivery, Research (Wash D C), 6 (2023) 0148.
[410] I.M.S. Degors, C. Wang, Z.U. Rehman, I.S. Zuhorn, Carriers Break Barriers in Drug Delivery: Endocytosis and Endosomal Escape of Gene Delivery Vectors, Acc. Chem. Res., 52 (2019) 1750-1760.
[411] A. Wittrup, A. Ai, X. Liu, P. Hamar, R. Trifonova, K. Charisse, M. Manoharan, T. Kirchhausen, J. Lieberman, Visualizing lipid-formulated siRNA release from endosomes and target gene knockdown, Nat. Biotechnol., 33 (2015) 870-876.
[412] J. Gilleron, W. Querbes, A. Zeigerer, A. Borodovsky, G. Marsico, U. Schubert, K. Manygoats, S. Seifert, C. Andree, M. Stoter, H. Epstein-Barash, L. Zhang, V. Koteliansky, K. Fitzgerald, E. Fava, M. Bickle, Y. Kalaidzidis, A. Akinc, M. Maier, M. Zerial, Image-based analysis of lipid nanoparticle-mediated siRNA delivery, intracellular trafficking and endosomal escape, Nat. Biotechnol., 31 (2013) 638-646.
[413] L. Zheng, S.R. Bandara, Z. Tan, C. Leal, Lipid nanoparticle topology regulates endosomal escape and delivery of RNA to the cytoplasm, Proc Natl Acad Sci U S A, 120 (2023) e2301067120.
[414] D. Schaffert, N. Badgujar, E. Wagner, Novel Fmoc-polyamino acids for solid-phase synthesis of defined polyamidoamines, Org. Lett., 13 (2011) 1586-1589.
[415] M. Jayaraman, S.M. Ansell, B.L. Mui, Y.K. Tam, J. Chen, X. Du, D. Butler, L. Eltepu, S. Matsuda, J.K. Narayanannair, K.G. Rajeev, I.M. Hafez, A. Akinc, M.A. Maier, M.A. Tracy, P.R. Cullis, T.D. Madden, M. Manoharan, M.J. Hope, Maximizing the Potency of siRNA Lipid Nanoparticles for Hepatic Gene Silencing In Vivo**, Angew. Chem., Int. Ed. Engl., 51 (2012) 8529-8533.
[416] S. Sabnis, E.S. Kumarasinghe, T. Salerno, C. Mihai, T. Ketova, J.J. Senn, A. Lynn, A. Bulychev, I. McFadyen, J. Chan, Ö. Almarsson, M.G. Stanton, K.E. Benenato, A Novel Amino Lipid Series for mRNA Delivery: Improved Endosomal Escape and Sustained Pharmacology and Safety in Non-human Primates, Mol. Ther., 26 (2018) 1509-1519.
[417] A. Krhač Levačić, S. Berger, J. Müller, A. Wegner, U. Lächelt, C. Dohmen, C. Rudolph, E. Wagner, Dynamic mRNA polyplexes benefit from bioreducible cleavage sites for in vitro and in vivo transfer, J. Controlled Release, 339 (2021) 27-40.

[418] D. Schaffert, C. Troiber, E.E. Salcher, T. Fröhlich, I. Martin, N. Badgujar, C. Dohmen, D. Edinger, R. Kläger, G. Maiwald, K. Farkasova, S. Seeber, K. Jahn-Hofmann, P. Hadwiger, E. Wagner, Solid-Phase Synthesis of Sequence-Defined T-, i-, and U-Shape Polymers for pDNA and siRNA Delivery, Angew. Chem., Int. Ed. Engl., 50 (2011) 8986-8989.
[419] Y. Rui, D.R. Wilson, S.Y. Tzeng, H.M. Yamagata, D. Sudhakar, M. Conge, C.A. Berlinicke, D.J. Zack, A. Tuesca, J.J. Green, High-throughput and high-content bioassay enables tuning of polyester nanoparticles for cellular uptake, endosomal escape, and systemic in vivo delivery of mRNA, Science advances, 8 (2022) eabk2855.
[420] Y. Lin, U. Wilk, J. Pöhmerer, E. Hörterer, M. Höhn, X. Luo, H. Mai, E. Wagner, U. Lächelt, Folate Receptor-Mediated Delivery of Cas9 RNP for Enhanced Immune Checkpoint Disruption in Cancer Cells, Small, 19 (2023) e2205318.
[421] M. Lyu, M. Yazdi, Y. Lin, M. Höhn, U. Lächelt, E. Wagner, Receptor-Targeted Dual pH-Triggered Intracellular Protein Transfer, ACS Biomater Sci Eng, 10 (2024) 99-114.
[422] C. Medina-Montano, M.L. Cacicedo, M. Svensson, M.J. Limeres, Y. Zeyn, J.E. Chaves-Giraldo, N. Röhrig, S. Grabbe, S. Gehring, M. Bros, Enrichment Methods for Murine Liver Non-Parenchymal Cells Differentially Affect Their Immunophenotype and Responsiveness towards Stimulation, Int. J. Mol. Sci., 23 (2022).
[423] X. Wang, B. Yu, W. Ren, X. Mo, C. Zhou, H. He, H. Jia, L. Wang, S.T. Jacob, R.J. Lee, K. Ghoshal, L.J. Lee, Enhanced hepatic delivery of siRNA and microRNA using oleic acid based lipid nanoparticle formulations, J Controlled Release, 172 (2013) 690-698.
[424] K. Paunovska, C.D. Sago, C.M. Monaco, W.H. Hudson, M.G. Castro, T.G. Rudoltz, S. Kalathoor, D.A. Vanover, P.J. Santangelo, R. Ahmed, A.V. Bryksin, J.E. Dahlman, A Direct Comparison of in Vitro and in Vivo Nucleic Acid Delivery Mediated by Hundreds of Nanoparticles Reveals a Weak Correlation, Nano Lett., 18 (2018) 2148-2157.
[425] S. Berger, M. Berger, C. Bantz, M. Maskos, E. Wagner, Performance of nanoparticles for biomedical applications: The in vitro/in vivo discrepancy, Biophysics Reviews, 3 (2022) 011303.
[426] S. Berger, U. Lächelt, E. Wagner, Dynamic cariers for therapeutic RNA delivery, Proc.Natl.Acad.Sci. USA, in revision (2023).
[427] D.C. Jürgens, L. Deßloch, D. Porras-Gonzalez, J. Winkeljann, S. Zielinski, M. Munschauer, A.L. Hörner, G. Burgstaller, B. Winkeljann, O.M. Merkel, Lab-scale siRNA and mRNA LNP manufacturing by various microfluidic mixing techniques – an evaluation of particle properties and efficiency, OpenNano, 12 (2023) 100161.
[428] S.G. Huayamares, M.P. Lokugamage, R. Rab, A.J. Da Silva Sanchez, H. Kim, A. Radmand, D. Loughrey, L. Lian, Y. Hou, B.R. Achyut, A. Ehrhardt, J.S. Hong, C.D. Sago, K. Paunovska, E.S. Echeverri, D. Vanover, P.J. Santangelo, E.J. Sorscher, J.E. Dahlman, High-throughput screens identify a lipid nanoparticle that preferentially delivers mRNA to human tumors in vivo, J Control Release, 357 (2023) 394-403.
[429] R.C. Steffens, E. Wagner, Directing the Way-Receptor and Chemical Targeting Strategies for Nucleic Acid Delivery, Pharm Res, 40 (2023) 47-76.

8 Publications

Research and review articles

Freitag, F., Wagner, E., *Optimizing synthetic nucleic acid and protein nanocarriers: The chemical evolution approach,* Adv Drug Deliv Rev (2021), 168, 30.

Haase, F., Pöhmerer, J., Yazdi, M., Grau, M., Zeyn, Y., Wilk, U., Burghardt, T., Höhn, M., Hieber, C., Bros, M., Wagner, E., Berger, S., *Lipoamino bundle LNPs for efficient mRNA transfection of dendritic cells and macrophages show high spleen selectivity,* Eur J Pharm Biopharm (2024) 194, 95-109.

Patent application

Wagner E, Peng, L, Berger S, Thalmayr S, Folda P, **Haase F**, Grau M, Germer J, Yazdi M, Weidinger E, Burghardt T, Steffens R, Seidl J, *Novel carriers for nucleic acid and/or protein delivery,* PCT/EP2023/082604.

9 Acknowledgements

Der Höhepunkt am Ende eines jeden Lebensabschnitts ist, wenn man einen Moment innehalten und all den Menschen danken kann, die diese Erfahrung ermöglicht und diese Zeit begleitet haben. Ohne euch alle wäre es nicht dasselbe gewesen.

Zuallererst möchte ich meinem Doktorvater Prof. Dr. Ernst Wagner danken, der all das hier erst möglich gemacht hat. Seine fachliche Expertise, seine Unterstützung und seine begeisternde Hingabe an die Forschung machen ihn zu einem ganz besonderen Vorbild. Ich bin dankbar für die wertvollen Diskussionen und Ratschläge und habe seinen immensen Erfahrungsschatz und sein Fachwissen sehr geschätzt.

Ein ganz großer Dank gilt auch all meinen Kollegen, die immer für mich da waren und mich in jeder Situation unterstützt haben. Ich danke Simone und Mina für ihr Engagement, die gute Zusammenarbeit und ihren wissenschaftlichen Input während der ganzen Zeit. Ihr habt mir geholfen meinen Weg durch den Forschungsdschungel zu finden. Der gemeinsame Ideenaustausch mit meinen Mitbewohnern Melina, Paul und Sophie, die Gespräche und wertvollen Diskussionen auf engstem Raum haben die Zeit extrem bereichert. Ich möchte Jana, Johanna, Ricarda und Vicky danken. Ihr wart nicht nur Kollegen, sondern Freunde, die die letzten Jahre sehr besonders gemacht haben. Außerdem danke ich Eric, Janin, Xianjin und Yi für die monatlichen Diskussionen im Cas 9 Meeting, genauso wie Anni, Elisa, Fengrong, Lun, Teo, Tobi und Uli für die Hilfe und Zusammenarbeit. Zusammen haben wir hier eine Menge durchgemacht - von all den Experimenten, die schiefgelaufen sind bis zu den genialen Durchbrüchen. Ihr wart nicht nur Kollegen, sondern auch Freunde, die Grund dafür waren, weshalb ich jeden Tag gerne in die Arbeit gekommen bin und diese Zeit zu etwas Besonderem gemacht haben.

Auch möchte ich mich bei Miriam für die Unterstützung und zahlreichen Tipps in der Zellkultur, bei Wolfgang für den technischen support und bei Markus für die liebevolle Betreuung der vielen kleinen Mäuschen bedanken.

Ich möchte auch all den Studenten danken, die ich über die vier Jahre betreuen dufte, um mit ihnen zusammen enzymatische Gehaltsbestimmungen durchzuführen oder aus einem Stück Schweineleber Enzyme zu isolieren. Insbesondere dankbar bin ich

Nicola und Elena, deren Bachelor- bzw. Masterarbeit ich mitbetreuen durfte und, die damit auch zu meiner eigenen Arbeit beigetragen haben.

Unendlich dankbar bin ich meiner Familie und Freunden. Ihr habt mich in allen Höhen und Tiefen ermutigt, unterstützt und mir den Rückhalt gegeben, den ich gebraucht habe. Tausend Dank an meinem Mann Christian, für seine unentwegte Unterstützung und die vielen, vielen Stunden Autofahrt zwischen Visp und München.

Abschließend möchte ich mich bei jedem Einzelnen bedanken, der mich in irgendeiner Form unterstützt hat, sei es durch aufmunternde Worte, fachliche Hilfe oder einfach durch das Teilen von Erfahrungen. Eure Beiträge haben meine Arbeit bereichert und meine persönliche Entwicklung gefördert.